SYNTHESIS AND BIOLOGICAL EVALUATION OF NEW CHOLINESTERASE INHIBITORS

Doctoral Thesis

Weiam A.Raheem A.Qader HUSSEIN

Eskişehir, 2017

SYNTHESIS AND BIOLOGICAL EVALUATION OF NEW CHOLINESTERASE INHIBITORS

Weiam A.Raheem A.Qader HUSSEIN

DOCTORAL THESIS

Department of Pharmaceutical Chemistry
Supervisor: Prof. Dr. Zafer Asım KAPLANCIKLI

Eskişehir
Anadolu University
Graduate School of Health Sciences
May, 2017

FINAL APPROVAL FOR THESIS

This thesis titled "Synthesis and Biological Evaluation of New cholinesterase Inhibitors" has been prepared and submitted by Weiam A.Raheem A.Qader Hussein in partial fullfillment of the requirements in "Anadolu University Directive on Graduate Education and Examination" for the Degree of PhD in Pharmaceutical Chemistry Department has been examined and approved in 17/05/2017.

Committee Members		Signature
Member (Supervisor)	: Prof. Dr. Zafer Asım KAPLANCIKLI	
Member	: Assoc. Prof. Dr. Yusuf ÖZKAY	
Member	: Assoc. Prof. Dr. Nafiz Öncü CAN	
Member	: Assoc. Prof. Dr. Murat ŞÜKÜROĞLU	
Member	: Assoc. Prof. Dr. Murat DURAN	

Prof. Dr. Dilek AK

Director

ABSTRACT

SYNTHESIS AND BIOLOGICAL EVALUATION OF
NEW CHOLINESTERASE INHIBITORS

Weiam A.Raheem A.Qader HUSSEIN

Department of Pharmaceutical Chemistry

Anadolu University, Graduate School of Health Sciences, May, 2017

Supervisor: Prof. Dr. Zafer Asım KAPLANCIKLI

Alzheimer's disease (AD) is a neurodegenerative disorder mostly influencing the elderly and causes death due to dementia. The main pathogenic feature connected with the progression of this multifactorial disease is the weakening of the cholinergic system in the brain. Cholinesterase (ChEs) inhibitors are recognized as one of the most promising targets in the treatment of AD. The inhibition of both enzymes has been approved as an appropriate therapeutic strategy to reduce the symptoms of disease and prevent disease progression; as well. The speed of medication explore has quickened detectably during the recent decade. Despite efforts to discover the original drugs, a radical treatment for this disease has not been found yet. A few drugs are approved by Food and Drug Administration to treat symptoms of AD. These medications are not ready to change or anticipate malady progression, they are, rather, palliative in easing the symptoms of malady. Inspired by what previously mentioned and by using simple and efficient synthetic way, 2-(9-acridinylamino)-2-oxoethyl piperazine/piperidine/morpholinecarbodithioate derivatives incorporating 9-aminoacridine and Donepezil like analogues were synthesized for the targeted modulation of acetylcholinesterase (AChE) and butyrylcholinesterase (BChE) activity. In general, we have achieved our desired aim, thus, eight derivatives demonstrated a specific and promising action against BChE. Furthermore, compound **4n** showed probable inhibitory activity against both enzymes. It has been found that the active compounds are well tolerated in the cytotoxicity test. Possible interactions between the lead compound **4n** and BChE enzyme were determined by a docking study. The findings obtained within this thesis will contribute to the development of new and effective synthetic anti-Alzheimer compounds and will ideally encourage future screening against AD. **Keywords:** Alzheimer diseases, acetylcholineesterase, butyrylcholinesterase, 9-aminoacridine, dithiocarbamates salts, docking study.

ÖZET

YENİ KOLİNESTERAZ İNHİBİTÖRLERİNİN
SENTEZİ VE BİYOLOJİK DEĞERLENDİRMESİ

Weiam A.Raheem A.Qader HUSSEIN

Farmasötik Kimya Anabilim Dalı

Anadolu Üniversitesi, Sağlık Bilimleri Enstitüsü, Mayıs, 2017

Danışman: Prof. Dr, Zafer Asım KAPLANCIKLI

Alzheimer hastalığı (AH), yaşlı insanlarda yaygın olarak görülen ve demansa bağlı olarak ölüme neden olan bir nörodejeneratif hastalıktır. Birçok nedeni olan bu hastalığın ilerlemesinde ana patojenik sebep, beyindeki kolinerjik sistemin zayıflamasıdır. Asetilkolinesteraz (AChE) ve bütirilkolinesteraz (BChE) inhibitörleri, AH tedavisinde en umut verici hedeflerden biri olarak kabul edilmektedir. Her iki enzimin inhibisyonu hastalığın belirtilerini azaltmak ve hastalık ilerlemesini önlemek için uygun bir terapötik strateji olarak kabul edilmektedir. Yeni ilaçların keşfedilme hızı son on yıl içinde fark edilebilir şekilde artmıştır. Fakat mevcut seçenekler son derece sınırlıdır. Orjinal ilaç geliştirme çabalarına rağmen, henüz bu hastalığa yönelik radikal bir tedavisi bulunamamıştır. Günümüzde birkaç ilaç AH'in semptomlarını tedavi etmek için Gıda ve İlaç İdaresi tarafından onaylanmıştır. Bu bilgiler ışığında, basit ve etkili bir sentetik yöntemle Takrin ve Donepezil analoğu 2-(9-akridinilamino)-2-oksoetil piperazin/piperidin/morfolinkarboditiyoat türevleri, AChE ve BChE inhibitör aktiviteleri hedeflenerek sentezlenmiştir. Genel olarak, hedefler doğrultusunda güçlü BChE inhibitör etkiye sahip farklı türevlere ulaşılmıştır. Sentezlenen bu bileşiklerden özellikle sekiz tanesi, BChE'ye spesifik ve umut verici inhibitör etki göstermiştir. Ayrıca, **4n** bileşiği hem AChE hem de BChE inhibitor etki sergilemiştir. Sentezlenen aktif bileşiklerin sağlıklı fibroblast hücreleri üzerindeki sitotoksisite testinde iyi tolere edildiği tesbit edilmiştir. En umut verici sonuçlara sahip olan **4n** bileşiğinin BChE enzimi ile olası önemli etkileşimleri Docking çalışması ile tespit edilmiştir. Bu tez kapsamında elde edilen bulgular, yeni ve etkili sentetik antiAlzheimer bileşiklerin geliştirilmesine ve hastalığın tedavisine yönelik ileriki çalışmalara katkı sağlayacaktır.

Anahtar Sözcükler: Alzheimer hastalıkları, asetilkolinesteraz, bütirilkolinesteraz, 9-aminoakridin, ditiyokarbamat tuzları, docking çalışması.

Working toward your dream is something you're could do if you are willing to work toward it. For me my dream is simply to fulfill my father's dream of seeing me a Ph.D. holder. I may not be able to repay your gift of kindness. But I have promised you to make your dream come true one day and it is the right time to tell you that..... Dearest dad, you could not wait until today. Please forgive me that I could not finish this earlier. This thesis is dedicated to you.

ACKNOWLEDGEMENTS

First and above all, I praise **ALLAH**, the almighty for giving me this chance and granting me the capability to continue effectively. During PhD course, I have been joined and upheld by a lot of people so; it is a delightful side that I have now the chance to express my appreciation to every one of them. Before anything else, I would like to express my sincere appreciation to my supervisor **Prof. Dr. Zafer Asım KAPLANCIKLI** my first teacher and supervisor. He has been an incredible teacher, and I have valued his counsel and guidance. From the earliest starting point, he has taught me to think, argue, and write more carefully and clearly. Perhaps more importantly, he has inspired me to be positive and empowered me as well to focus on goodness. I could not have imagined having a great, communicative and extremely helpful supervisor for my PhD study like you. I am deeply indebted to the help of **Assoc. Prof. Dr. Yusuf ÖZKAY** for his direction and support in doing this project work, his excited view on research has made a profound impact on me. I honestly can't thank you enough for all the knowledge and encouragement you have shared with me inside and outside the thesis. To you, my gratitude is deep.

I also appreciate the help of **Res. Asst. Begüm Nurpelin SAĞLIK** for examining the biological activity of the newly synthesized compounds and for doing docking procedure, thanks for being so accommodating and helpful person. I also thankful and appreciate the help of the **Res. Asst. Serkan LEVENT** for recording and interpretation of NMR spectra and for having shared many experiences and thoughts with me throughout the last years in addition for his kindly answers to my general questions. I would also like to thank **Mr. Murat KOZANLI** for recording the numerous mass spectra. My special thanks to **Res. Asst. Derya OSMANİYE** for help and support. I also appreciate the help of **Assoc. Prof. Dr. Sinem ILGIN** and **Miss. Büşra KORKUT** for doing the toxicity test for the active derivatives. I'm most grateful and appreciate **Prof. Dr. Gülhan TURAN-ZITOUNI** for her spiritual supports for me during my PhD study. I will never forget the time that we were together, I would like just to thank you for everything. I also thankful and appreciate the help of **Assoc. Prof. Dr. Ahmet Çağrı KARABURUN and Assoc. Prof. Dr. Leyla YURTTAŞ** whose, through numerous inspection, sincere encouragement and discussions, gave me numerous tips and thoughts on the best way to take every

necessary step. I am also thankful to **Prof. Dr. Nalan GÜNDOĞDU KARABURUN,** I really learned a lot from you. You are my favorite teacher. There is nothing that can come close to the unspoken support of my elder brother **ABDUL-LATIF** it would not have been possible without your support to get this scholarship. This was all the resultant of your efforts and help. I would like to thank you for being with us through the journey of processing. Financial support was provided from the **ADEN UNIVERSITY** and **Turks Abroad and Related Communities (YTB)** at various points, for which I am very grateful. It was a good opportunity to work at the **ANADOLU UNIVERSITY**. What a fantastic place to work**.** I just want to pass along my appreciation for the services provided and facilities service**s**. I might want to express my thanks to **My Colleagues (Betül, Ulviye, Asaf ……)** at the **Laboratory of Pharmaceutical Chemistry of the Anadolu University, Faculty of Pharmacy** and other members in the **Department of Pharmaceutical Chemistry** for making a cordial working atmosphere. I also, want to say thank you to **Mr. Ömer UYGUR** for all the laughs and for being such a positive influence.

I want to express my gratitude and deepest appreciation to my dear **MOM** and **DAD**…. you both gave me a real education you both inspired me to have ambition you both told me that the sky is my limit for success and victory you made me fit whatever I am today is because of you two. I believe my parents always watched me from somewhere, even they died. May **ALLAH** grant them a place in Jannat Al Firdous. Last, but not least, I might want to give special thanks to **My Sister Kamla,** if you hadn't been beside me it would have been totally impossible for me to finish this thesis, Hereby, I would like to thank you for everything. To all my **Brothers and Sisters** for they have provided help in several ways and for their backing and love which are a wellspring of my life. I need to express my appreciation and most profound thankfulness to my lovely sweets kids **Nasser** and **Aala** who's without their love; I could not have finished this work. I would rather thank my close friend actually my sister **Wafa Farooq** I don't know how I can say thank you to a person who understands the all things I never say and never says anything I don't understand. I cannot finish without thanking and expressing my special gratitude to my husband, **Fawaz AL-HEIBSHY** I know that you did not want to be named, it was you who kept the crucial of our family and who has merrily upheld me in each condition and in all parts of my life. I don't have any wishes in life as long as I have you, I've got it all.

17/05/2017

STATEMENT OF COMPLIANCE WITH ETHICAL PRINCIPLES AND RULES

I hereby truthfully declare that this thesis is an original work prepared by me; that I have behaved in accordance with the scientific ethical principles and rules throughout the stages of preparation, data collection, analysis and presentation of my work; that I have cited the sources of all data and information that could be obtained within the scope of this study, and included these sources in the references section; and that this study has been scanned for plagiarism with scientific plagiarism detection program used by Anadolu University, and that "it does not have any plagiarism" whatsoever. I also declare that, if a case contrary to my declaration is detected in my work at any time, I hereby express my consent to all the ethical and legal consequences that are involved.

Weiam A.Raheem A.Qader HUSSEIN

CONTENTS

Page

LIST OF TABLES

Page

LIST OF FIGURES

LIST OF SCHEMES

Page

LIST OF ABBREVIATIONS

ACh	Acetylcholine
AChE	Acetylcholinesterase
AChEI	Acetylcholinesterase inhibitor
AD	Alzheimer's disease
ADME	Absorption, distribution, metabolism and excretion
ATC	Acetylthiocholine
ATR	Attenuated total reflection
Aβ	Amyloid-β
BBB	Blood-brain barrier
BChE	Butyrylcholinesterase
BSA	Bovine serum albumin
BTC	Butyrylthiocholine
^{13}C-NMR	Carbon-13 nuclear magnetic resonance
CAS	Catalytic active site
ChAT	Choline acetyltransferase
ChE	Cholinesterase
CNS	Central nervous system
CNS	Central nervous system
DMEM	Dulbecco's modified Eagle's medium
DMF	Dimethylformamide
DMSO	Dimethyl sulfoxide
DMSO-d_6	Deuterated dimethyl sulfoxide
DNA	Deoxyribonucleic acid

DTCs	Dithiocarbamates
DTNB	5,5'-Dithiobis (2-nitrobenzoic acid)
EDTA	Ethylenediaminetetraacetic acid
ESI	Electrospray ionization
Et3N	Triethylamine
EtOH	Ethanol
FDA	Food and drug administration
FT-IR	Fourier transform infrared spectroscopy
^{1}H-NMR	Proton nuclear magnetic resonance
HBA	Hydrogen bond acceptor
HBD	Hydrogen bond donor
IC_{50}	Half maximal inhibitory concentration
IT-TOF	Ion trap and time-of-flight technologies
LCMS	Liquid chromatography mass spectrometry
M.p	Melting point
M.W	Molecular weight
m/z	Mass-to-charge ratio
MAO	Monoamine oxidase
MD	Molecular dynamics
MeOH	Methanol
MG	Myasthenia gravis
MLP	Molecular lipophilicity potential
MTT	[3-(4,5-dimethyl-2-thiazol)-2,5-diphenyl-2*H*-tetrazolium bromide]
NMDA	N-methyl-D-aspartate

NMR	Nuclear magnetic resonance spectroscopy
NSAID	Non-steroidal anti-inflammatory drug
NTB	2-Nitro-5-thiobenzoic acid
OD	Optical density
PAS	Peripheral anionic site
PBS	Phosphate buffer saline
PDB	Protein data bank
r.t	Room temperature
SAR	Structure activity relationship
SBVS	Structure-based virtual screening
tcAChE	Torpedo californica Acetylcholinesterase
TEA	Triethyl amine
THF	Tetrahydrofuran
TLC	Thin layer chromatography
Topo-1	Topoisomerase-I

1. INTRODUCTION

Alzheimer's disease (AD) is a neurological ailment and one of the most common cause of dementia in the age group above 60 years for which there is no radical cure. It is estimated from the world population that more than 35.6 million people are living with AD now and this may increase to 65.7 million by 2030 and 115.4 million by 2050 (Anders and Martin,2010, p.10). According to World health organization (WHO) report, more than 50% persons with AD, over half people with AD live in the developing word and are expressed to go up to 70% by 2025 (http-1). To date, a few elements including low levels of acetylcholine (ACh), oxidative anxiety, dyshomeostasis of biometals furthermore, amyloid-β (Aβ) stores have been exhibited to be related with AD pathogenesis, and a few speculations in light of these components have been proposed to clarify the component of AD advancement (Melnikova, 2007, p.341-342). In this way, new remedial advances are presently under advance.

Carbamates are the most generally contemplated class of anticholinesterase operators and impressive research on them in connection to AD has been expert. Rivastigmine, a dual acetylcholinesterase (AChE) and butyrylcholinesterase (BChE) inhibitor, is one of the most broadly utilized anticholinesterase operators bearing carbamate gather, which looks like the ester linkage of ACh (Shen, 2004, p.298-307; Lemke et al., 2008, p.327). Dithiocarbamates (DTCs) have pulled in a lot of intrigue in therapeutic science because of the way that new compelling mixes can be acquired by the bioisosteric substitution of carbamate moiety with dithiocarbamate moiety. They are likewise critical pharmacophores due to their lipophilicity, which is pivotal for the conveyance of central nervous system (CNS) medications to their site of activity through the blood-brain barrier (BBB) (Madalageri and Kotresh, 2012, p.2697-2703; Turan-Zitouni, Özdemir and Güven, 2005, p.96-104). The basic differences of known AChE inhibitors and the probability to investigate obvious mode of action have fortified works that affirmed the action of new AChE inhibitors like tacrine and donepezil. On the premise of these discoveries and in attempting to develop new drugs for the treatment of AD, and because of Tacrine treatment is connected with a high rate of serum aminotransferase which rises during treatment and has been connected to a few examples of clinically obvious, intense liver harm. In addition, there are no reviews accessible about utilizing acetylated 9-aminoacridine as anticholinesterase inhibitor till now and in

regarding to structurally related compounds consequently, it made more sense and become logical to develop new hybrid of 9-aminoacridine and dithiocarbamates analogues as a hopeful therapeutic approach for the symptomatic refinement in AD. Furthermore, since AChE inhibitors ought to endure a center ring framework that cooperates with PAS, a basic part which bind to CAS, and a suitable connection, for example, O , CH_2, CONH, and CONH(CH_2)n, between the center ring framework to satisfy the main structural necessity for active and strong enzyme inhibitors (Leurs et al., 2005, p.107-120). Based on this empirical knowledge, we aimed to improve AChE/BChE inhibitory activity by doing the following structural changes: 9-aminoacridine represents a center ring while a basic part is replaced by a heterocyclic ring (piperazine/piperidine or morpholine) and finally (thiocarbamoylthio)acetamide part represents the connection.

To begin a new medication disclosure and to discover new biologically active compounds, the study incorporated **(a)** In vitro biological assays, against AChE and BChE keeping in mind the specific goal to decide the compounds IC_{50} combined with **(b)** Molecular docking studies to assess the docking status and interatomic interactions in consideration of the active compounds. Because of BBB permeability is very essential for drugs that specifically target the CNS since the ability of the drug molecules to penetrate the BBB constitutes a major obstacle for CNS drug candidates and should be considered in drug discovery efforts. Therefore, it is of great importance to calculate this property for the new compounds. Accordingly, **(c)** BBB permeability and drug likeness score (DLS) predictions data were calculated for active compounds in the series. **(d)** Finally, the MTT cytotoxicity test was carried out for active derivatives in order to observe possible toxicity.

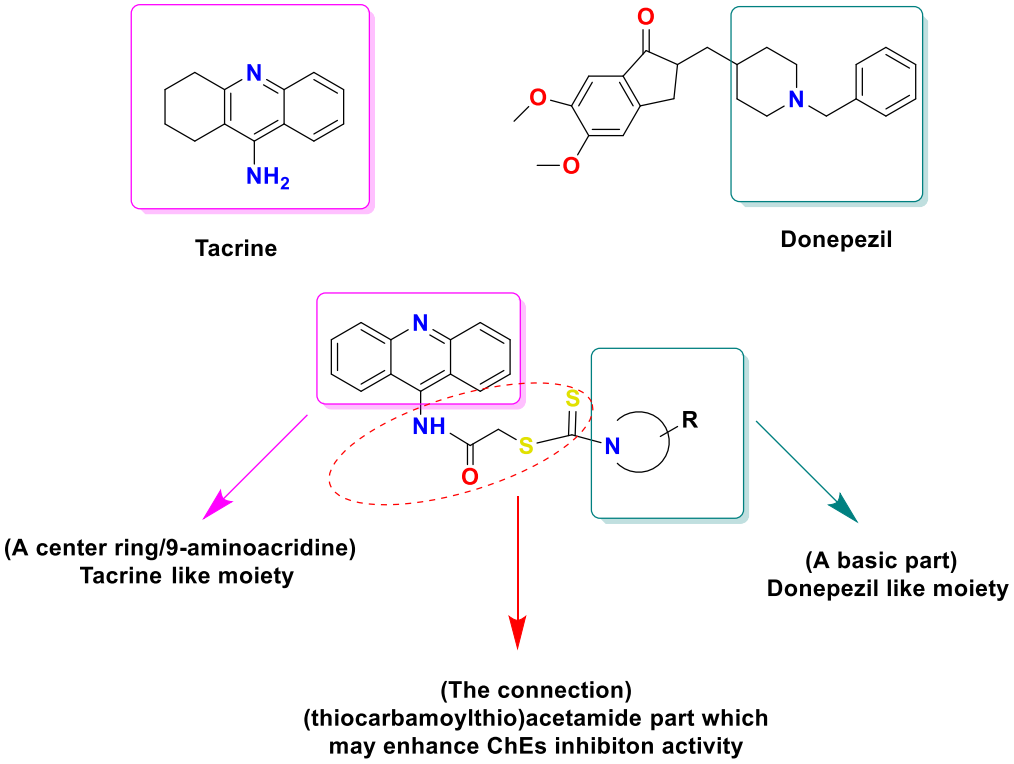

Scheme 1.1. *Design Strategy of Recently Synthesized Derivatives*

2. LITERATURE REVIEW

2.1. Alzheimer's Disease (AD)

AD is a non-convertible, precocious brain disorder that slowly destroys memory and thinking skills, and, ultimately, the ability to perform simple tasks. Most people with AD, symptoms first appear in their mid-60s. AD is the most common cause of dementia in the elderly people. The disease is named after Dr. Alois Alzheimer (Figure 2.1.) in 1906 observed changes in the brain tissue of a woman who died of an extraordinary mental disorder. Its symptoms include amnesia, language problems, and uncertain behavior. After she died, he inspected her brain and found many anomalous clumps (now called amyloid plaques) and tangled bundles of fibers (now called Neurofibrillary or tau tangles). These plaques and tangles in the brain until now considered to be one of the main characteristics of AD. Another characteristic is the loss of linkages between the nerve cells (neurons) in the brain. Neurons deliver messages among the various parts of the brain and from the brain to the muscles and organs in the body. While treatment can help control signs in some people, until the present time there is no treatment for this harmful disease. Researchers continue disentangle complicated brain changes arising from onset and the progression of AD. It is probable that brain damage begins a decade or more before the memory and other cognitive problems become apparent. During the pre-clinical stage of AD, people seem to have no symptoms, but the toxic changes occur in the brain. Abnormal deposits of proteins form amyloid plaques and tau tangles over the brain, and once the healthy neurons no longer work lose the communication with other neurons, and pass away.

Figure 2.1. *Dr. Alois Alzheimer (1864-1915)*
Reference: *http-2*

Damage originally appears to take place in the hippocampus, a part of the brain a substantial in the formation of memories. The greater the neurons die, the additional portion of the brain affected. During the final stage of Alzheimer's, damage prevalent and cortical tissue has declined significantly. Assessment varies, but experts assume that more than 5 million Americans are affected from AD. If the disease cannot be effectively treated or prevented, the number of people with this will considerably increase if current demographic trends continue. This is because an increased risk of AD with age, as in the United States (US) population ages. Alzheimer's is a slow-developed ailment that advances in three phases-an early, preclinical phase without any side effects, a center phase of intellectual disability, and a last phase of Alzheimer's dementia. The time from diagnosis to death differs-more meager as 3 or 4 years if the individual is elder than 80 when analyzed to the length of at least 10 years if the individual is more youthful. AD nowadays is the key cause of death in the United States, but according to recent assessment it will be the third cause of death directly after cardiovascular disease and cancer (http-3).

2.1.1. Patho physiology of AD

AD is driven by two procedures: extracellular deposition of beta amyloid-Aβ and intracellular gathering of tau protein. Both these compounds are insoluble. Aβ is the fundamental part of senileplaques and tau is the segment of neurofibrillary tangles. Aβ deposition is particular for AD and is thought to be essential. Tau gathering is likewise

observed in other degenerative diseases and is thought to be optional. (Figure 2) (http-4) In AD, cholinesterase (ChE) action, particularly that of BChE, is additionally found in association with the characteristic Aβ plaques (Stribley et al., 2000; p.1320-1331). Additionally, BChE movement related with Aβ plaques likewise gives off an impression of being a component that recognizes AD pathology from plaques introduce in the brains of people without dementia (Mesulam and Geula; 1994, p.722-727). The function(s) of BChE in Aβ plaques in AD remain(s) ambiguous. One of the most interesting studies carried out in this area showed that when BChE progresses toward becoming related with plaques, it advances role is the conversion of "harmless" plaques to "damaging" plaques. (Guillozet et al., 1997, p.909-918). So, BChE represents a proper imaging target for early diagnosis and treatment of AD.

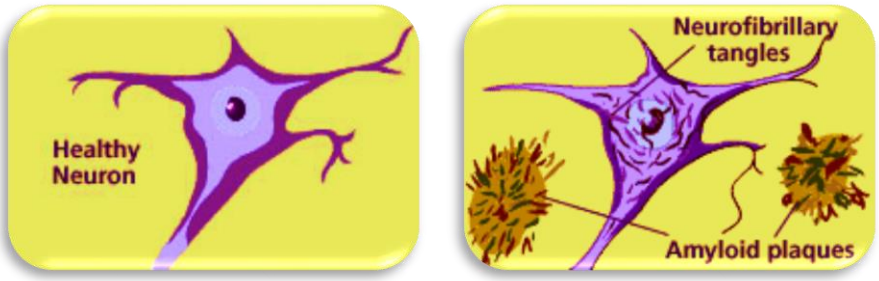

Figure 2.2. *Patho Physiology of (AD)*
Reference: *http-5*

It is apparent that AD pathology is complicated, various factors are included and the final result is a systemic fall of cholinergic neurotransmission alongside neuronal cell death, all things considered leading to dementia signs and symptoms. Among them, *N*-methly-D-aspartate (NMDA) excitotoxicty, increase in peroxides production, monoamine oxidase (MAO) enzymes, and non-steroidal anti-inflammatory drugs pathways are the most important (Hoey, Williams and Perkinton, 2009, p.29, 4442-4460) (Figure 2.3).

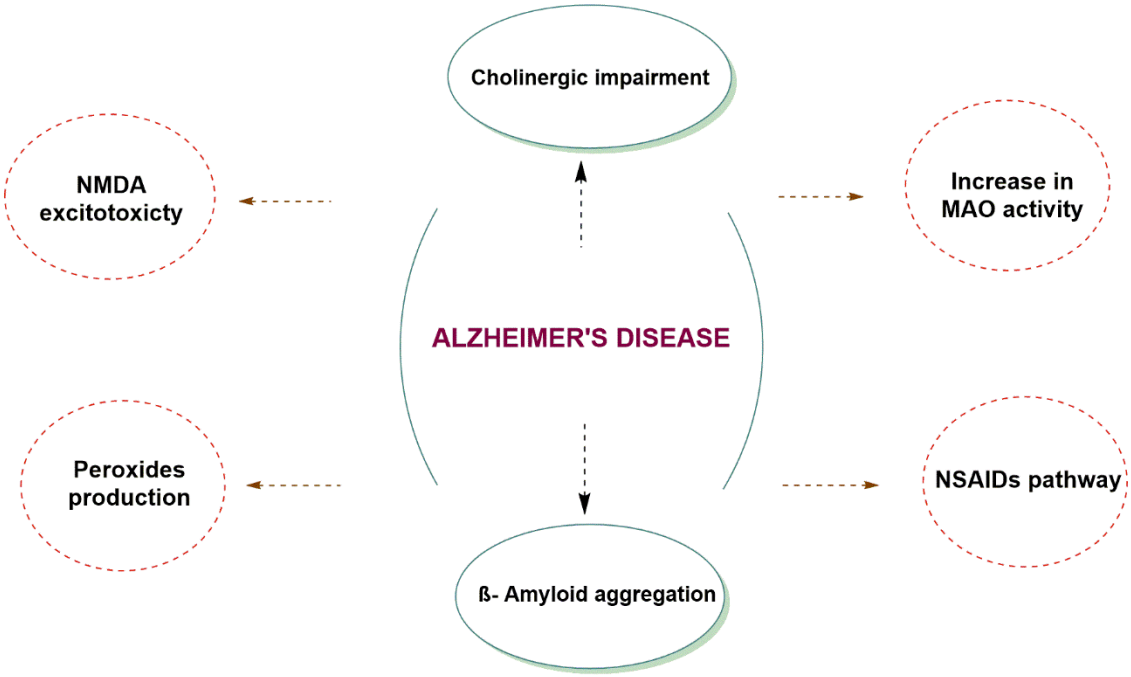

Figure 2.3. *Important Key Factors in AD Pathology.*

2.2. The Cholinergic Hypothesis

This is one of the oldest and most studied hypotheses totalized the pathogenesis of AD. The hypothesis suggests that impairments in cholinergic neurotransmission, dependent on the neurotransmitter acetylcholine (ACh), are to be faulted for the fast decrease in subjective capacity of AD patients. The cholinergic section of the CNS, primarily distributed within the cerebrum and cerebellum, is related with subjective capacity and general physical mindfulness. Besides ACh, other key players in the cholinergic theory are the ChE enzymes: AChE and BChE which are responsible for ACh degradation (Selkoe, 2002, p. 789-791).

2.2.1. The cholinesterase (ChE) enzymes

Learning of ChEs structure is essential for understanding their high catalytic efficacy as well as for the purpose, of rational drug design it is important to know everything related to these vital enzymes. ChEs are a family of enzymes that catalyzes the hydrolysis of ACh, a basic procedure taking into account the rebuilding of the cholinergic neuron. The two sorts of ChE are: (AChE; EC 3.1.1.7) and (BChE; EC 3.1.1.8). AChE is one of the well-known compounds, which plays an imperative part in the CNS. The availability of AChE crystal structures for distinct species with and without

ligands gives a strong premise to structure-based plan of novel AChE inhibitors (Barril, Orozco and Luque, 2001, p.255-266).

The AChE structure has been widely investigated since 1990s. The first experiment with X-ray was completed on AChE in the electric eel, Torpedo californica (tcAChE), because of its accessibility (Sussman et al.,1991, p.872-879). The results got have prompt to a casual model until the commercialization of human recombinant AChEs (Pohanka,2011, p.219-229). Target enzyme comprises of a narrow gorge with two separate ligand binding sites: the catalytic active site (CAS) and the peripheral anionic site (PAS) Fig. (3) (Bolognesi et al.,2005, p.465-473; Guo et al.,2004, p.5492-5500). The gorge itself is a narrow hydrophobic channel with a length of about 20Å, connecting the PAS to the active site (Sussman et al.,1991, p.872-879). It is surrounded by aromatic amino acids empowering a high selectivity for ACh.Substrate penetration is permitted by cation-π interactions between ACh quaternary ammonium atom and π electrons of phenylalanine (F), tryptophan (W) and tyrosine (Y) aromatic cores (Ripoll et al.,1993, p.5128-5132; Koellner et al.,2002, p.721-725).

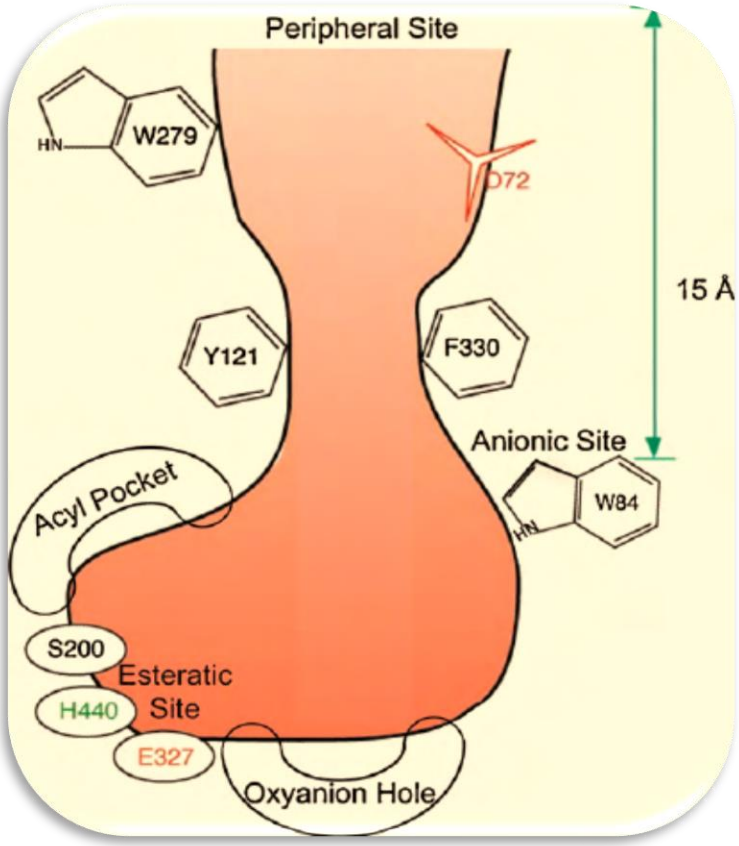

Figure 2.4. *Diagrammatic Illustration about AChE Active Sites*
Reference: *http-6*

The AChE catalytic active site is located at the bottom of the gorge and it comprises serine (S)-histidine (H)-glutamate (E), the catalytic triad (the same in AChE and BChE) within an esteratic site. The anionic site (also called α -anionic site) is another portion of the active site, and it is near to the esteratic site, while the esteratic site hydrolyzes the ester bond, the anionic site interacts with the acetylcholine quaternary ammonium atom and it is responsible for its proper orientation (Pohanka,2011, p.219-229; Johnson and Moore, 2006, p. 217-225).

The primary alcohol moiety of the serine residue (catalytic triad) participates in a transesterification reaction with ACh, resulting in acetylation of the enzyme. A neighboring group, the imidazole ring (part of a histidine residue) participates and facilitates the acetyl group transfer. The subsequent acetylated serine moiety is amazingly labile and quickly undergoes spontaneous hydrolytic cleavage to liberate acetate anion and to regenerate the active catalytic surface (Cannon,2003, p.39-108). The peripheral anionic site (additionally called β-anionic site) is located at the active center gorge entry, to approximately 14 Å from the main active site (Kryger, Silman and Sussman,1998, p.191-194). Tryptophan, tyrosine, and aspartate (D) amino acids residues are the most significant in the PAS (Johnson and Moore,2006, p.217-225).

This PAS incorporates binding sites for allosteric ligands (activators and inhibitors) (Bolognesi et al., 2005, p.465-473). Ligand binding to the PAS affects enzymatic activity through a combination of both by steric blockade of ligands moving through the gorge, and by allosteric change of the catalytic triad conformation (Bourne et al., 2003, p.1-12). Both enzymes contain a catalytic triad that is enclosed of the amino acids serine (Ser), histidine (His), and glutamic acid (Glu) which are occupying the bottom of a gorge (Nicolet et al; 2003, p. 41141-41147). AChE is narrower than that of BChE, this is essentially because of to the aromatic residues Tyr-124 and Trp-286 which are situated at the gorge entrance and which are possessed by Gln-119 and Ala-277 in BChE (Figure 2.5a and Figure 2.5b). Inside the gorge, there is a contrast in the acyl binding site residues which in AChE consist of the aromatic residues Phe-295 and Phe-297, while BChE contains the smaller residues Leu-286 and Val-288 (Nicolet et al; 2003, p.41141-41147). This permits BChE to bind bulkier substrates into the active site while in AChE it's just the opposite.

It is notable that AChE exists in two unique structures (with the same active sites): the globular forms, consisting of monomer (G1), dimer (G2) and tetramer (G4), and the

asymmetric forms. In the human brain, the plenty AChE forms are G4 and G1 (Rakonczay and Brimijoin,1988, p.85-93). A selective loss of the membrane-associated AChE molecular form G4 has been recognized in the AD brain, while the G1 form is relatively preserved (Rakonczay,2003, p.183-189). The enzyme acetylcholinesterase AChE plays a primary role in acetylcholine-mediated neurotransmission. It is concentrated at cholinergic synapses throughout the central nervous system and at neuromuscular synapses where it quickly hydrolyzes acetylcholine. It is this activity, rather than re-uptake by transporters as with other neurotransmitter systems, that terminates cholinergic neurotransmission (Massoulie et al., 1993, p.31-91). At therapeutic level, the utilization of AChE inhibitors is used to increase synaptic levels of acetylcholine in diseases that reduce acetylcholine neurotransmission, such as AD (Ballard, 2002, p.64-70). However, BChE activity regularly increments in patients with AD, while AChE action stays unaltered or decays. Both enzymes therefore represent right therapeutic targets for improving the cholinergic shortfall considered to be responsible for the declines in cognitive and behavioral characteristic of AD (Greig, Lahiri and Sambamurti, 2002, p.77-91).

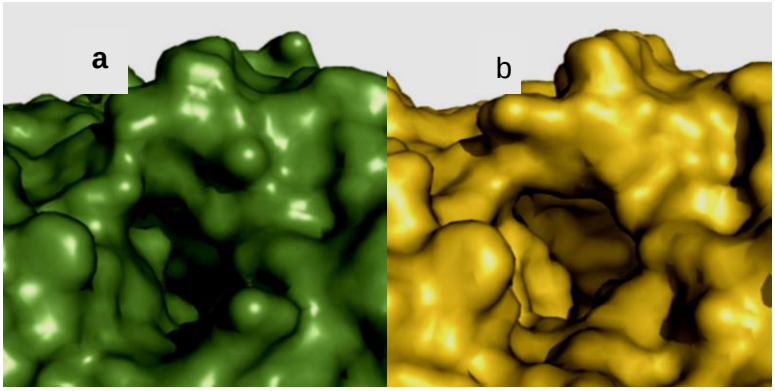

Figure 2.5. *The Active Site Entrance of **a)** Human AChE (Dvir et al., 2010, p.10- 22) and **b)** Human BChE (Ngamelue et al., 2007, p. 723-727)*

2.2.1.1. Acetylcholinesterase (AChE)

AChE, otherwise called, cholinesterase, acetylcholine acetylhydrolase, true cholinesterase and choline esterase I, is viewed as the principle catalyst in the cholinesterase family. AChE is found in many tissues, however most outstandingly in neuromuscular junctions (Guerra et al., 2005, p.57-61), brain cholinergic synapses (Adler et al., 2011, p. 909-920), autonomic ganglia (Vernino et al., 2008, p. 1926-1932). AChEs

best referred to for its capacity as a modulator of neurotransmission by hydrolysing acetylcholine (Figure 2.6). Acetylcholine is synthesized by choline acetyltransferase and packed into synaptic vesicles where it is stored until discharged into the synaptic cleft (Gauthier, 2002, p. 616-623). A continuous receptor stimulation by acetylcholine results in side effects, like as convulsion, vomiting, confusion and respiratory failure (Eddleston et al., 2008, p. 597-607). Then again, an absence of acetylcholine diminishes receptor incitement which can be seen for instance as the subjective weakness happening in AD (Garcia-Alloza et al., 2005, p. 442-449). Thus, keeping a balance of acetylcholine activity is essential. The structure of AChE has been broadly examined and right around 50 % of the structures distributed in the Protein Data Bank (PDB) (http://www.rcsb.org/pdb/home/home.do) to date have been readied utilizing the electric ray (Torpedo californica) enzyme, 36 % utilizing mouse enzyme and just 8 % utilizing the human AChE. The first crystal structure of AChE was determined in 1991 utilizing Torpedo californica (Harel et al., 1993, p. 9031-9035) while the first structure of human AChE developed in 2000 (Kryger et al., 2000, p. 1385-1394) (Figure 2.7).

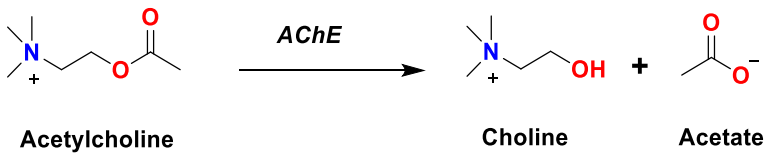

Figure 2.6. *Hydrolysis of Acetylcholine by Acetylcholinesterase*

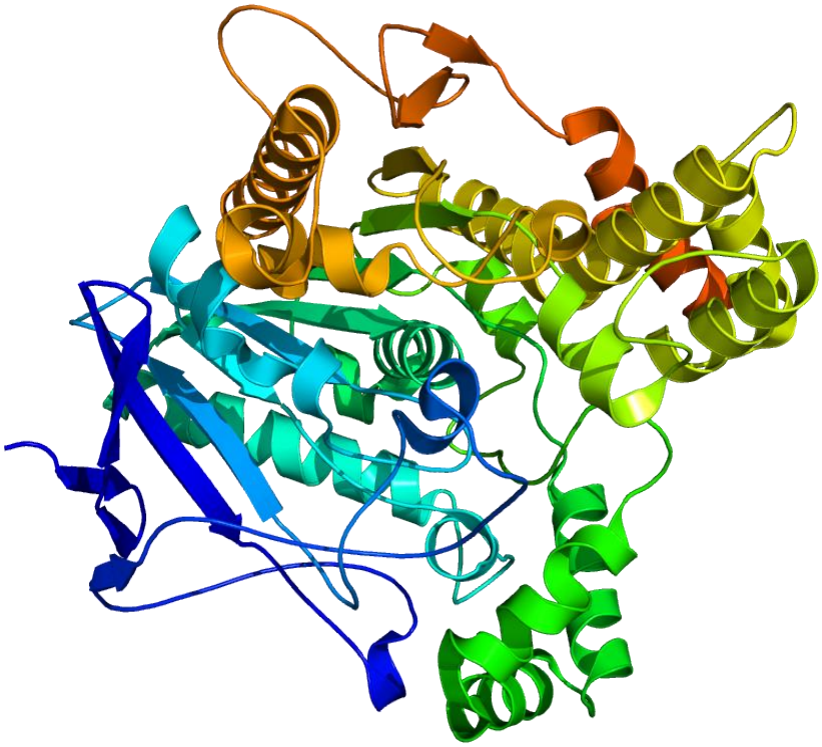

Figure 2.7. *Crystallographic Structure of Acetylcholinesterase (E.C. 3.1.1.7) From Torpedo Californica Based on PDB*

2.2.1.2. Butyrylcholinesterase (BChE)

BChE, also familiar as e.g. pseudocholinesterase, acylcholine acylhydrolase, non-specific cholinesterase and choline esterase II. Unlike AChE, BChE is more active in the peripheral tissue than in the brain (Liston et al., 2004, p. 9-17) and for the most part found in serum and glial cells, additionally, it is present in neurons (Darvesh et al., 1998, p. 374-390). As opposed to AChE, the crystal structures of BChE that are currently available in PDB utilize the human enzyme. The first crystal structure of a human BChE was explained in 2003 (Nicolet et al., 2003, p. 41141-41147) (Figure 2.8). BChE has been implicated in in different physiological procedures, the most conspicuous being the hydrolysis of a few choline and non-choline esters, for example acetylcholine (Mesulam et al., 2002,p. 627-639), succinylcholine (Kaufman et al., 2011,p.21) and cocaine (Xue et al., 2011,p. 290-297) in this way, having an essential influence in neurotransmission and anesthesia .In contrast to AChE, which is sensitive to organophosphates, BChE is not influenced by them and is in truth being examined for use as a detoxification agent for organophosphates (Mumford and Troyer, 2011,p. 29-34).

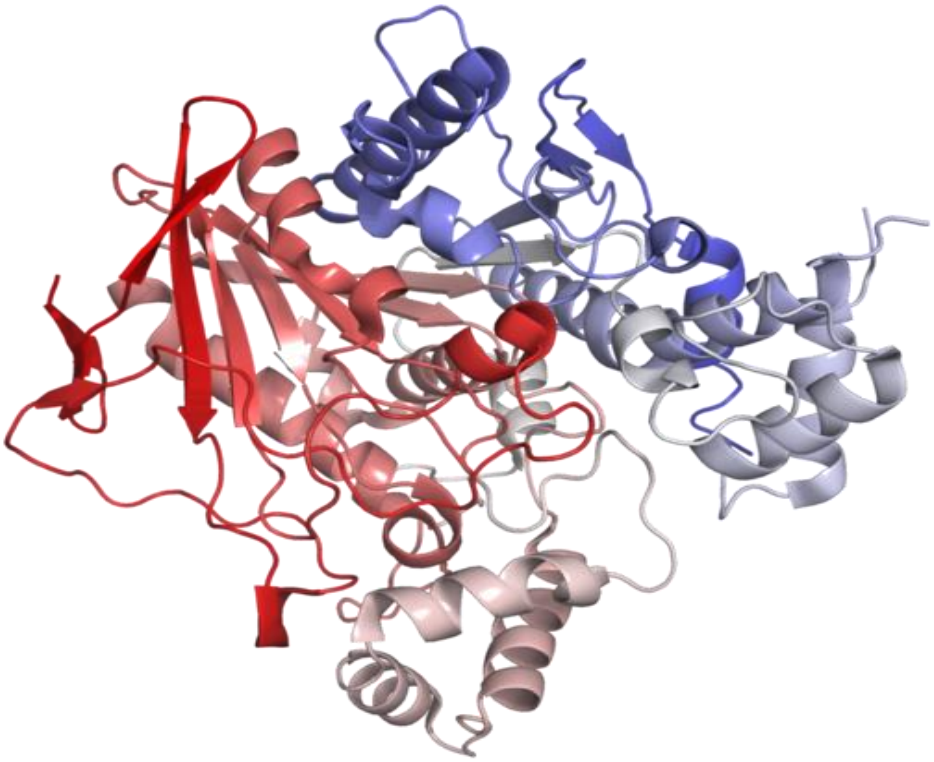

Figure 2.8. *The First Crystal Structure of Human BChE (PDB ID: 1POI (Nicolet et al., 2003) Drawn with PyMOL*

2.3. Therapeutic Approaches of AD

2.3.1. Pharmacological approach therapy of AD

Up to now, medications that have been affirmed by Food and Drug Administration (FDA) for the treatment of Alzheimer's ailment incorporate acetylcholinesterase inhibitors (AChEI) for gentle to direct cases, and memantine, a NMDA (N-methyl-D-aspatarte) receptor foe for the treatment of moderate to serious Alzheimer's sickness dementia. These medications appear to be equipped for delivering humble symptomatic change in a few patients (Clark and Karlawish, 2003; Cummings, 2004; Scarpini et al, 2003), however, none of the accessible medications have the capacity to treat or stop the progress of the disease. There is an extraordinary medicinal need to grow new healing procedures and drugs for the fundamental pathogenic components of Alzheimer's sickness and, consequently, to give helpful lead compounds to controlling and battling against AD (Mehta, Adem and Sabbagh, 2012, p.7).

The majority of the AD medicines have been centered around the hindrance of AChE to improve cholinergic neurotransmission by expanding ACh accessibility in the

synaptic cleft. A decline of ACh in the mind of AD patients gives off an impression of being a basic component in creating dementia (Rakonczay,2003, p.183-189). Today, an acetylcholinesterase inhibitor AChEI is regularly utilized after the AD diagnosis (Tayeb et al., 2012, p.8-25).

AChE has turned out to be the most suitable therapeutic target for symptomatic change in AD because of the cholinergic deficiency is a reliable and early finding in AD. Inhibition of AChE was thought to be achievable as a restorative target because of demonstrated adequacy of inhibition of AChE as a treatment for myasthenia gravis (MG) demonstrating that the methodology was possible. However, selective inhibition of the AChE initially proved to be daunting. Before tacrine, physostigmine, the exemplary AChE inhibitor (AChEI) was examined as a treatment for AD. Really, the AChEIs approved by the US FDA for the symptomatic treatment of patients with mild or moderate AD include: Donepezil (a benzyl piperidine), Rivastigmine (a carbamate) and Galantamine (a tertiary alkaloid). But, they don't stop the progression of the ailment or modify its ultimate results. Clinical experience has demonstrated that AChE hindrance is a feasible restorative way to deal with the palliative treatment of AD. A standout amongst the most widely recognized untoward effects of such treatment is gastrointestinal complaints following stimulation of peripheral autonomic cholinergic nerve system. Physostigmine was in this way surrendered as a result of poor tolerability. Four medications are as of now accessible for AD treatment: galantamine, rivastigmine, donepezil, and memantine. The initial three are AChE inhibitors and memantine is definitely not. A large portion of the medications that are accessible for treatment of AD target both AChE and BChE, in any case, some are more particular than others. These features combine between the current ChEIs (donepezil, rivastigmine, and galantamine) (a) they reduce cognitive, functional, and behavioral decline in AD, (b) their efficacies appear similar (c) their benefits are sustained with treatment persistence, (d) their benefits are generally dose-related (until limited by side-effects at very high doses), and (e) they appear to be relatively safe and well tolerated. AChE remains a very practical focus for the symptomatic change since the cholinergic shortage is a reliable and early finding in AD. In this way tacrine, donepezil, rivastigmine, furthermore, galantamine (Table.2.1.) were created and endorsed for the symptomatic treatment of AD. From that point forward, various cholinesterase inhibitors (ChEI) continue to be developed. These include newer ChEIs such as physostigmine derivatives (Phenserine and Tolserine), naturally derived

ChEIs like for examples huperzine A, huperzine B, hybrids, and synthetic analogues. Since AD is a multifactorial sickness, the creative model is of the "one molecule, various targets" approach. Hybrids combine BBB permeability with drugs targeting multiple receptors become an important strategy. The multipotent approach includes many ways like for example; novel tacrine-donepezil hybrids, dual inhibitors of AChE and MAO, serotonin transporters and potent cholinesterase inhibitors with antioxidant and neuroprotective properties (Samadi et al., 2010, p.5861-5872).

The unwanted effects profiles are obscure in humans at present. Concerning the synthetic analogs, they are under progression since, the targeted pharmacological improvement, hepatotoxicity and known gastrointestinal reactions might be avoided. The danger of creating synthetic analogs is that they won't have the potency what's more, their BBB permeability may not have achieved as ChEIs or they may have unexpected pharmacological properties. The first synthetic analog created was Tacrine or 9-amino-1,2,3,4-tetrahydroacridine; however, utilizing the medication caused dose dependent reversible liver lethality (Korabecny et al., 2010, p.6093-6095). Ladostigil is another synthetic analog for AD, with neuroprotective, multimodal brain specific monoamine oxidase, and cholinesterase inhibitor properties (Weinreb et al., 2011, p.191-215). This pharmacological way continues to be effective with many hopeful compounds. Other therapeutic approaches for AD – including those more almost focused to the pathogenesis of the disease–will likewise be inspected. These possibly disease modifying medications incorporate amyloid-β-peptide immunization, secretase inhibitors, cholesterol-lowering medications, metal chelators, and anti-inflammatory agents (Elio, Schelterns and Feldman, 2003, p. 539–547).

Table 2.1. *Current Alzheimer's Treatments*

Drug Name	Brand Name	Class	FDA Approved
Tacrine	Cognex®	ChEIs	1993
Donepezil	Aricept®	ChEIs	1996
Rivastigmine	Exelon®	ChEIs	2000
Galantamine	Razadyne®	ChEIs	2001
Memantine	Namenda®	NMDA antagonist	2003

2.3.2. Non-Pharmacological Approach Therapy of AD

For all intents and purposes at this point of time there is no cure for Alzheimer. But apart from therapeutic interventions, attempts should be possible to deal with the disease and treat the indications by the parental figures in a non-pharmacologic way. Alongside medications, physical exercise, social involvement as well as proper nutrition are crucial in treating the side effects of AD. The objective of non-pharmacologic treatment in AD however sounds straightforward yet clinically remains a test where the parental figure has an imperative part to play; first thing is to give a quiet organized environment where comfort, dignity of the afflicted person is kept up and the patient stays working to the extent that this would be possible (Zeisel and Raia,2000, p. 331-340; Weiner and Gray,1994, p.6-12). Treatment in a non-pharmacologic way intends to improve the quality of life to treat the disease symptoms. It is not a simple task for a care giver to increment practical freedom, reduce the requirement for psychoactive drugs, prolong life, decrease the requirement for restrictions, reduce usual hospital admissions, reduce depression and enhance spirit. While treating AD patients in non-pharmacologic way one of the significant foundation is how we comprehend the distressed individual and help him to understand and accept himself (Reisberg et al., 1996, p.2-4; Sclan et al., 1996, p.11-819). The issue with dementia is that individuals experiencing it are sometimes confused with sensory information and expected to process it in the same way a healthy person would. So, researches looking at whether if you modify the sensory demands placed on someone, their performance improves, even in simple tasks, for example, eating, or putting on socks and shoes. It likewise does a great deal of work with nursing homes and care homes in upskilling their staff, who are not qualified specialists or medical caretakers themselves, and additionally with the managers in taking a gander at where they can adjust zones of the home to make them calmer, for lower stimulation, and different regions for high stimulation (http-7).

Figure 2.9. *Especially Designed Room for (AD) Patients in Concerning with Sensory Approaches*
Reference: *(http-7)*

2.4. Docking Studies for Donepezil and Tacrine Analoques

Özkay et al., have been designed and synthesized 14 new benzothiazole–piperazine compounds as acetylcholine esterase (AChE) inhibitors. According to the docking results, the interactions of most active comounds and AChE enzyme enable to explain the proper binding with the active region of AChE in a like manner as donepezil, thus they able to bind with the gorge and with both CAS and PAS (Özkay et al.,2014, p.39-42).

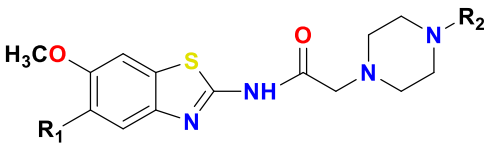

Figure 2.10. *New Benzothiazole–Piperazine Compounds as ChEs Inhibitors*

Soyer et al., have been synthesized a series of 4-phthalimidobenzenesulfonamide derivatives and were assessed for their inhibiton action against AChE and BChE. Molecular docking investigations of the most active compound in AChE demonstrated that this compound can associate with both the CAS and PAS of AChE. In the base of the gorge, the phthalimide moiety interface with Trp84 by means of the π–π connection and the oxygen atom of sulfonamide make a hydrogen bond with hydroxyl group of Tyr121 (Soyer et al., 2016, p.13-19).

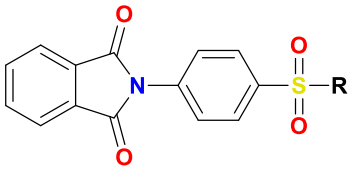

Figure 2.11. *New 4-phthalimidobenzenesulfonamide Derivatives as AChE Inhibitors*

A series of novel tacrine derivatives and tacrine−coumarin hybrid were designed, synthesized, and biologically assessed for their inhibitory effect on both AChE and BChE. Molecular modeling studies proven that these hybrids target both the CAS and PAS of AChE (Hamulakova et al.,2014, p.7073−7084).

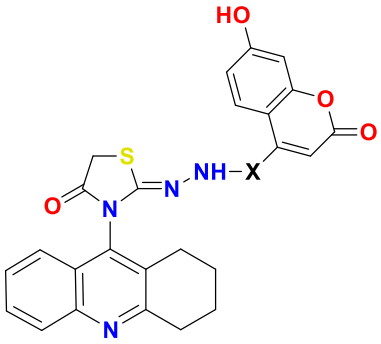

Figure 2.12. *Novel tacrine−coumarin hybrid as ChEs Inhibitors*

2.5. Acridines

Among the multidisciplinary nitrogen based heterocycles, acridines are an essential class of aza-heterocyclic compounds with momentous properties in many critical fields, which makes them a remunerating point for research. Contrasted with their significance, a moderately low number of surveys on acridines, and their derivatives have appeared (Galy, Morel, Boyer and Elguero, 1996, p.1551-1560). The high number of late original copies gives proof of the substantial utilization of this ring framework in the synthesis of many bioactive compounds (Denny, 2002, p.1655-65).

Acridine is well-known as Dibenzo[b,e]pyridine or 2,3,5,6-dibenzopyridine or 2,3benzoquinoline or by 10-azaanthracene. Acridine is an aromatic compound with hydrophobic behavior that's means it is insoluble in water (http-8). Furthermore, it is colorless to light yellow crystals having melting point 107-110°C. It has irritating odor,

lachrymator, carcinogenic and mutagenic effects (Ames, Sims, and Grover, 1972. p.47-49).

In 1856, William Henry Perkins an English scientist outline a procedure to synthesize quinine be that as it may, his work came about not in quinine, but instead in the principal engineered material color called "mauve or mauveine. This left the improvement of the manufactured color industry in Germany. In old time microbiologists utilized these novel colors to recolor and in this manner, improve the visibility of microorganisms under the magnifying instrument. Paul Ehrlich saw that methylene blue **(1)** was especially viable in recoloring malaria parasites. He excused that this color may likewise be specifically harmful to the parasite. In 1891, Ehrlich and Guttmann cured two malaria parasites patients with methylene blue, which became the original synthetic drug ever used in the treatment. In spite of the fact that it was not utilized further that time, methylene blue constituted the reason for the improvement of manufactured antimalarials. In the 1920s, physicists at Bayer in Germany began to alter the structure of methylene blue. A key change was the substitution of one methyl group by a dialkylaminoalkyl side chain and then the connection of the diethylaminoisopentylamino side chain with an acridine heterocycle gave mepacrine (quinacrine) **(2)**. When the US was cut off from its quinine supply thus of the Japanese occupation of Indonesia in 1942, significant endeavors were embraced in the US to reproduce the manufactured pathway to mepacrine from German patent writing. Mepacrine became the principle agent for the prophylaxis and treatment of malaria for the soldiers during the Pacific war (Meshnick, 2001, p.15-25).

Acridine was initially created as dyes as mentioned before and during the early 20^{th} century its pharmacological properties were assessed (Puneet et al., 2013, p.79-85). It assumes an imperative part in different drugs. Various helpful therapeutic agents depend on acridine core, for example, quinacrine (antimalarial), acriflavine and proflavine (disinfectants), ethacridine (abortifacient), amsacrine and nitracine (anticancer), and tacrine (anti-alzheimer) (Figure 2.10).

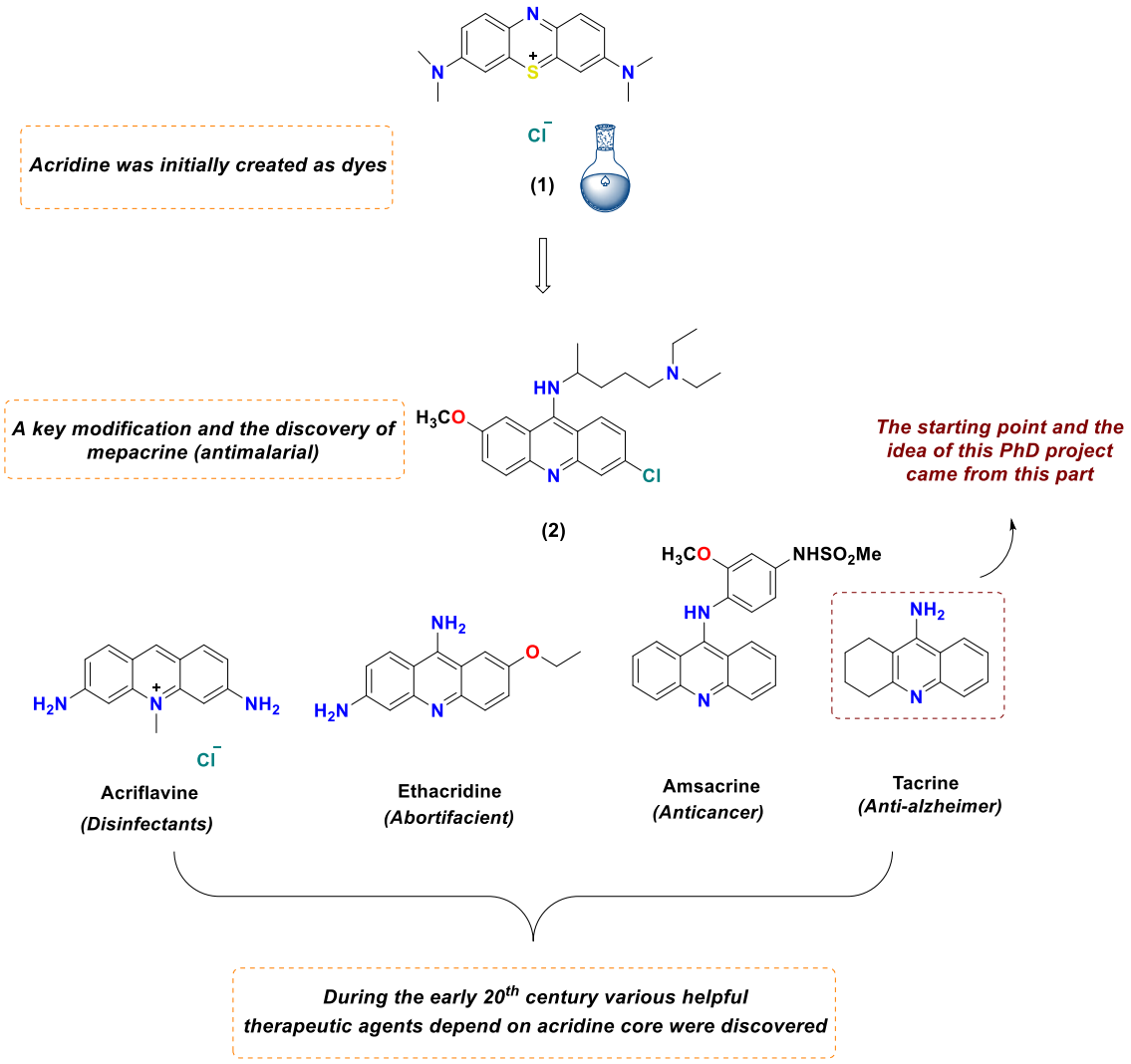

Figure 2.13. *Historical Development of Acridine Derivatives from Dye to Effective Medicines*

2.5.1. Chemistry

Acridine is acquired from high boiling part of coal tar (Ramesh kumar, Mandeep kaur and Meena Kumarı, 2012, p.3-9). It is isolated from coal tar by shaking out with dilute sulfuric acid, and then precipitating from sulfuric acid solution with potassium dichromate. The subsequent acridine dichromate is degredate in the last step by ammonia. Acridine and its homologues are stable compounds of weakly basic character. Acridine has a pKa estimation of 5.6, like that of pyridine (Ramesh kumar, Mandeep kaur and Meena kumarı, 2012, p.3-9).

2.5.2. Synthesis

A few techniques are accounted for the syntheses of acridines and its derivative acridinone, among them just those imperatives are discussed below:

2.5.2.1. Ullmann synthesis

The condensation of primary amine with aromatic aldehyde/aromatic carboxylic acid in the presence of strong mineral acids (H_2SO_4/HCl), followed by dehydrogenation, yield acridines (Jourdan, 1885, p. 1444-1456).

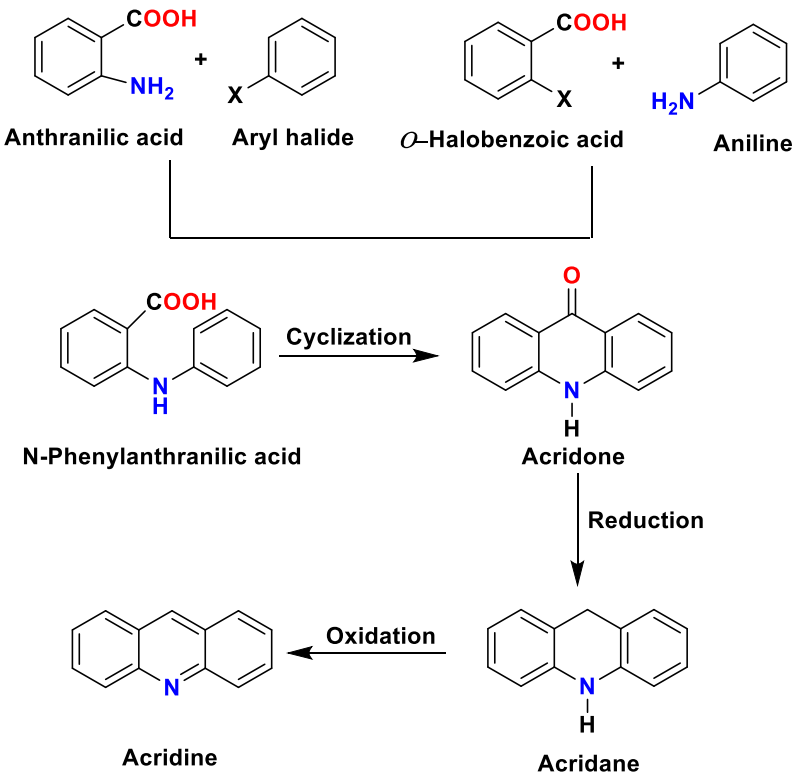

Figure 2.14. *Ullmann Synthesis*

2.5.2.2. Bernthsen synthesis

Bernthsen synthesis involves the reaction of diphenylamine with carboxylic acid in the presence of zinc chloride, resulting in the formation of acridine (Frank, 1962, p. 2658–2659).

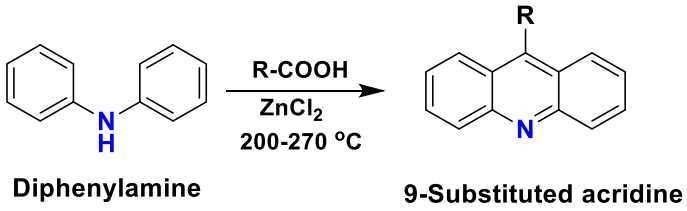

Figure 2.15. *Bernthsen Synthesis*

2.5.2.3. Friedlander synthesis

In this synthesis, the salt of anthranilic acid is treated with cyclohex-2-enone at120^{o}C to obtain 9-methylacridine (http-9).

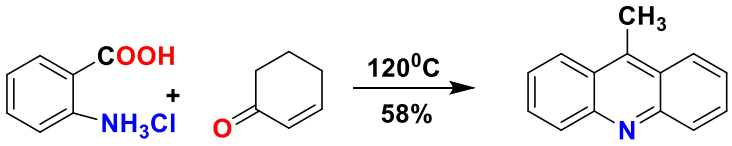

Figure 2.16. *Friedlander Synthesis*

2.5.2.4. From diphenylamines

The reaction of diphenylamine in the presence of $ZnCl_2$ give 9-phenylacridine as a result (Morrin Acheson, 1973, p.28-29).

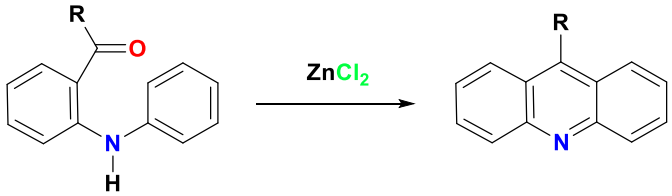

Figure 2.17. *Synthesis of Acridine from Diphenylamines*

2.5.3. Pharmacological uses

Various marketed preparations in view of the acridine core are accessible. These preparations represent different pharmacological activities. Bucricaine (butyl-(1,2,3,4-tetrahydroacridin-9-yl)amine) is utilized topically for surface anesthesia of eye what's more, given by infusion for infilteration anesthesia, peripheral nerve block and spinal anesthesia. Quinacrine (2-methoxy-6-chloro-9-(1-diethylamino-3-methylpropanamine)acridine) is additionally known as mepacrine. It goes about as

gametocytocide. It crushes the sexual erythrocytic types of plasmodia and acts as antimalarial agent. 9-Aminoacridine goes about as disinfectant. Proflavin (3,6-diaminoacridine) is found to be active as bacteriostatic against numerous Gram positive microscopic organisms. Nitracrine (1-nitro-9-(dimethylaminopropylamino)acridine) causes the DNA damage and for this reason it used as an anticancer agent (Gniazdowski and Szmigiero, 1995, p.473). Acriflavin (3,6-diamino-10-methylacridinium chloride) is utilized as germ-free for skin and mucous memberanes (http-10). The 9-arylacridine derivatives cooperate firmly with topoisomerase-I (Topo-1) and go about as anticancer agent (Takemura et al., 1995, p.366).

2.5.4. Literatures survey of *N*-(9-acridinyl)-2-chloroacetamide derivatives and their analogues as cholinesterase inhibitors

There are reported synthetic approaches for synthesis of *N*-(acridin-9-yl)-2-chloroacetamide derivatives but, until now not reported as AChEI , thus (Viktor et al., 1906.p. 1906-8) have been reported the synthesized of new Xylocaine analogs of the type $RNHCOCH_2NEt_2$ where R is acridine or its derivatives gave compounds with biological activity approximating that of Procaine but with considerably lower toxicity.

Wald et al. have been designed and synthesized a series of novel acridine-like class of compounds from which *N*-(9-acridinyl)-2-chloroacetamide derivatives also have been synthesized and have demonstrated efficiency in treating cancer but not as AChEI (Wald et al., 2015, patent).

Owing to the advanced chemotherapeutic activities of acridine, a lot of research activity has been directed toward this class in latest years but the major part of the known compounds either has antibacterial or cytotoxic activity. In addition, there are some derivatives which have been reported to have AChE inhibition activity but either in form of acridone or 1,2,3,4-tetrahydro form. Thus, Zhou et al., were synthesized a series of 5,6-dihydrobenzo[c]acridin-7-ol derivatives (Figure 3.8.) and evaluated for their AChE-inhibition and neuroprotective effects (Zhou et al., 2009, p.623-628).

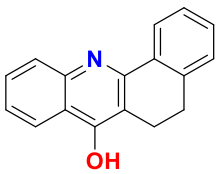

Figure 2.18. *5,6-Dihydrobenzo[c]acridin-7-ol Derivatives*

Mohammadi-Khanaposhtani et al. have been designed and synthesized a novel series of acridone linked to 1,2,3-triazole derivatives (Figure 3.9.) and evaluated in vitro for their AChE and BChE inhibitory activities (Mohammadi-Khanaposhtani et al., 2015, p.799-806).

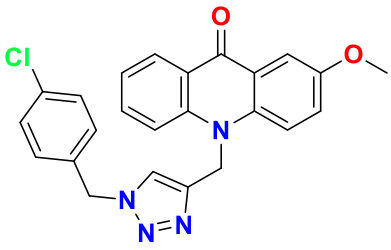

Figure 2.19. *Acridone Linked to 1,2,3-Triazole Derivatives*

Kálai et al., have been synthesized a new series of tacrine-nitroxide and nitroxide precursor hybrid. The new compounds were tested for their scavenging ability, AChE inhibitor activity and protective ability against Aβ-induced cytotoxicity. As a result, they found that tacrine analogs with five and six-membered nitroxides and piperazine spacers showed the best action (Kálai et al., 2014, p.343-350).

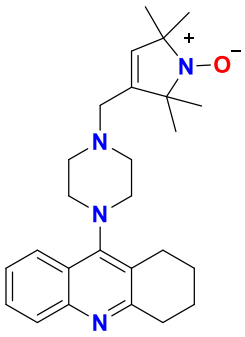

Figure 2.20. *A New Series of Tacrine-Nitroxide and Nitroxide Precursor Hybrid*

Camps et al., have been synthesized several new (tacrine-huperzine A hybrids) and tested as AChE inhibitors. Among the derivatives, the more active were those with chloro and fluoro substituents (Pelayo et al., 2000, p.4657-4666).

A new series of donepezil-tacrine hybrid related derivatives have been synthesized. These molecules have been tested for their inhibitory activity against ChE enzymes. One of the synthesised compounds arised as a strong and selective AChE inhibitor (Alonso et al., 2005, p.6588–6597).

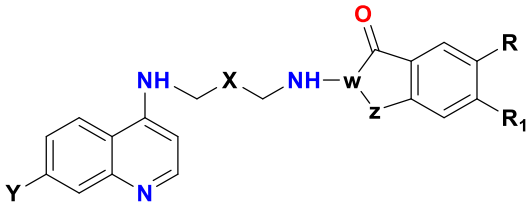

Figure 2.21. *A New Series of Donepezil–Tacrine Hybrid Related Derivatives*

2.6. Structurally Related Literatures to Donepezil

Donepezil is an important drugs of AChE inhibitors with longer and more specific activity with limited sides effects (Andreani et al., 2006, p.4011–4014). Recent studies have shown that the impact of AChE inhibitors is not really limited to cholinesterase restraint but rather that they may additionally improve the symptoms of AD through discharge of amyloid precursor protein (Pákáski and Kálmán, 2008, p.103-111).

Shen et al., reported the synthesis of 2-phenoxy-indan-1-one as donepezil like derivatives. In vitro AChE inhibition study performed and as a result, the donepezil IC_{50} value used as a reference. The most active derivative was found to be 2- (4- (3- (diethylamino) propanoyl) phenoxy) -5,6-dimethoxy-2,3-dihydro-1H-1-with IC_{50} about 0.00078 ± 0.00012 μM (Shen et al.,2008, p.7646-7653).

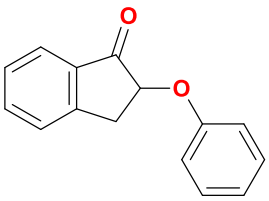

Figure 2.22. *A New Series of 2-phenoxy-indan-1-one as Donepezil Like Derivatives*

Ali et al., have been synthesized a new derivative of spiro-pyrrolothiazolyloxindoles and evaluate their inhibiton activity against AChE. As a result

of activity studies compound with pyridine ring, was the best inhibitor in their series with IC_{50} value was found to be 0.11 ± 0.1 μM (Ali et al., 2012, p.508-511).

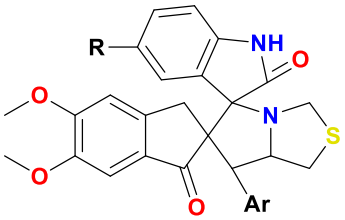

Figure 2.23. *A New Series of Spiro-pyrrolothiazolyloxindoles*

Meng et al., have been synthesized and investigated the anticholinesterase activities of their derivatives. In vitro AChE test compound 5-[2-(piperidin-1-yl)ethoxy]-2-(pyridin-4-yl-methylene)-2,3-dihydro-1*H*-inden-1-one has an IC_{50} value of 0.0018 ± 0.00007 μM. It was reported to be the most active inhibitor in the series. Made in the vitro BChE activity test, the IC_{50} value of the same compound was 9.5 ± 0.241 μM (Meng et al., 2012, p.4462-4466).

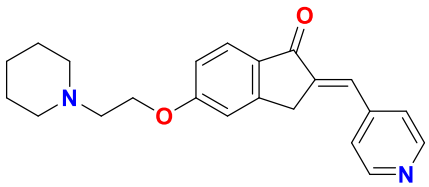

Figure 2.24. *A New Donepezil Like Series of 5-[2-(piperidin-1-yl)ethoxy]-2-(pyridin-4-yl-methylene)-2,3-dihydro-1H-inden-1-one*

In a study conducted in 2013, donepezil-hydrazinonicotinamide hybrid were synthesized and their biological effects were investigated. As a result of AChE inhibition studies the most active compound was *N*-[5-[[2-[(4-benzylpiperidin-1-yl)methyl]-1-oxo-2,3-dihydro-5-yl]oxy]phenyl]-4-hydrazinylbenzamide with an IC_{50} value of 2.659×10^{-3} μM (Zurek et al., 2013, p.137-144).

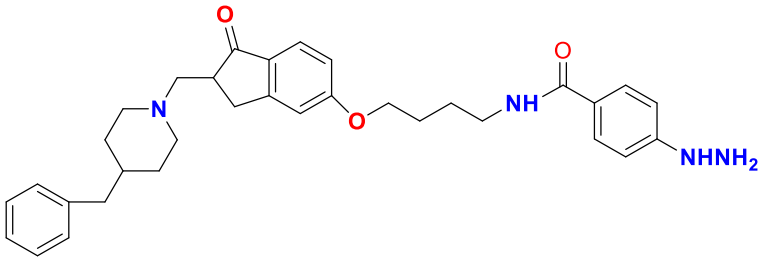

Figure 2.25. *A New Donepezil-hydrazinonicotinamide Hybrid*

2.7. Dithiocarbamates

2.7.1. Introduction

Organosulfur compounds are vital intermediates for the synthesis of different naturally active molecules (Brooks, 1989, p.62). DTCs are a group of organosulfur compounds that have broadly been utilized as pesticides as a part of agriculture for additional than 50 years with a few items being as of now presented in the 1930s (Tisdale and Williams, 1934, p.193). The first derivative of a DTCs to accomplish prominence as a fungicide was tetramethylthiuram disulfide. The yearly utilization of DTCs is between 25,000 and 35,000 metric tonnes (http-11). Most of the DTCs are connected as fungicides and a few of them are classified by the WHO as being hazardous (http-12)

In industry, DTCs are utilized as accelerators for rubber vulcanization, rubber antioxidants, slimicides in pulp and paper as well as in sugar production, in waste water treatment, and as antifoulant for water cooling systems (Wales and Helliker, 2002, p.1-3; Monser and Adhoum,2002, p.137-146). The first DTCs were prepared from a monoamine and carbon disulfide in 1934 (Gullino, et al., 2010, p.1076-1087). In 1940, W. F. Hester of Rohm and Haas, Inc. prepared a dithiocarbamate from a diamine. Hester's compound, disodium ethylene bisdithiocarbamate (nabam), can be viewed as the principal genuine ethylene bisdithiocarbamate. A patent was honored on the compound in 1943, and the distributed investigative report showed up in print in the same year (Dimond, Heuberger and Horsfall, 1943, p.1095–1097). Tetraethylthiuram disulfide, also called disulfiram (Figure 2.11), has been utilized as a part of the treatment of alcoholism for additional than 50 years (Szolar, 2007, p.191-200). These days, DTCs have drawn a considerable measure of importunate because of their nearness in different naturally active compounds (Dhooghe and Kime, 2006, p.513–535). Thus, compounds having sulfur functional

groups alongside another useful group are of great interest due to more than one pharmacophore inside one compound (Cen et al., 2004, p.6914-6920). The good nucleophilic character and the one of a special redox property of the sulfur atom in DTCs compounds make it a key buildup for chemical catalysis, protein collapsing, redox ability and the most needful property is a regulation, which is a vital for cell vitality digestion system, motility and subsistence of cellular systems (Westrop, Georg and Coombs, 2009, p.33485-33494). The above properties of DTC group make it a flexible pharmacophore and thus, it is utilized as a part of the compounds of organic interest. Amid the past decade, numbers of DTCs were combined and assessed for different natural activities (Wynne, Jensen and Snow, 2003, p.3733–3735).

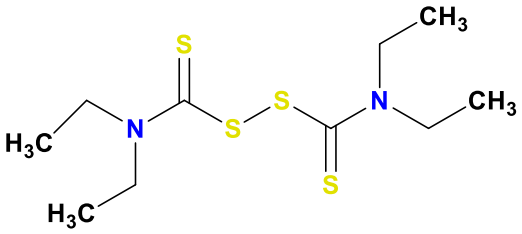

Figure 2.26. *Structure of Disulfiram*

Carbamates as pyridostigmine, rivastigmine, and physostigmine constitute a class of AChE inhibitors. Even so, carbamates have a relatively short duration of action and restricted penetration to BBB (Lieske et al., 1991, p.215-223).

DTCs have pulled in a lot of enthusiasm in medicinal chemistry because of the way that new viable derivatives can be picked up by the bioisosteric supplanting of carbamate moiety with dithiocarbamate moiety. They are additionally imperative pharmacophores as a result of their lipophilicity, which is essential for the delivery of CNS drugs to their site of action through the BBB (Madalageri and Kotresh, 2012, p.2697-2703; Silverman, 2004, p.11-12; Pliska et al., 1996, p.401-415).

2.7.2. Synthesis

DTCs are formed by the exothermic response between carbon disulphide and either ammonia or a primary or secondary amine in the presence of a base. The base might be a soluble base, for example, sodium hydroxide or abundance of the amine. Ammonium dithiocarbamate is created by the reaction of alkali and carbon disulphide. The free

dithiocarbamicf acid can be gotten by treatment of the ammonium dithiocarbamate with cold acid. Monoalkyldithiocarbamates are formed from the exothermic reaction between carbon disulphide and a monoalkylamine; they break down on long remaining in soluble base. No such trouble is experienced in the preparation of dialkyldithioearbamates (Miller and Latimer, 1962, p.246; Zuman and Zahradnik, 1957, p.135; Zahradni and Zuman, 1959, p.1132).

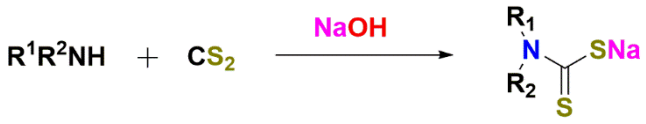

Figure 2.27. *General Way for Synthesis of dithiocarbamates*

2.7.3. Literatures survey of piperazine-dithiocarbamate derivatives as ChEs inhibitors

Yurttaş et al. published a series of novel thiazole-piperazine compounds to investigate their AChE and BChE inhibition activity. As a result of the in vitro enzymatic studies performed, when the IC_{50} value of donepezil is 0.054 μM, the 2-(4-benzylpiperazin-1-yl)-*N*-[4-(2-methylthiazol-4-yl)-phenyl]acetamide has an IC_{50} value of 0.011 μM, for this reason it has been reported this compound as the best from the other compounds in the same series (Yurttaş et al., 2013, p. 1040–1047).

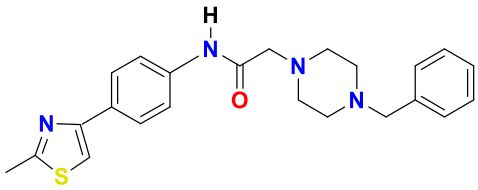

Figure 2.28. *2-(4-benzylpiperazin-1-yl)-N-[4-(2-methylthiazol-4-yl)-phenyl]acetamide Compound* as a *Potent AChE Inhibitor*

Gundogdu-Karaburun, was designed a series of novel new 2-[(5-substituted-4-methylthiazol-2-yl)amino]-2-oxoethyl 4-substitutedpiperazine-1-carbodithioate derivatives and evaluated for AChE inhibitory activity . The compound 2-[(4-methyl-5-phenylthiazol-2-yl)amino]-2-oxoethyl-4-[2-(dimethylamino)ethyl]piperazine-1-

carbodioate showed an inhibition of AChE by 86.40 ± 0.25% at 1 μM concentration as a result of an anticholinesterase activity study (Gundogdu-Karaburun, 2014, p.814-823).

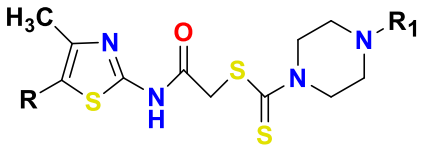

Figure 2.29. *Novel 2-[(5-substituted-4-methylthiazol-2-yl)amino]-2-oxoethyl 4-substitutedpiperazine-1-carbodithioate Derivatives* as *ChEs Inhibitors*

Altıntop et al. have been designed and synthesized a series of piperazine-dithiocarbamate derivatives which were evaluated for their anticholinesterase effects on AChE and BChE. The resulting enzymatic tests indicated that the compound with 4-(trifluoromethyl)benzyl-4-ethylpiperazine-1-carbodioate derivative was the most effective AChE inhibitor with an IC_{50} value of 0.53 ± 0.001 μM. The effect of the same compound on the BChE enzyme is indicated by an IC_{50} value of 3.64 ± 0.072 μM (Altıntop et al., 2013, p.571–576).

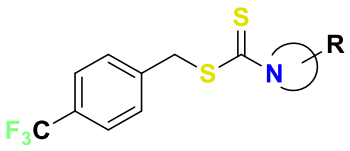

Figure 2.30. *Novel Piperazine-Dithiocarbamate Derivatives as ChEs Inhibitors*

Altintop et al. were reported novel dithiocarbamates with pyrazolines scaffold and evaluated for their AChE inhibitory activity. Among all compounds, compound 7 bearing 2-dimethylaminoethyl and 3,4-methylenedioxyphenyl moieties was also found to be the most active inhibitor of BChE. It was found that this compound has 0.72 ± 0.06 μg / mL inhibitor activity against AChE enzyme and 7.46 ± 0.83 μg / mL inhibitory activity on BChE enzyme (Altintop et al., 2013, p. 189-199).

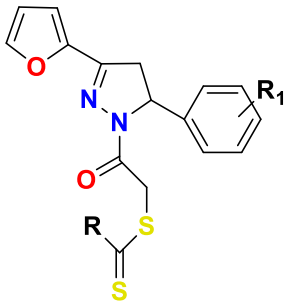

Figure 2.31. *Pyrazoline Derivatives Bearing a Dithiocarbamate Moiety as ChEs Inhibitors*

Abu Mohsen has been studied Some 2-[(1-methyl-1*H*-benzimidazol-2-yl)amino]-2-oxoethy-l-4-substitutedpiperazine-1-carbodithioate derivatives as anticholinesterase activity. None of the compounds showed notable anticholinesterase activity (Abu Mohsen, 2014, p.10-19).

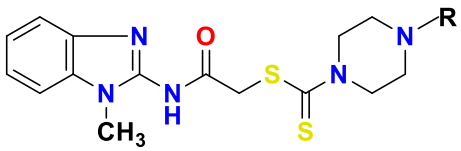

Figure 2.32. *2-[(1-Methyl-1H-benzimidazol-2-yl)amino]-2-oxoethyl 4-substitutedpiperazine-1-carbodithioate Derivatives as ChEs Inhibitors*

Mohsen et al. have been studied some new compounds of 2-[(6-substitutedbenzothiazol-2-yl)amino]-2-oxoethyl 4-substitutedpiperazine-1-carbodithioate derivatives and screened for their ability to inhibit AChE using a modificated Ellman's method. According to the result of the in vitro AChE enzymatic studies, it was found that the compound 2-[(6-nitrobenzothiazol-2-yl) amino]-2-oxoethyl 4-(2-[dimethylamino)ethyl]piperazine-1-carbodithioate is the most active one with IC_{50} value about 4.27 ± 0.76 μM (Mohsen et al., 2015, p. 176-183).

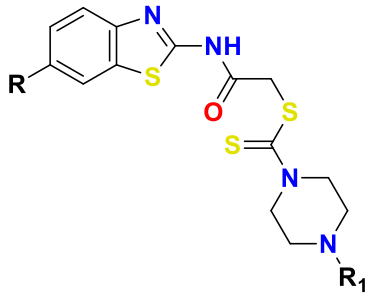

Figure 2.33. *2-[(6-Substituted benzothiazol-2-yl)amino]-2-oxoethyl 4-substituted piperazine-1-carbodithioate Derivatives as ChEs Inhibitors*

Abu Mohsen has been reported the synthesize of new 2-[(5-substituted-4-methylthiazole-2-yl)amino]-2-oxoethy-l-4substitutedpiperazine-1-carbodithionate derivatives and examine their antibacterial, antifungal effects as well as AChE inhibitory action. Despite there is no considerable inhibitory activity was observed for AChE inhibition activity of the newly tested compounds (Abu Mohsen, 2014, p. 222-228).

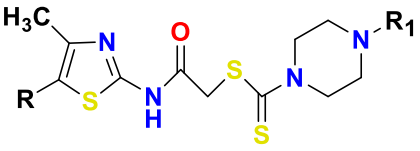

Figure 2.34. *2-(5-Substituted-4-methylthiazole-2-yl)amino]-2-oxoethyl-4substitutedpiperazine-1-carbodithionate Derivatives as ChEs Inhibitors*

Levent et al. have been synthesized new piperazine and piperidine dithiocarbamates and studied their inhibitory potencies against ChEs enzymes. 2-[4-(2-dimethylaminoethyl)piperazin-1-yl-dithiocarbamoyl]-3,4-dichloroacetophenone was found the most active compound against AChE with a IC_{50} value of 11.82 μM (Levent et al., 2016, p.1-6).

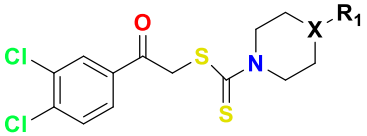

Figure 2.35. *New Piperazine and Piperidine Dithiocarbamates Derivatives as ChEs Inhibitors*

2.7.4. Literatures survey of piperidine/morpholine-dithiocarbamate derivatives as cholinesterase inhibitors

Sağlık et al. have investigated in vitro ChEs enzyme activity of *N*-[4-(Piperidin-1-yl)phenyl]-2-(piperidinyl/morpholinyl-thiocarbonylthio)acetamide derivatives. In general, the synthesized compounds showed low enzyme inhibition activity (Sağlık et al., 2014, p.1-9).

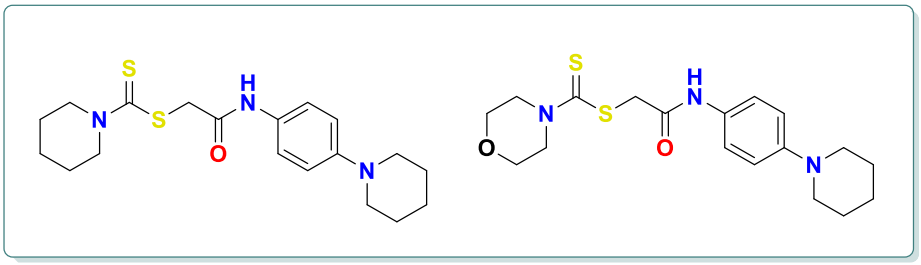

Figure 2.36. *N-[4-(Piperidin-1-yl)phenyl]-2-(piperidin-1-yl-thiocarbonylthio)acetamide Derivatives as ChEs Inhibitors*

Altıntop et al. have been designed and synthesized 4-(trifluoromethyl)benzyl piperidinyl/morpholinylcarbodithioate and 4-(trifluoromethyl)-benzyl 4-methylpiperidine-1-carbodithioate which were evaluated for their anticholinesterase effects on AChE and BChE. None of them was active (Altıntop et al., 2013, p.571–576).

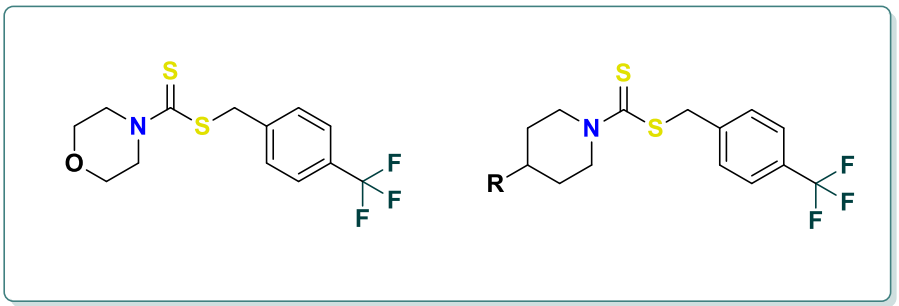

Figure 2.37. *4-(Trifluoromethyl)benzyl piperidine/morpholincarbodithioate Derivatives as ChEs Inhibitors*

Levent et al. have been synthesized new piperazine and piperidine dithiocarbamates and studied their inhibitory potencies against ChEs enzymes as mentioned previously (page 25) (Levent et al., 2016, p.1-6).

Considering the above depicted synthetic approaches, we have designed another analogue of *N*-substituted dithiocarbamoic acids that can be helpful by using a parallel method of synthesis.

3. EXPERIMENTAL PROCEDURES, ANALYTICAL DATA AND BIOLOGICAL EVALUATION

3.1. Experimental Part

3.1.1. General Information

All chemicals were purchased from Sigma-Aldrich Chemicals (Sigma-Aldrich Corp., St. Louis, MO, USA) or Merck Chemicals (Merck KGaA, Darmstadt, Germany). Melting points of the synthesized compounds were assessed by a MP90 digital melting point apparatus (Mettler Toledo, Ohio, USA) and were uncorrected. ^{1}H-NMR and ^{13}C-NMR spectrum were recorded on the Bruker Fourier 300 (Bruker Bioscience, Billerica, MA, USA) in DMSO-d_6. The IR spectra were obtained on a Shimadzu, IR Affinity 1S (Shimadzu, Kyoto, Japan). Mass spectra of the compounds were taken in negative and positive mode using electron spray ionization (ESI) ionization technique in LCMS-IT-TOF (Shimadzu, Kyoto, Japan) from the solutions of the samples in methanol. The purities of compounds were checked by TLC on silica gel 60 F254 (Merck KGaA, Darmstadt, Germany).

3.1.2. General Synthetic Procedure A

Synthesis of N-(9-acridinyl)-2-chloroacetamide derivatives (2)

Chloroacetyl chloride (30 mmol, 2.4 mL) in THF (10 mL) was added dropwise with stirring to a mixture of 9-aminoacridine (**1**) (20 mmol 3.9 g) and triethylamine (40 mmol 5.6 mL in THF (50 mL) at 0-5 °C and stirred for 4 hours. The solvent was evaporated under reduced pressure. The residue was washed with water to remove triethylamine hydrochloride and crystallized from ethanol (Wang et al., 2005, p. 4667-4678).

3.1.3. General Synthetic Procedure B

Synthesis of sodium N-substituted piperazine/morpholine/piperidine dithiocarbamates (3a-3u)

Ethanolic solution (10 mL) of sodium hydroxide (10 mmol, 0.4g) was added to an ethanolic solution (10 mL) of the secondary amine (10 mmol). The mixture was cooled in an ice bath additionally, carbon disulfide (100 mmol, 6.0 mL) was added dropwise with continuous stirring for 1 h at room temperature. The percipitates were filtrated and washed with diethyl-ether to get a white to pale-yellow colored product in 70- 90 % yield (Karali, 1999, p.422-426).

3.1.4. General Synthetic Procedure C

Synthesis of 2-(9-acridinylamino)-2-oxoethyl 4-piperazinyl/morpholinyl/piperidinylcarbodithioate derivatives (4a-4u):

Equimolar quantity (5 mmol) of appropriate sodium *N*,*N*-disubstituted dithiocarbamate (**3**) and of *N*-(9-acridinyl)-2-chloroacetamide (**2**) in acetone (10 mL) were refluxed for 8 hours. The mixture was cooled and percipitate filtrated. The residue was washed with water and crystallized from ethanol to obtain the final product as was accomplished according to **Scheme 3.1.** Some properties of the compounds are given in **Table 3.1.**

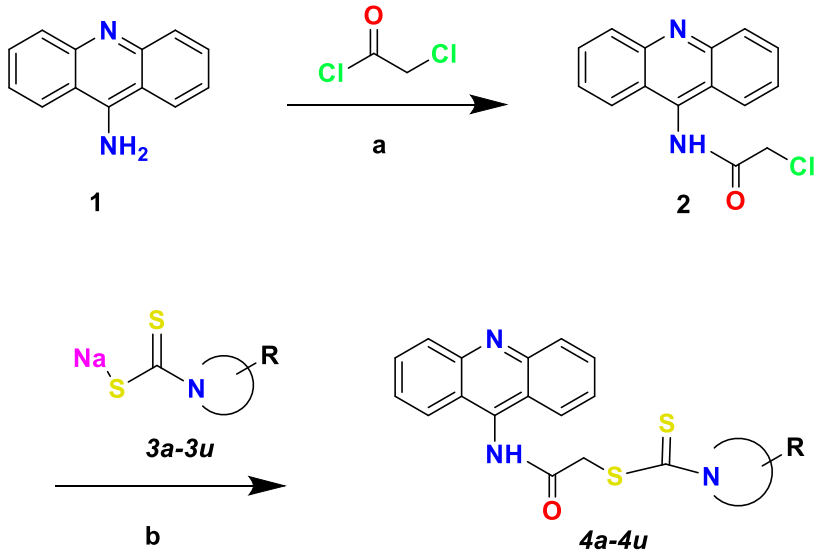

Scheme 3.1. *Synthesis of the Compounds (**4a-4u**). **a**: $(C_2H_5)_3N$ / THF / 0°C Then rt, **b**: Acetone / Reflux.*

Table 3.1. *Some properties of the compounds (**4a-4u**)*

Comp.	Het.	R	Yield (%)	m.p. (°C)	Molecular formula	Molecular weight
4a	Piperazinyl	4-(2-(dimethylamino)ethyl	88.5	200.6	$C_{24}H_{29}N_5OS_2$	467.65
4b	Piperazinyl	4-(3-(dimethylamino)propyl	85.7	153.8	$C_{25}H_{31}N_5OS_2$	481.68
4c	Piperazinyl	4-ethyl	81.0	221.7	$C_{22}H_{24}N_4OS_2$	424.58
4d	Piperazinyl	4-(4-nitrophenyl)	90.5	248.2	$C_{26}H_{23}N_5O_3S_2$	517.62
4e	Piperazinyl	4-(2-hydroxyethyl)	84.4	219.2	$C_{22}H_{24}N_4O_2S_2$	440.58
4f	Piperazinyl	4-phenyl	94.5	oil	$C_{26}H_{24}N_4OS_2$	472.63
4g	Piperazinyl	4-methyl	95.3	243.2	$C_{21}H_{22}N_4OS_2$	410.55
4h	Piperazinyl	4-(4-methoxyphenyl)	89.4	243.8	$C_{27}H_{26}N_4O_2S_2$	502.65
4i	Piperazinyl	4-(4-chlorophenyl)	97.0	213.6	$C_{26}H_{23}ClN_4OS_2$	506.07
4j	Piperazinyl	4-(pyrimidin-2-yl)	84.3	248.4	$C_{24}H_{22}N_6OS_2$	474.60
4k	Piperazinyl	4-benzyl	91.4	222.3	$C_{27}H_{26}N_4OS_2$	486.65
4l	Piperazinyl	4-cyclohexyl	88.4	225.4	$C_{26}H_{30}N_4OS_2$	478.67
4m	Piperazinyl	4-benzhydryl	84.3	137.0	$C_{33}H_{30}N_4OS_2$	562.75
4n	Piperazinyl	4-[4-(trifluoromethyl)benzyl]	87.7	161.5	$C_{28}H_{25}F_3N_4OS_2$	554.65
4o	Piperazinyl	4-(4-methylbenzyl)	91.0	205.8	$C_{28}H_{28}N_4OS_2$	500.68
4p	Piperazinyl	4-(4-fluorophenyl)	96.4	227.7	$C_{26}H_{23}FN_4OS_2$	490.62
4q	Piperazinyl	4-(2-furoyl)	95.5	218.9	$C_{25}H_{22}N_4O_3S_2$	490.60
4r	Morpholinyl	H	89 .2	237.8	$C_{20}H_{19}N_3O_2S_2$	397.51
4s	Piperidinyl	H	84.4	265.4	$C_{21}H_{21}N_3OS_2$	395.54
4t	Piperidinyl	2-methyl	93.3	114.3	$C_{22}H_{23}N_3OS_2$	409.57
4u	Piperidinyl	4-benzyl	90.7	230.4	$C_{28}H_{27}N_3OS_2$	485.66

3.1.5. TLC Studies

All the synthesis steps were utilized by TLC applications to control the reactions. In the TLC studies, aluminum plaques coated with silicagel 60 F_{254} as adsorbent and saturated with previously suitable solvent mixtures were used. The ethanolic solutions of the starting materials used in the synthesis and the samples taken for a certain period from the reaction medium were applied to the plaques using capillary tubes and dragged within the moving phases. The ultraviolet light (254 nm and 366 nm).

According to the TLC applications, it is decided to finish or continue the reactions. In each of the synthesis steps within the thesis, the appropriate mobile phases used in the TLC applications were determined by making a selection of different solvent mixtures. It was determined that the appropriate mobile phase for the control of the compounds synthesized in methods A, B and C was petroleum ether: ethyl acetate (2 : 1).

3.1.6. Detection of Melting Points

The Mettler Toledo MP90 Melting Point System (melting point determination device) was used to determine the melting points (m.p) of the compounds. Synthetic materials were placed in the reservoirs of the device by putting a one-half open capillary pipes up to 0.5 cm. When the process is complete, the melting points of the compounds are recorded following the videos taken from the device.

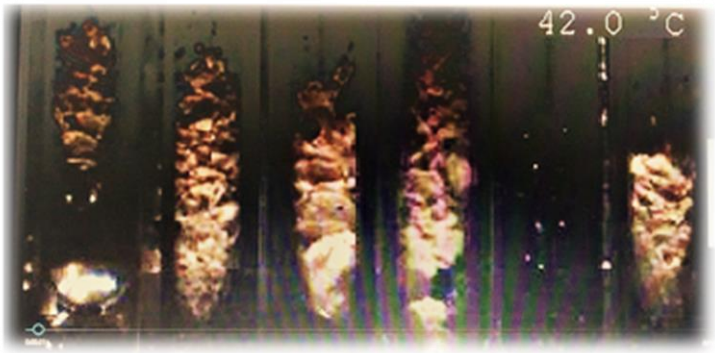

Figure 3.1. *Detection of Melting Points by Using the Mettler Toledo MP90*

3.1.7. Determination of anticholinesterase activity

AChE and BChE enzyme inhibitor activities of the compounds synthesized in the thesis were investigated by Ellman method (Ellman et al., 1961, p.88-95). Milipor, distilled water obtained from Milli-Q Synthesis A10 purification device was used at every step of the method. Care has been taken to ensure that all solutions used are freshly

prepared and consumed within 1 week after preparation. BioTek-Precision Power robotic pipetting system was utilized in the partitioning of the solutions prepared in the enzyme inhibition study, the application of the test compounds to the 96-well plates, and the addition of the enzyme substrate solutions. The creation, monitoring and retrieval of the spectrophotometric measurements of the enzyme protocol were performed on the BioTek-Synergy H1 Microplate Reader.

3.1.7.1. Preparation of AChE and BChE enzyme solution

Electric eel AChE was used, while acetylthiocholine iodide (AChI) was employed as the substrate of the reaction (Goran et al., 2007, p. 223-227). To dissolve the lyophilized AChE / BChE enzyme, 1% gelatin solution is prepared, then 500 U / mL concentration of AChE / BChE enzyme gelatin solution was prepared. 1 mL of the enzyme solution was diluted to 100 mL of water, by this way a 5 U / mL of enzyme stock solution was obtained. From the stock solution prepared before 0.7 mL was stored at -20 °C. Then, just prior to use, allow to a 0.7 mL of stock solution to warm at room temperature and again diluted with water to 1.4 mL to yield a solution of 2.5 units/mL.

3.1.7.2. Preparation of (0.075 M) acetylthiocholine iodide (ATC)

0.217 g of ATC was dissolved in small quantity of water and dilute to 10 mL. The prepared solution was stored at -20 °C in 0.4 mL portions until use.

3.1.7.3. Preparation of (0.075 M) butyrylthiocholine iodide (BTC)

0.237 g of BTC was dissolved in small quantity of water and dilute to 10 mL. The prepared solution was stored at -20 °C in 0.4 mL portions until use.

3.1.7.4. Preparation of (0.01 M) dithiobisnitrobenzoic acid (DTNB)

0.396 g of DTNB was dissolved in water, 0.15 g of sodium bicarbonate was added and diluted to 100 mL with water. The prepared solution was stored at -20 °C in 3 mL portions until use.

3.1.7.5. Preparation of phosphate buffer (pH = 8.0)

13.61 g of Potassium dihydrogen phosphate was dissolved in 1 L of water. The pH of the prepared solution was adjusted to 8.0 ± 0.1 in a controlled manner using a pH meter with 0.1 N potassium hydroxide solution. The adjusted buffer solution was made ready for use by filtration through disposable filters with a porosity of 0.22 μm. The prepared solution was stored at 4 °C until use.

3.1.7.6. Preparation of synthesized compounds solutions (Inhibitor Solutions)

The synthesized compounds in the anticholinesterase activity studies were prepared at a concentration of 10^{-3}-10^{-9} M in aqua solution of dimethylsulfoxide (DMSO) 2 %. The compounds were first prepared at 10^{-3} M concentration and then switched to other concentrations with 1/10 serial dilutions.

3.1.7.7. AChE and BChE inhibition study

Inhibition potency of the compounds against AChE and BChE have been determined using Ellman's method (Ellman et al., 1961, p.88-95). Enzyme solutions were prepared in gelatin solution (1%), at aconcentration of 2.5 units/mL. Synthesized compounds and donepezil were prepared at 10^{-3} M and 10^{-4} M concentrations using in aqua solution of DMSO 2%. AChE or BChE solution (20 µL/well) and compound solution (20 µL/well) were added to phosphate buffer (140 µL/well, pH 8± 0.1) and incubated at 25°C for 5 min. The reaction was started by adding the chromogenic reagent 5,5-dithio-bis(2-nitrobenzoic acid) (DTNB) (20 µL/well, 10 mM) and the substrates acetylthiocholine iodine (ATCI) or butrylthiocholine iodine (BTCI) (10 µL/well, 75 mM) to the enzyme-inhibitor mixture. The production of the yellow anion was recorded for 10 min at 412 nm. As a control, an identical solution of the enzyme without the inhibitor was processed. Control and inhibitor readings were corrected with blank-reading. All processes were assayed in four independent wells. The same procedure was followed for further concentrations (10^{-5}-10^{-9} M, 20 µL/well) of donepezil and selected compounds indicating ≥ 50% inhibition at initial concentrations (10^{-3} and 10^{-4} M, 20 µL/well). The concentrations of the samples that inhibit the breakdown of the substrate (acetylcholine) by 50% (IC_{50}) were determined by linear regression analysis between the inhibition percentage versus the samples concentration by using the Excel program (Dhanasekaran et al., 2015, p. 012-016., Özkay et al.,2014, p.39-42) (Figure 3.2). Absorbance differences between the two readings were taken and % inhibition rates were calculated according to the following formula:

$$\% \text{ inhibition} = \frac{[(A(C)-A(B))-(A(I)-A(B))]}{(A(C)-A(B))} \times 100 \quad (1)$$

Blank (B) **:** The well in which the inhibitor compound and substrate is not added.
Control (C) **:** The well where the inhibitor compound is not added.
A(B) **:** Difference in absorbance reading for blank.
A(C) **:** Difference in absorbance reading for control.
A(I) **:** Difference in absorbance reading for inhibitor compounds.

The IC_{50} value was calculated from the plots of enzyme activity against concentrations by applying regression analyses on GraphPad Prism Version 6.

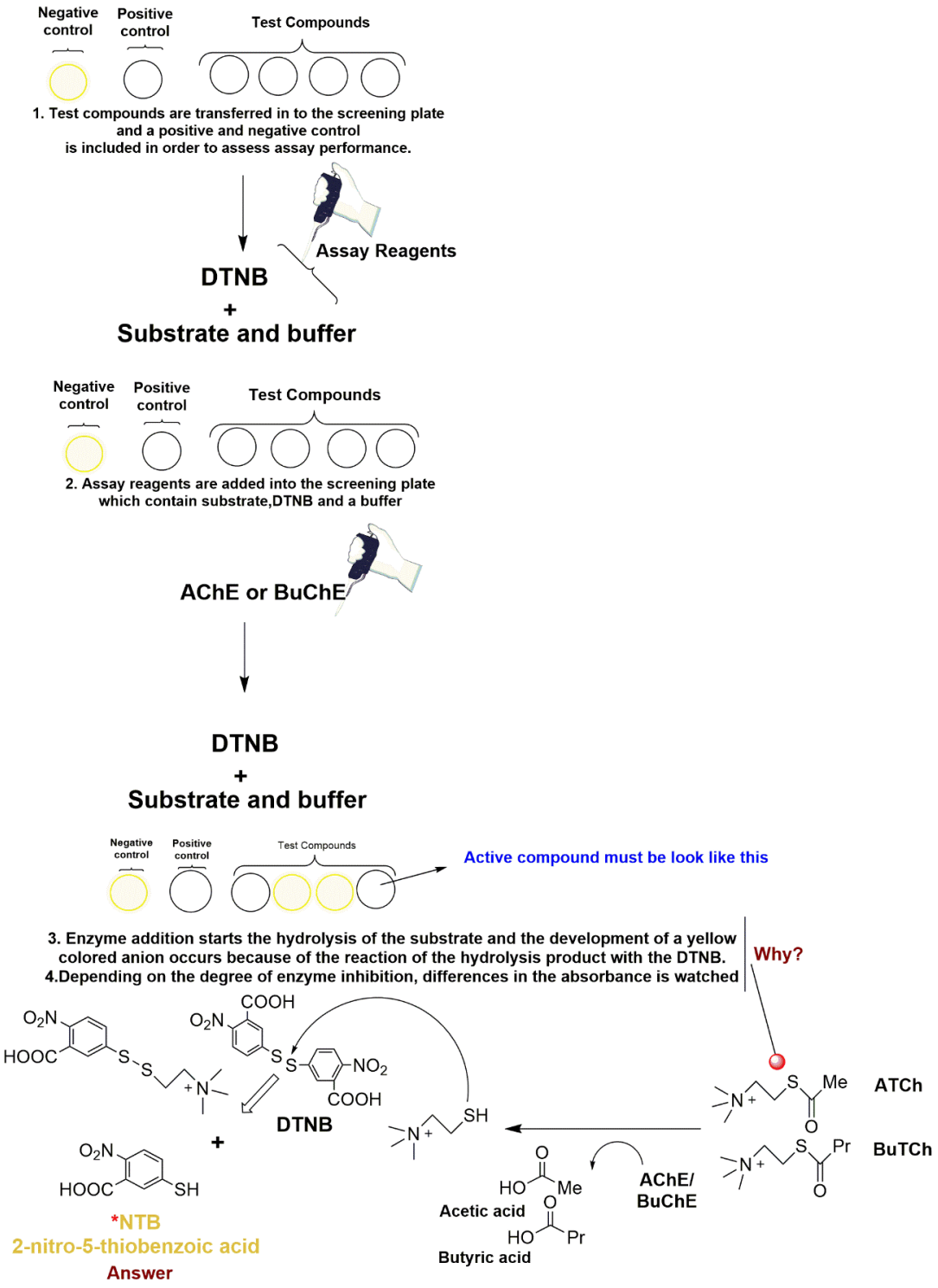

A yellow chromophore detected at wavelengths of 405-412 nm as its concentration increases, the ability of the derivative to inhibit the ChEs decreases

Figure.3.2. *Explanation of Ellman Assay*

3.1.7.8. Enzyme kinetics

In kinetic studies, the assay protocol specified in the inhibition study is identical. However, unlike the inhibition method, the concentrations of the most active inhibitor compound **4n** at the calculated IC_{50} values were used. Substrate (BTCI) solution with 10 serial dilutions at different concentrations in the range of 150-0.2929 mM were prepared as well and used. Measurements were performed in two different ways, in the presence of and without inhibitor. First, compound **4n** at the calculated IC_{50} values were used and then added to the wells (20 µL/well). BChE was added to the plate (20 µL/well) and enzyme inhibitor mixture was incubated at 25°C for 5 min. The reaction was started by adding DTNB (20 µL/well) and the various concentrations of BTCI as mentioned before (10 µL/well). The production of the yellow anion was recorded for 10 min at 412 nm. A parallel control without inhibitor was used for comparison. All processes were assayed in four independent wells. The results were analyzed as Lineweaver-Burk plots using Microsoft Office Excel 2013 (Demir Özkay et al., 2016, p.5387-5394).

3.1.8. Molecular Docking

A structure based in silico procedure was applied to discover the binding modes of most active compound **4n** to BChE enzyme active sites. The crystal structures of Homo sapiens BChE (PDB ID: 4BDS) (Nachon et al., 2013, p.393-399) which was crystallized with the reference drug (tacrine) of enzyme activity assay, was retrieved from the Protein Data Bank server (www.pdb.org). The structure of ligand was assembled utilizing the Schrödinger Maestro (Schrödinger, 2016) interface and then was submitted to the Protein Preparation Wizard protocol of the Schrödinger Suite 2016 Update 2 (Schrödinger, 2016). The ligand was prepared by the LigPrep 3.8 (Schrödinger, 2016) to assign the protonation states at pH 8.0±1.0 and the atom types, accurately. Bond orders were assigned and hydrogen atoms were added to the structures. The grid generation was formed using Glide 7.1 (Schrödinger, 2016) program and docking runs were performed with single precision docking mode (SP).

3.1.9. 3D Structure of the Active Compounds

The 3D structure of the active compounds was visualized by using the Molinspiration Galaxy 3D Structure Generator (http-13).

3.1.10. Cell Viability Assay and Selectivity Indexes

Healthy mouse embryonic fibroblast (NIH3T3 cell line) was used for cytotoxicity tests. NIH3T3 cells were incubated in Dulbecco's modified Eagle's medium (DMEM) supplemented with fetal calf serum (Hyclone, Thermo Scientific, USA), 100 IU/mL penicillin (Hyclone, Thermo Scientific, USA) and 100 mg/mL streptomycin (Hyclone, Thermo Scientific, USA) and 7.5% $NaHCO_3$ at 37 °C in a humidified atmosphere of 95% air and 5% CO_2. NIH3T3 cells were seeded at 1 x 10^4 cells into each well of 96-well plates. After 24 hours of incubating period, the culture mediums were removed and compounds were added to culture medium at 0.000316 μM - 1 mM concentrations. After 24 hours of incubation, cytotoxicity test was performed using the MTT assay (Figure 3.3), which measures mitochondrial activity in a NIH3T3 cell culture.

This assay is based on the reduction of yellow MTT dye by metabolically active eukaryotic cells to form the purple formazan product. The assay is generally used to examine cell viability and to estimate cell culture growth (Berridge, Herst and Tan, 2005, p.127-152). First, the cells were washed phosphate buffer saline (PBS). MTT and fresh culture medium solution were mixed at 1:9 ratio. Then, 100 μL of this mixture was added to all wells. The plate was incubated for 3 hours at 37 ºC, 5% CO_2. After 3 hours, the contents of the wells were removed and DMSO was added 100 μL / well. The optic densities (OD) of plates were read at 540 nm. Inhibition % was calculated for each concentration according to the formula below and IC_{50} values were determined by plotting a dose response curve of inhibition % versus compound concentrations tested (Demir Özkay et al., 2016, p.5387-5394). We additionally investigated selectivity indexes (SI) for active derivatives since, a compound selectivity is an important issue when developing a new drug. In many instances, an absence of selectivity can translate to increased toxicity. SI is calculated as a ratio of cellular toxicity and IC_{50} values (in μM) for enzymes.

$$\% \text{ inhibition} = 100 - \frac{(OD\ of\ sample\ )}{(OD\ of\ solvent\ )} \times 100 \qquad (2)$$

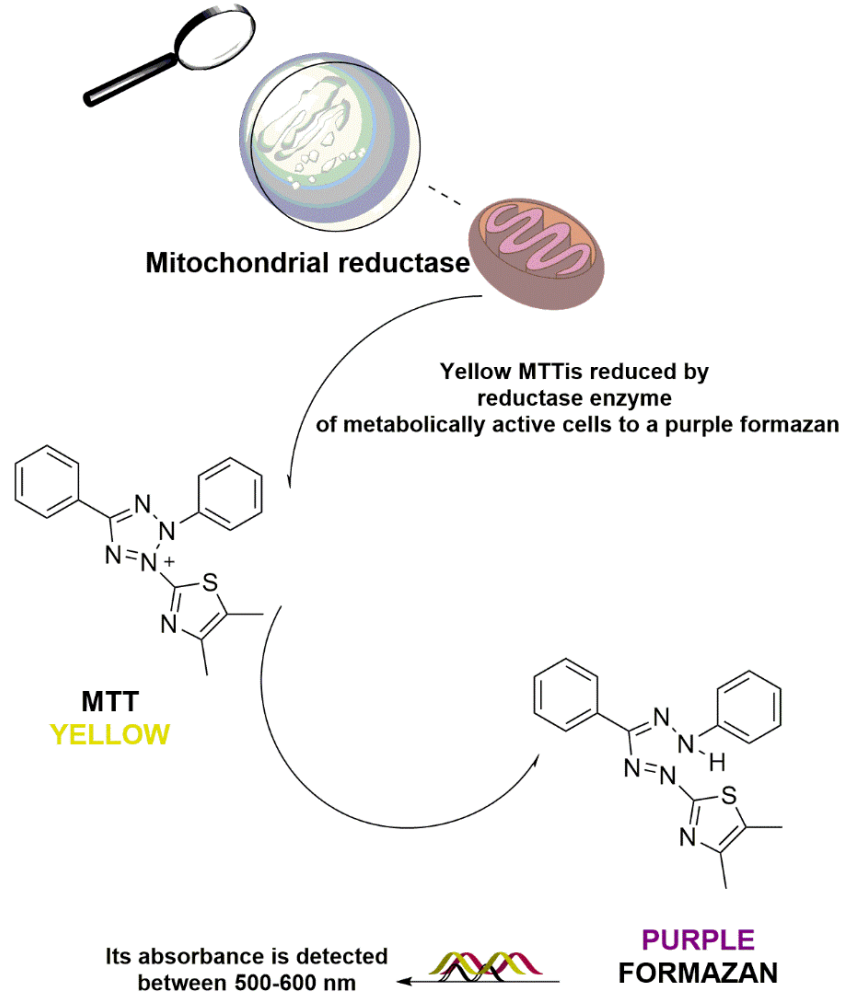

Figure 3.3. *MTT Cell Viability Assay*

3.1.11. BBB Permeability and Drug-Likeness Score (DLS)

With a specific end goal to assess some important biological parameters for the active compounds (**4a, 4b, 4e, 4i, 4m, 4n, 4o and 4t**), BBB and DLS were predicted by using an online BBB Predictor and the Molsoft's chemical fingerprints mode, respectively (http-14; http-15).

3.1.12. Statistical Analysis

All data generated from the experiments were calculated as mean ±SD. The IC_{50} values were calculated from the plots of enzyme activity against concentrations by applying regression analyses on GraphPad Prism Version 6. In addition, the IC_{50} values and the cytotoxic properties (in MTT cell viability assay) of the active substances were determined by non-linear regression analysis. Concerning the enzyme kinetics, the results were analyzed as Lineweaver-Burk plots using Microsoft Office Excel 2013.

4. RESULTS AND DISCUSSION

4.1. Synthesis of the Compounds

4.1.1. Synthesis of *N*-(9-acridinyl)-2-chloroacetamide (2)

Synthesized according to method A. Experimental m.p. 111.9 ºC. Yield: 89.2% (Wang et al., 2005, p. 4667-4678).

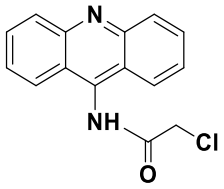

4.1.2. Synthesis of sodium piperazine/morpholine/piperidine dithiocarbamates (3)

The following derivatives were synthesized according to the method B:

Sodium 4-(2-(dimethylamino)ethyl)piperazine-1-carbodithioate (3a)

Experimental m.p. 214.3 ºC. Yield: 88.3% (Karaburun et al., 2011, p.811-815).

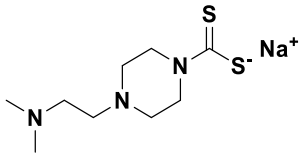

Sodium 4-(3-(dimethylamino)propyl)piperazine-1-carbodithioate (3b)

Experimental m.p. 199.9 ºC. Yield: 89.1% (Gundogdu-Karaburun, 2014, p. 814-823).

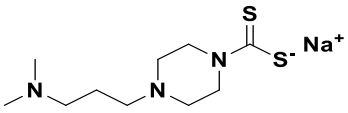

Sodium 4-ethylpiperazine-1-carbodithioate (3c)

Experimental m.p. 231.7 ºC. Yield: 93.9%.

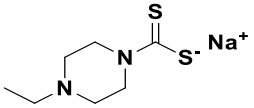

Sodium 4-(4-nitrophenyl)piperazine-1-carbodithioate (3d)

Experimental m.p. 176.3 ^{o}C. Yield: 90.5% (Parveena et al., 2015, p.32-39).

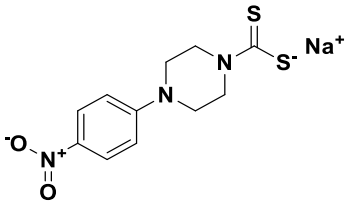

Sodium 4-(2-hydroxyethyl)piperazine-1-carbodithioate (3e)

Experimental m.p. 156.7 ^{o}C. Yield: 94.5% (Garcia-Fontan and Rodriguez-Seoane.,1993, p. 211-215).

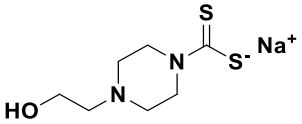

Sodium 4-phenylpiperazine-1-carbodithioate (3f)

Experimental m.p. 166.9 ^{o}C. Yield: 98.9% (Turan-Zitouni et al., 2011, p. 830-837).

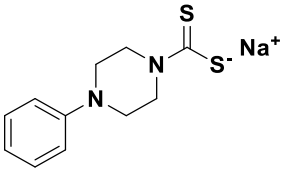

Sodium 4-methylpiperazine-1-carbodithioate (3g)

Experimental m.p. 252.9 ^{o}C. Yield: 88.0%.

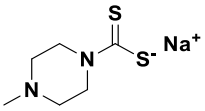

Sodium 4-(4-methoxyphenyl)piperazine-1-carbodithioate (3h)

Experimental m.p. 211.1^{o}C. Yield: 96.9% (Hayat, Rehman and Haleem Khan, 2017.p.279-295).

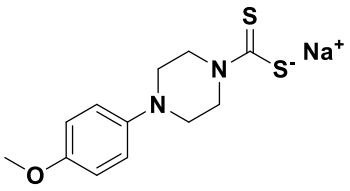

Sodium 4-(4-chlorophenyl)piperazine-1-carbodithioate (3i)

Experimental m.p. 255.7 ^{o}C. Yield: 98.2% (Yin, Xue and Wang, 2006, p.873-880).

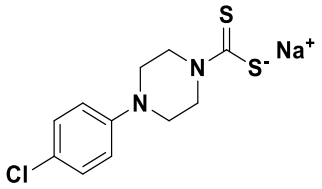

Sodium 4-(pyrimidin-2-yl)piperazine-1-carbodithioate (3j)

Experimental m.p. 219.5 ^{o}C. Yield: 96.4% (Yurttas et al., 2014, p.815-824).

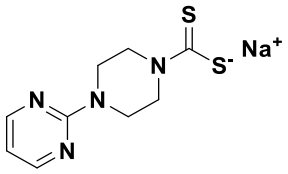

Sodium 4-benzylpiperazine-1-carbodithioate (3k)

Experimental m.p. 187.3 ^{o}C. Yield: 93.0% (Onder, Incesu and Ozkay, 2015, p.508-517).

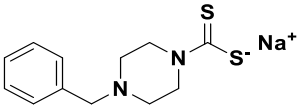

Sodium 4-cyclohexylpiperazine-1-carbodithioate (3l)

Experimental m.p. 145.9 ^{o}C. Yield: 92.2% (Kuppukkannu, Corrado and Gurunathan-Senthilkumar, 2016, p.2489-2500).

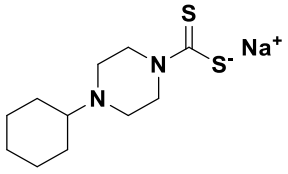

Sodium 4-benzhydrylpiperazine-1-carbodithioate (3m)

Experimental m.p. 232.7 ^{o}C. Yield: 95.9% (Kapanda Coco et al., 2012, p.5774-5783).

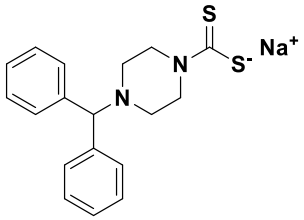

Sodium 4-(4-(trifluoromethyl)benzyl)piperazine-1-carbodithioate (3n)

Experimental m.p. 171.1 ^{o}C. Yield: 83.5% (Levent et al.,2016, p.510-519).

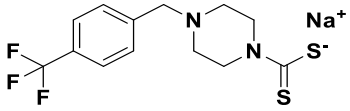

Sodium 4-(4-methylbenzyl)piperazine-1-carbodithioate (3o)

Experimental m.p. 167.7 ^{o}C. Yield: 86.5% (Abu Mohsen, 2014, p.10-19).

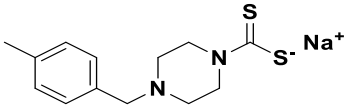

Sodium 4-(4-fluorophenyl)piperazine-1-carbodithioate (3p)

Experimental m.p. 203.6 ^{o}C. Yield: 97.0% (Zhiyong et al., 2007, p.919-925).

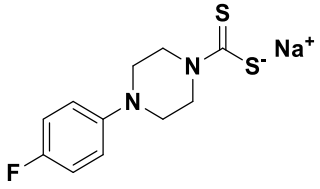

Sodium 4-(furan-2-carbonyl)piperazine-1-carbodithioate (3q)

Experimental m.p. 184.9 ^{o}C. Yield: 87.7% (Levent et al.,2016, p.510-519).

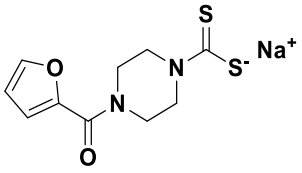

Sodium morpholine-4-carbodithioate (3r)

Experimental m.p. 269.4 ^{o}C.Yield: 88.6%.

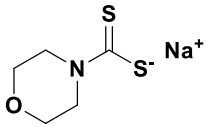

Sodium piperidine-1-carbodithioate (3s)

Experimental M.p. 134.8 ^{o}C. Yield: 90.8% (Mafud and Gambardella Maria Teresa, 2011, p.942).

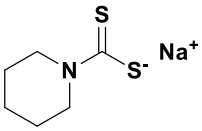

Sodium 2-methylpiperidine-1-carbodithioate (3t)

Experimental m.p. 155.7 ^{o}C. Yield: 98.8% (Forrest-Thomas P and Ray, S,1970, p.1537).

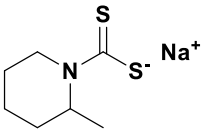

Sodium 4-benzylpiperidine-1-carbodithioate (3u)

Experimental m.p. 179.5 ^{o}C. Yield: 80.5% (Mandalapu et al., 2016, p.820-839).

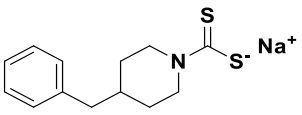

4.3.1. Synthesis of 2-(9-acridinylamino)-2-oxoethyl piperazinyl/morpholinyl/piperidinylcarbodithioate derivatives (4a-u)

The final derivatives were synthesized according to the method C.

2-(9-Acridinylamino)-2-oxoethyl 4-(2-(dimethylamino)ethyl)piperazine-1-carbodithioate (4a)

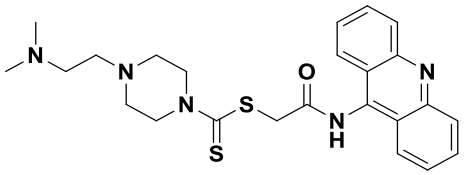

Yield: 88.5 %, **M.p.**: 200.6 °C.

FTIR (ATR, cm^{-1}): 3269 (amide N-H), 2769-2972 (aliphatic C-H), 1662 (C=O), 1463-1506 (C=N and C=C), 1232 (C=S), 756 (out of plane C-H bending).

^{1}H-NMR (300 MHz, DMSO-*d*$_6$; δ, ppm): 2.17-2.18 (6H, d, *J*=2.37 Hz, N($\underline{CH_3}$)$_2$), 2.43-2.44 (4H, t, *J*=2.52 Hz, $\underline{CH_2}$-$\underline{CH_2}$), 2.48-2.55 (4H, m, piperazine $C_{3,5}$-H), 3.97 and 4.25 (4H, two bs, piperazine $C_{2,6}$-H-), 4.62 (2H, s, CO$\underline{CH_2}$), 7.57-7.62 (2H, t, *J*=7.50 Hz, Ar-H), 7.82-7.87 (2H, t, *J*=7.65 Hz, Ar-H), 8.14-8.17 (2H, d, *J*=8.70 Hz, Ar-H), 8.25-8.28 (2H, d, *J*=8.61 Hz, Ar-H), 11.06 (1H, s, -NH-).

^{13}C-NMR (75 MHz, DMSO-*d*$_6$; δ, ppm): 45.70 (CH_3), 50.39 (CH_2), 51.63 (CH_2), 52.86 (CH_2), 55.18 (CH_2), 56.73 (CH_2), 123.15 (C), 125.36 (CH), 126.20 (CH), 129.59 (CH), 130.93 (CH), 140.60 (C), 149.38 (C-9 in 9-aminoacridine), 167.43 (C=O), 194.92 (C=S).

HRMS (m/z): $[M+H]^+$ calcd for $C_{24}H_{29}N_5OS_2$: 468.1886 ; found 468.1874.

DOPNALAB

	Item	Value
	Acquired Date&Time	17.08.2016 11:28:09
	Acquired by	System Administrator
	Filename	C:\Users\dopnalab\Desktop\derya\wiam\yw-11.ispd
	Spectrum name	yw-11
	Sample name	yw-1
	Sample ID	
	Option	
	Comment	
	No. of Scans	10
	Resolution	4 [cm-1]
	Apodization	Happ-Genzel

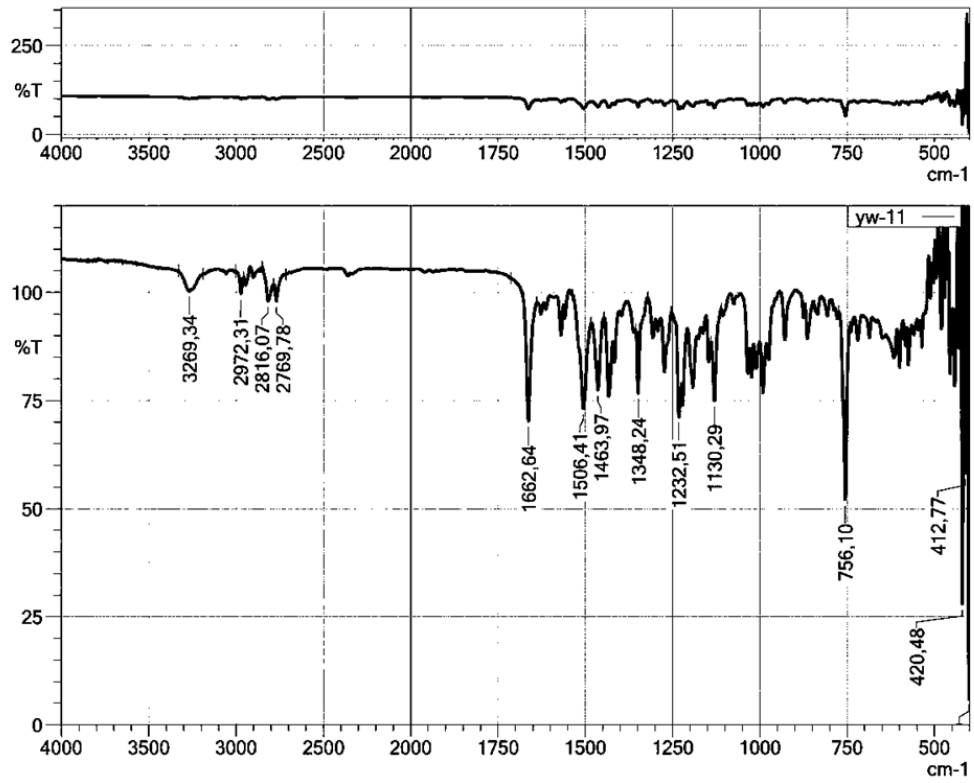

Figure 4.1. *IR Spectrum of Compound **4a***

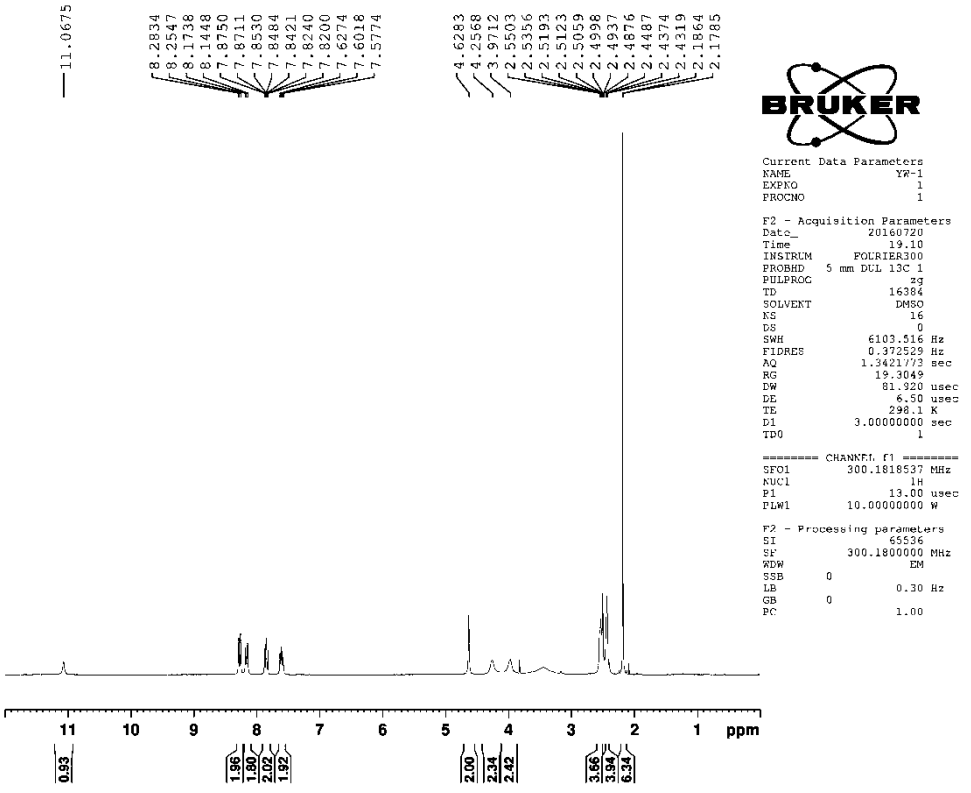

Figure 4.2. *The [1]H-NMR Spectrum of Compound **4a***

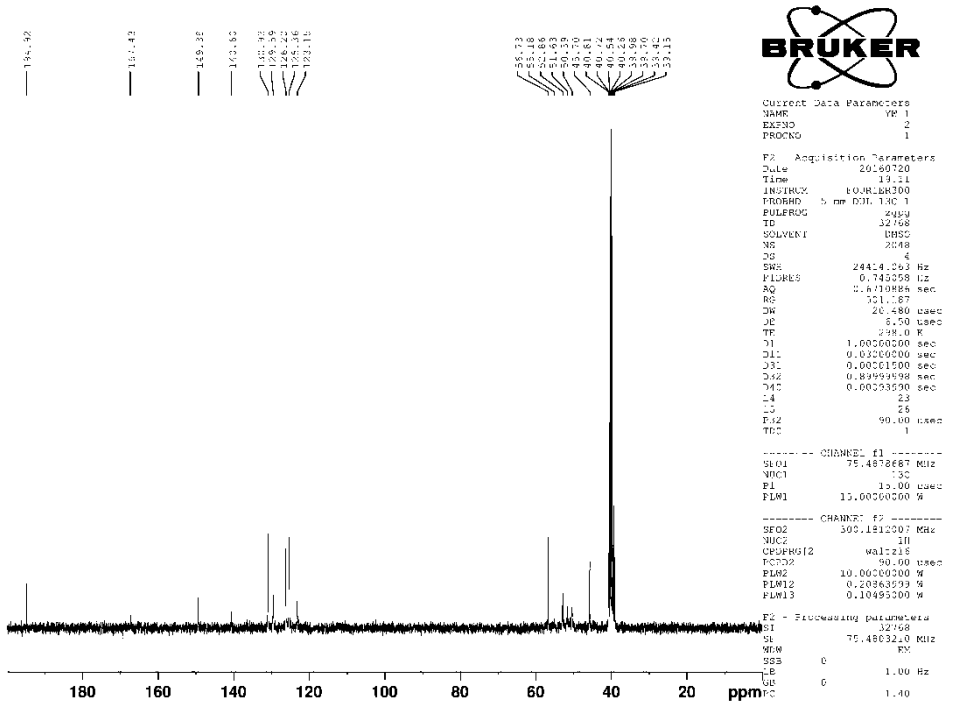

Figure 4.3. *The [13]C-NMR Spectrum of Compound **4a***

Formula Predictor Report - YW-1_16.lcd

Page 1 of 1

Data File: C:\LabSolutions\Data\Analiz\GTuran\YW-1_16.lcd

Elmt	Val.	Min	Max	Elmt	Val.	Min	Max	Elmt	Val.	Min	Max	Elmt	Val.	Min	Max	Use Adduct
H	1	29	30	O	2	0	5	Cl	1	0	0	I	3	0	0	H
C	4	0	30	F	1	0	3	Br	1	0	0					
N	3	0	6	S	2	0	3	Ru	2	0	0					

Error Margin (ppm):	5	DBE Range:	0.0 - 20.0	Electron Ions:	both
HC Ratio:	unlimited	Apply N Rule:	yes	Use MSn Info:	no
Max Isotopes:	3	Isotope RI (%):	1.00	Isotope Res:	10000
MSn Iso RI (%):	10.00	MSn Logic Mode:	AND	Max Results:	500

Event#: 1 MS(E+) Ret. Time : 1.973 -> 2.080 Scan# : 297 -> 313

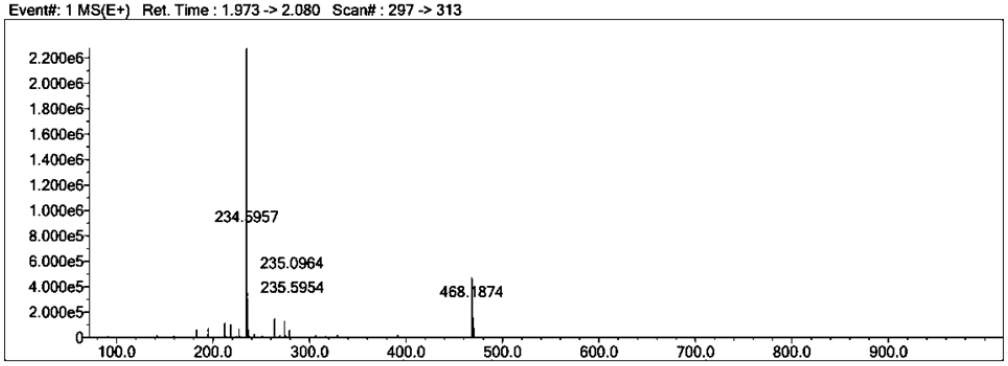

Measured region for 468.1874 m/z

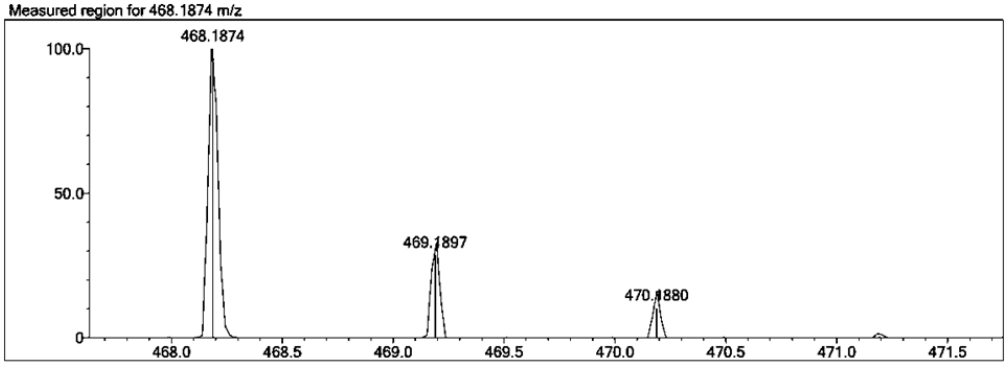

C24 H29 N5 O S2 [M+H]+ : Predicted region for 468.1886 m/z

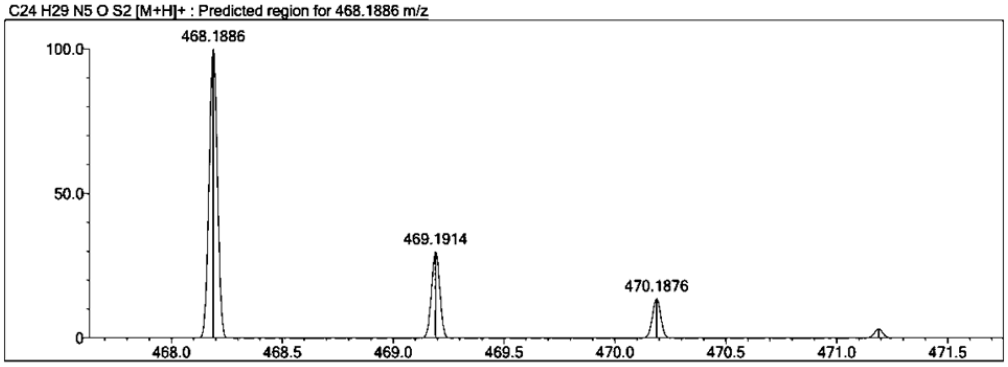

Rank	Score	Formula (M)	Ion	Meas. m/z	Pred. m/z	Df. (mDa)	Df. (ppm)	Iso	DBE
1	79.19	C24 H29 N5 O S2	[M+H]+	468.1874	468.1886	-1.2	-2.56	82.40	13.0

Figure 4.4. *Mass Spectrum of Compound **4a***

2-(9-Acridinylamino)-2-oxoethyl 4-(3-(dimethylamino)propyl)piperazine-1-carbodithioate (4b)

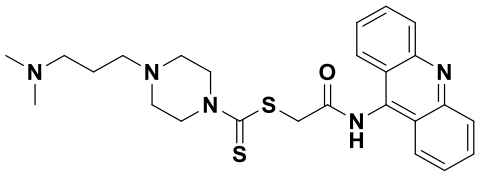

Yield: 85.7 %, **M.p.**: 153.8 °C.

FTIR (ATR, cm^{-1}): 3340 (amide N-H), 2777-2947 (aliphatic C-H), 1653 (C=O), 1411-1458 (C=N and C=C), 1209 -1263 (C=S), 758 (out of plane C-H bending).

^{1}H-NMR (300 MHz, DMSO-*d*$_6$; δ, ppm): 1.47-1.56 (2H, m, CH_2-$\underline{CH_2}$-CH_2), 2.08 (6H, s, N($\underline{CH_3}$)$_2$), 2.15-2.20 (2H, t, *J*=7.10 Hz, CH_2-$CH_2\underline{CH_2}$N(CH_3)$_2$), 2.24-2.29 (2H, d, *J*=7.36 Hz, $\underline{CH_2}CH_2CH_2$), 2.41-2.42 (4H, d, *J*= 0.87, piperazine $C_{3,5}$-H), 3.98 and 4.26 (4H, two s, piperazine $C_{2,6}$-H), 4.65 (2H, s, CO$\underline{CH_2}$), 7.57-7.62 (2H, q, *J*=7.62 Hz, Ar-H)4, 7.81-7.87 (2H, m, Ar-H), 8.14-8.17 (2H, d, *J*=8.70 Hz, Ar-H), 8.26-8.29 (2H, d, *J*=8.70 Hz, Ar-H), 11.19 (1H, s, -NH-).

^{13}C-NMR (75 MHz, DMSO-*d*$_6$; δ, ppm): 24.92 (CH_2), 45.72 (CH_2), 50.39 (CH_3), 51.61(CH_2), 52.87 (CH_2), 55.19 (CH_2), 56.73 (CH_2), 123.16 (C), 125.37 (CH), 126.21 (CH), 129.60 (CH), 130.94 (CH), 140.64 (C), 149.39 (C-9 in 9-aminoacridine), 167.44 (C=O),194.92 (C=S) .

HRMS (m/z): $[M+H]^+$ calcd for $C_{25}H_{31}N_5OS_2$: 482.2043 ; found 482.2047.

DOPNALAB

	Item	Value
	Acquired Date&Time	29.12.2016 15:10:11
	Acquired by	System Administrator
	Filename	C:\Users\dopnalab\Desktop\derya\wiam\yw-22.ispd
	Spectrum name	yw-22
	Sample name	YW-2
	Sample ID	
	Option	
	Comment	
	No. of Scans	10
	Resolution	4 [cm-1]
	Apodization	Happ-Genzel

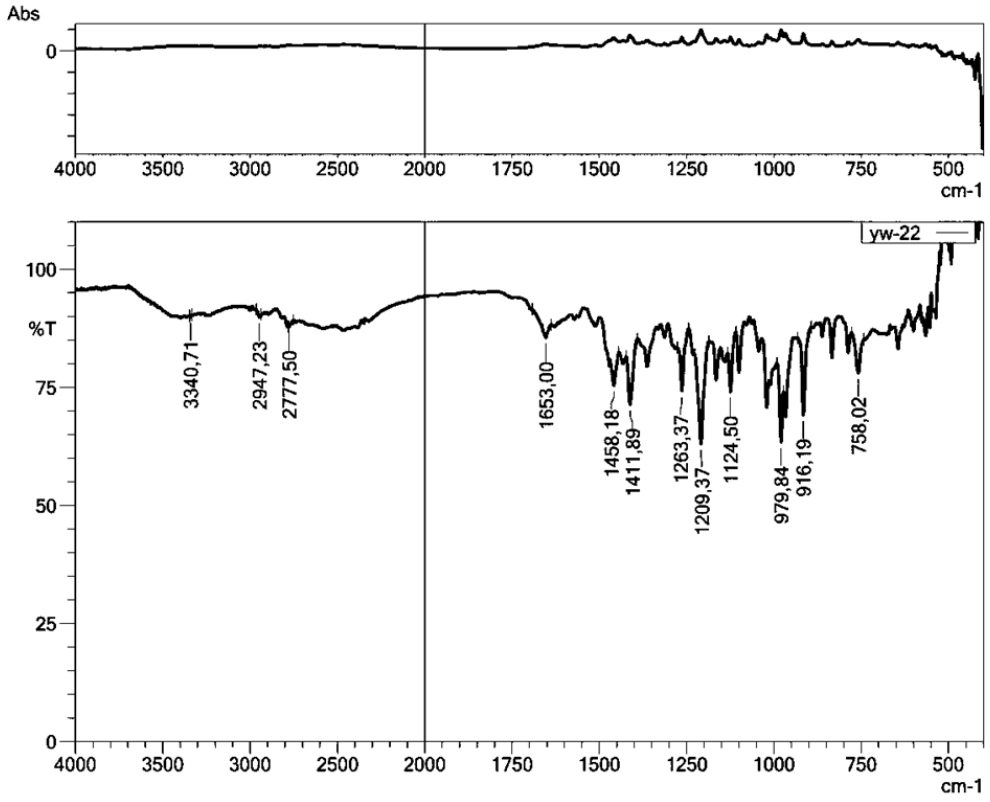

Figure 4.5. *IR Spectrum of Compound **4b***

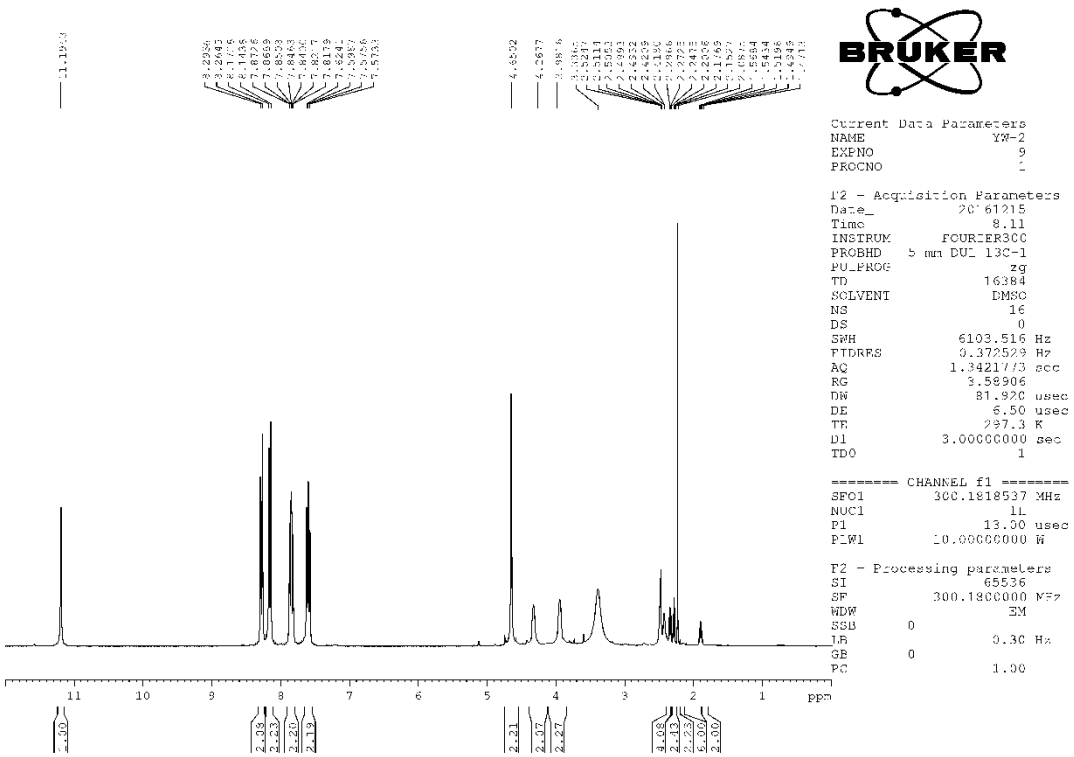

Figure 4.6. *The [1]H-NMR Spectrum of Compound **4b***

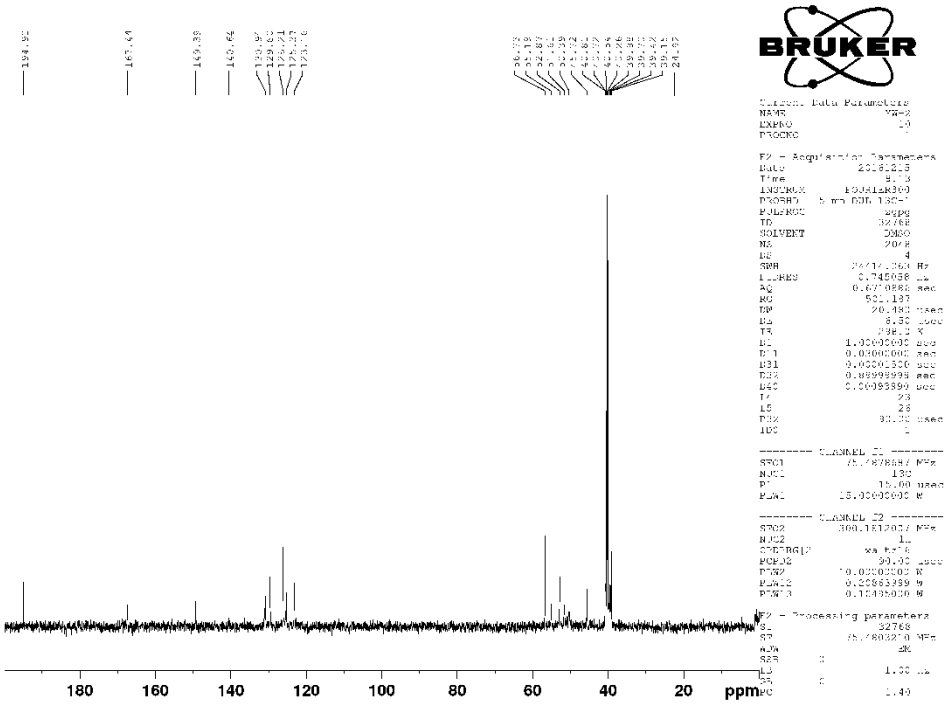

Figure 4.7. *The [13]C-NMR Spectrum of Compound **4b***

Formula Predictor Report - YW-2_17.lcd

Page 1 of 1

Data File: C:\LabSolutions\Data\Analiz\GTuran\YW-2_17.lcd

Elmt	Val.	Min	Max	Elmt	Val.	Min	Max	Elmt	Val.	Min	Max	Elmt	Val.	Min	Max	Use Adduct
H	1	31	31	O	2	0	5	Cl	1	0	0	I	3	0	0	H
C	4	0	30	F	1	0	3	Br	1	0	0					
N	3	0	6	S	2	0	3	Ru	2	0	0					

Error Margin (ppm):	5	DBE Range:	0.0 - 20.0	Electron Ions:	both
HC Ratio:	unlimited	Apply N Rule:	yes	Use MSn Info:	no
Max Isotopes:	3	Isotope RI (%):	1.00	Isotope Res:	10000
MSn Iso RI (%):	10.00	MSn Logic Mode:	AND	Max Results:	500

Event#: 1 MS(E+) Ret. Time : 1.267 -> 1.320 - 2.240 -> 6.975 Scan# : 191 -> 199 - 337 -> 1047

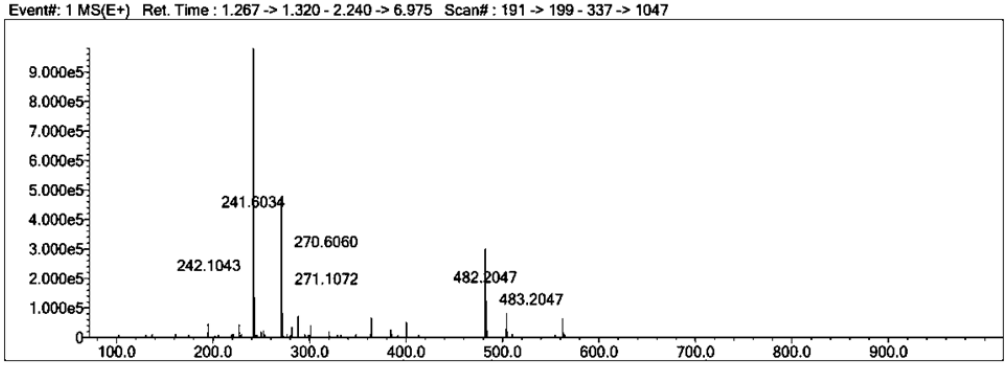

Measured region for 482.2047 m/z

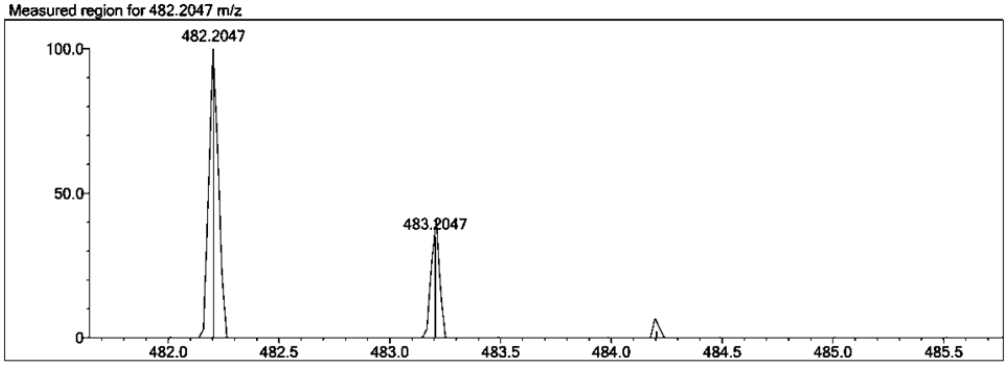

C25 H31 N5 O S2 [M+H]+ : Predicted region for 482.2043 m/z

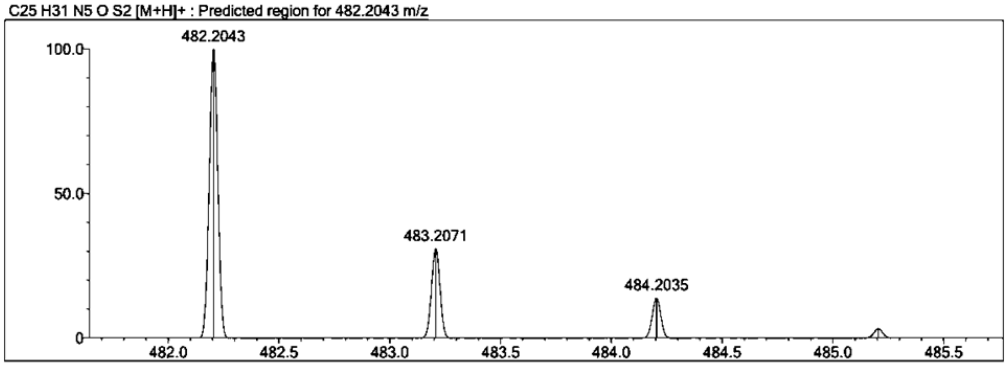

Rank	Score	Formula (M)	Ion	Meas. m/z	Pred. m/z	Df. (mDa)	Df. (ppm)	Iso.	DBE
1	62.68	C25 H31 N5 O S2	[M+H]+	482.2047	482.2043	0.4	0.83	62.68	13.0

Figure 4.8. *Mass Spectrum of Compound **4b***

2-(9-Acridinylamino)-2-oxoethyl 4-ethylpiperazine-1-carbodithioate (4c)

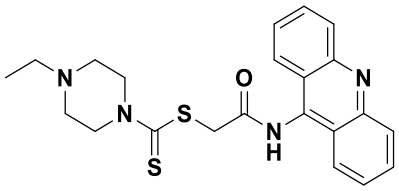

Yield: 81.0 %, **M.p.**: 221.7 °C.

FTIR (ATR, cm^{-1}): 3232 (amide N-H), 2358-2974 (aliphatic C-H), 1654 (C=O), 1435-1508 (C=N and C=C), 1219-1271 (C=S),732-758 (out of plane C-H bending).

^{1}H-NMR (300 MHz, DMSO-*d*$_6$; δ, ppm): 0.98-1.03 (3H, t, *J*=7.15 Hz, $CH_2\underline{CH_3}$), 2.33-2.40 (2H, q, *J*=7.15 Hz, $\underline{CH_2}CH_3$), 2.47-2.50 (4H, m, piperazine $C_{3,5}$-H), 3.98 and 4.26 (4H, two s, piperazine $C_{2,6}$-H), 4.65 (2H, s, $CO\underline{CH_2}$), 7.57-7.62 (2H, t, *J*=7.45 Hz, Ar-H), 7.81-7.87 (2H, t, *J*=7.63 Hz, Ar-H), 8.14-8.17 (2H, d, *J*=8.70 Hz, Ar-H), 8.26-8.29 (2H, d, *J*=8.55 Hz, Ar-H), 11.19 (1H, s, -NH-).

^{13}C-NMR (75 MHz, DMSO-*d*$_6$; δ, ppm):12.34 (CH_3), 50.92 (CH_2), 51.06 (CH_2), 51.50 (CH_2), 52.21 (CH_2), 123.15 (C), 125.42 (CH), 126.18 (CH), 129.57 (CH), 130.91 (C), 140.65 (C), 149.38 (C-9 in 9-aminoacridine),167.43 (C=O),195.01 (C=S).

HRMS (m/z): $[M+H]^+$ calcd for $C_{22}H_{24}N_4OS_2$: 425.1464 ; found 425.1459.

DOPNALAB

	Item	Value
	Acquired Date&Time	17.08.2016 11:40:13
	Acquired by	System Administrator
	Filename	C:\Users\dopnalab\Desktop\derya\wiam\yw-31.ispd
	Spectrum name	yw-31
	Sample name	yw-3
	Sample ID	
	Option	
	Comment	
	No. of Scans	10
	Resolution	4 [cm-1]
	Apodization	Happ-Genzel

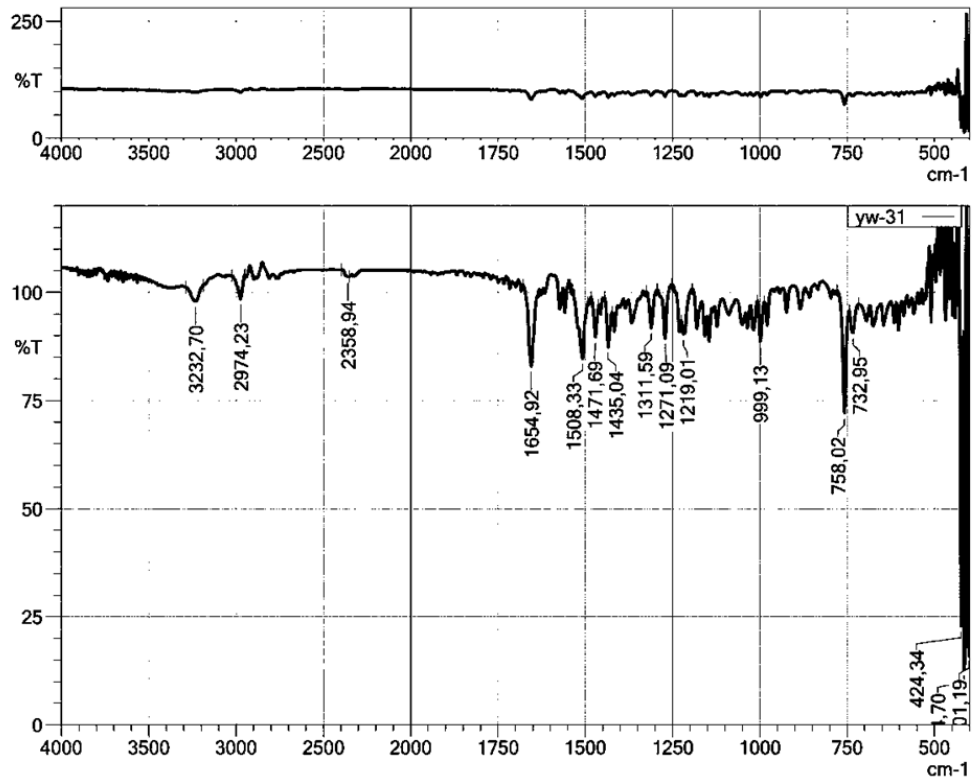

Figure 4.9. *IR Spectrum of Compound* ***4c***

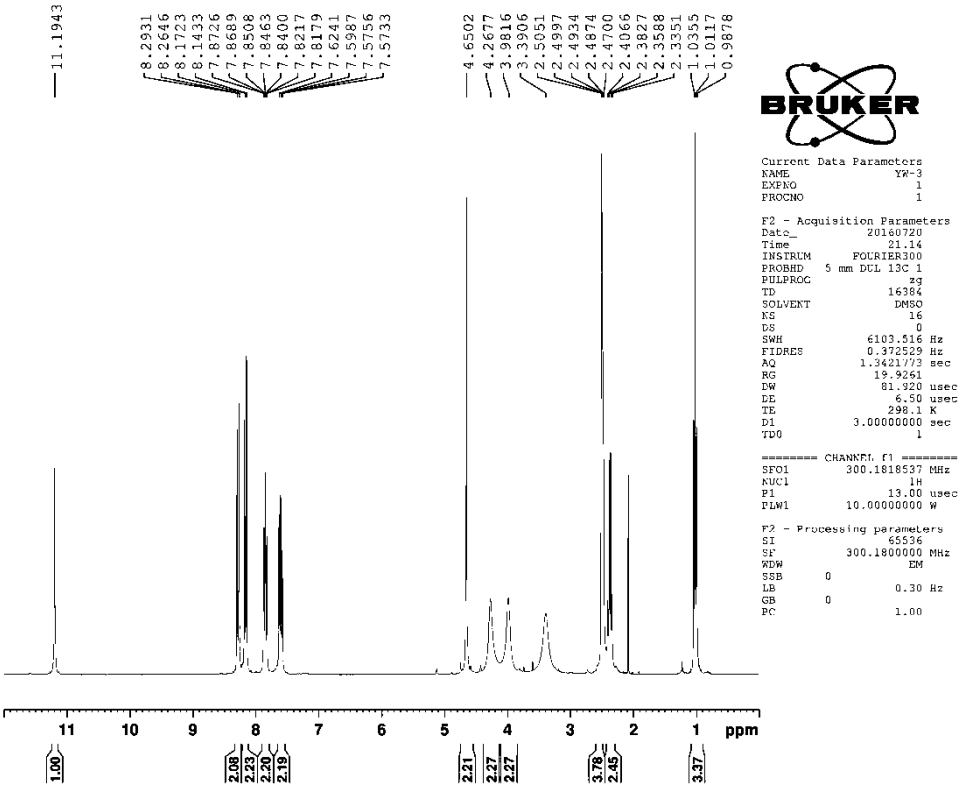

Figure 4.10. *The [1]H-NMR Spectrum of Compound* ***4c***

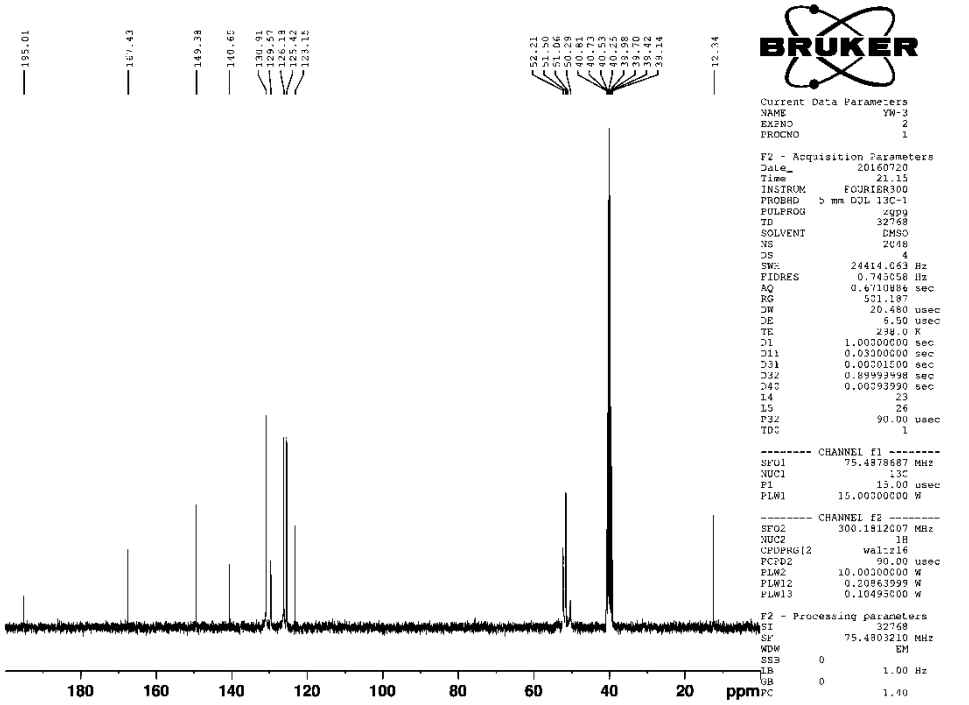

Figure 4.11. *The [13]C-NMR Spectrum of Compound* ***4c***

Formula Predictor Report - YW-3_18.lcd

Page 1 of 1

Data File: C:\LabSolutions\Data\Analiz\GTuran\YW-3_18.lcd

Elmt	Val.	Min	Max	Elmt	Val.	Min	Max	Elmt	Val.	Min	Max	Elmt	Val.	Min	Max	Use Adduct
H	1	24	24	O	2	0	5	Cl	1	0	0	I	3	0	0	H
C	4	0	30	F	1	0	3	Br	1	0	0					
N	3	0	6	S	2	0	3	Ru	2	0	0					

Error Margin (ppm):	5	DBE Range:	0.0 - 20.0	Electron Ions:	both
HC Ratio:	unlimited	Apply N Rule:	yes	Use MSn Info:	no
Max Isotopes:	3	Isotope RI (%):	1.00	Isotope Res:	10000
MSn Iso RI (%):	10.00	MSn Logic Mode:	AND	Max Results:	500

Event#: 1 MS(E+) Ret. Time : 1.093 -> 2.240 - 1.027 -> 1.566 Scan# : 165 -> 337 - 155 -> 235

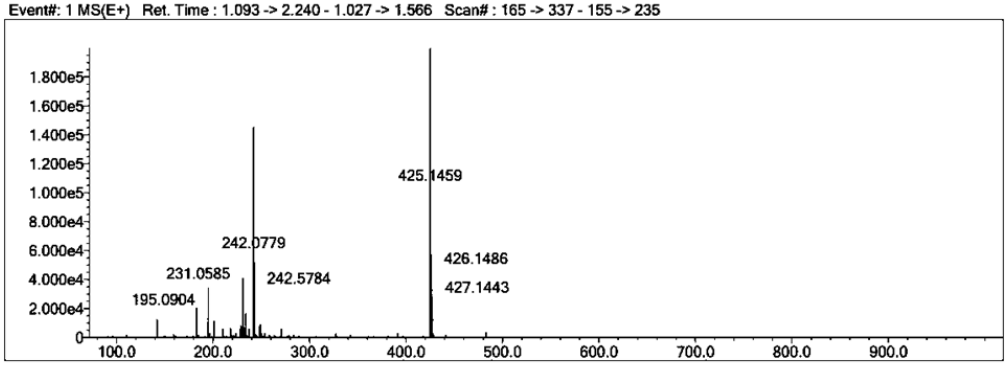

Measured region for 425.1459 m/z

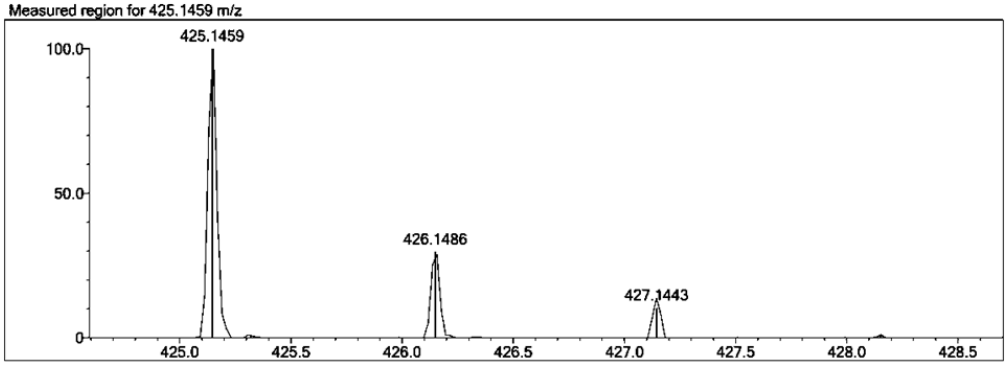

C22 H24 N4 O S2 [M+H]+ : Predicted region for 425.1464 m/z

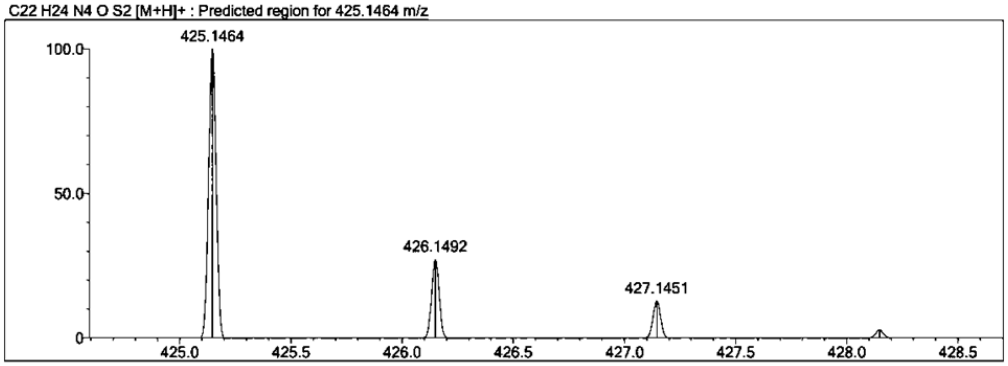

Rank	Score	Formula (M)	Ion	Mass. m/z	Pred. m/z	Df. (mDa)	Df. (ppm)	Iso.	DBE
1	83.23	C22 H24 N4 O S2	[M+H]+	425.1459	425.1464	-0.5	-1.18	83.61	13.0

Figure 4.12. *Mass Specturum of Compound **4c***

2-(9-Acridinylamino)-2-oxoethyl 4-(4-nitrophenyl)piperazine-1-carbodithioate (4d)

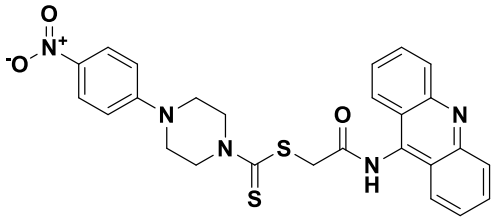

Yield: 90.5%, **M.p.**: 248.2 °C.

FTIR (ATR, cm^{-1}): 3238 (amide N-H), 2976 (aliphatic C-H), 1670 (C=O), 1417-1598 (C=N and C=C), 1213-1280 (C=S),752 (out of plane C-H bending).

^{1}H-NMR (300 MHz, DMSO-*d*$_6$; δ, ppm): 3.74 (4H, s, piperazine $C_{3,5}$-H), 4.19 and 4.42 (4H, two bs, piperazine $C_{2,6}$-H), 4.68 (2H, s, CO$\underline{CH_2}$), 6.93-6.96 (2H, d, *J*=9.51Hz, Ar-H), 7.59-7.63 (2H, t, *J*=6.61 Hz, Ar-H), 7.82-7.87 (2H, t, *J*=7.65 Hz, Ar-H), 8.07-8.10 (2H, d, *J*=9.42 Hz, Ar-H), 8.14-8.17 (2H, d, *J*=8.70 Hz, Ar-H), 8.27-8.30 (2H, d, *J*=8.49 Hz, Ar-H), 11.10 (1H, s, -NH-).

^{13}C-NMR (75 MHz, DMSO-*d*$_6$; δ, ppm): 45.19 (CH_2), 48.92 (CH_2), 50.62(CH_2), 112.31 (C), 123.16 (CH), 125.36 (CH), 126.24 (CH), 126.26 (CH), 129.60 (CH), 130.93 (CH), 137.29(C), 140.57(C), 149.38 (C), 154.16 (C-9 in 9-aminoacridine), 167.33 (C=O), 195.41 (C=S).

HRMS (m/z): $[M+H]^+$ calcd for $C_{26}H_{23}N_5O_3S_2$: 518.1315 ; found 518.1299.

DOPNALAB

	Item	Value
	Acquired Date&Time	17.08.2016 11:45:20
	Acquired by	System Administrator
	Filename	C:\Users\dopnalab\Desktop\derya\wiam\yw-41.ispd
	Spectrum name	yw-41
	Sample name	yw-4
	Sample ID	
	Option	
	Comment	
	No. of Scans	10
	Resolution	4 [cm-1]
	Apodization	Happ-Genzel

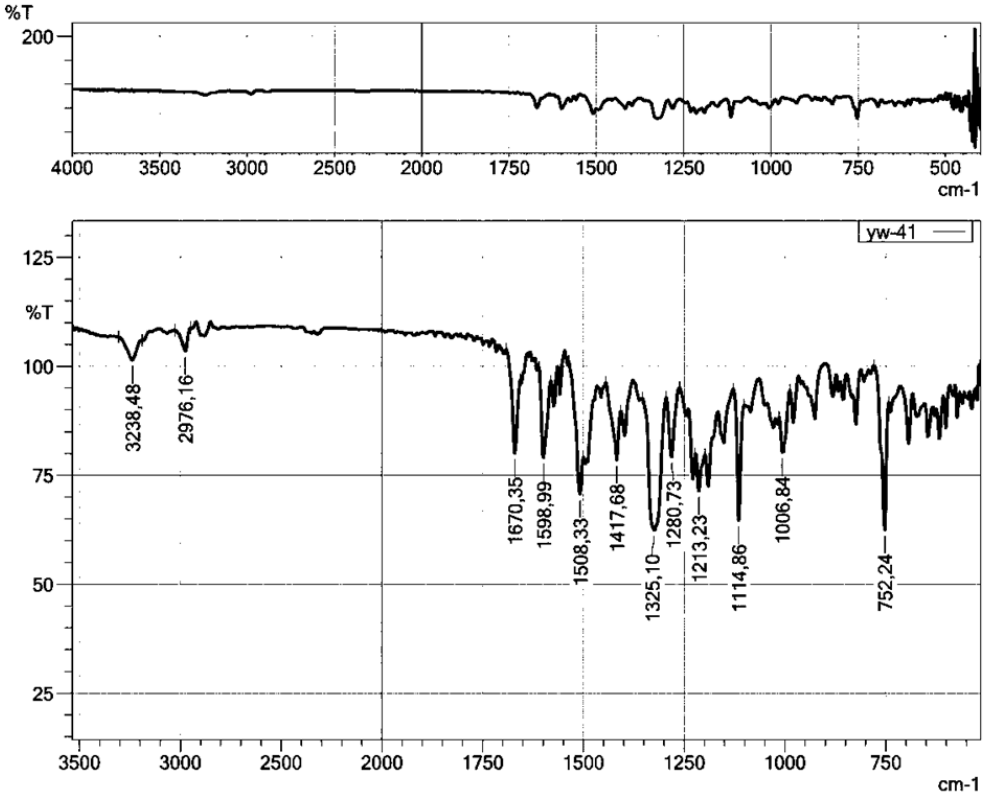

Figure 4.13. *IR Spectrum of Compound **4d***

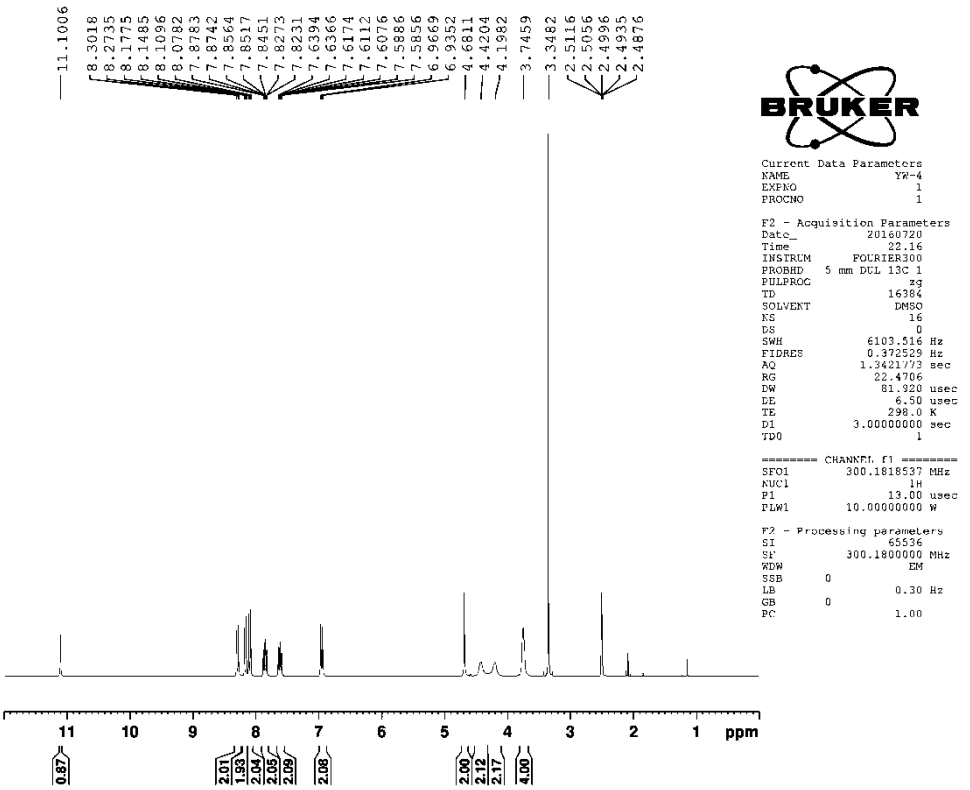

Figure 4.14. *The [1]H-NMR Spectrum of Compound **4d***

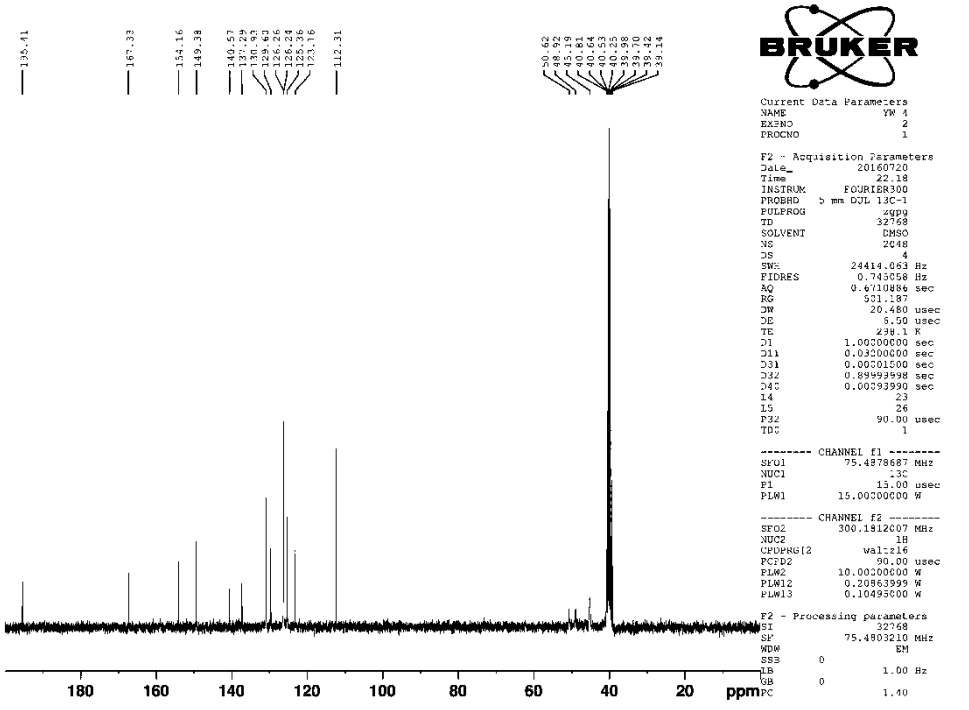

Figure 4.15. *The [13]C-NMR Spectrum of Compound **4d***

Formula Predictor Report - YW-4_1.lcd

Page 1 of 1

Data File: C:\LabSolutions\Data\Analiz\Murat\YW-4_1.lcd

Elmt	Val.	Min	Max	Elmt	Val.	Min	Max	Elmt	Val.	Min	Max	Elmt	Val.	Min	Max	Use Adduct
H	1	23	40	O	2	0	3	Cl	1	0	0	I	3	0	0	H
C	4	6	27	F	1	0	0	Br	1	0	0					
N	3	0	9	S	2	0	2	Ru	2	0	0					

Error Margin (ppm): 5
HC Ratio: unlimited
Max Isotopes: 3
MSn Iso RI (%): 10.00

DBE Range: 9.0 - 30.0
Apply N Rule: yes
Isotope RI (%): 1.00
MSn Logic Mode: AND

Electron Ions: both
Use MSn Info: no
Isotope Res: 10000
Max Results: 500

Event#: 1 MS(E+) Ret. Time : 5.787 -> 6.013 - 6.360 -> 9.898 Scan# : 869 -> 903 - 955 -> 1485

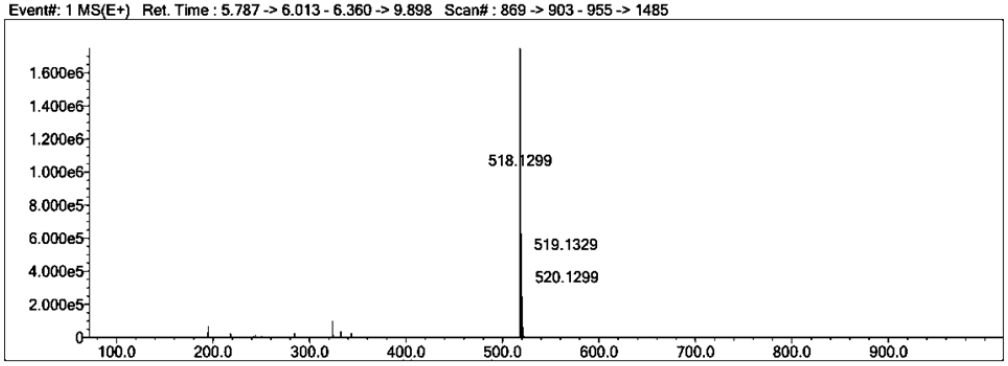

Measured region for 518.1299 m/z

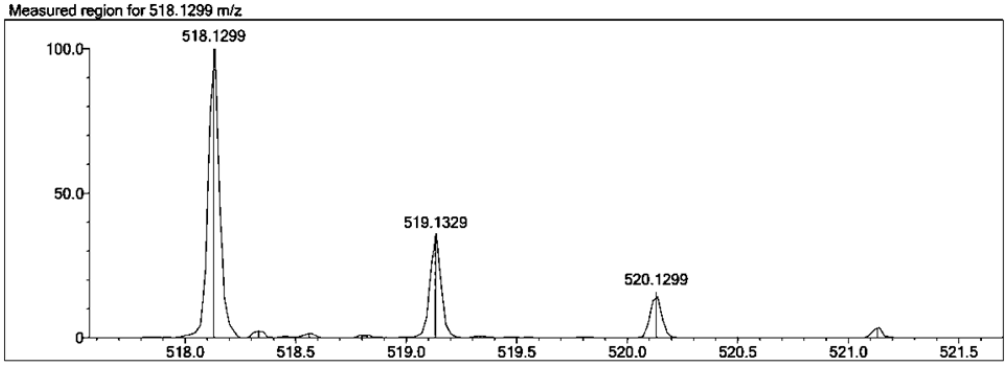

C26 H23 N5 O3 S2 [M+H]+ : Predicted region for 518.1315 m/z

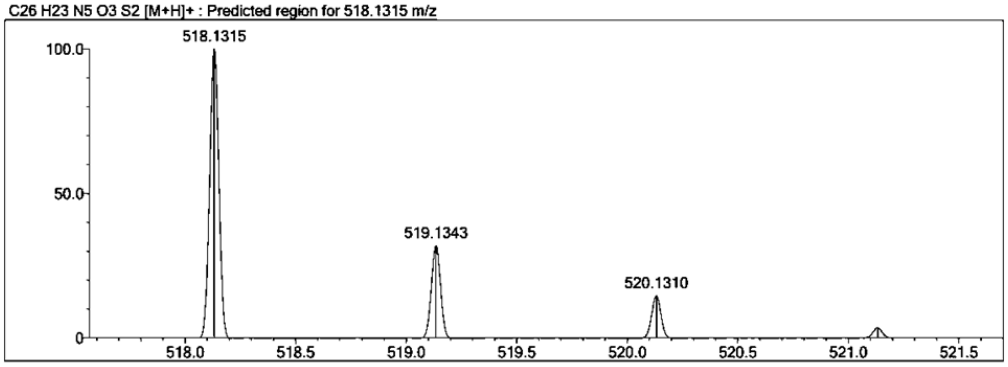

Rank	Score	Formula (M)	Ion	Meas. m/z	Pred. m/z	Df. (mDa)	Df. (ppm)	Iso.	DBE
1	92.30	C26 H23 N5 O3 S2	[M+H]+	518.1299	518.1315	-1.6	-3.09	97.39	18.0

Figure 4.16. *Mass Spectrum of Compound **4d***

2-(9-Acridinylamino)-2-oxoethyl 4-(2-hydroxyethyl)piperazine-1-carbodithioate (4e)

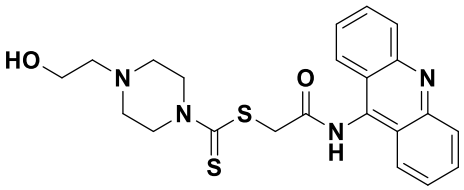

Yield: 84.4%, **M.p.**: 219.2 °C.

FTIR (ATR, cm^{-1}): 3226 (amide N-H), 2978 (aliphatic C-H), 1660 (C=O), 1433-1558 (C=N and C=C), 1228 (C=S), 758 (out of plane C-H bending).

^{1}H-NMR (300 MHz, DMSO-d_6; δ, ppm): 2.49-2.50 (2H, t, *J*=1.72 Hz, OH-CH_2-$\underline{CH_2}$-), 2.61 (4H, s, piperazine $C_{3,5}$-H), 3.54 (2H, s, OH-$\underline{CH_2}$-CH_2-), 4.00 and 4.28 (4H, s, piperazine $C_{2,6}$-H), 4.64 (2H, s, CO$\underline{CH_2}$), 7.58-7.62 (2H, t, *J*=7.38 Hz, Ar-H), 7.82-7.87 (2H, t, *J*=7.39 Hz, Ar-H), 8.14-8.17 (2H, d, *J*=8.64 Hz, Ar-H), 8.26-8.28 (2H, d, *J*=8.58 Hz, Ar-H), 11.10 (1H, s, -NH-).

^{13}C-NMR (75 MHz, DMSO-d_6; δ, ppm): 50.17 (CH_2), 51.36 (CH_2), 52.87 (CH_2), 58.73 (CH_2), 59.83 (CH_2), 123.16 (C), 125.37 (CH), 126.21 (CH), 129.59 (CH), 130.93 (CH), 140.60 (C), 149.38 (C-9 in 9-aminoacridine), 167.41 (C=O), 195.07 (C=S).

HRMS (m/z): $[M+H]^+$ calcd for $C_{22}H_{24}N_4O_2S_2$: 441.1413 ; found 441.1406.

DOPNALAB

	Item	Value
	Acquired Date&Time	17.08.2016 11:51:56
	Acquired by	System Administrator
	Filename	C:\Users\dopnalab\Desktop\derya\wiam\yw-51.ispd
	Spectrum name	yw-51
	Sample name	yw-5
	Sample ID	
	Option	
	Comment	
	No. of Scans	10
	Resolution	4 [cm-1]
	Apodization	Happ-Genzel

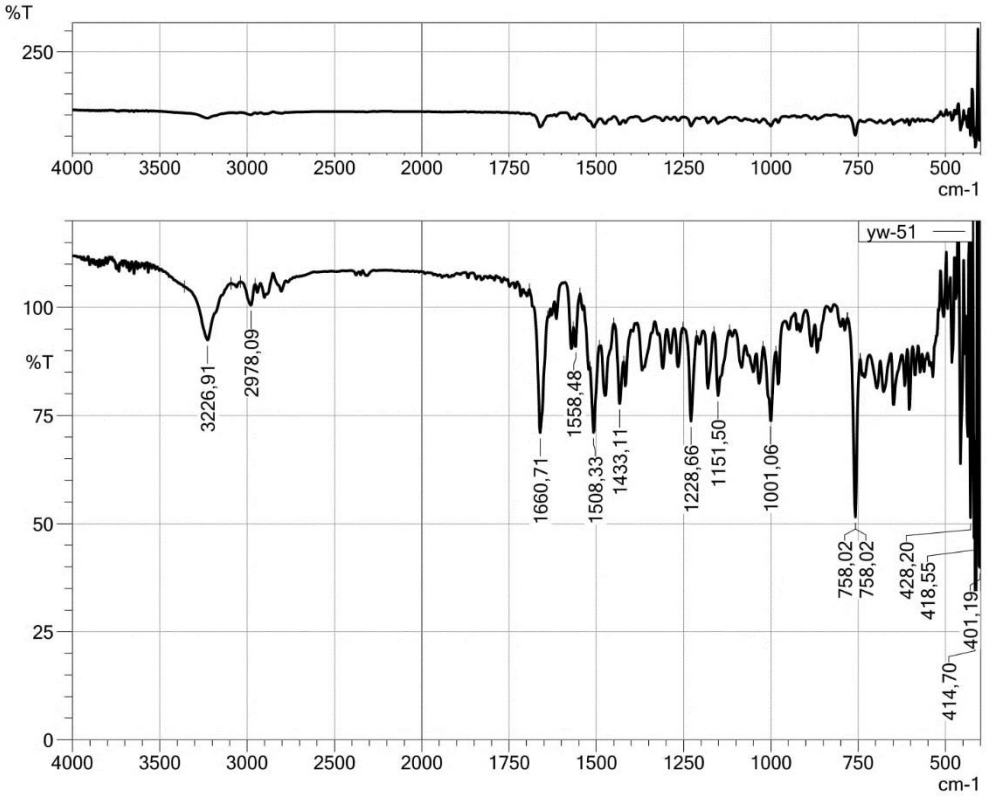

Figure 4.17. *IR Spectrum of Compound* ***4e***

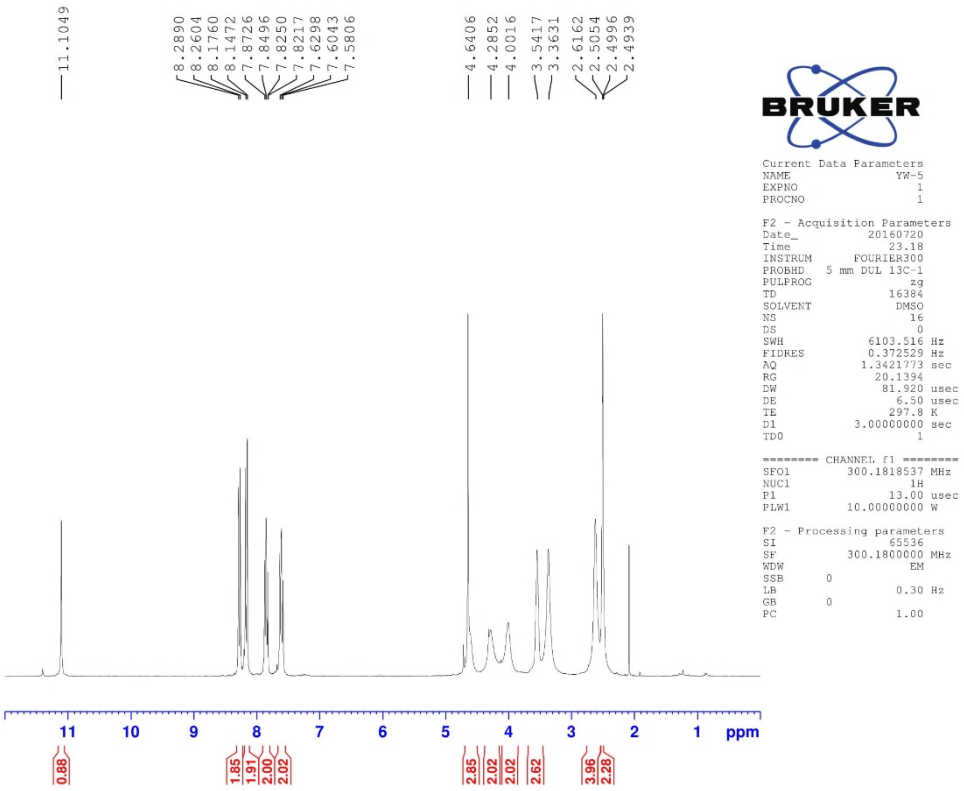

Figure 4.18. *The [1]H-NMR Spectrum of Compound* ***4e***

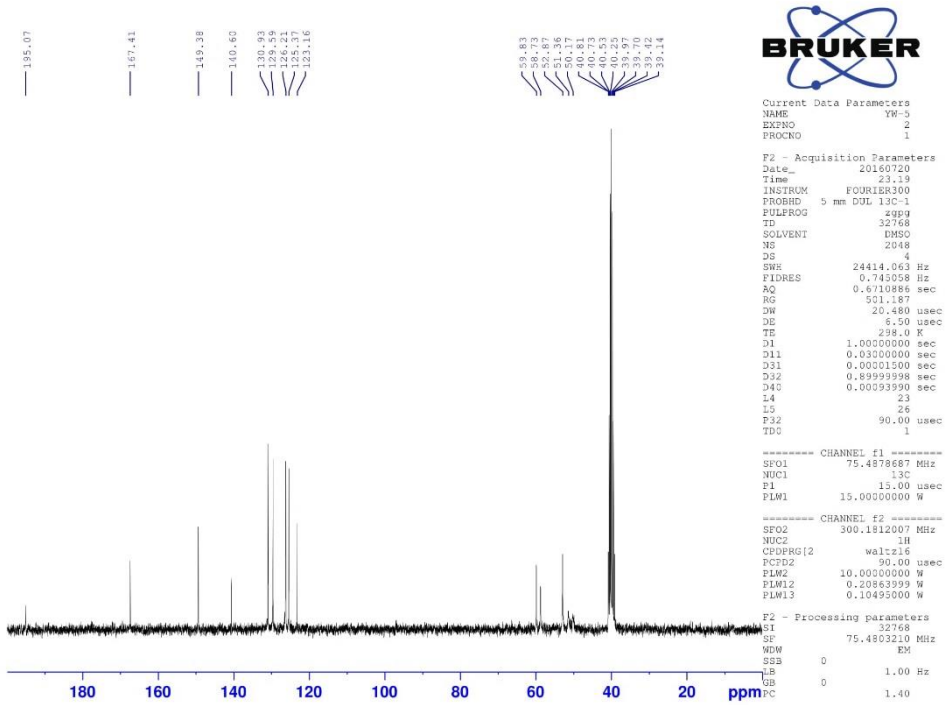

Figure 4.19. *The [13] C-NMR Spectrum of Compound* ***4e***

Formula Predictor Report - YW-5_19.lcd

Page 1 of 1

Data File: C:\LabSolutions\Data\Analiz\GTuran\YW-5_19.lcd

Elmt	Val.	Min	Max	Elmt	Val.	Min	Max	Elmt	Val.	Min	Max	Elmt	Val.	Min	Max	Use Adduct
H	1	24	24	O	2	0	5	Cl	1	0	0	I	3	0	0	H
C	4	0	30	F	1	0	3	Br	1	0	0					
N	3	0	6	S	2	0	3	Ru	2	0	0					

Error Margin (ppm): 5
HC Ratio: unlimited
Max Isotopes: 3
MSn Iso RI (%): 10.00

DBE Range: 0.0 - 20.0
Apply N Rule: yes
Isotope RI (%): 1.00
MSn Logic Mode: AND

Electron Ions: both
Use MSn Info: no
Isotope Res: 10000
Max Results: 500

Event#: 1 MS(E+) Ret. Time : 1.360 -> 1.840 - 3.227 -> 9.598 Scan# : 205 -> 277 - 485 -> 1441

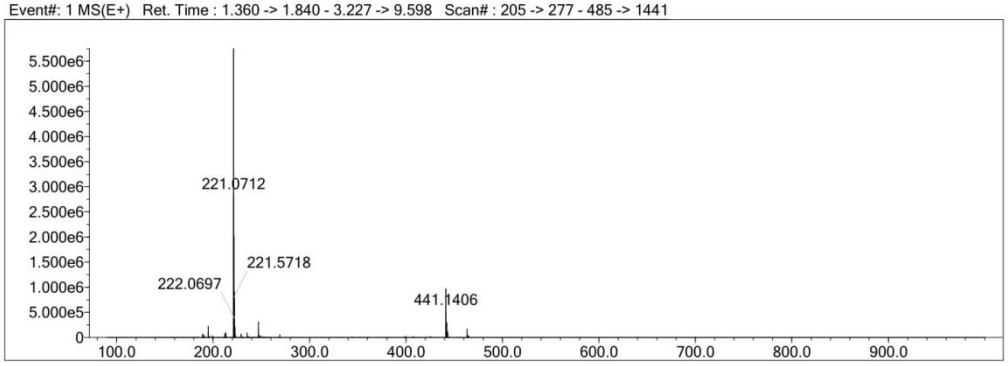

Measured region for 441.1406 m/z

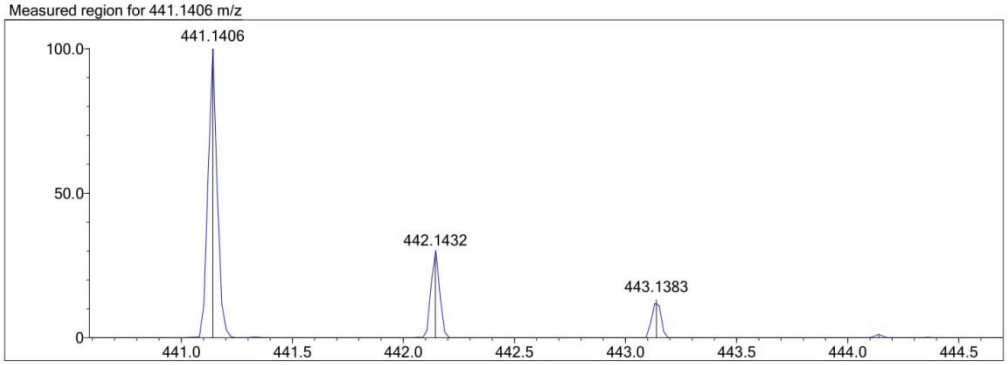

C22 H24 N4 O2 S2 [M+H]+ : Predicted region for 441.1413 m/z

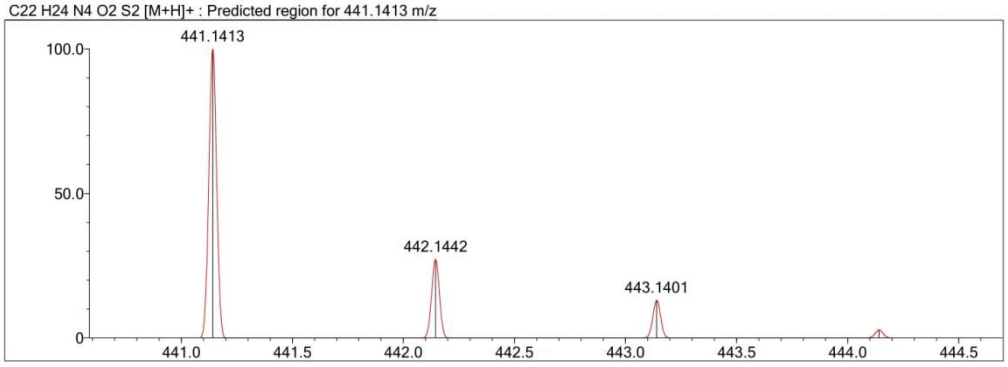

Rank	Score	Formula (M)	Ion	Meas. m/z	Pred. m/z	Df. (mDa)	Df. (ppm)	Iso	DBE
1	97.53	C22 H24 N4 O2 S2	[M+H]+	441.1406	441.1413	-0.7	-1.59	98.99	13.0

Figure 4.20. *Mass Spectrum of Compound* ***4e***

2-(9-Acridinylamino)-2-oxoethyl 4-phenylpiperazine-1-carbodithioate (4f)

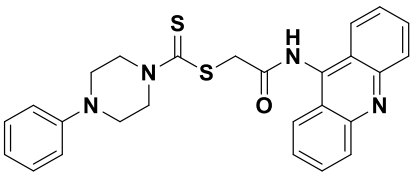

Yield: 94.5%, **M.p.**: oil.

FTIR (ATR, cm-1): 3352 (amide N-H), 2881 (aliphatic C-H), 1660 (C=O), 1417-1506 (C=N and C=C), 1228 (C=S), 756-883 (out of plane C-H bending).

^{1}H-NMR (300 MHz, DMSO-*d*$_6$; δ, ppm): 3.31-3.35 (4H, d, J =9.36 Hz, piperazine $C_{3,5}$-H), 4.15 and 4.42 (4H, two bs, piperazine $C_{2,6}$-H), 4.66 (2H, s, CO$\underline{CH_2}$), 6.78-6.83 (1H, t, *J*=7.24 Hz, Ar-H), 6.94-6.97 (2H, d, *J*=8.01 Hz, Ar-H), 7.21-7.26 (2H, t, *J*=7.93 Hz, Ar-H), 7.58-7.63 (2H, t, *J*=7.60 Hz, Ar-H), 7.82-7.86 (2H, t, J=6.66 Hz, Ar-H), 8.14-8.17 (2H, d, *J*=8.70 Hz, Ar-H), 8.27-8.30 (2H, d, *J*=8.52 Hz, Ar-H), 11.08 (1H, s,-NH-).

^{13}C-NMR (75 MHz, DMSO-*d*$_6$; δ, ppm): 48.06 (CH_2), 50.05 (CH_2), 51.34 (CH_2), 115.93 (C), 119.74 (CH), 123.16 (CH), 125.35 (CH), 126.23 (CH), 129.53 (CH), 129.60 (CH), 130.93 (CH), 140.58 (C), 149.38 (C),150.49 (C-9 in 9-aminoacridine),167.39 (C=O), 195.25 (C=S).

HRMS (m/z): $[M+H]^+$ calcd for $C_{26}H_{24}N_4OS_2$: 473.1464; found 473.1471.

DOPNALAB

	Item	Value
	Acquired Date&Time	17.08.2016 11:58:11
	Acquired by	System Administrator
	Filename	C:\Users\dopnalab\Desktop\derya\wiam\yw-61.ispd
	Spectrum name	yw-61
	Sample name	yw-6
	Sample ID	
	Option	
	Comment	
	No. of Scans	10
	Resolution	4 [cm-1]
	Apodization	Happ-Genzel

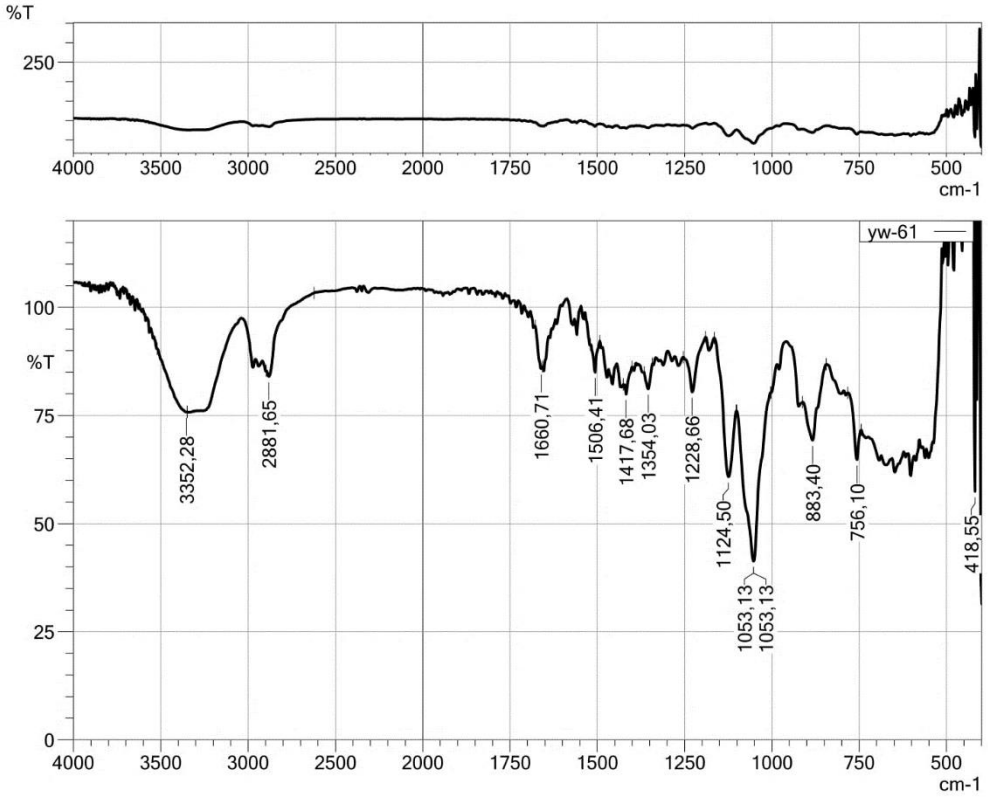

Figure 4.21. *IR Spectrum of Compound **4f***

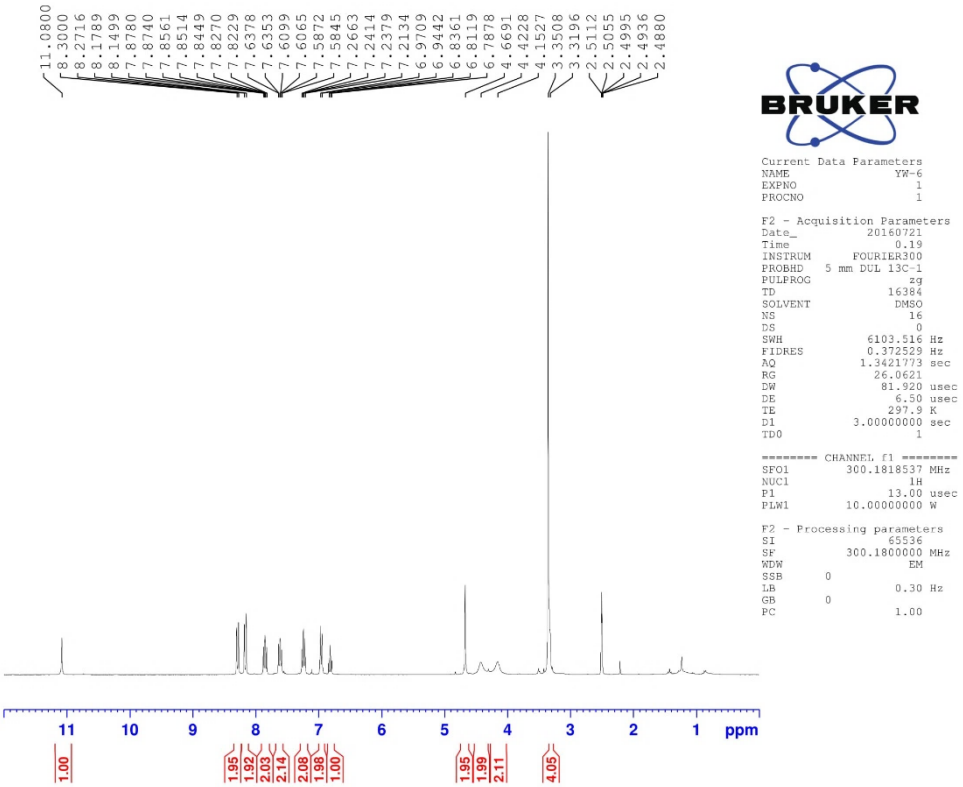

Figure 4.22. *The [1]H-NMR Spectrum of Compound* ***4f***

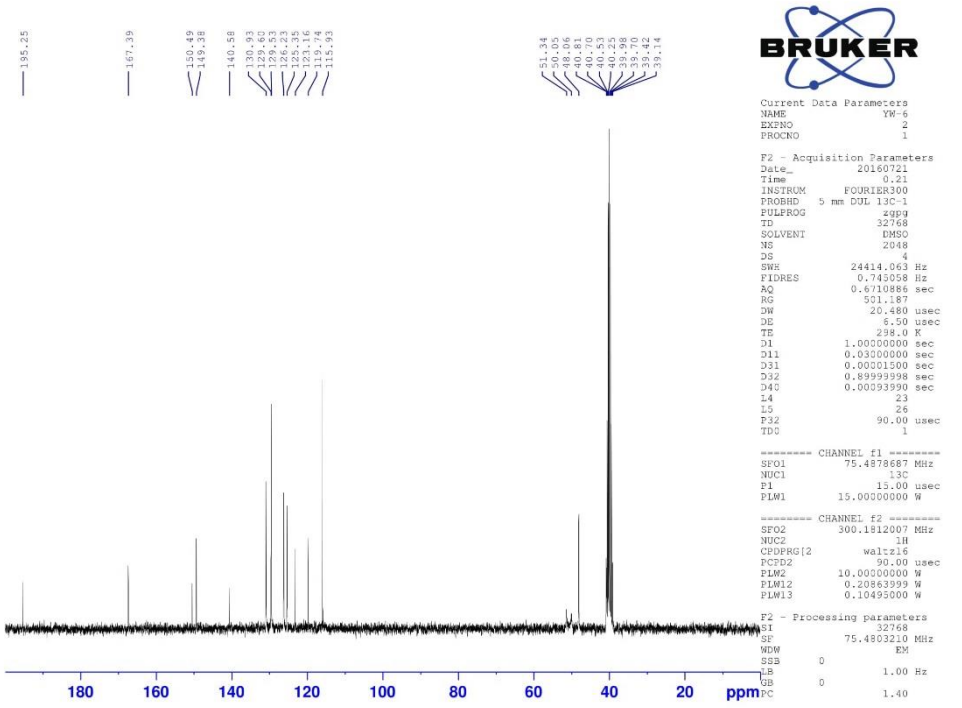

Figure 4.23. *The [13]C-NMR Spectrum of Compound* ***4f***

Formula Predictor Report - YW-6_1.lcd

Page 1 of 1

Data File: C:\LabSolutions\Data\Analiz\Murat\YW-6_1.lcd

Elmt	Val.	Min	Max	Elmt	Val.	Min	Max	Elmt	Val.	Min	Max	Elmt	Val.	Min	Max	Use Adduct
H	1	23	40	O	2	0	3	Cl	1	0	0	I	3	0	0	H
C	4	6	27	F	1	0	0	Br	1	0	0					
N	3	0	9	S	2	0	2	Ru	2	0	0					

Error Margin (ppm): 5
HC Ratio: unlimited
Max Isotopes: 3
MSn Iso RI (%): 10.00

DBE Range: 9.0 - 30.0
Apply N Rule: yes
Isotope RI (%): 1.00
MSn Logic Mode: AND

Electron Ions: both
Use MSn Info: no
Isotope Res: 10000
Max Results: 500

Event#: 1 MS(E+) Ret. Time : 6.360 -> 6.573 - 7.333 -> 9.306 Scan# : 955 -> 987 - 1101 -> 1397

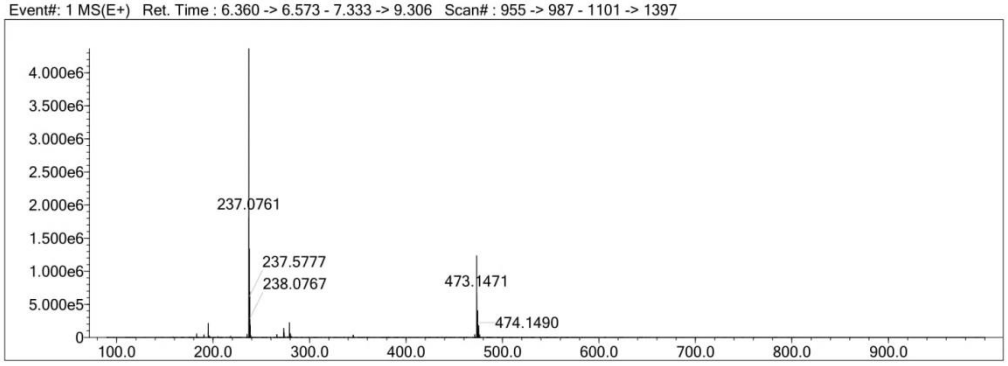

Measured region for 473.1471 m/z

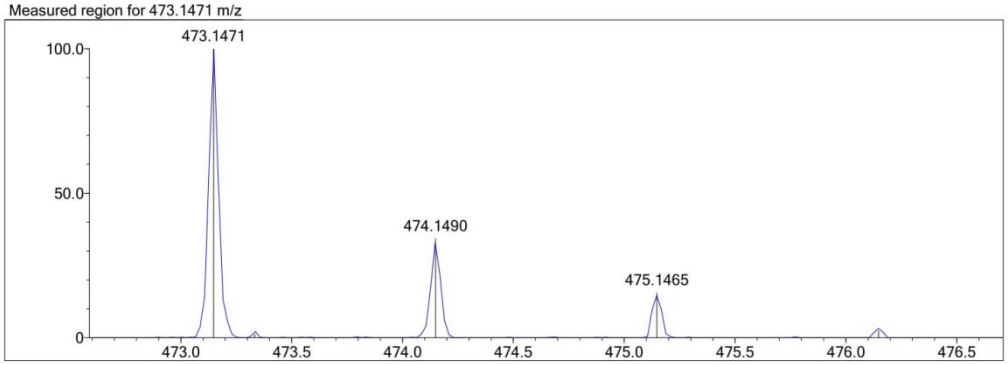

C26 H24 N4 O S2 [M+H]+ : Predicted region for 473.1464 m/z

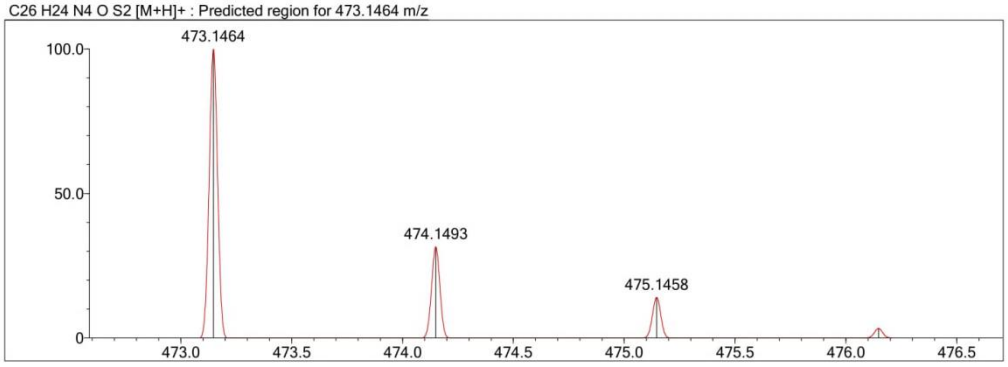

Rank	Score	Formula (M)	Ion	Meas. m/z	Pred. m/z	Df. (mDa)	Df. (ppm)	Iso	DBE
1	98.80	C26 H24 N4 O S2	[M+H]+	473.1471	473.1464	0.7	1.48	100.00	17.0

Figure 4.24. *Mass Spectrum of Compound **4f***

2-(9-Acridinylamino)-2-oxoethyl 4-methylpiperazine-1-carbodithioate (4g)

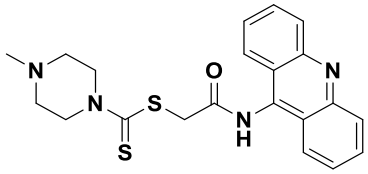

Yield: 95.3 %, **M.p.**: 243.2 °C.

FTIR (ATR, cm^{-1}): 3226 (amide N-H), 2783-2976 (aliphatic C-H), 1651 (C=O), 1435-1571(C=N and C=C), 1224-1288 (C=S), 758 (out of plane C-H bending).

^{1}H-NMR (300 MHz, DMSO-*d*$_6$; δ, ppm): 2.21 (3H, s, CH_3), 2.42-2.45 (4H, t, *J*= 4.50 Hz, piperazine $C_{3,5}$-H), 3.99 and 4.27 (4H, two s, piperazine $C_{2,6}$-H), 4.61 (2H, s, CO$\underline{CH_2}$), 7.58-7.63 (2H, t, *J*=7.51 Hz, Ar-H), 7.82-7.87 (2H, t, *J*=7.30 Hz, Ar-H), 8.15-8.18 (2H, d, *J*=8.70 Hz, Ar-H), 8.25-8.28 (2H, d, *J*=8.64 Hz, Ar-H), 10.94 (1H, s, -NH-).

^{13}C-NMR (75 MHz, DMSO-*d*$_6$; δ, ppm): 45.58 (CH_2), 50.26 (CH_3), 51.57 (CH_2), 54.45 (CH_2), 123.16 (CH), 125.30 (CH), 126.25 (CH), 129.26 (CH), 130.94 (CH), 140.52 (CH), 149.38 (C-9 in 9-aminoacridine), 167.40 (C=O), 195.11 (C=S).

HRMS (m/z): $[M+H]^+$ calcd for $C_{21}H_{22}N_4OS_2$: 411.1308 ; found 411.1307.

DOPNALAB

	Item	Value
	Acquired Date&Time	17.08.2016 12:02:49
	Acquired by	System Administrator
	Filename	C:\Users\dopnalab\Desktop\derya\wiam\yw-71.ispd
	Spectrum name	yw-71
	Sample name	yw-7
	Sample ID	
	Option	
	Comment	
	No. of Scans	10
	Resolution	4 [cm-1]
	Apodization	Happ-Genzel

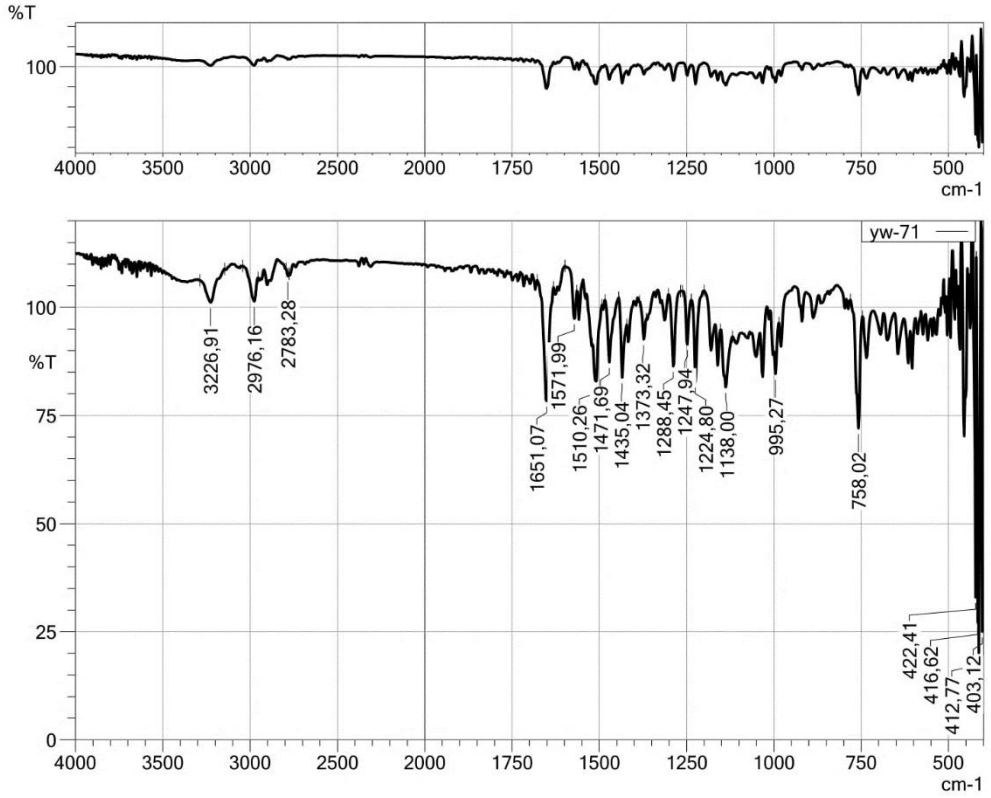

Figure 4.25. *IR Spectrum of Compound **4g***

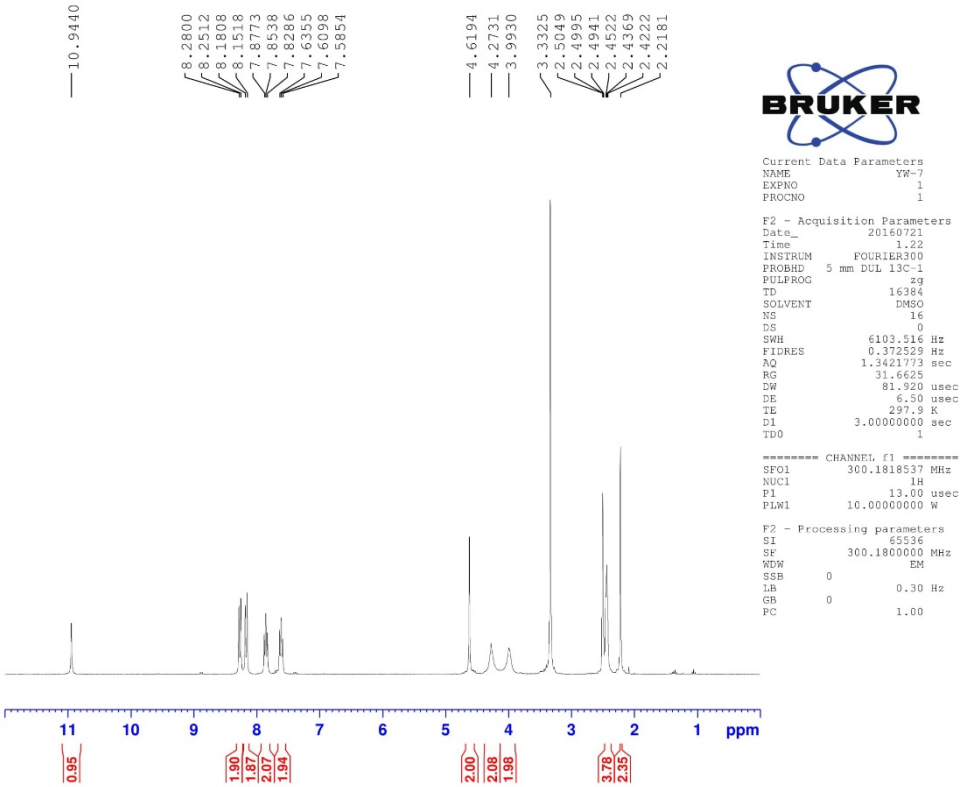

Figure 4.26. *The [1]H-NMR Spectrum of Compound* ***4g***

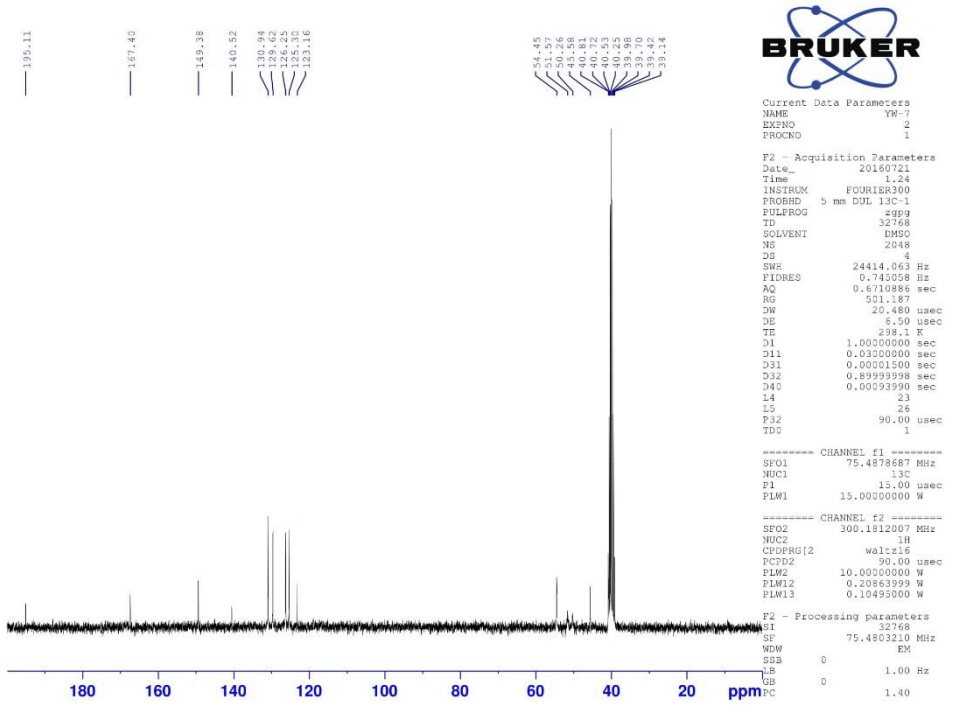

Figure 4.27. *The [13]C-NMR Spectrum of Compound* ***4g***

Formula Predictor Report - YW-7_20.lcd

Page 1 of 1

Data File: C:\LabSolutions\Data\Analiz\GTuran\YW-7_20.lcd

Elmt	Val.	Min	Max	Elmt	Val.	Min	Max	Elmt	Val.	Min	Max	Elmt	Val.	Min	Max	Use Adduct
H	1	22	22	O	2	0	5	Cl	1	0	0	I	3	0	0	H
C	4	0	30	F	1	0	3	Br	1	0	0					
N	3	0	6	S	2	0	3	Ru	2	0	0					

Error Margin (ppm): 5
HC Ratio: unlimited
Max Isotopes: 3
MSn Iso RI (%): 10.00

DBE Range: 0.0 - 20.0
Apply N Rule: yes
Isotope RI (%): 1.00
MSn Logic Mode: AND

Electron Ions: both
Use MSn Info: no
Isotope Res: 10000
Max Results: 500

Event#: 1 MS(E+) Ret. Time : 1.560 -> 2.053 Scan# : 235 -> 309

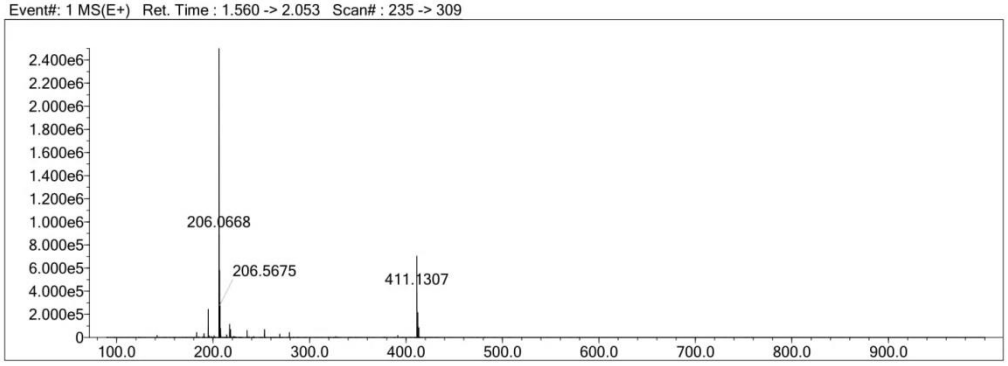

Measured region for 411.1307 m/z

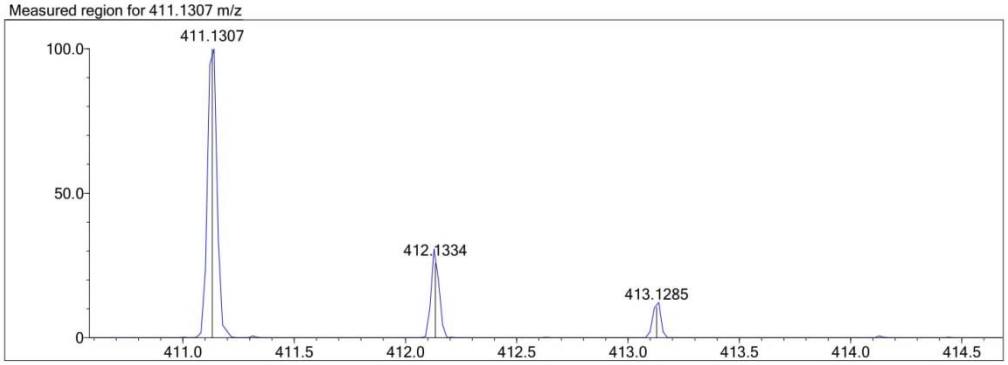

C21 H22 N4 O S2 [M+H]+ : Predicted region for 411.1308 m/z

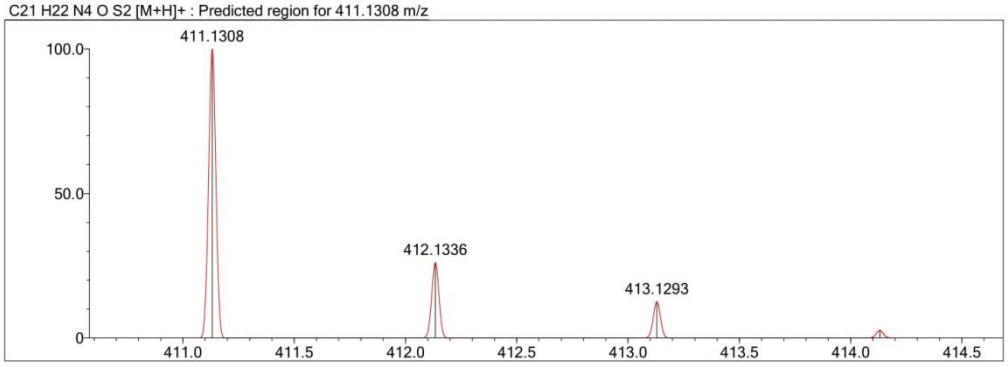

Rank	Score	Formula (M)	Ion	Meas. m/z	Pred. m/z	Df. (mDa)	Df. (ppm)	Iso	DBE
1	94.77	C21 H22 N4 O S2	[M+H]+	411.1307	411.1308	-0.1	-0.24	94.77	13.0

Figure 4.28. *Mass Spectrum of Compound **4g***

2-(9-Acridinylamino)-2-oxoethyl 4-(4-methoxyphenyl)piperazine-1-carbodithioate (4h)

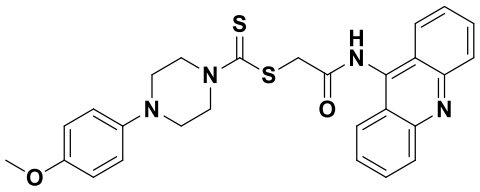

Yield: 89.4%, **M.p.**: 243.8 °C.

FTIR (ATR, cm-1): 3284 (amide N-H), 3057-2945 (aliphatic C-H), 1664 (C=O), 1431-1508 (C=N and C=C), 1215 (C=S), 707-756 (out of plane C-H bending),

^{1}H-NMR (300 MHz, DMSO-*d*$_6$; δ, ppm): 3.16-3.35 (4H, s, piperazine $C_{3,5}$-H), 3.68 (3H, s, O$\underline{CH_3}$), 4.14 and 4.42 (4H, two s, piperazine $C_{2,6}$-H), 4.66 (2H, s, CO$\underline{CH_2}$), 6.81-6.84 (2H, d, *J*=8.49 Hz, Ar-H), 6.90-6.93 (2H, d, *J*=8.37 Hz, Ar-H), 7.59-7.64 (2H, t, *J*=7.33 Hz, Ar-H), 7.82-7.87 (2H, t, *J*=7.36 Hz, Ar-H), 8.16-8.18 (2H, d, *J*=8.61 Hz, Ar-H), 8.27-8.30 (2H, d, *J*=8.55 Hz, Ar-H), 10.97 (1H, s, -NH-).

^{13}C-NMR (75 MHz, DMSO-*d*$_6$; δ, ppm): 49.82 (CH_2), 51.42 (CH_2), 55.67 (CH_3), 60.21 (CH_2), 114.82 (C), 118.37 (CH), 123.16 (CH), 125.30 (CH), 126.25 (CH), 129.62 (CH), 130.94 (CH), 140.50 (C), 144.87 (C), 149.39 (C),153.88 (C-9 in 9-aminoacridine), 167.39 (C=O), 195.24 (C=S).

HRMS (m/z): $[M+H]^+$ calcd for $C_{27}H_{26}N_4O_2S_2$: 503.1570; found 503.1547.

DOPNALAB

	Item	Value
	Acquired Date&Time	17.08.2016 12:08:19
	Acquired by	System Administrator
	Filename	C:\Users\dopnalab\Desktop\derya\wiam\yw-81.ispd
	Spectrum name	yw-81
	Sample name	yw-8
	Sample ID	
	Option	
	Comment	
	No. of Scans	10
	Resolution	4 [cm-1]
	Apodization	Happ-Genzel

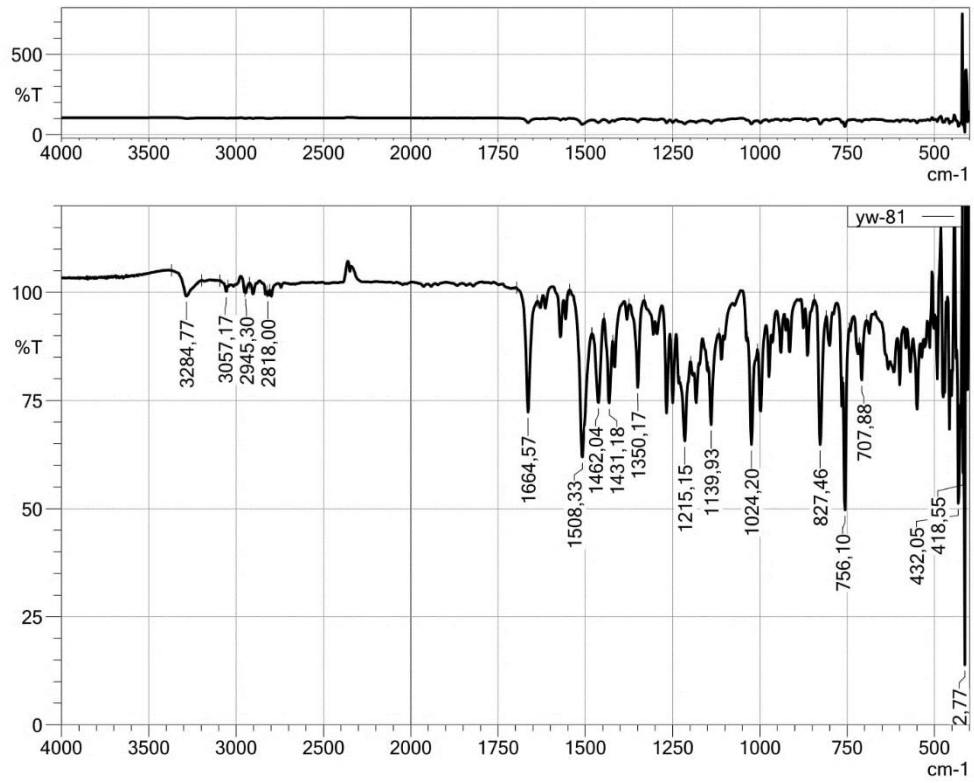

Figure 4.29. *IR Spectrum of Compound* ***4h***

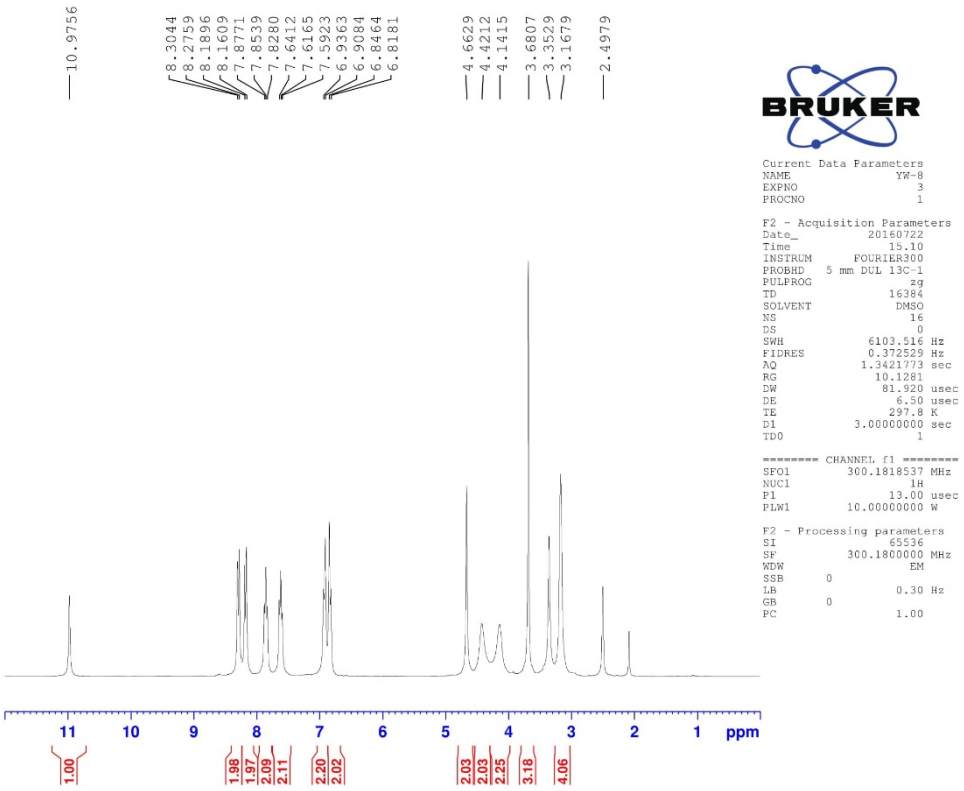

Figure 4.30. *The [1]H-NMR Spectrum of Compound* ***4h***

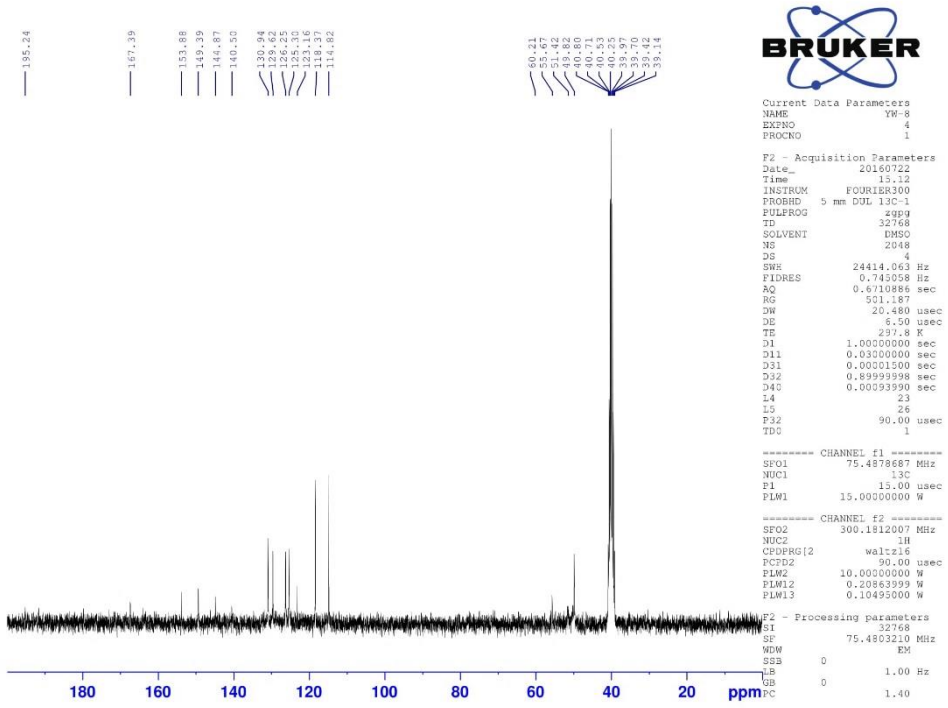

Figure 4.31. *The [13]C-NMR Spectrum of Compound* ***4h***

Formula Predictor Report - YW8-R_5.lcd

Page 1 of 1

Data File: C:\LabSolutions\Data\Analiz\GTuran\YW8-R_5.lcd

Elmt	Val.	Min	Max	Elmt	Val.	Min	Max	Elmt	Val.	Min	Max	Elmt	Val.	Min	Max	Use Adduct
H	1	26	40	O	2	0	2	Cl	1	0	0	I	3	0	0	H
C	4	6	27	F	1	0	0	Br	1	0	0					
N	3	0	9	S	2	0	2	Ru	2	0	0					

Error Margin (ppm): 10
HC Ratio: unlimited
Max Isotopes: 3
MSn Iso RI (%): 10.00

DBE Range: 9.0 - 30.0
Apply N Rule: yes
Isotope RI (%): 1.00
MSn Logic Mode: AND

Electron Ions: both
Use MSn Info: no
Isotope Res: 10000
Max Results: 500

Event#: 1 MS(E+) Ret. Time : 6.107 -> 6.200 - 8.547 -> 9.315 Scan# : 917 -> 931 - 1283 -> 1399

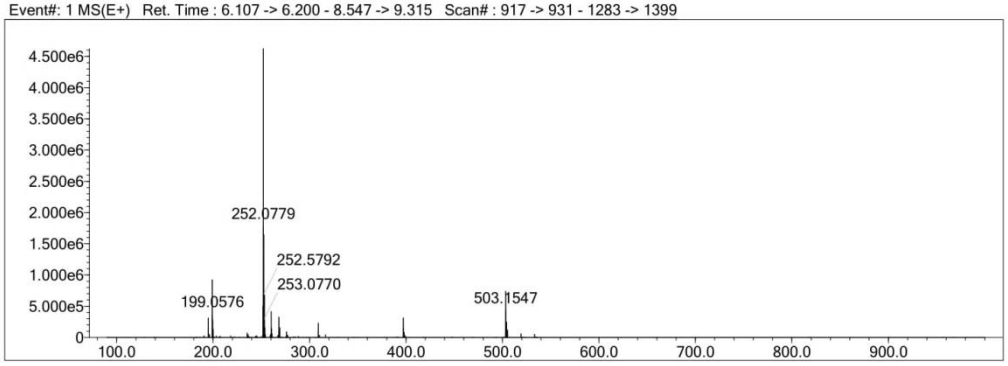

Measured region for 503.1547 m/z

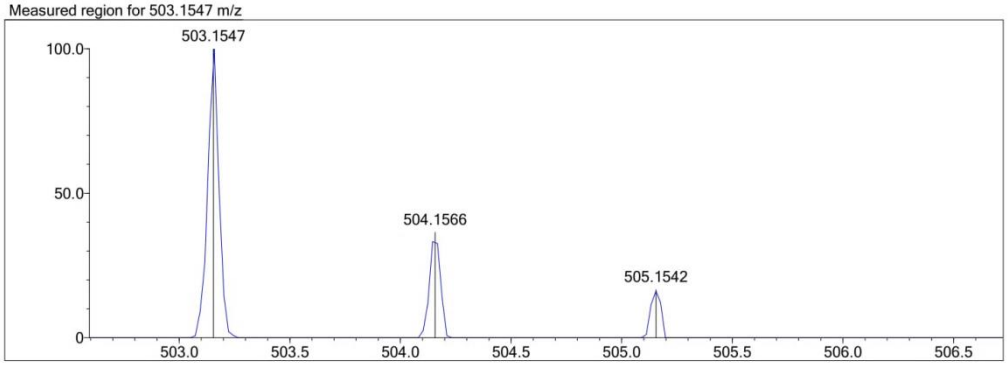

C27 H26 N4 O2 S2 [M+H]+ : Predicted region for 503.1570 m/z

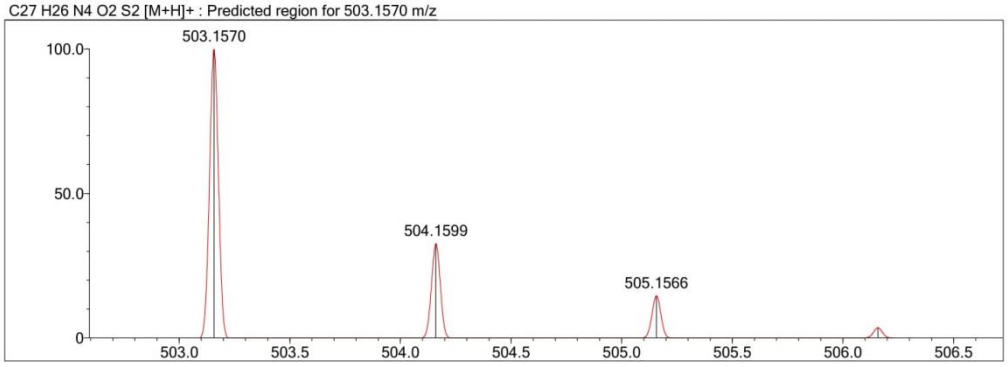

Rank	Score	Formula (M)	Ion	Meas. m/z	Pred. m/z	Df. (mDa)	Df. (ppm)	Iso	DBE
1	88.35	C27 H26 N4 O2 S2	[M+H]+	503.1547	503.1570	-2.3	-4.57	97.01	17.0

Figure 4.32. *Mass Spectrum of Compound **4h***

2-(9-Acridinylamino)-2-oxoethyl 4-(4-chlorophenyl)piperazine-1-carbodithioate (4i)

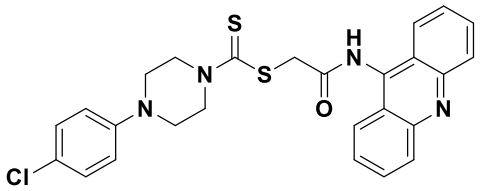

Yield: 97.0%, **M.p.**: 213.6 °C.

FTIR (ATR, cm^{-1}): 3223 (amide N-H), 2706-2912 (aliphatic C-H), 1672 (C=O), 1417-1573 (C=N and C=C), 1226 (C=S), 815 (para aromatic substitution), 756 (out of plane C-H bending).

^{1}H-NMR (300 MHz, DMSO-d_6; δ, ppm): 2.44-2.50 (4H, q, *J*=5.77 Hz ,piperazine $C_{3,5}$-H), 4.02 and 4.45 (4H, two bs, piperazine $C_{2,6}$-H), 4.60 (2H, s, CO$\underline{CH_2}$), 6.97-7.00 (2H, d, *J*=9.12 Hz, Ar-H), 7.25-7.28 (2H, d, *J*=8.97 Hz, Ar-H), 7.57-7.62 (2H, t, *J*=7.53 Hz, Ar-H), 7.81-7.85 (2H, t, *J*=5.88 Hz, Ar-H), 8.14-8.17 (2H, d, *J*=8.70 Hz, Ar-H), 8.27-8.30 (2H, d, *J*=8.61 Hz, Ar-H), 11.22 (1H, s, -NH-).

^{13}C-NMR (75 MHz, DMSO-d_6; δ, ppm): 45.59 (CH_2), 49.82 (CH_2), 51.03 (CH_2), 117.26 (CH), 117.97 (CH), 123.15 (CH), 125.24 (CH), 126.19 (CH), 129.21 (CH), 129.26 (CH), 129.56 (CH), 130.92 (CH), 140.65 (C), 149.36 (C-9 in 9-aminoacridine), 167.39 (C=O), 195.34 (C=S).

HRMS (m/z): $[M+H]^+$ calcd for $C_{26}H_{23}ClN_4OS_2$: 507.1075 ; found 507.1069.

DOPNALAB

	Item	Value
	Acquired Date&Time	17.08.2016 12:10:19
	Acquired by	System Administrator
	Filename	C:\Users\dopnalab\Desktop\derya\wiam\yw-91.ispd
	Spectrum name	yw-91
	Sample name	yw-9
	Sample ID	
	Option	
	Comment	
	No. of Scans	10
	Resolution	4 [cm-1]
	Apodization	Happ-Genzel

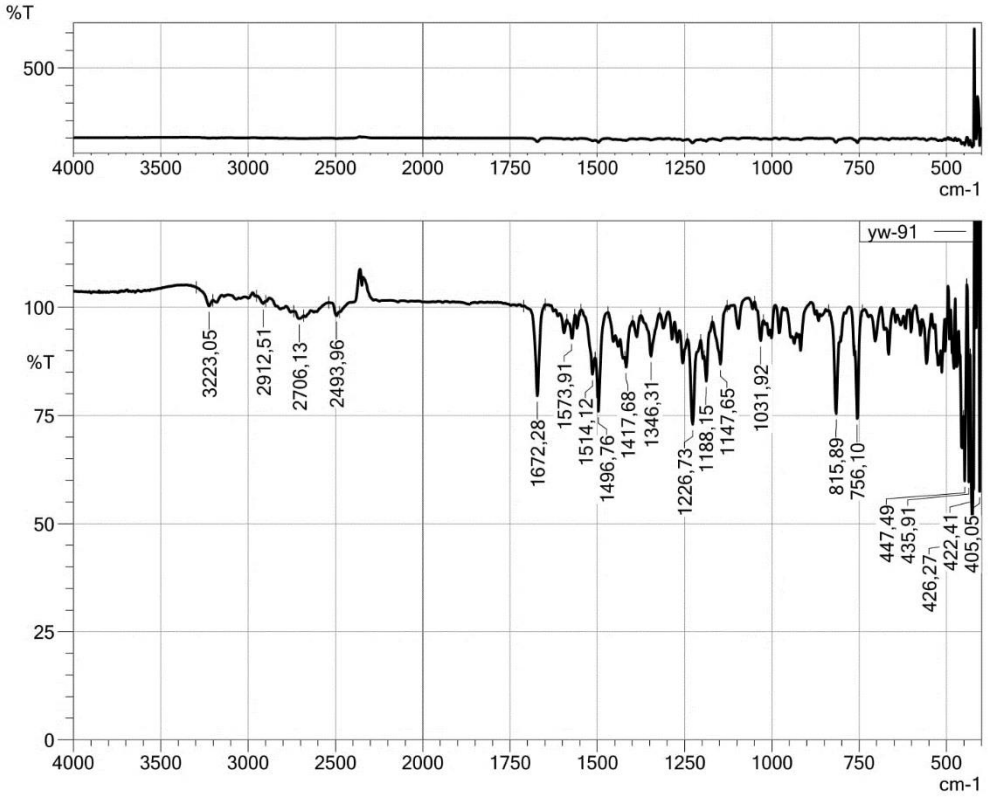

Figure 4.33. *IR Spectrum of Compound **4i***

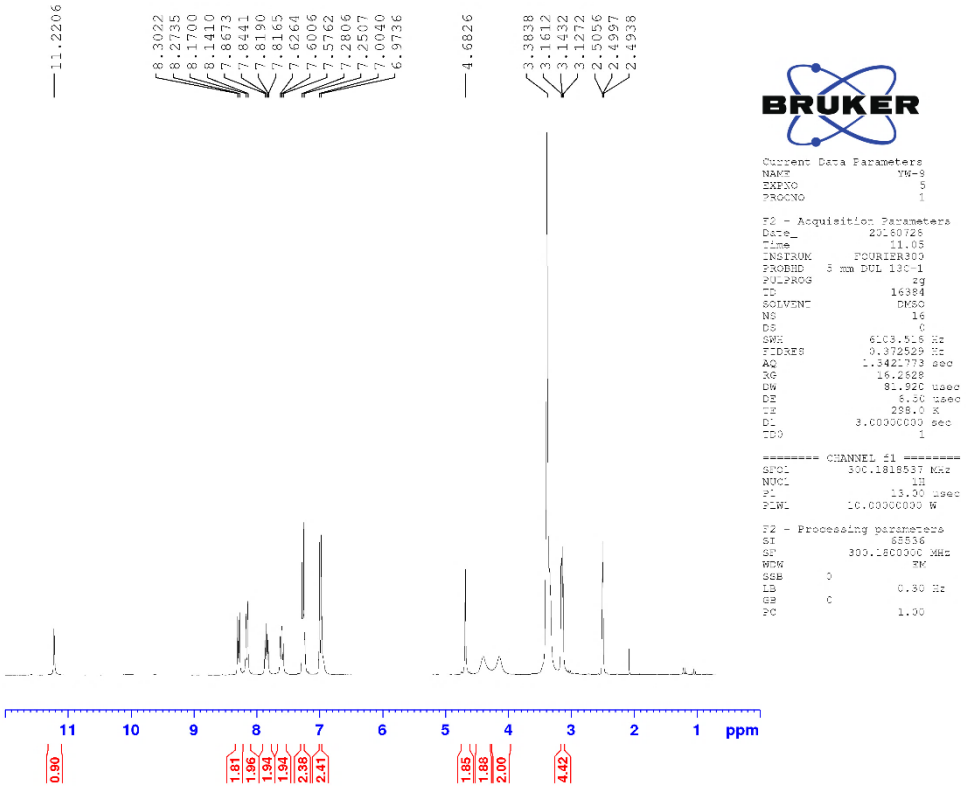

Figure 4.34. *The [1]H-NMR Spectrum of Compound **4i***

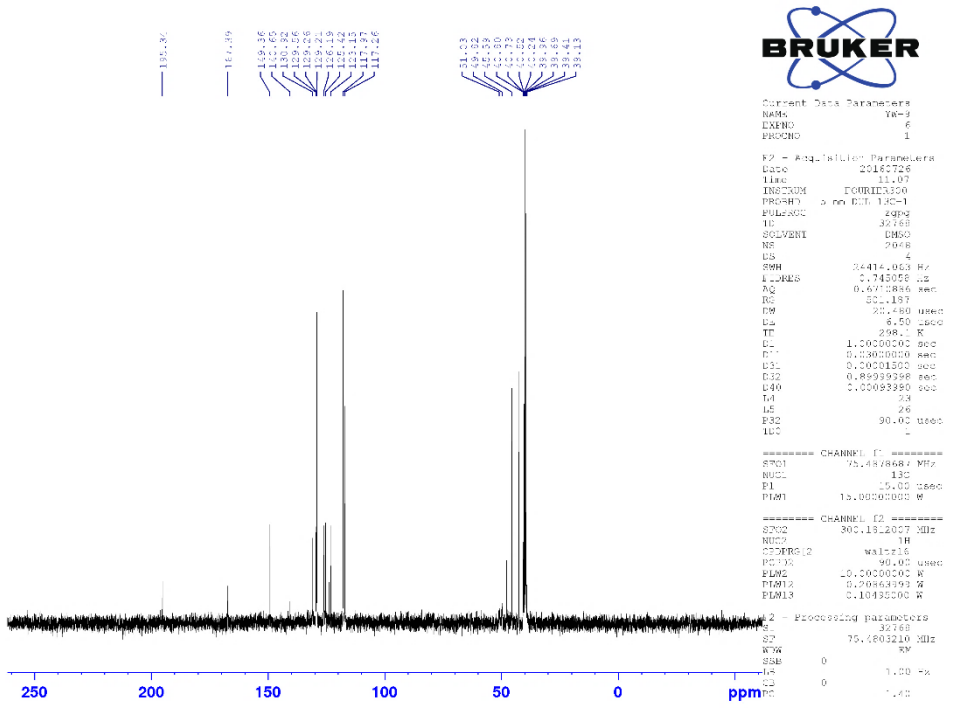

Figure 4.35. *The [13]C-NMR Spectrum of Compound **4i***

Formula Predictor Report - YW-9_22.lcd

Page 1 of 1

Data File: C:\LabSolutions\Data\Analiz\GTuran\YW-9_22.lcd

Elmt	Val.	Min	Max	Elmt	Val.	Min	Max	Elmt	Val.	Min	Max	Elmt	Val.	Min	Max	Use Adduct
H	1	23	23	O	2	0	5	Cl	1	0	1	I	3	0	0	H
C	4	0	40	F	1	0	3	Br	1	0	0					
N	3	0	6	S	2	0	3	Ru	2	0	0					

Error Margin (ppm): 5
HC Ratio: unlimited
Max Isotopes: 3
MSn Iso RI (%): 10.00

DBE Range: 0.0 - 20.0
Apply N Rule: yes
Isotope RI (%): 1.00
MSn Logic Mode: AND

Electron Ions: both
Use MSn Info: no
Isotope Res: 10000
Max Results: 500

Event#: 1 MS(E+) Ret. Time : 8.093 -> 8.693 - 9.560 -> 10.891 Scan# : 1215 -> 1305 - 1435 -> 1635

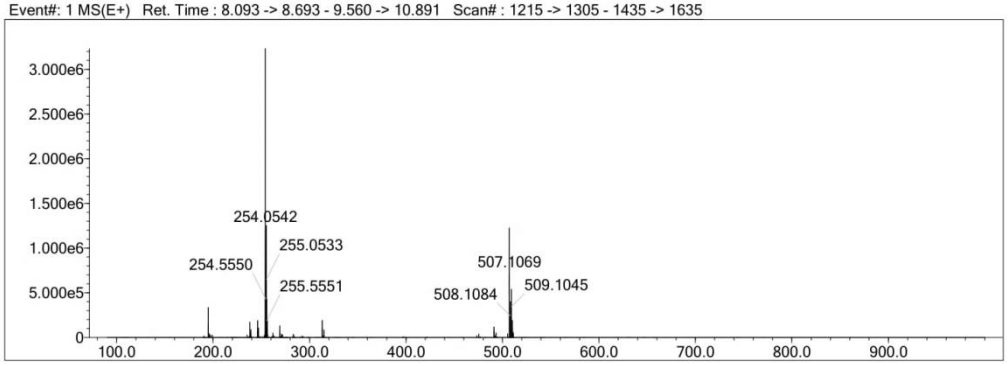

Measured region for 507.1069 m/z

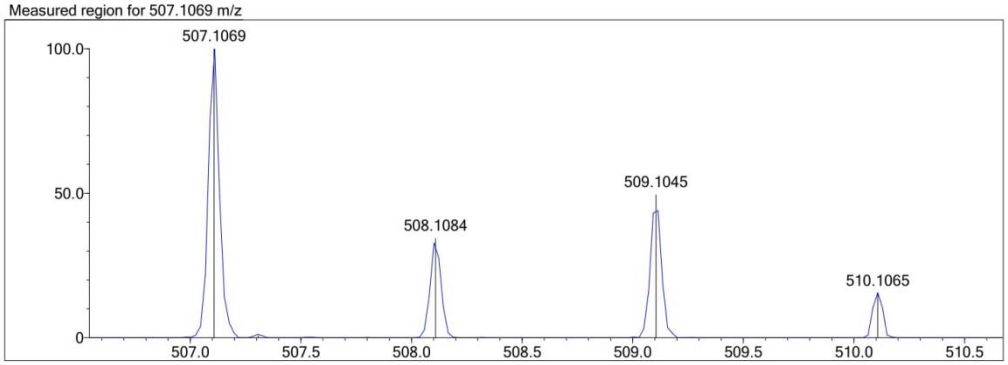

C26 H23 N4 O S2 Cl [M+H]+ : Predicted region for 507.1075 m/z

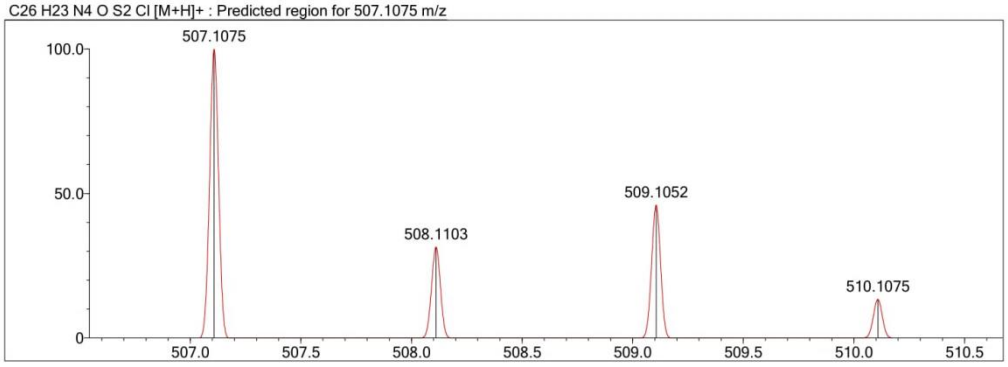

Rank	Score	Formula (M)	Ion	Meas. m/z	Pred. m/z	Df. (mDa)	Df. (ppm)	Iso	DBE
1	91.62	C26 H23 N4 O S2 Cl	[M+H]+	507.1069	507.1075	-0.6	-1.18	92.03	17.0

Figure 4.36. *Mass Spectrum of Compound **4i***

2-(9-Acridinylamino)-2-oxoethyl 4-(pyrimidin-2-yl)piperazine-1-carbodithioate (4j)

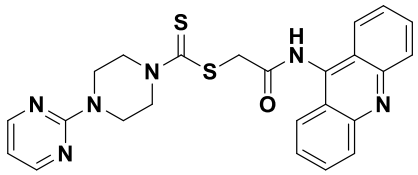

Yield: 84.3%, **M.p.**: 248.4 °C.

FTIR (ATR, cm^{-1}): 3263 (amide N-H), 2852-2897 (aliphatic C-H), 1662 (C=O), 1425-1583 (C=N and C=C), 1222-1257 (C=S), 759-792 (out of plane C-H bending).

^{1}H-NMR (300 MHz, DMSO-*d*$_6$; δ, ppm): 3.91 (4H, s , piperazine $C_{3,5}$-H), 4.13 and 4.38 (4H, two s, piperazine $C_{2,6}$-H), 4.68 (2H, s, CO$\underline{CH_2}$), 6.67-6.70 (1H, t, *J*=4.74 Hz, Ar-H), 7.58-7.63 (2H, t, *J*=7.56 Hz, Ar-H), 7.82-7.87 (2H, t, *J*=7.42 Hz, Ar-H), 8.14-8.18 (2H, d, *J*=8.73 Hz, Ar-H), 8.27-8.30 (2H, d, *J*=8.64 Hz, Ar-H), 8.39-8.41 (2H, d, *J*=4.74 Hz, Ar-H), 11.16 (1H, s, -NH-).

^{13}C-NMR (75 MHz, DMSO-*d*$_6$; δ, ppm): 42. 97 (CH_2), 49.82 (CH_2), 51.20 (CH_2), 111.11 (C), 123.16 (CH), 125.40 (CH), 126.20 (CH), 129.57 (CH), 130.93 (CH), 140.63 (C), 149.37 (CH), 158.48 (C), 161.29 (C-9 in 9-aminoacridine), 167.39 (C=O), 195.43 (C=S).

HRMS (m/z): $[M+H]^+$ calcd for $C_{24}H_{22}N_6OS_2$: 475.1369; found 475.1366.

DOPNALAB

	Item	Value
	Acquired Date&Time	17.08.2016 12:14:18
	Acquired by	System Administrator
	Filename	C:\Users\dopnalab\Desktop\derya\wiam\yw-101.ispd
	Spectrum name	yw-101
	Sample name	yw-10
	Sample ID	
	Option	
	Comment	
	No. of Scans	10
	Resolution	4 [cm-1]
	Apodization	Happ-Genzel

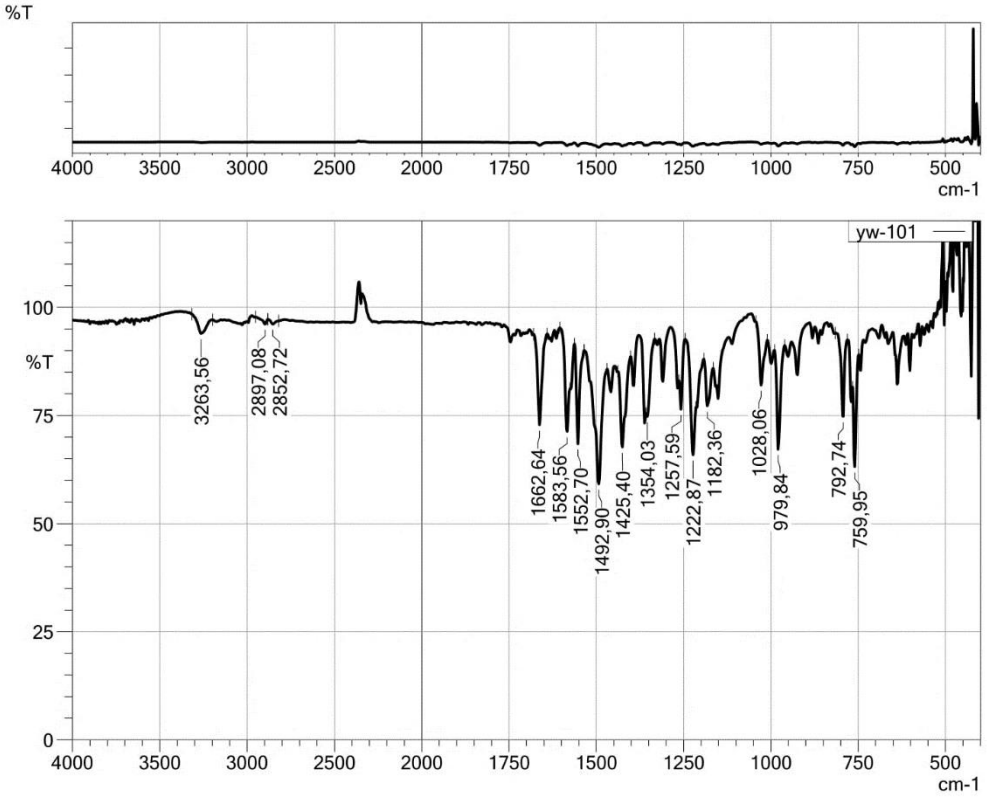

Figure 4.37. *IR Spectrum of Compound **4j***

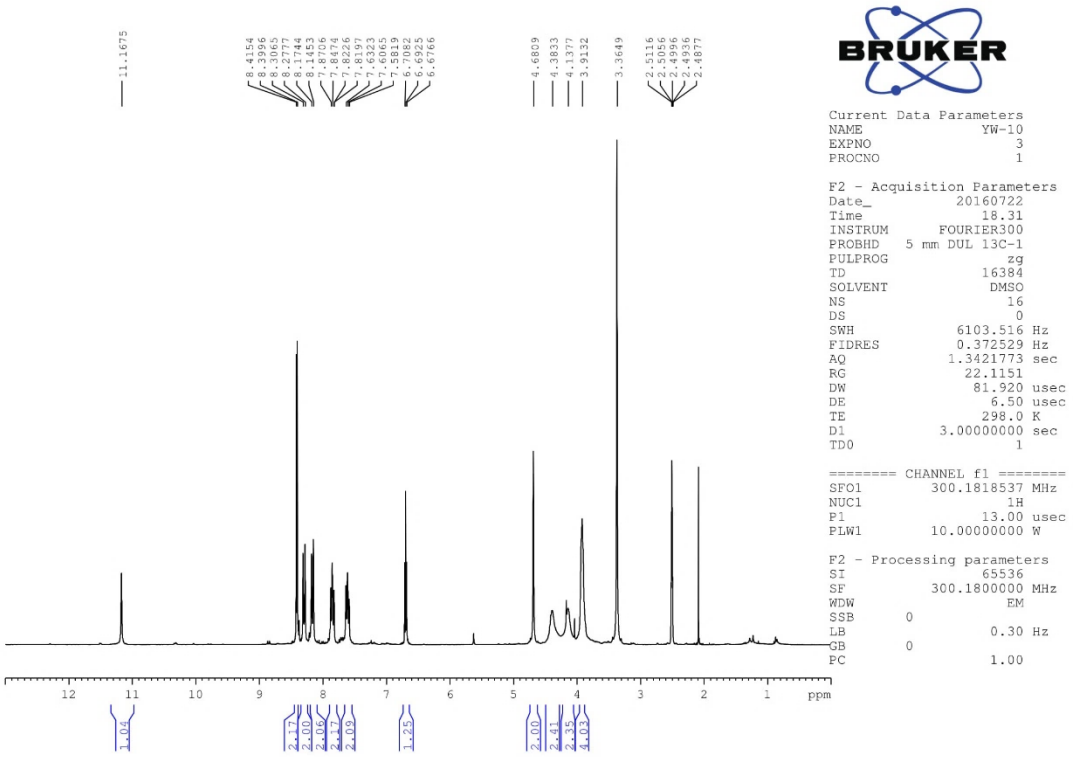

Figure 4.38. *The [1]H-NMR Spectrum of Compound* ***4j***

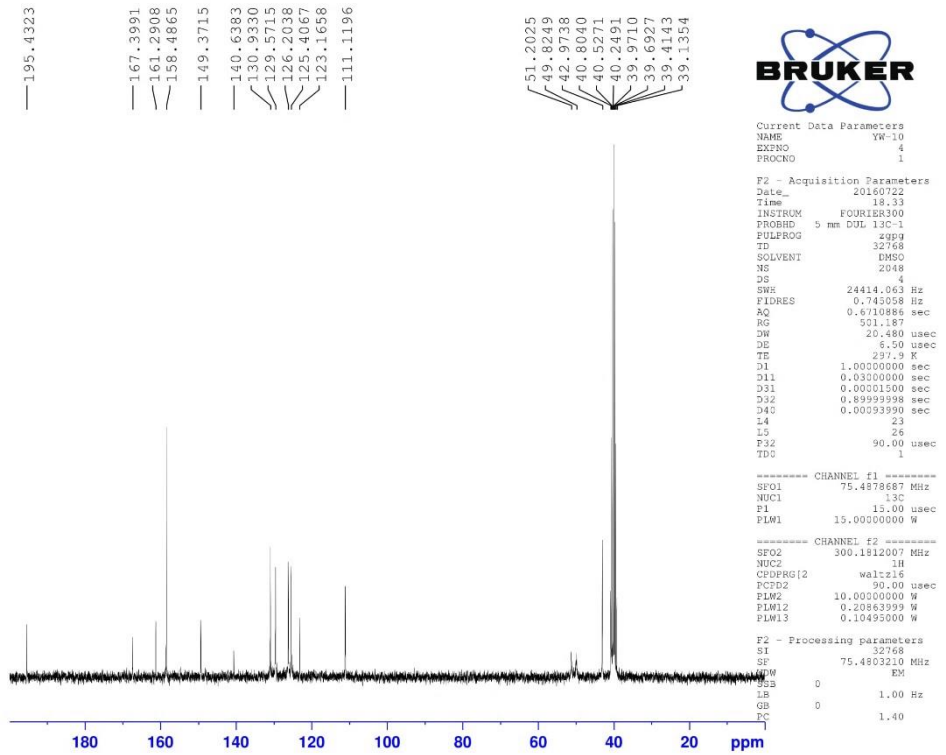

Figure 4.39. *The [13]C-NMR Spectrum of Compound* ***4j***

Formula Predictor Report - YW-10_23.lcd

Page 1 of 1

Data File: C:\LabSolutions\Data\Analiz\GTuran\YW-10_23.lcd

Elmt	Val.	Min	Max	Elmt	Val.	Min	Max	Elmt	Val.	Min	Max	Elmt	Val.	Min	Max	Use Adduct
H	1	22	22	O	2	0	5	Cl	1	0	0	I	3	0	0	H
C	4	0	40	F	1	0	3	Br	1	0	0					
N	3	0	6	S	2	0	3	Ru	2	0	0					

Error Margin (ppm):	5	DBE Range:	0.0 - 20.0	Electron Ions:	both
HC Ratio:	unlimited	Apply N Rule:	yes	Use MSn Info:	no
Max Isotopes:	3	Isotope RI (%):	1.00	Isotope Res:	10000
MSn Iso RI (%):	10.00	MSn Logic Mode:	AND	Max Results:	500

Event#: 1 MS(E+) Ret. Time : 5.413 -> 6.120 - 6.600 -> 9.525 Scan# : 813 -> 919 - 991 -> 1429

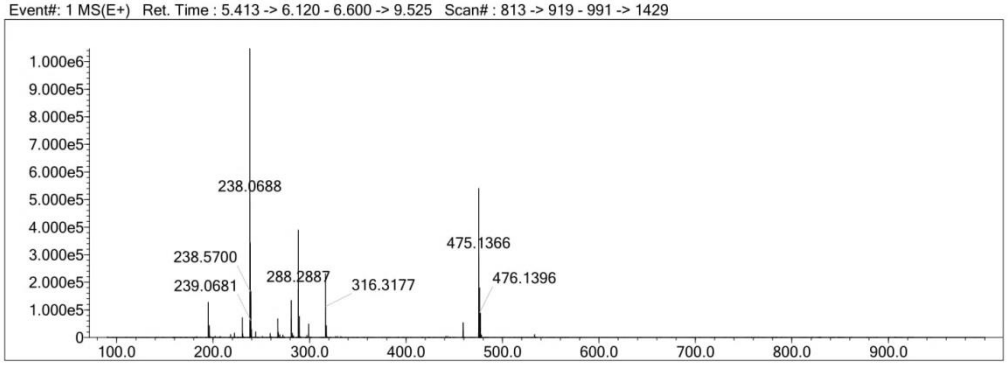

Measured region for 475.1366 m/z

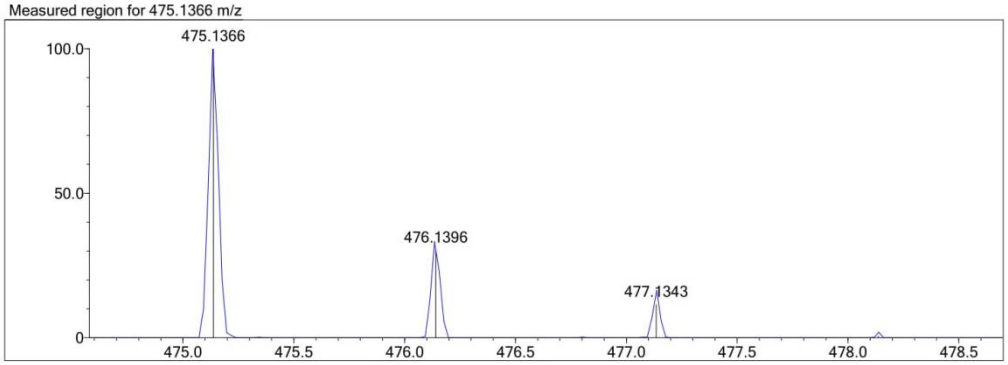

C24 H22 N6 O S2 [M+H]+ : Predicted region for 475.1369 m/z

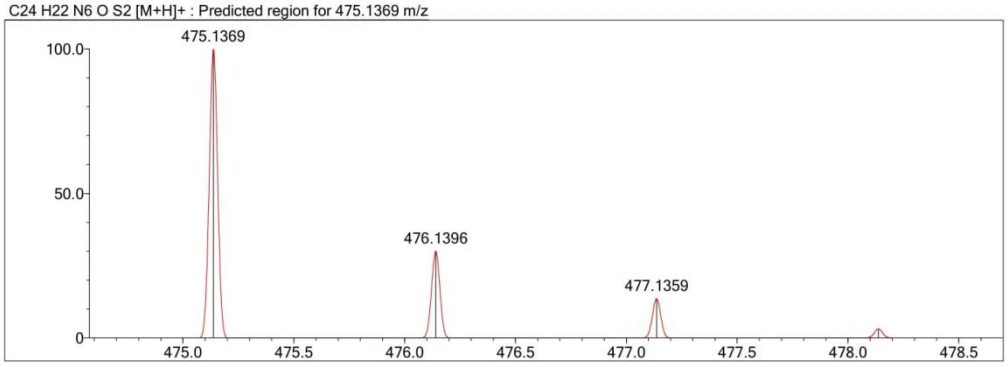

Rank	Score	Formula (M)	Ion	Meas. m/z	Pred. m/z	Df. (mDa)	Df. (ppm)	Iso	DBE
1	91.24	C24 H22 N6 O S2	[M+H]+	475.1366	475.1369	-0.3	-0.63	91.24	17.0

Figure 4.40. *Mass Spectrum of Compound **4j***

2-(9-Acridinylamino)-2-oxoethyl 4-benzylpiperazine-1-carbodithioate (4k)

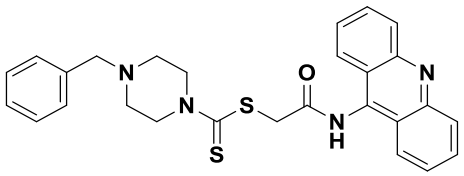

Yield: 91.4%, **M.p.**: 222.3 °C.

FTIR (ATR, cm^{-1}): 3248 (amide N-H), 2818-2908 (aliphatic C-H), 1668 (C=O), 1417-1510 (C=N and C=C), 1230 (C=S), 731-756 (out of plane C-H bending).

^{1}H-NMR (300 MHz, DMSO-*d*$_6$; δ, ppm): 3.53 and 3.99 (4H, two bs, piperazine $C_{2,6}$-H), 4.28 (2H, s, C_6H_5-$\underline{CH_2}$-), 4.62 (2H, s, CO$\underline{CH_2}$), 7.26-7.32 (5H, m, Ar-H), 7.57-7.62 (2H, t, *J*=7.51 Hz, Ar-H), 7.82-7.87 (2H, t, *J*=7.51 Hz, Ar-H), 8.14-8.17 (2H, d, *J*=8.70 Hz, Ar-H), 8.25-8.28 (2H, d, *J*=8.64 Hz, Ar-H), 11.05 (1H, s, -NH-).

^{13}C-NMR (75 MHz, DMSO-*d*$_6$; δ, ppm): 50.38 (CH_2), 51.66 (CH_2), 52.43 (CH_2), 61.76 (CH_2), 123.15 (C), 125.34 (CH), 126.22 (CH), 127.60 (CH), 128.73 (CH), 129.42 (CH), 129.59 (CH), 130.93 (CH), 138.01 (C), 140.58 (C), 149.37 (C-9 in 9-aminoacridine), 167.41 (C=O),195.00 (C=S).

HRMS (m/z): $[M+H]^+$ calcd for $C_{27}H_{26}N_4OS_2$: 487.1621; found 487.1622.

DOPNALAB

	Item	Value
	Acquired Date&Time	17.08.2016 12:17:19
	Acquired by	System Administrator
	Filename	C:\Users\dopnalab\Desktop\derya\wiam\yw-111.ispd
	Spectrum name	yw-111
	Sample name	yw-11
	Sample ID	
	Option	
	Comment	
	No. of Scans	10
	Resolution	4 [cm-1]
	Apodization	Happ-Genzel

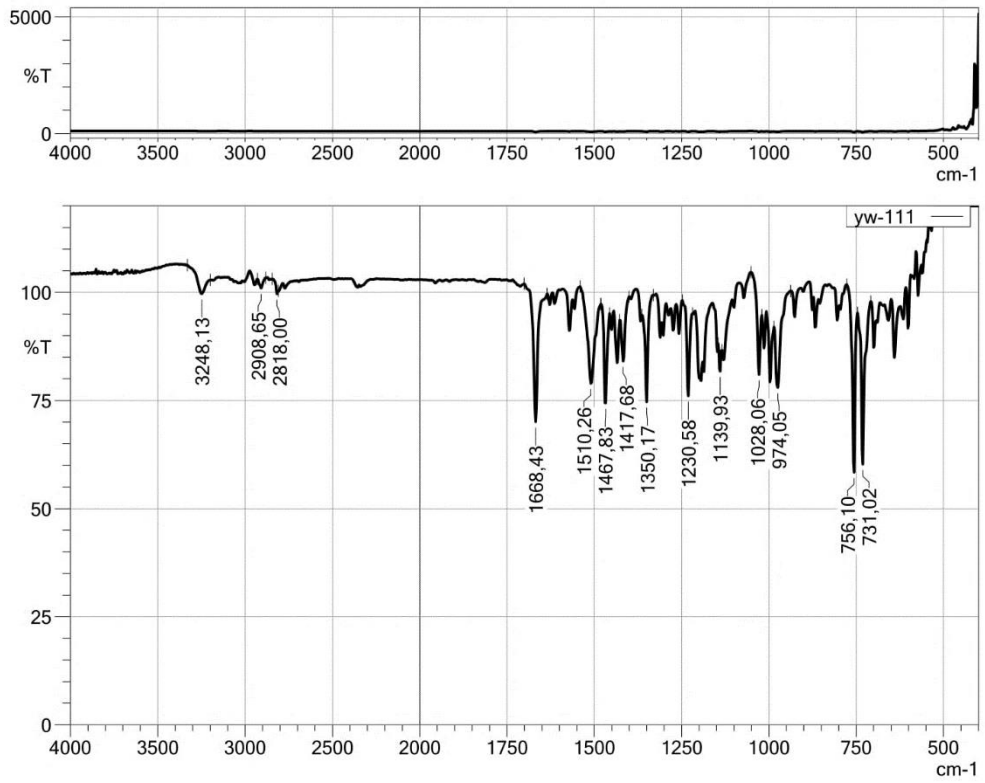

Figure 4.41. *IR Spectrum of Compound **4k***

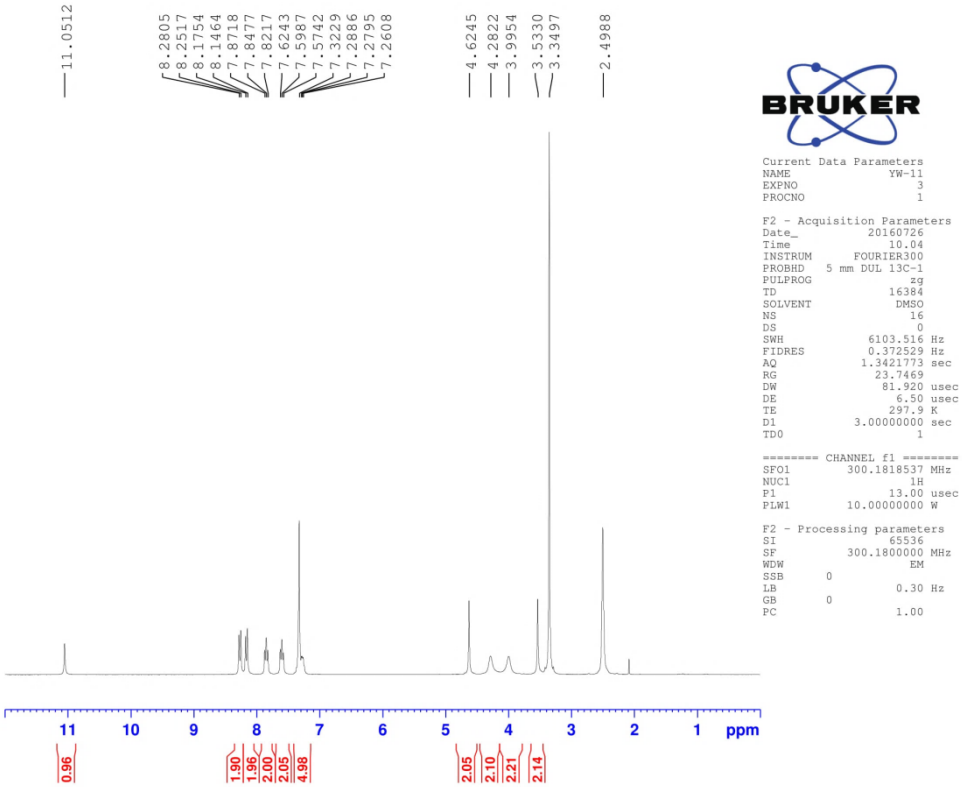

Figure 4.42. *The [1]H-NMR Spectrum of Compound* ***4k***

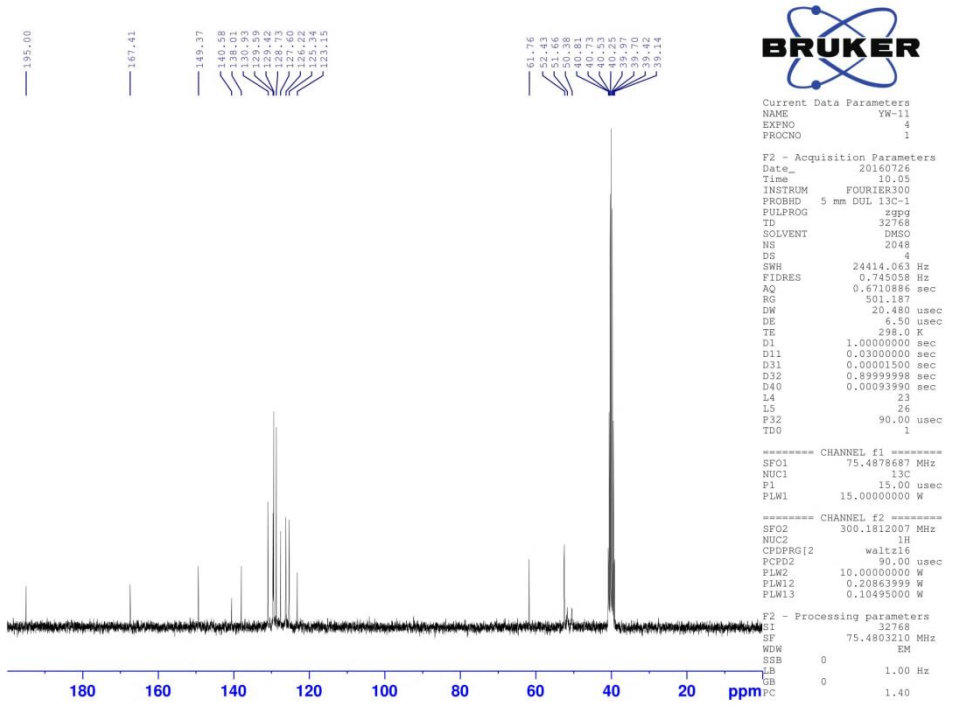

Figure 4.43. *The [13]C-NMR Spectrum of Compound* ***4k***

Formula Predictor Report - YW-11_24.lcd

Page 1 of 1

Data File: C:\LabSolutions\Data\Analiz\GTuran\YW-11_24.lcd

Elmt	Val.	Min	Max	Elmt	Val.	Min	Max	Elmt	Val.	Min	Max	Elmt	Val.	Min	Max	Use Adduct
H	1	26	26	O	2	0	5	Cl	1	0	0	I	3	0	0	H
C	4	0	40	F	1	0	3	Br	1	0	0					
N	3	0	6	S	2	0	3	Ru	2	0	0					

Error Margin (ppm): 5
HC Ratio: unlimited
Max Isotopes: 3
MSn Iso RI (%): 10.00

DBE Range: 0.0 - 20.0
Apply N Rule: yes
Isotope RI (%): 1.00
MSn Logic Mode: AND

Electron Ions: both
Use MSn Info: no
Isotope Res: 10000
Max Results: 500

Event#: 1 MS(E+) Ret. Time : 4.027 -> 4.213 - 8.947 -> 10.536 Scan# : 605 -> 633 - 1343 -> 1581

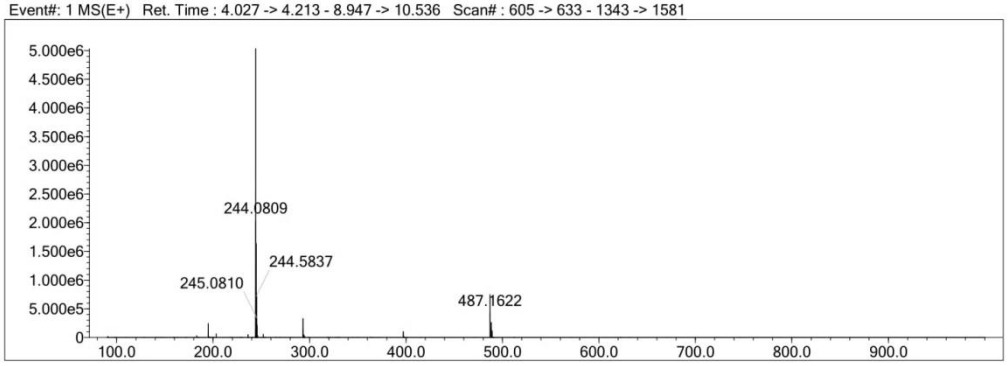

Measured region for 487.1622 m/z

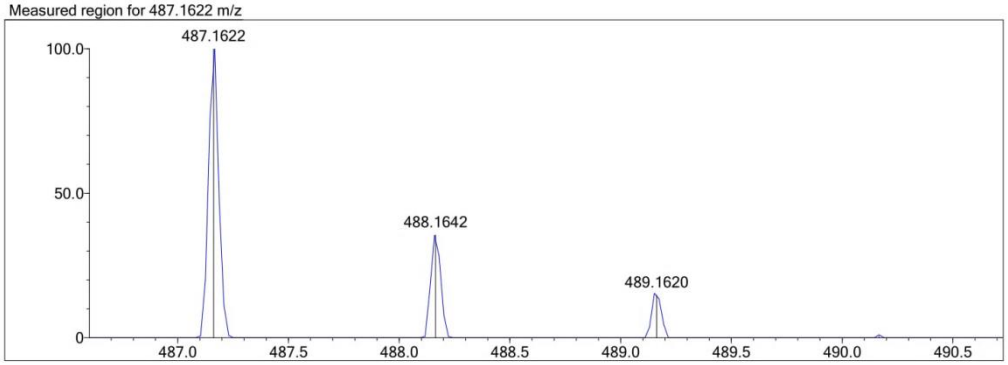

C27 H26 N4 O S2 [M+H]+ : Predicted region for 487.1621 m/z

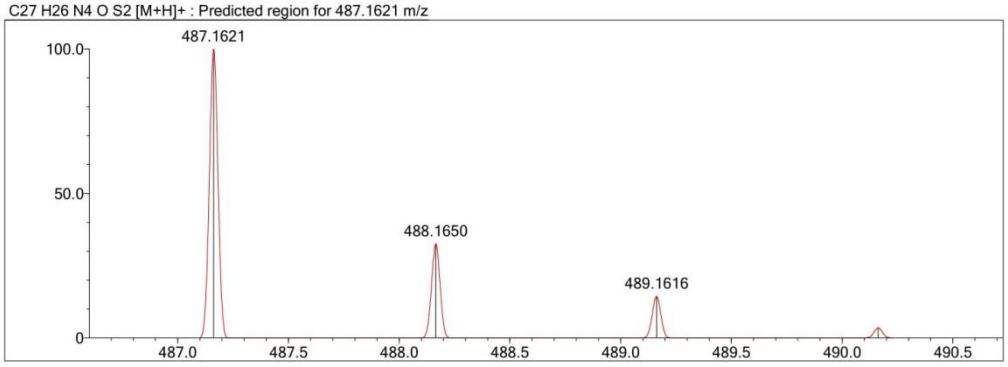

Rank	Score	Formula (M)	Ion	Meas. m/z	Pred. m/z	Df. (mDa)	Df. (ppm)	Iso	DBE
1	86.54	C27 H26 N4 O S2	[M+H]+	487.1622	487.1621	0.1	0.21	86.54	17.0

Figure 4.44. *Mass Spectrum of Compound **4k***

2-(9-Acridin-ylamino)-2-oxoethyl 4-cyclohexylpiperazine-1-carbodithioate (4l)

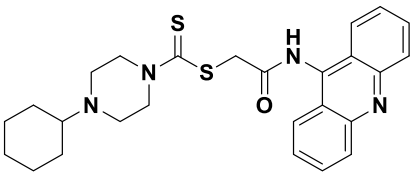

Yield: 88.4%, **M.p.**: 225.4°C.

FTIR (ATR, cm^{-1}): 3309 (amide N-H), 2357-2931 (aliphatic C-H), 1676 (C=O), 1469-1566 (C=N and C=C), 1230-1274 (C=S), 754-866 (out of plane C-H bending).

^{1}H-NMR (300 MHz, DMSO-d_6; δ, ppm): 1.03-1.18 (6H, m , cyclohexyl - CH_2-), 1.54-1.57 (1H, d, *J*=11.19 Hz, cyclohexyl - CH-), 1.72 (4H, s, cyclohexyl –CH_2-), 2.60 (4H, s, piperazine $C_{3,5}$-H), 3.94 and 4.24 (4H, two bs, piperazine $C_{2,6}$-H), 4.62 (2H, s, CO$\underline{CH_2}$), 7.57-7.62 (2H, t, *J*=7.51 Hz, Ar-H), 7.82-7.87 (2H, t, *J*=7.62 Hz, Ar-H), 8.14-8.17 (2H, d, *J*=8.67 Hz, Ar-H), 8.25-8.28 (2H, d, *J*=8.64 Hz, Ar-H), 11.04 (1H, s, -NH-).

^{13}C-NMR (75 MHz, DMSO-d_6; δ, ppm): 25.68 (CH_2), 26.26 (CH_2), 28.76 (CH_2), 48.59 (CH_2), 50.90 (CH_2), 52.19 (CH_2), 62.73 (CH), 123.15 (C), 125.36 (CH), 126.20 (CH), 129.58 (CH), 130.93 (CH), 140.62 (C), 149.37 (C-9 in 9-aminoacridine), 167.44 (C=O), 194.71 (C=S).

HRMS (m/z): $[M+H]^+$ calcd for $C_{26}H_{30}N_4OS_2$: 479.1934 ; found 479.1929.

DOPNALAB

	Item	Value
	Acquired Date&Time	17.08.2016 12:19:04
	Acquired by	System Administrator
	Filename	C:\Users\dopnalab\Desktop\derya\wiam\yw-121.ispd
	Spectrum name	yw-121
	Sample name	yw-12
	Sample ID	
	Option	
	Comment	
	No. of Scans	10
	Resolution	4 [cm-1]
	Apodization	Happ-Genzel

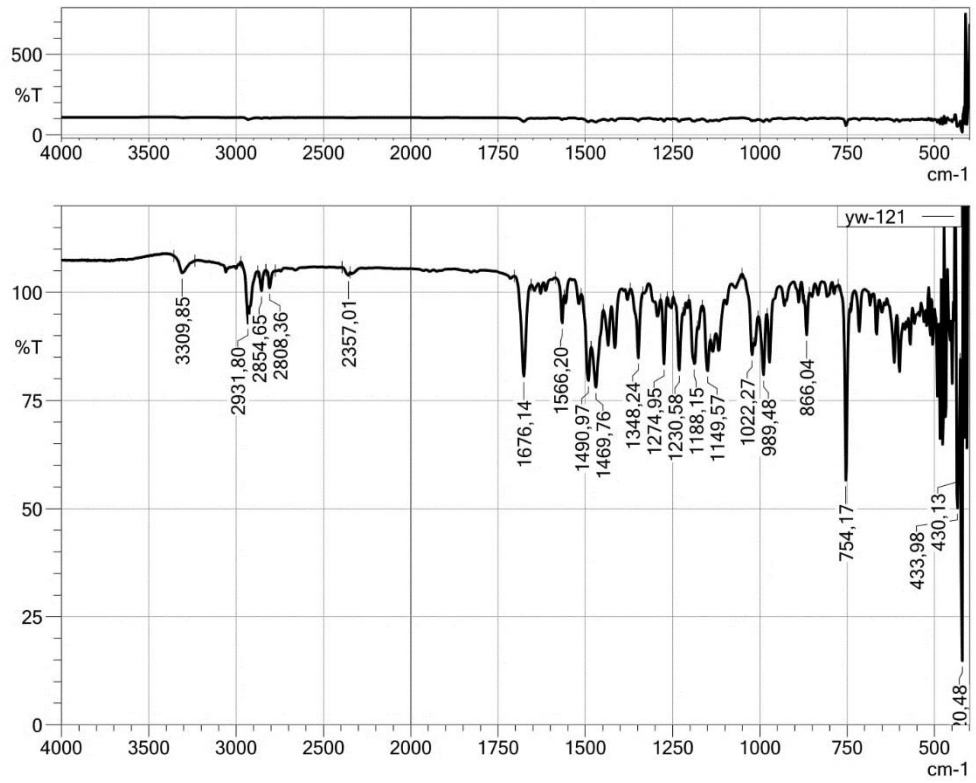

Figure 4.45. *IR Spectrum of Compound* ***4l***

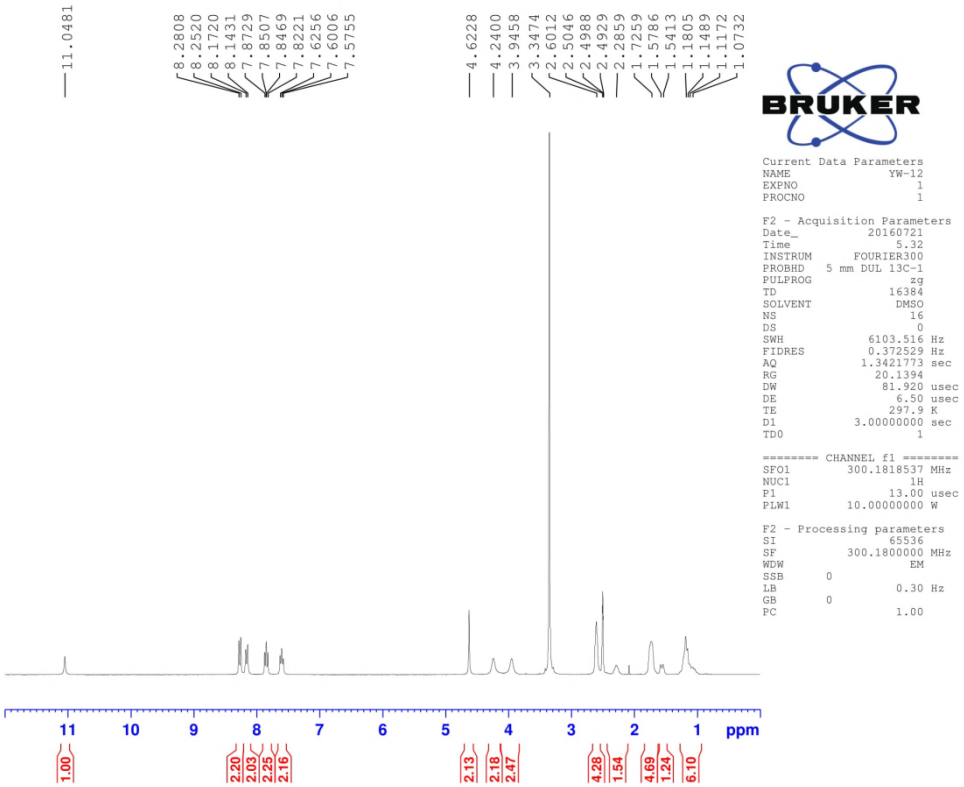

Figure 4.46. *The [1]H-NMR Spectrum of Compound* ***4l***

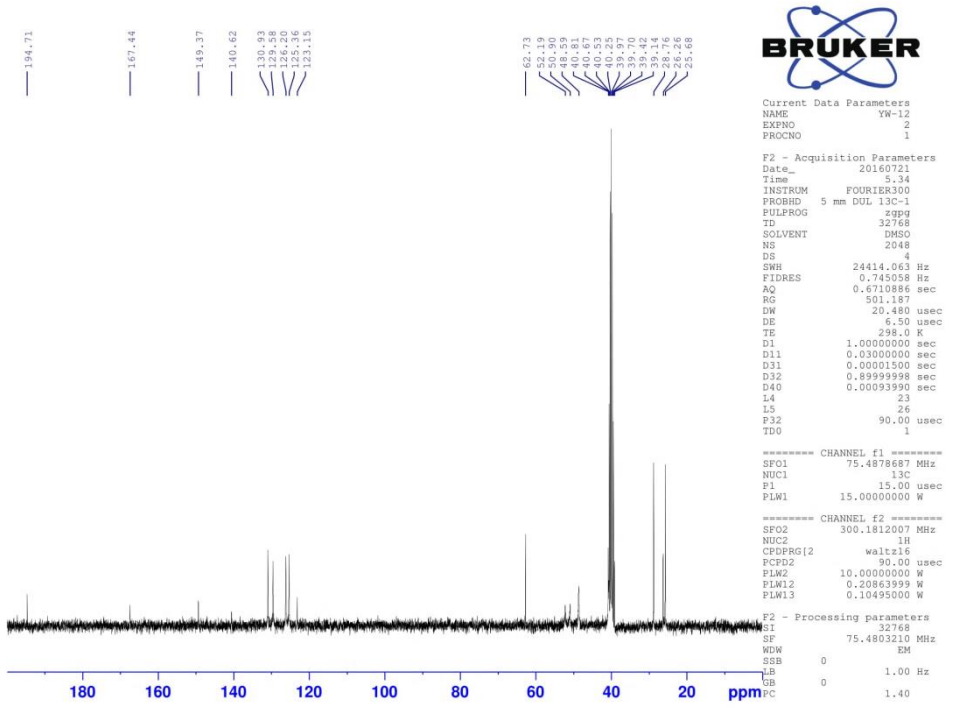

Figure 4.47. *The [13]C-NMR Spectrum of Compound* ***4l***

Formula Predictor Report - YW-12_25.lcd

Page 1 of 1

Data File: C:\LabSolutions\Data\Analiz\GTuran\YW-12_25.lcd

Elmt	Val.	Min	Max	Elmt	Val.	Min	Max	Elmt	Val.	Min	Max	Elmt	Val.	Min	Max	Use Adduct
H	1	30	40	O	2	0	2	Cl	1	0	0	I	3	0	0	H
C	4	6	33	F	1	0	0	Br	1	0	0					
N	3	0	9	S	2	0	2	Ru	2	0	0					

Error Margin (ppm):	5	DBE Range:	9.0 - 30.0	Electron Ions:	both
HC Ratio:	unlimited	Apply N Rule:	yes	Use MSn Info:	no
Max Isotopes:	3	Isotope RI (%):	1.00	Isotope Res:	10000
MSn Iso RI (%):	10.00	MSn Logic Mode:	AND	Max Results:	500

Event#: 1 MS(E+) Ret. Time : 2.347 -> 2.547 - 0.013 -> 1.466 Scan# : 353 -> 383 - 3 -> 221

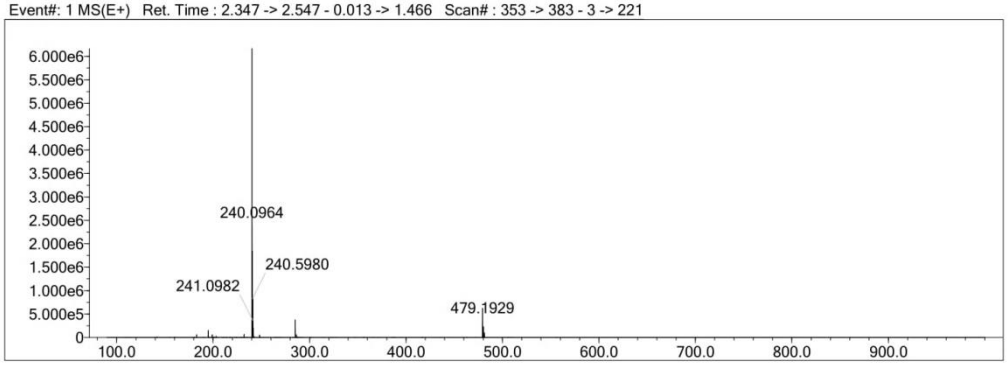

Measured region for 479.1929 m/z

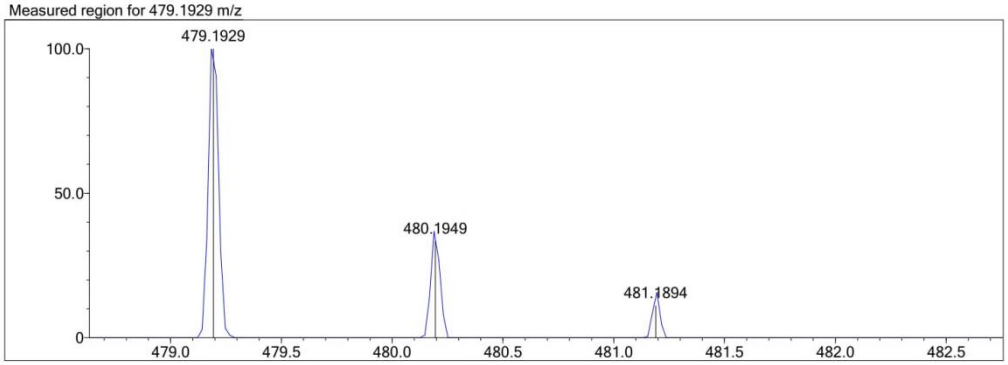

C26 H30 N4 O S2 [M+H]+ : Predicted region for 479.1934 m/z

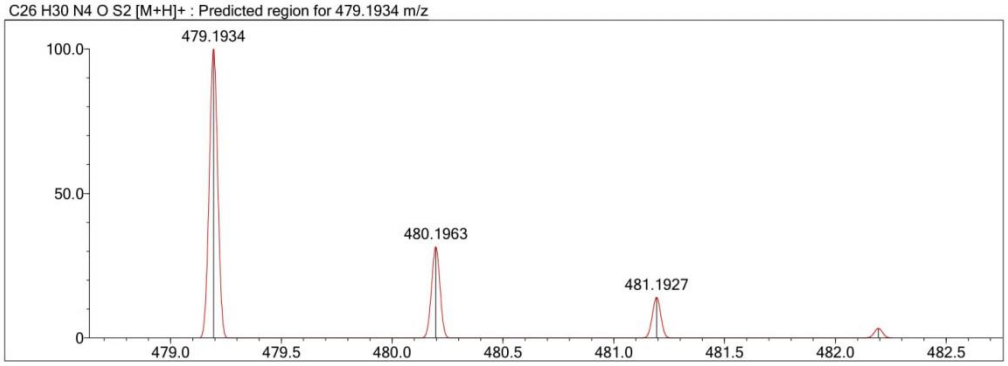

Rank	Score	Formula (M)	Ion	Meas. m/z	Pred. m/z	Df. (mDa)	Df. (ppm)	Iso	DBE
1	88.17	C26 H30 N4 O S2	[M+H]+	479.1929	479.1934	-0.5	-1.04	88.26	14.0

Figure 4.48. *Mass Spectrum of Compound **4l***

2-(9-Acridinylamino)-2-oxoethyl 4-benzhydrylpiperazine-1-carbodithioate (4m)

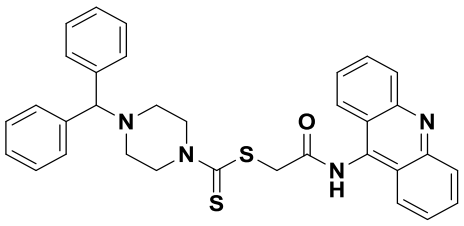

Yield: 84.3%, **M.p.**: 137.0 °C.

FTIR (ATR, cm^{-1}): 3246 (amide N-H), 2355-2920 (aliphatic C-H), 1656 (C=O), 1427-1571 (C=N and C=C), 1226-1284 (C=S), 705-758 (out of plane C-H bending).

^{1}H-NMR (300 MHz, DMSO-*d*$_6$; δ, ppm): 2.44-2.50 (4H, d, *J*=5.77 Hz, piperazine $C_{3,5}$-H), 4.02 and 4.28 (4H, two s, piperazine $C_{2,6}$-H), 4.40 (1H, s, $C_{12}H_{10}$-CH-), 4.60 (2H, s, $COCH_2$), 7.18-7.23 (3H, t, *J*=7.00 Hz, Ar-H), 7.29-7.32 (4H, t, *J*=7.36 Hz, Ar-H), 7.44 (4H, s, Ar-H), 7.57-7.62 (2H, t, *J*=7.56 Hz, Ar-H), 7.82-7.88 (2H, m , Ar-H), 7.15-7.18 (2H, d, *J*=8.70 Hz, Ar-H), 7.24-7.27 (2H, d, *J*=8.64 Hz, Ar-H), 11.02 (1H, s, -NH-).

^{13}C-NMR (75 MHz, DMSO-*d*$_6$; δ, ppm): 51.40 (CH_2), 60.71 (CH_2), 72.73 (CH_2), 74.59 (CH), 117.94 (C), 123.10 (CH), 125.38 (CH), 126.28 (CH), 127.61 (CH), 128.13 (CH), 129.14 (CH), 131.16 (CH), 140.93 (C), 142.61 (C), 149.12 (C-9 in 9-aminoacridine), 167.43 (C=O), 195.05 (C=S).

HRMS (m/z): $[M+H]^+$ calcd for $C_{33}H_{30}N_4OS_2$: 563.1934; found 563.1924.

DOPNALAB

	Item	Value
	Acquired Date&Time	17.08.2016 12:21:00
	Acquired by	System Administrator
	Filename	C:\Users\dopnalab\Desktop\derya\wiam\yw-131.ispd
	Spectrum name	yw-131
	Sample name	yw-13
	Sample ID	
	Option	
	Comment	
	No. of Scans	10
	Resolution	4 [cm-1]
	Apodization	Happ-Genzel

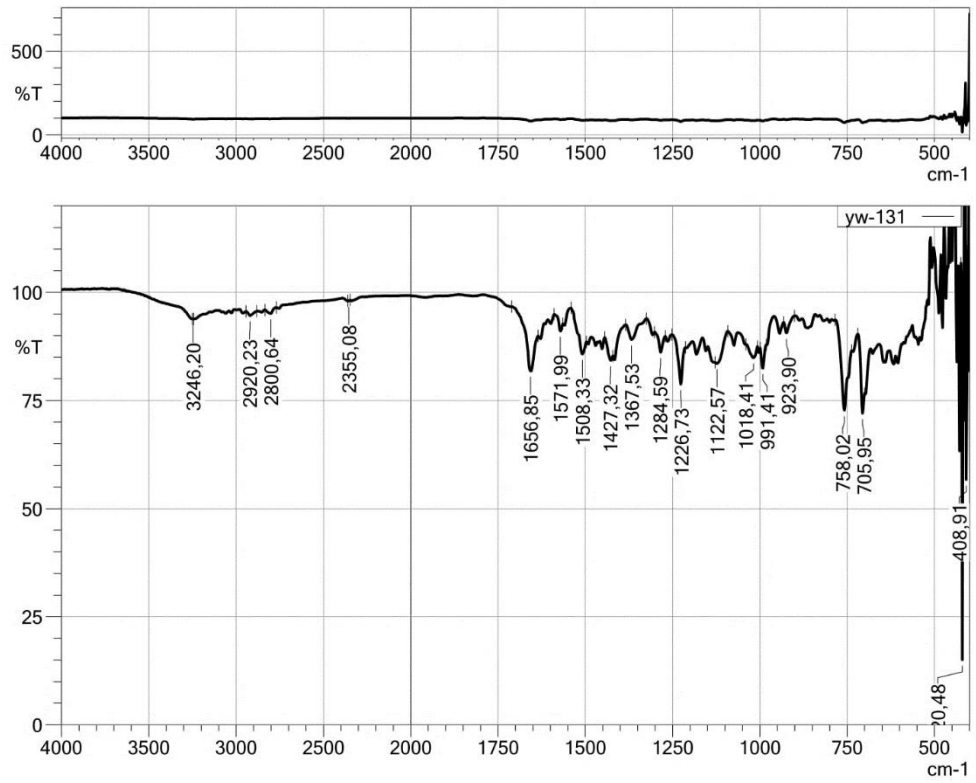

Figure 4.49. *IR Spectrum of Compound* ***4m***

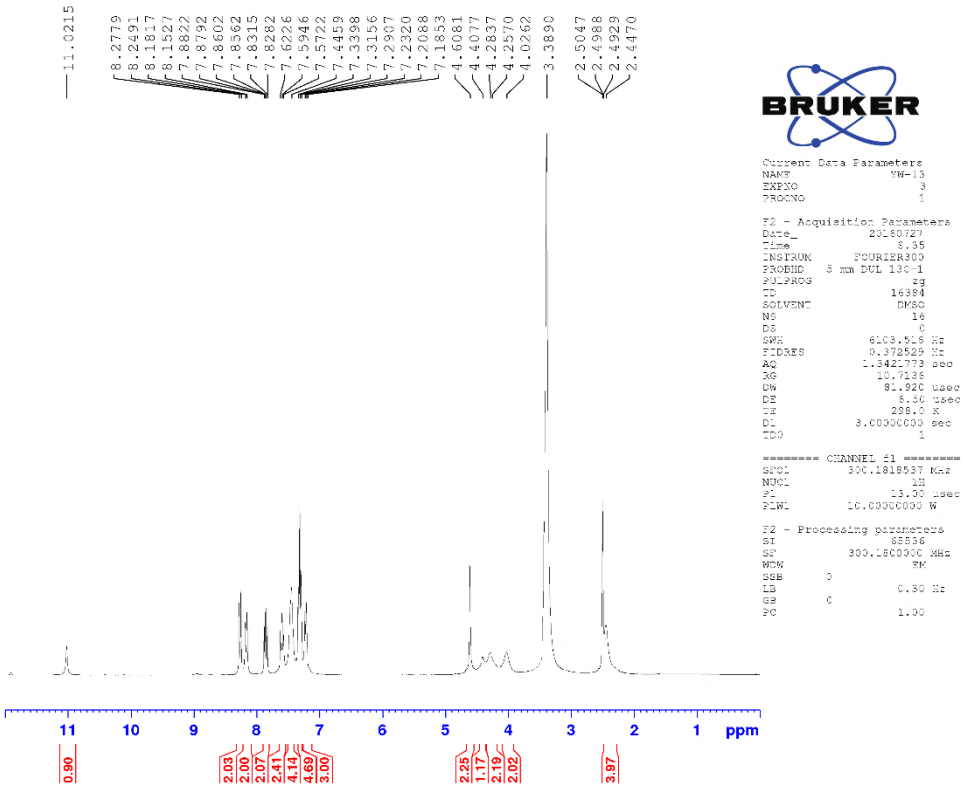

Figure 4.50. *The [1]H-NMR Spectrum of Compound* ***4m***

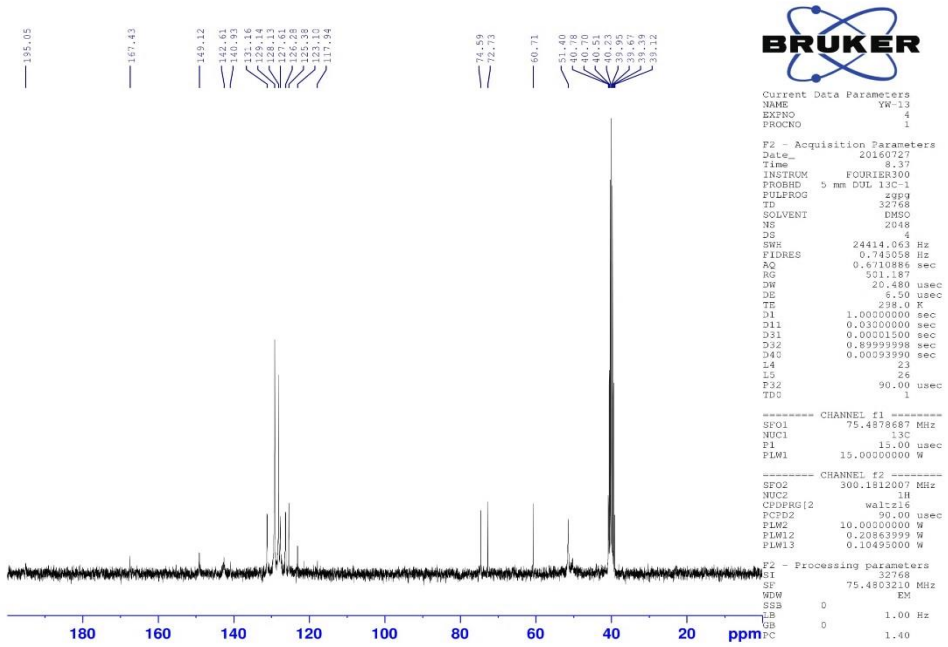

Figure 4.51. *The [13]C-NMR Spectrum of Compound* ***4m***

Formula Predictor Report - YW-13_26.lcd

Page 1 of 1

Data File: C:\LabSolutions\Data\Analiz\GTuran\YW-13_26.lcd

Elmt	Val.	Min	Max	Elmt	Val.	Min	Max	Elmt	Val.	Min	Max	Elmt	Val.	Min	Max	Use Adduct
H	1	28	40	O	2	0	2	Cl	1	0	0	I	3	0	0	H
C	4	33	33	F	1	0	0	Br	1	0	0					
N	3	0	9	S	2	0	2	Ru	2	0	0					

Error Margin (ppm): 5
HC Ratio: unlimited
Max Isotopes: 3
MSn Iso RI (%): 10.00

DBE Range: 9.0 - 30.0
Apply N Rule: yes
Isotope RI (%): 1.00
MSn Logic Mode: AND

Electron Ions: both
Use MSn Info: no
Isotope Res: 10000
Max Results: 500

Event#: 1 MS(E+) Ret. Time : 7.280 -> 7.627 Scan# : 1093 -> 1145

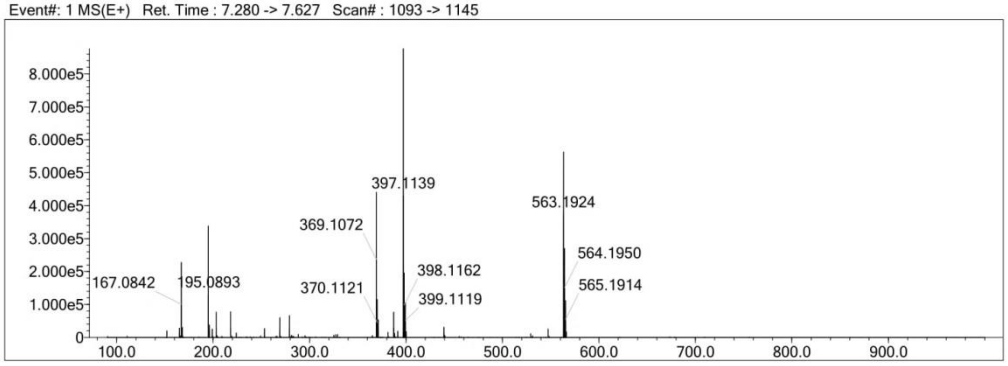

Measured region for 563.1924 m/z

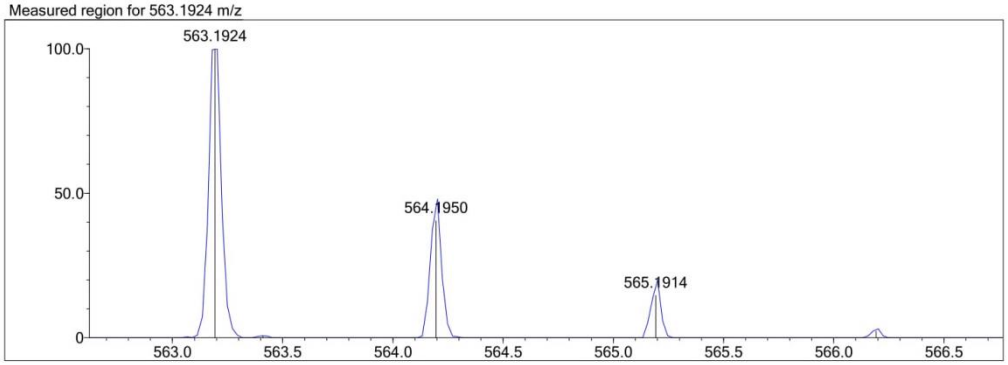

C33 H30 N4 O S2 [M+H]+ : Predicted region for 563.1934 m/z

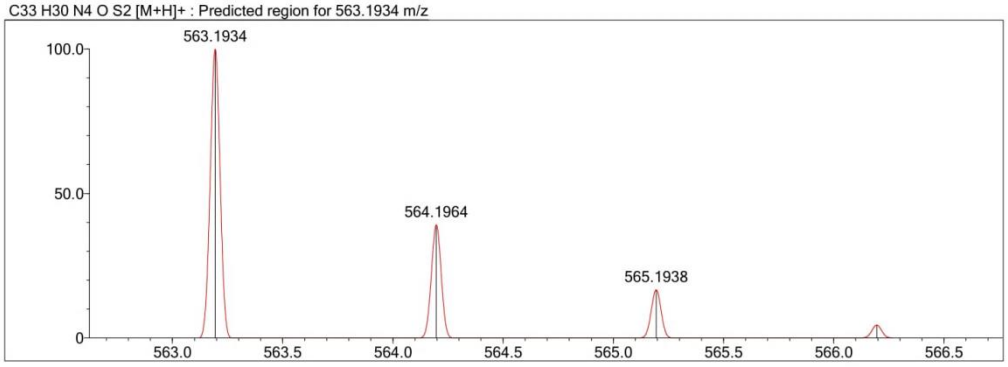

Rank	Score	Formula (M)	Ion	Meas. m/z	Pred. m/z	Df. (mDa)	Df. (ppm)	Iso	DBE
1	86.13	C33 H30 N4 O S2	[M+H]+	563.1924	563.1934	-1.0	-1.78	87.85	21.0

Figure 4.52. *Mass Spectrum of Compound **4m***

2-(9-Acridinylamino)-2-oxoethyl 4-(4-(trifluoromethyl)benzyl)piperazine-1-carbodithioate (4n)

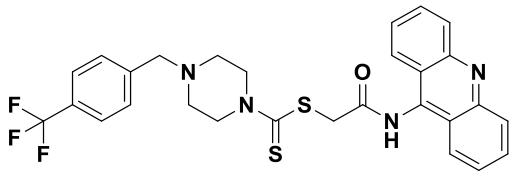

Yield: 87.7%, **M.p.**: 161.5°C.

FTIR (ATR, cm^{-1}): 3232 (amide N-H), 2814-2920 (aliphatic C-H), 1653 (C=O), 1415-1510 (C=N and C=C), 1219 (C=S), 756 (out of plane C-H bending).

^{1}H-NMR (300 MHz, DMSO-*d*$_6$; δ, ppm): 2.48-2.52 (4H, t, *J*=5.10 Hz, piperazine $C_{3,5}$-H), 3.62 and 4.00 (4H, two s, piperazine $C_{2,6}$-H), 4.29 (2H, s, C_6H_5-$\underline{CH_2}$-), 4.62 (2H, s, CO$\underline{CH_2}$), 7.55-7.57 (2H, d , *J*=7.92 Hz, Ar-H), 7.60-7.62 (2H, d, *J* =7.74 Hz, Ar-H), 7.68-7.71 (2H, d, *J*=8.16 Hz Ar-H), 7.82-7.87 (2H, t, *J*=7.80 Hz, Ar-H), 7.14-7.17 (2H, d , *J*=8.76 Hz, Ar-H), 7.25-7.27 (2H, d, *J*=8.58 Hz, Ar-H), 11.01 (1H, s, -NH-).

^{13}C-NMR (75 MHz, DMSO-*d*$_6$; δ, ppm): 52.44 (CH_2), 60.83 (CH_2), 72.72 (CH_2), 125.00 (q, *J*=214.9 Hz, CF_3), 123.15 (CH), 125.31 (CH), 125.60 (q, *J* =3.6 Hz, trifluoromethylphenyl $C_{3,3'}$), 126.23 (CH), 129.58 (CH), 129.96 (q, *J* =39.8 Hz, trifluoromethylphenyl C_4), 129.98 (CH), 130.93 (C), 140.56 (C), 143.21 (C), 149.37 (C-9 in 9-aminoacridine), 167.41 (C=O), 195.11 (C=S).

HRMS (m/z): $[M+H]^+$ calcd for $C_{28}H_{25}F_3N_4OS_2$: 555.1495; found 555.1493.

DOPNALAB

	Item	Value
	Acquired Date&Time	17.08.2016 12:23:01
	Acquired by	System Administrator
	Filename	C:\Users\dopnalab\Desktop\derya\wiam\yw-141.ispd
	Spectrum name	yw-141
	Sample name	yw-14
	Sample ID	
	Option	
	Comment	
	No. of Scans	10
	Resolution	4 [cm-1]
	Apodization	Happ-Genzel

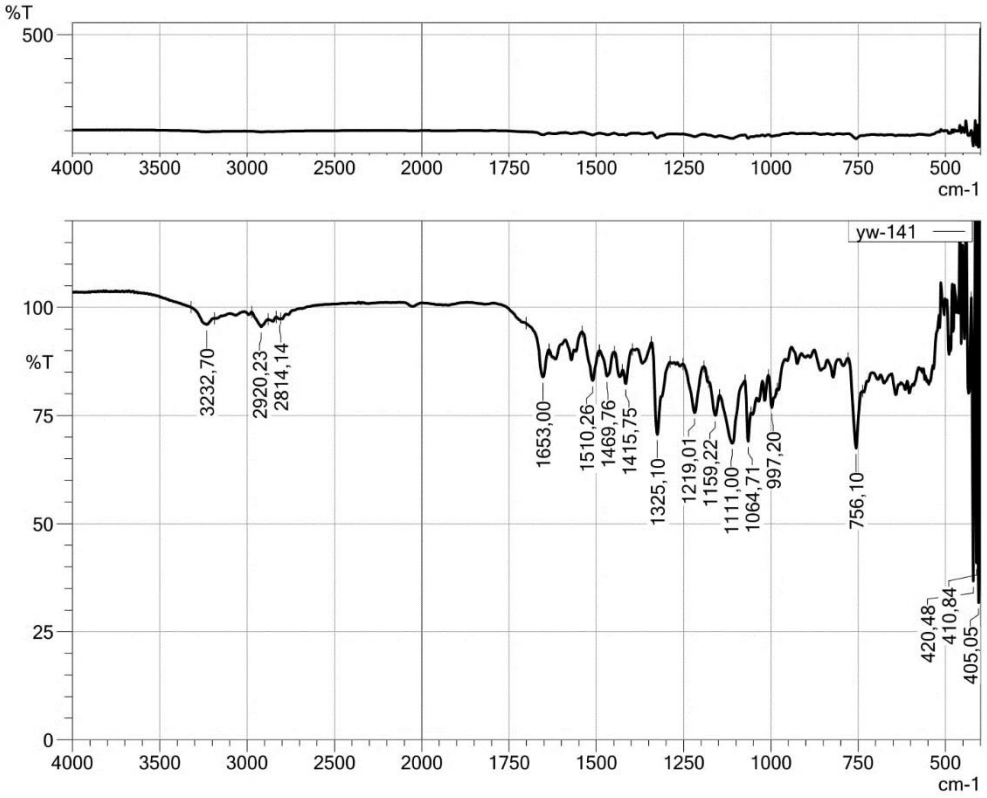

Figure 4.53. *IR Spectrum of Compound **4n***

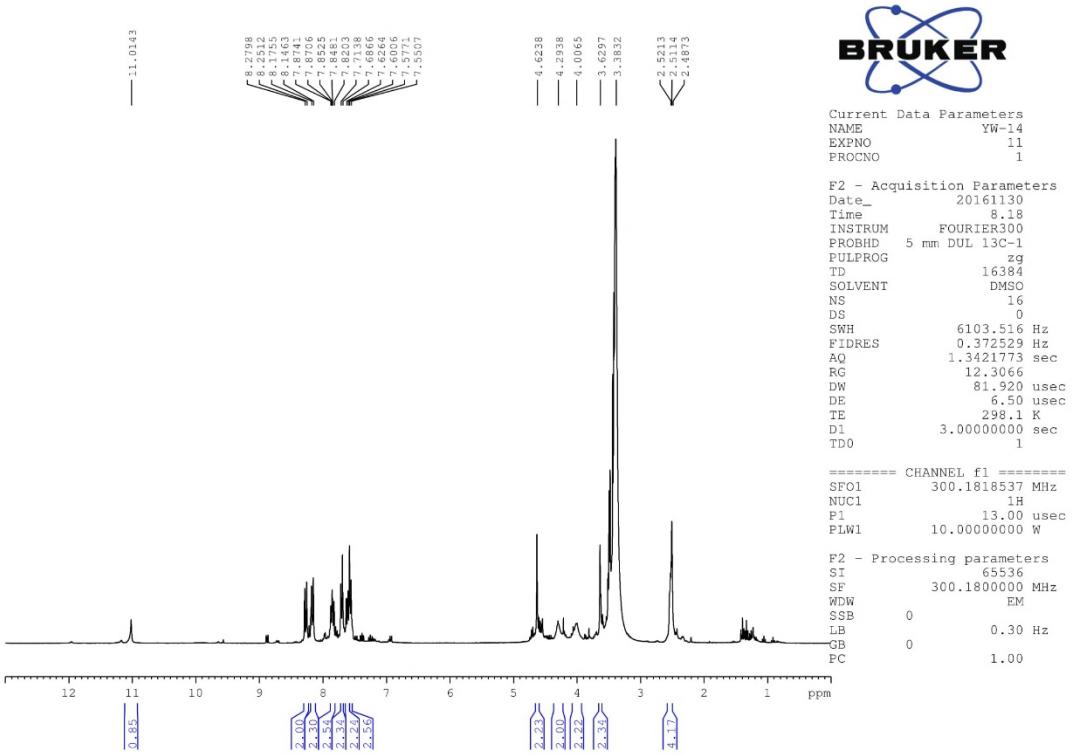

Figure 4.54. *The [1]H-NMR Spectrum of Compound **4n***

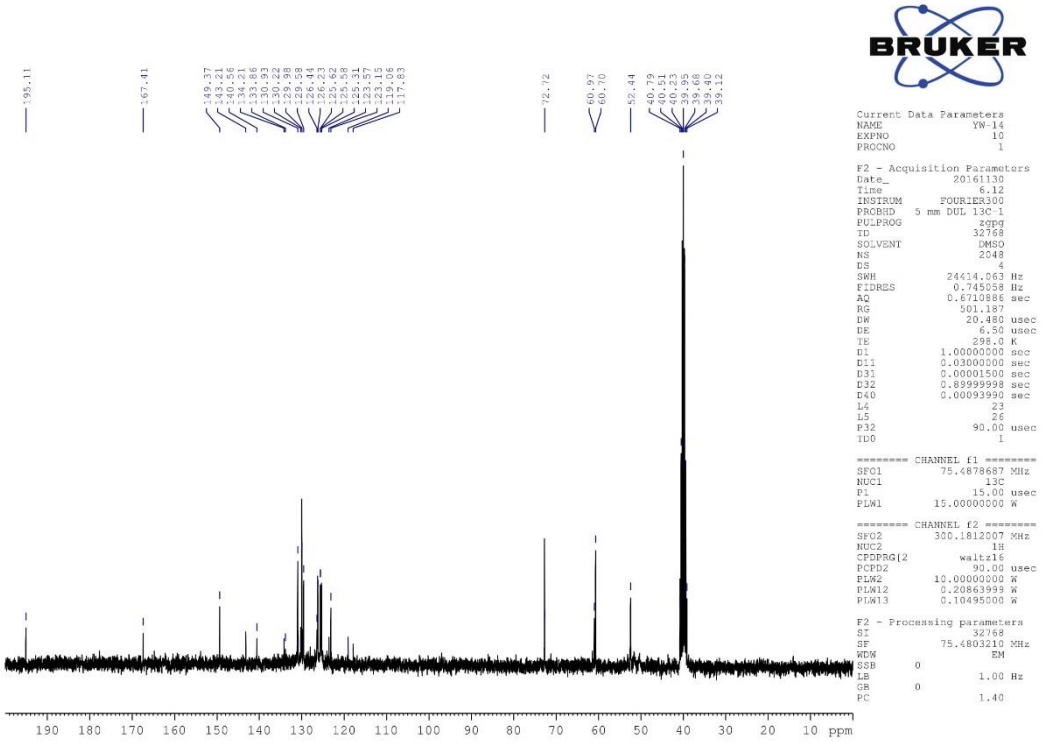

Figure 4.55. *The [13]C-NMR Spectrum of Compound **4n***

Formula Predictor Report - YW-14_27.lcd

Page 1 of 1

Data File: C:\LabSolutions\Data\Analiz\GTuran\YW-14_27.lcd

Elmt	Val.	Min	Max	Elmt	Val.	Min	Max	Elmt	Val.	Min	Max	Elmt	Val.	Min	Max	Use Adduct
H	1	0	40	O	2	0	2	Cl	1	0	0	I	3	0	0	H
C	4	0	33	F	1	0	3	Br	1	0	0					
N	3	0	9	S	2	0	2	Ru	2	0	0					

Error Margin (ppm): 5
HC Ratio: unlimited
Max Isotopes: 3
MSn Iso RI (%): 10.00

DBE Range: 9.0 - 20.0
Apply N Rule: yes
Isotope RI (%): 1.00
MSn Logic Mode: AND

Electron Ions: both
Use MSn Info: no
Isotope Res: 10000
Max Results: 500

Event#: 1 MS(E+) Ret. Time : 4.920 -> 6.160 - 6.027 -> 10.936 Scan# : 739 -> 925 - 905 -> 1641

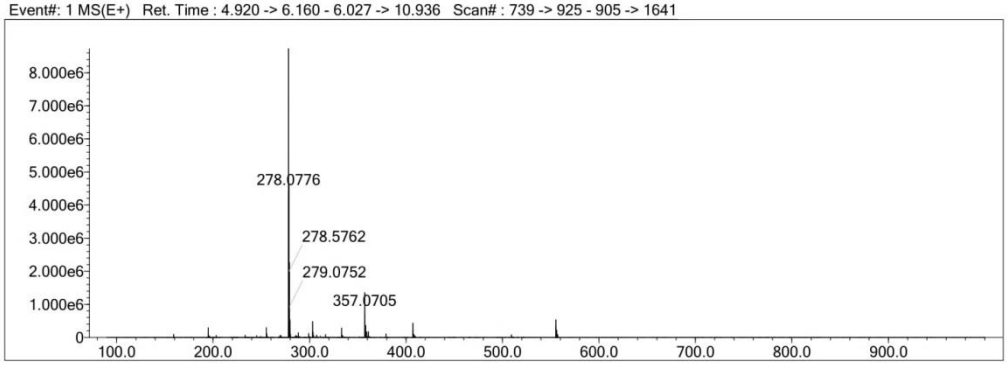

Measured region for 555.1493 m/z

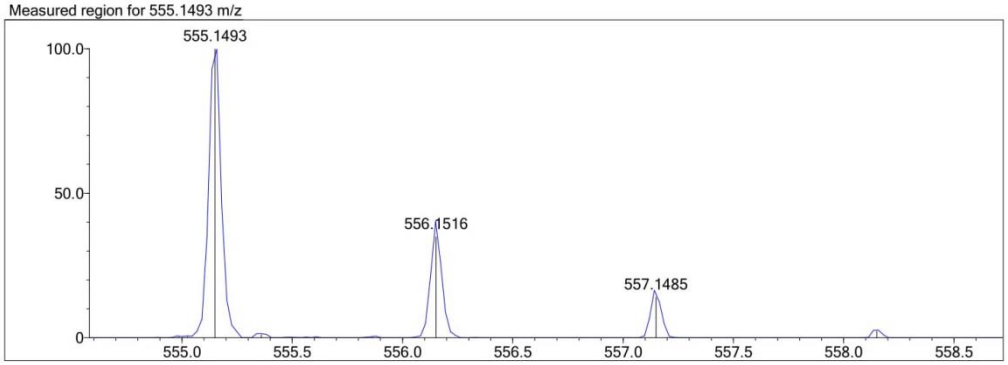

C28 H25 N4 O F3 S2 [M+H]+ : Predicted region for 555.1495 m/z

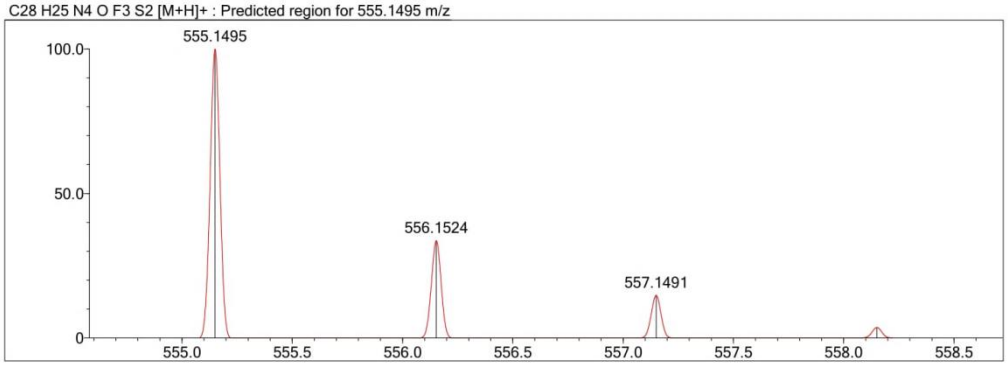

Rank	Score	Formula (M)	Ion	Meas. m/z	Pred. m/z	Df. (mDa)	Df. (ppm)	Iso	DBE
1	93.64	C28 H25 N4 O F3 S2	[M+H]+	555.1493	555.1495	-0.2	-0.36	93.64	17.0

Figure 4.56. *Mass Spectrum of Compound* ***4n***

2-(9-Acridinylamino)-2-oxoethyl 4-(4-methylbenzyl)piperazine-1-carbodithioate (4o)

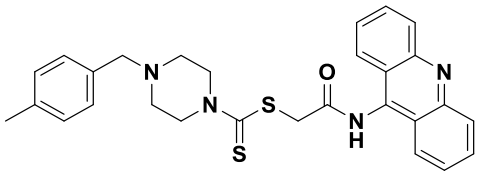

Yield: 91.0%, **M.p.**: 205.8 °C.

FTIR (ATR, cm^{-1}): 3255 (amide N-H), 2792-2902 (aliphatic C-H), 1654 (C=O), 1435-1508 (C=N and C=C), 1220 (C=S), 759 (out of plane C-H bending).

^{1}H-NMR (300 MHz, DMSO-*d*$_6$; δ, ppm): 2.27 (3H, s, - CH_3), 2.47-2.50 (4H, m , piperazine $C_{3,5}$-H), 3.47 (2H, s,C_6H_5-$\underline{CH_2}$), 3.98 and 4.26 (4H, two s, piperazine $C_{2,6}$-H), 4.63 (2H, s, CO$\underline{CH_2}$), 7.11-7.14 (2H, d, *J*=7.92 Hz, Ar-H), 7.18-7.20 (2H, d, *J* =7.95 Hz, Ar-H), 7.56-7.61 (2H, t, *J*=7.50 Hz , Ar-H), 7.86-7.81 (2H, t, *J*=7.41 Hz, Ar-H), 8.14-8.17 (2H, d, *J*=8.70 Hz, Ar-H), 8.25-8.28 (2H, d, *J*=8.64 Hz, Ar-H), 11.15 (1H, s, -NH-).

^{13}C-NMR (75 MHz, DMSO-*d*$_6$; δ, ppm): 21.16 (CH_3), 50.42 (CH_2), 51.62 (CH_2), 52.36 (CH_2), 61.50 (CH_2), 123.15 (C), 125.39 (CH), 126.18 (CH), 129.29 (CH), 129.42 (CH), 129.57 (CH), 130.91 (CH), 134.84 (C), 36.66 (C), 140.63 (C), 149.37(C-9 in 9-aminoacridine), 167.42 (C=O), 194.98 (C=S).

HRMS (m/z): $[M+H]^+$ calcd for $C_{28}H_{28}N_4OS_2$: 501.1777.; found 501.1774.

DOPNALAB

	Item	Value
	Acquired Date&Time	17.08.2016 12:24:51
	Acquired by	System Administrator
	Filename	C:\Users\dopnalab\Desktop\derya\wiam\yw-151.ispd
	Spectrum name	yw-151
	Sample name	yw-15
	Sample ID	
	Option	
	Comment	
	No. of Scans	10
	Resolution	4 [cm-1]
	Apodization	Happ-Genzel

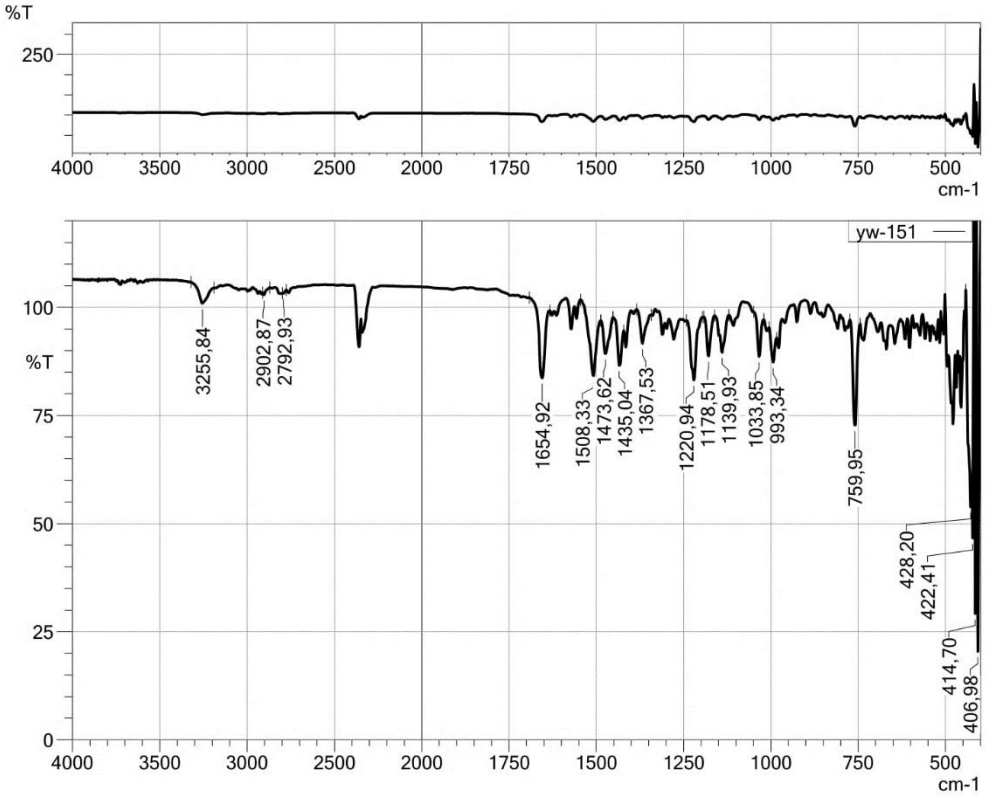

Figure 4.57. *IR Spectrum of Compound* ***4o***

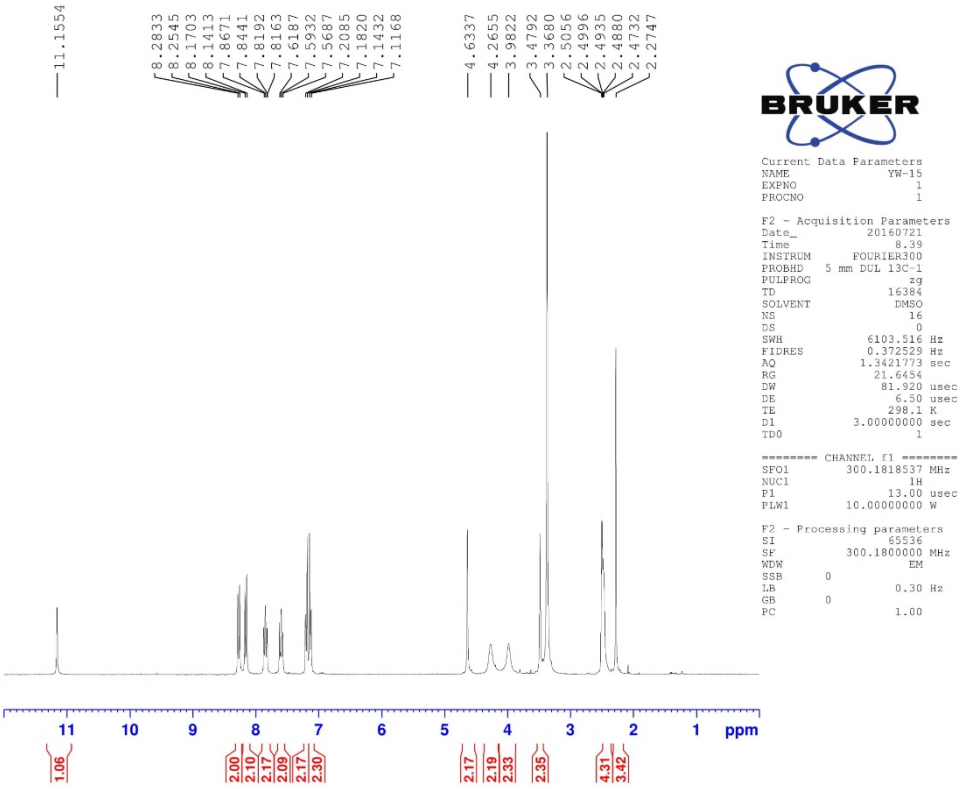

Figure 4.58. *The [1]H-NMR Spectrum of Compound* ***4o***

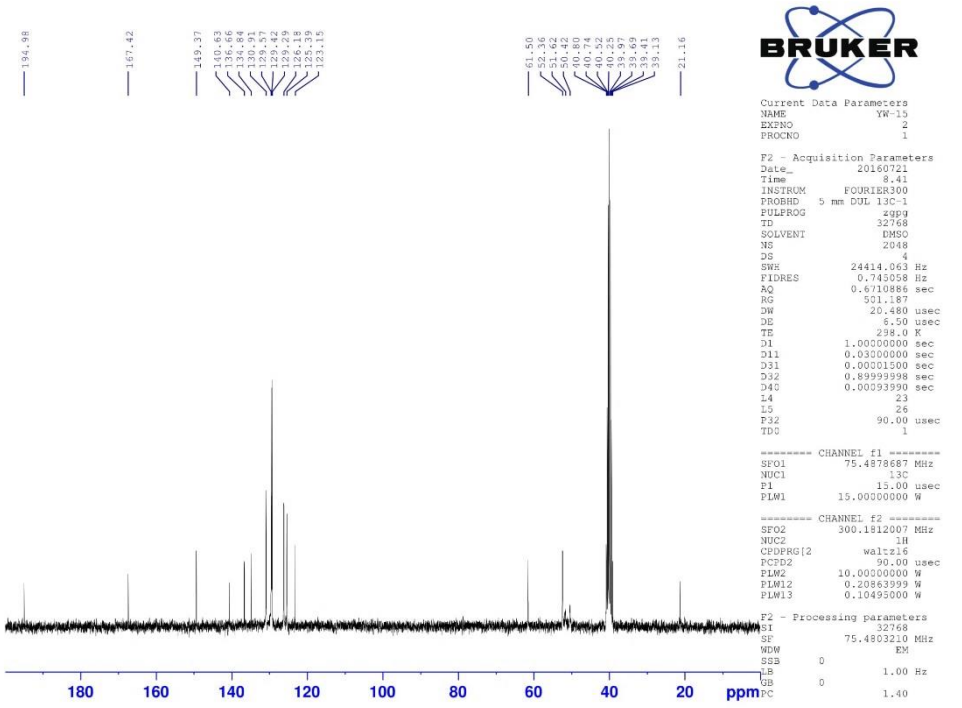

Figure 4.59. *The [13]C-NMR Spectrum of Compound* ***4o***

Formula Predictor Report - YW-15_28.lcd

Page 1 of 1

Data File: C:\LabSolutions\Data\Analiz\GTuran\YW-15_28.lcd

Elmt	Val.	Min	Max	Elmt	Val.	Min	Max	Elmt	Val.	Min	Max	Elmt	Val.	Min	Max	Use Adduct
H	1	28	40	O	2	0	2	Cl	1	0	0	I	3	0	0	H
C	4	28	28	F	1	0	3	Br	1	0	0					
N	3	0	9	S	2	0	2	Ru	2	0	0					

Error Margin (ppm): 5
HC Ratio: unlimited
Max Isotopes: 3
MSn Iso RI (%): 10.00

DBE Range: 9.0 - 20.0
Apply N Rule: yes
Isotope RI (%): 1.00
MSn Logic Mode: AND

Electron Ions: both
Use MSn Info: no
Isotope Res: 10000
Max Results: 500

Event#: 1 MS(E+) Ret. Time : 5.627 -> 6.600 - 6.173 -> 9.570 Scan# : 845 -> 991 - 927 -> 1437

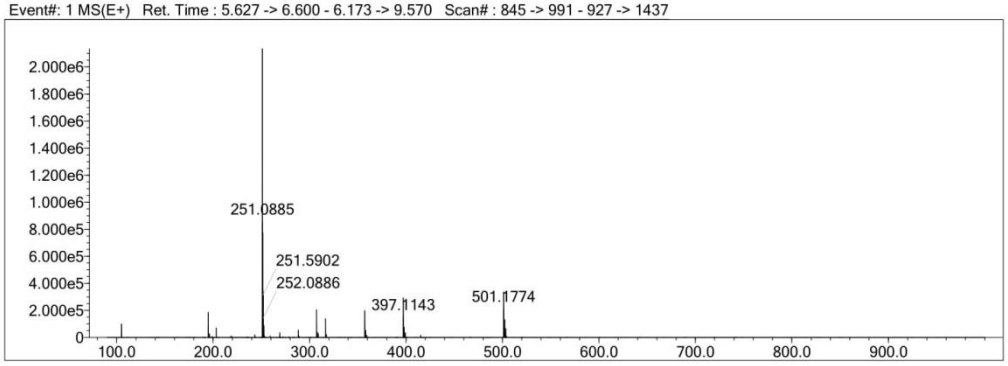

Measured region for 501.1774 m/z

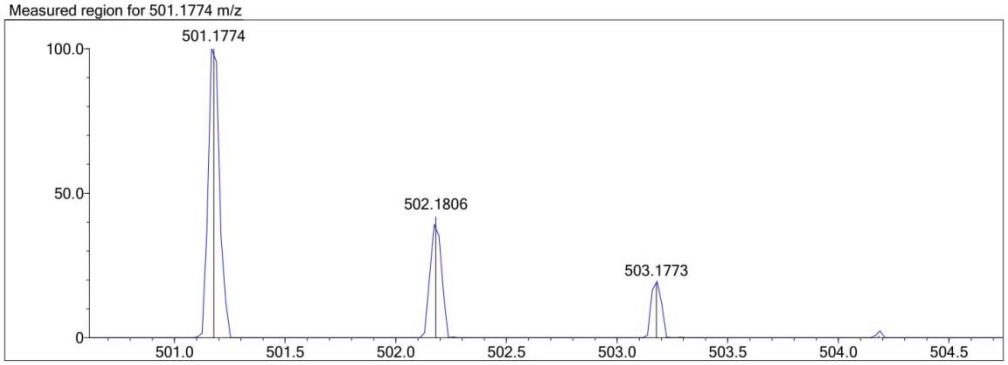

C28 H28 N4 O S2 [M+H]+ : Predicted region for 501.1777 m/z

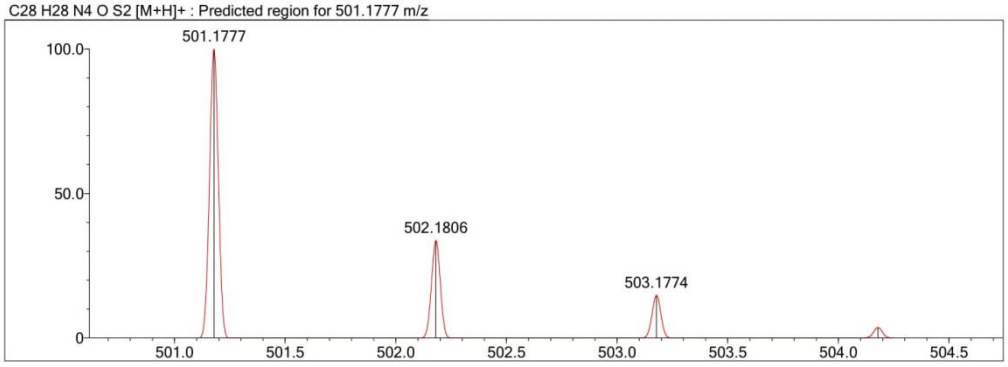

Rank	Score	Formula (M)	Ion	Meas. m/z	Pred. m/z	Df. (mDa)	Df. (ppm)	Iso	DBE
1	78.20	C28 H28 N4 O S2	[M+H]+	501.1774	501.1777	-0.3	-0.60	78.20	17.0

Figure 4.60. *Mass Spectrum of Compound* ***4o***

2-(9-Acridinylamino)-2-oxoethyl 4-(4-fluorophenyl)piperazine-1-carbodithioate (4p)

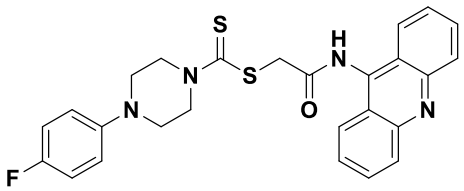

Yield: 96.4%, **M.p.**: 227.7 °C.

FTIR (ATR, cm^{-1}): 3257 (amide N-H), 2800-2906 (aliphatic C-H), 1653 (C=O), 1433 (C=N and C=C), 1213 (C=S), 1029 (C-F), 825 (1,4-disubstituted benzene), 756 (out of plane C-H bending).

^{1}H-NMR (300 MHz, DMSO-*d*$_6$; δ, ppm): 3.24-3.27 (4H, t, *J*=4.83 Hz, piperazine $C_{3,5}$-H), 4.16 and 4.39 (4H, two s, piperazine $C_{2,6}$-H), 4.67 (2H, s,CO$\underline{CH_2}$), 6.94-6.99 (2H, m, Ar-H), 7.04-7.10 (2H, t, *J*=8.85 Hz, Ar-H), 7.58-7.63 (2H, t, *J*=7.60 Hz , Ar-H), 7.82-7.87 (2H, t, *J*=7.66 Hz, Ar-H), 8.15-8.18 (2H, d, *J*=8.73 Hz, Ar-H), 8.27-8.30 (2H, d, *J*=8.64 Hz, Ar-H), 11.07 (1H, s, -NH-).

^{13}C-NMR (75 MHz, DMSO-*d*$_6$; δ, ppm): 48.96 (CH_2), 50.05 (CH_2), 51.36 (CH_2), 115.90 (d, *J* =21.8 Hz, fluorophenyl $C_{3,3'}$), 117.90 (d, *J* =7.5 Hz, fluorophenyl $C_{2,2'}$), 123.17 (CH), 125.35 (CH), 126.23 (CH), 129.61 (CH), 130.92 (CH), 140.57 (CH), 147.42 (d, *J* =2.3 Hz, fluorophenyl C_1), 149.40 (C-9 in 9-aminoacridine), 156.78 (d, *J* =234.8 Hz, fluorophenyl C_4), 167.38 (C=O), 195.34 (C=S). HRMS (m/z): $[M+H]^+$ calcd for $C_{26}H_{23}FN_4OS_2$: 490.62.; found 491.13.

HRMS (m/z): $[M+H]^+$ calcd for $C_{26}H_{23}FN_4OS_2$: 491.1370; found 491.1354.

DOPNALAB

	Item	Value
	Acquired Date&Time	29.12.2016 15:13:52
	Acquired by	System Administrator
	Filename	C:\Users\dopnalab\Desktop\derya\wiam\yw-161.ispd
	Spectrum name	yw-161
	Sample name	YW-16
	Sample ID	
	Option	
	Comment	
	No. of Scans	10
	Resolution	4 [cm-1]
	Apodization	Happ-Genzel

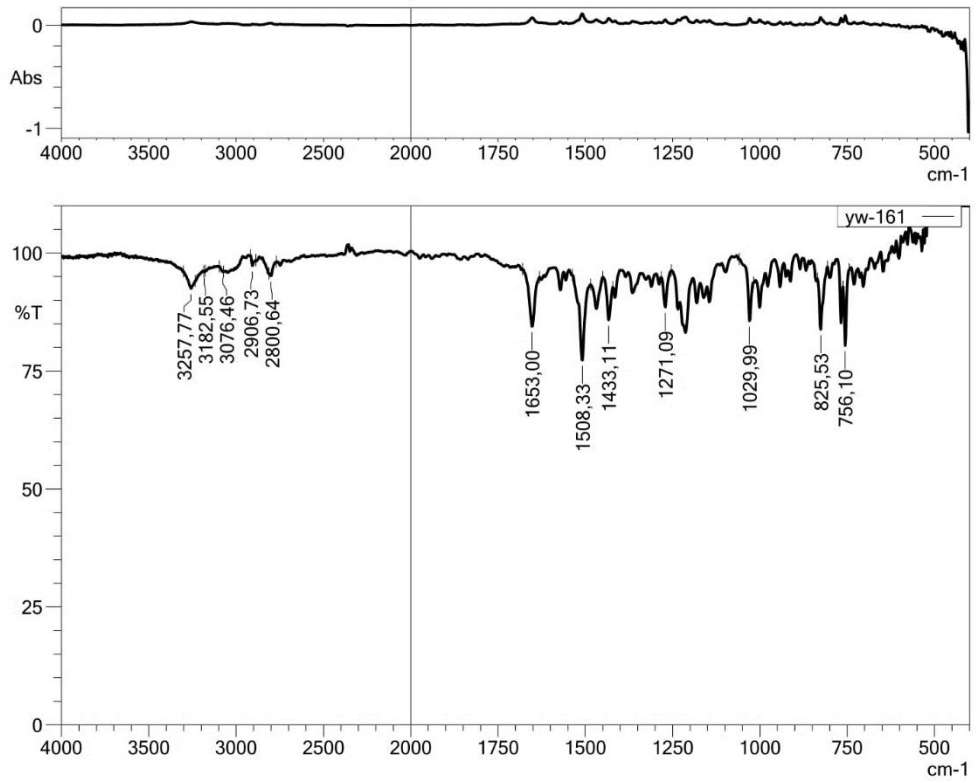

Figure 4.61. *IR Specturum of Compound **4p***

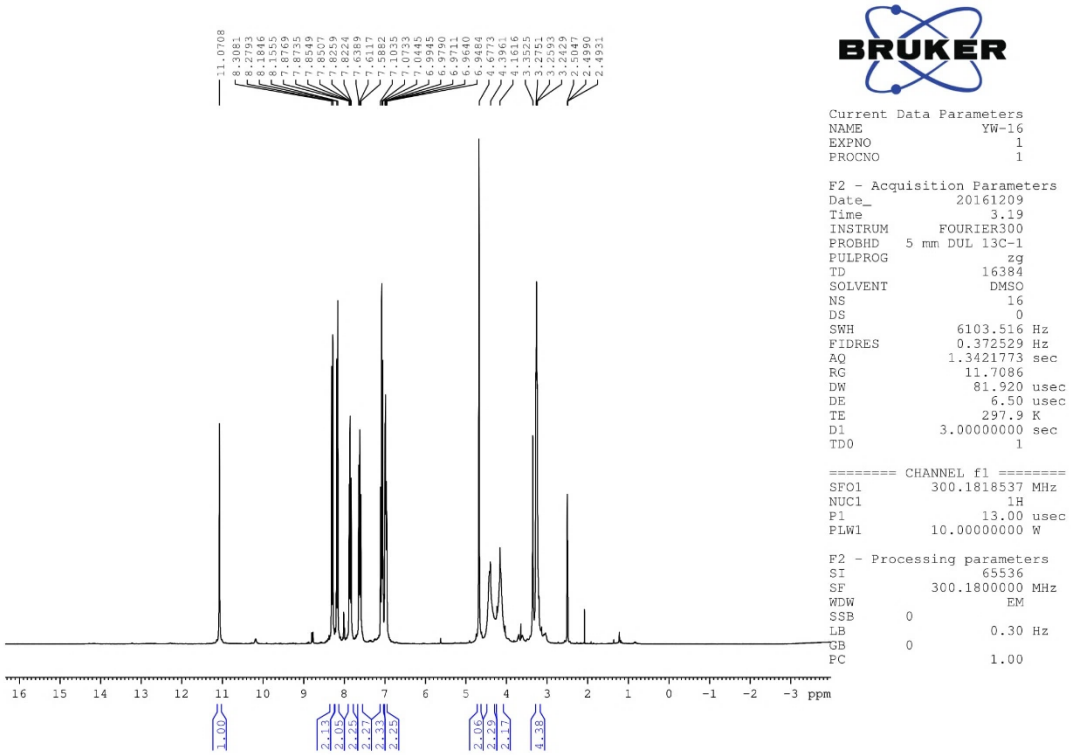

Figure 4.62. *The [1]H-NMR Specturum of Compound* ***4p***

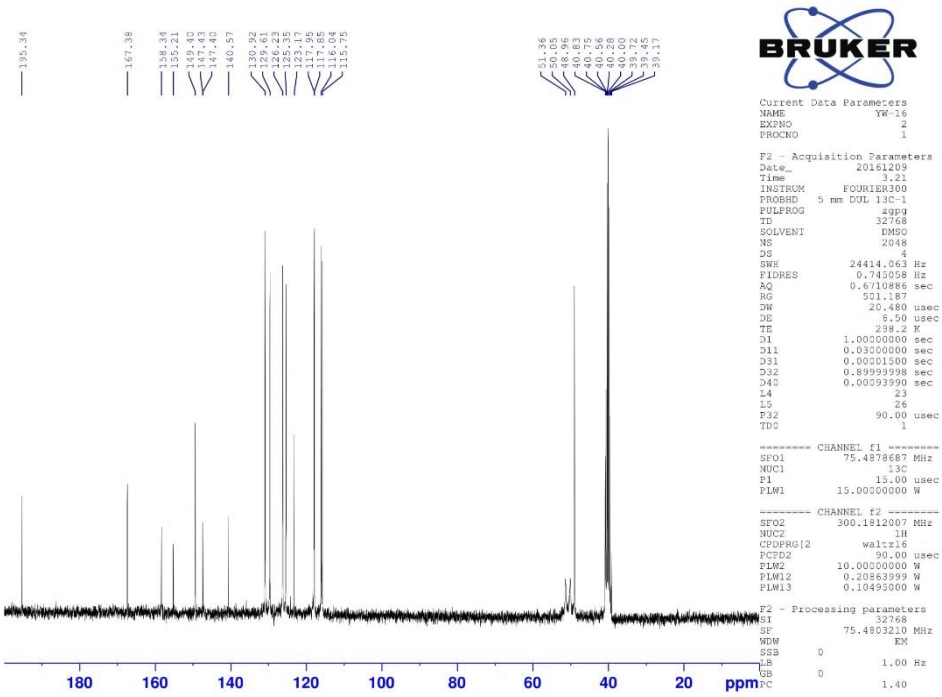

Figure 4.63. *The [13]C-NMR Specturum of Compound* ***4p***

Formula Predictor Report - YW-16_33.lcd

Page 1 of 1

Data File: C:\LabSolutions\Data\Analiz\GTuran\YW-16_33.lcd

Elmt	Val.	Min	Max	Elmt	Val.	Min	Max	Elmt	Val.	Min	Max	Elmt	Val.	Min	Max	Use Adduct
H	1	7	25	O	2	1	7	Cl	1	0	1	I	3	0	0	H
C	4	17	30	F	1	1	1	Br	1	0	0					
N	3	4	7	S	2	2	3	Ru	2	0	0					

Error Margin (ppm): 10
HC Ratio: unlimited
Max Isotopes: 3
MSn Iso RI (%): 10.00

DBE Range: 14.0 - 19.0
Apply N Rule: yes
Isotope RI (%): 1.00
MSn Logic Mode: AND

Electron Ions: both
Use MSn Info: no
Isotope Res: 10000
Max Results: 500

Event#: 1 MS(E+) Ret. Time : 5.413 -> 5.667 Scan# : 813 -> 851

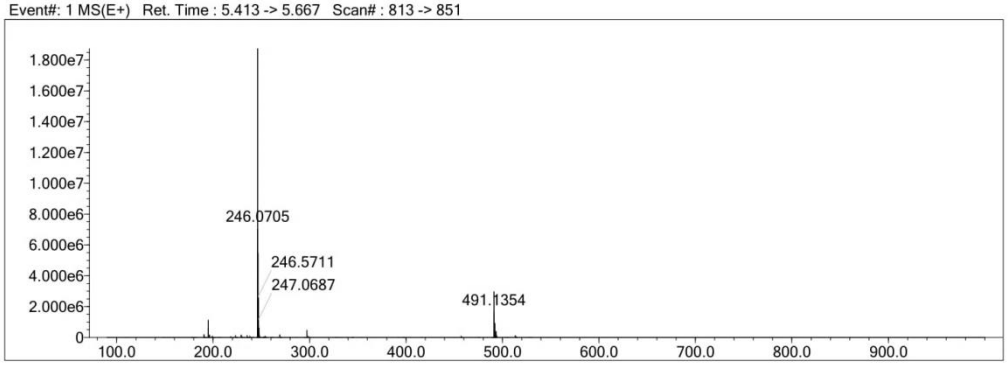

Measured region for 491.1354 m/z

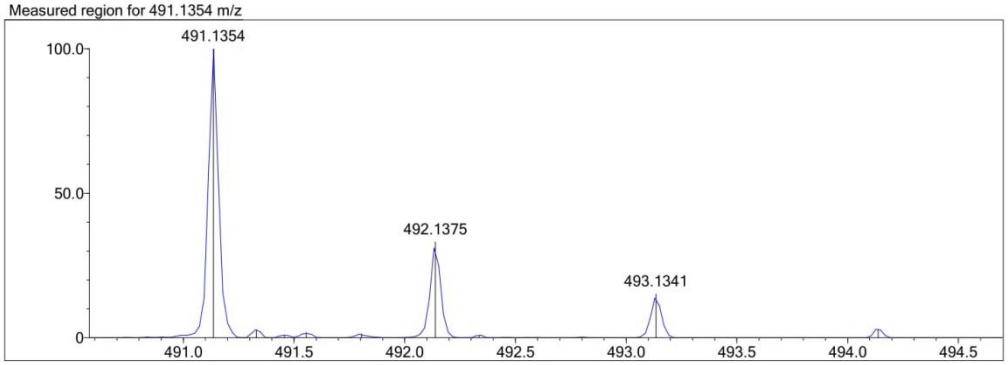

C26 H23 N4 O F S2 [M+H]+ : Predicted region for 491.1370 m/z

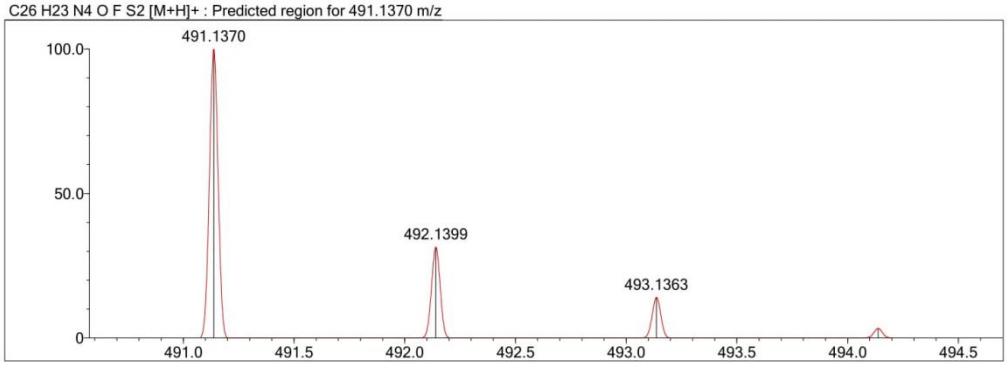

Rank	Score	Formula (M)	Ion	Meas. m/z	Pred. m/z	Df. (mDa)	Df. (ppm)	Iso	DBE
1	94.35	C26 H23 N4 O F S2	[M+H]+	491.1354	491.1370	-1.6	-3.26	100.00	17.0

Figure 4.64. *Mass Specturum of Compound* ***4p***

2-(9-Acridinylamino)-2-oxoethyl 4-(furan-2-carbonyl)piperazine-1-carbodithioate (4q)

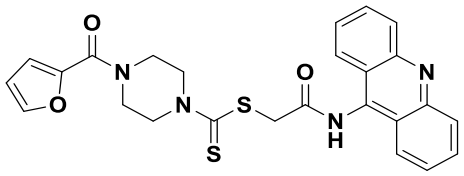

Yield: 95.5%, **M.p.**: 218.9 °C.

FTIR (ATR, cm^{-1}): 3255 (amide N-H), 2895-2995 (aliphatic C-H), 1653 (furan-2-carbonyl), 1616 (amide C=O), 1423 (C=N and C=C), 1215 (C=S), 758 (out of plane C-H bending).

^{1}H-NMR (300 MHz, DMSO-*d*$_6$; δ, ppm): 3.88 (4H, s, piperazine $C_{3,5}$-H), 4.12 and 4.36 (4H, two s, piperazine -CH_2), 4.68 (2H, s, CO$\underline{CH_2}$), 6.64-6.65 (1H, m , Ar-H), 7.07-7.08 (2H, d, *J* =3.39 Hz, Ar-H), 7.57-7.63 (2H, t, *J*=7.59 Hz , Ar-H), 7.81-7.87 (3H, t, *J*=8.14 Hz, Ar-H), 8.14-8.17 (2H, d, *J*=8.70 Hz, Ar-H), 8.27-8.30 (2H, d, *J*=8.64 Hz, Ar-H), 11.21 (1H, s, -NH-).

^{13}C-NMR (75 MHz, DMSO-*d*$_6$; δ, ppm): 49.61 (CH_2), 51.09 (CH_2), 111.91 (C), 116.62 (CH), 123.16 (CH), 125.41 (CH), 126.20 (CH), 129.57 (CH), 130.92 (CH), 140.64 (CH), 145.62 (C), 147.08 (C), 149.38 (C), 158.97 (C-9 in 9-aminoacridine), 167.35 (C=O), 195.67 (C=S).

HRMS (m/z): $[M+H]^+$ calcd for $C_{25}H_{22}N_4O_3S_2$: 491.1206. ; found 491.1186.

DOPNALAB

	Item	Value
	Acquired Date&Time	29.12.2016 15:16:38
	Acquired by	System Administrator
	Filename	C:\Users\dopnalab\Desktop\derya\wiam\yw-171.ispd
	Spectrum name	yw-171
	Sample name	YW-17
	Sample ID	
	Option	
	Comment	
	No. of Scans	10
	Resolution	4 [cm-1]
	Apodization	Happ-Genzel

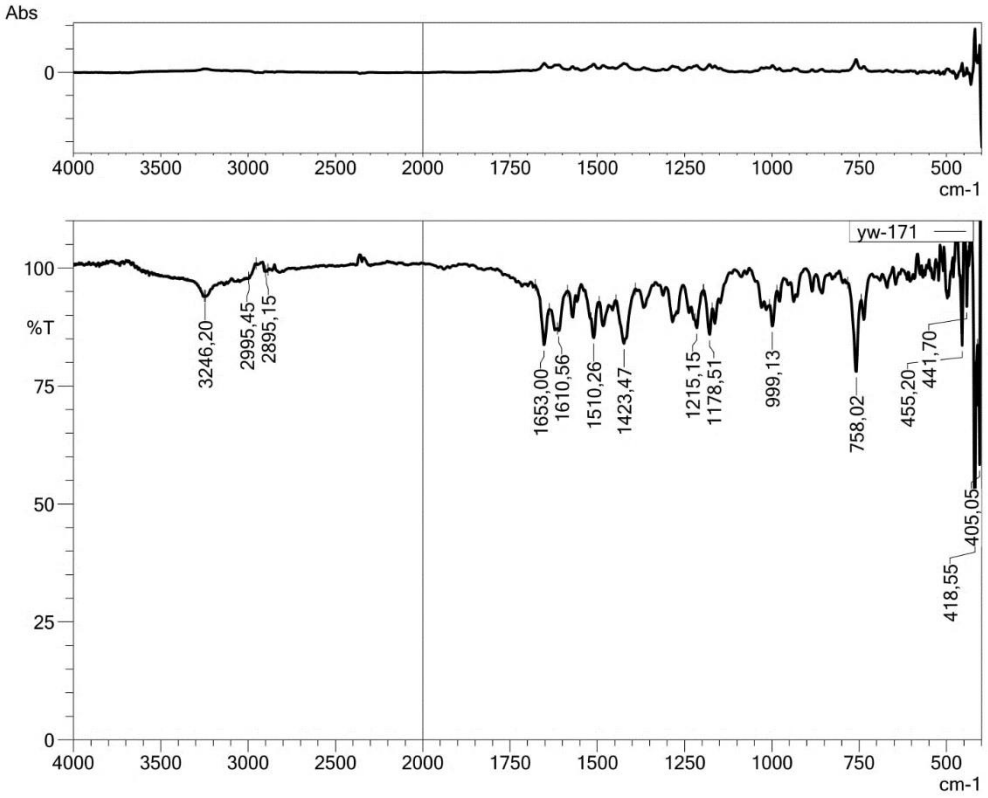

Figure 4.65. *IR Specturum of Compound* ***4q***

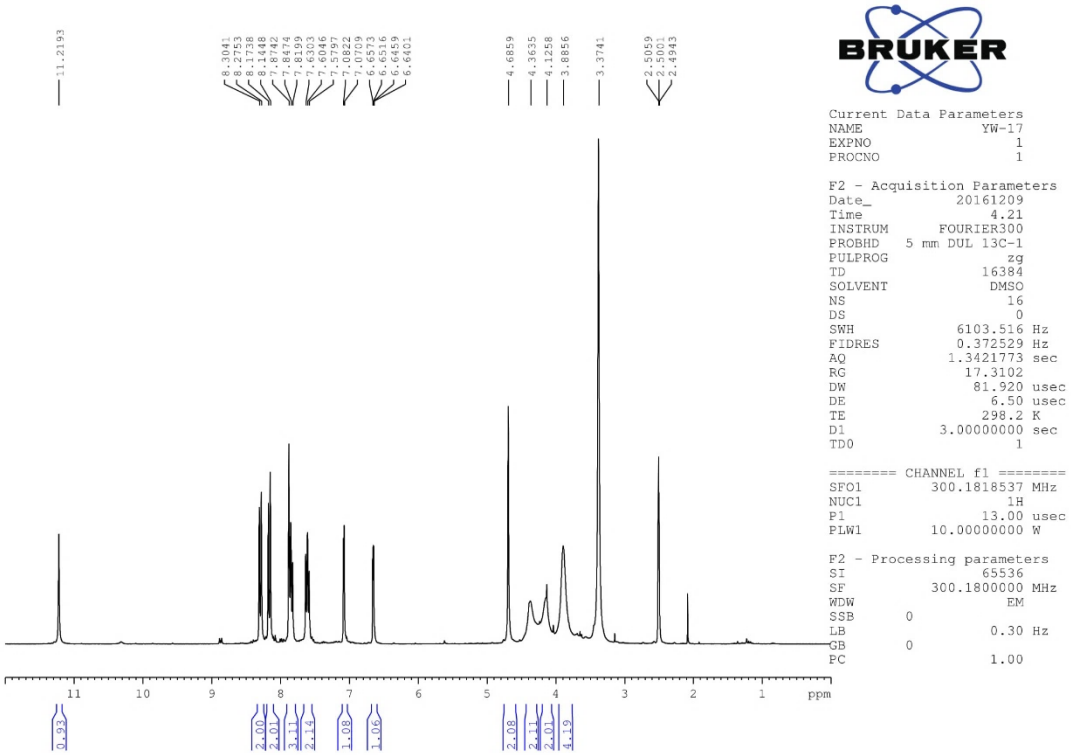

Figure 4.66. *[1]H-NMR Specturum of Compound **4q***

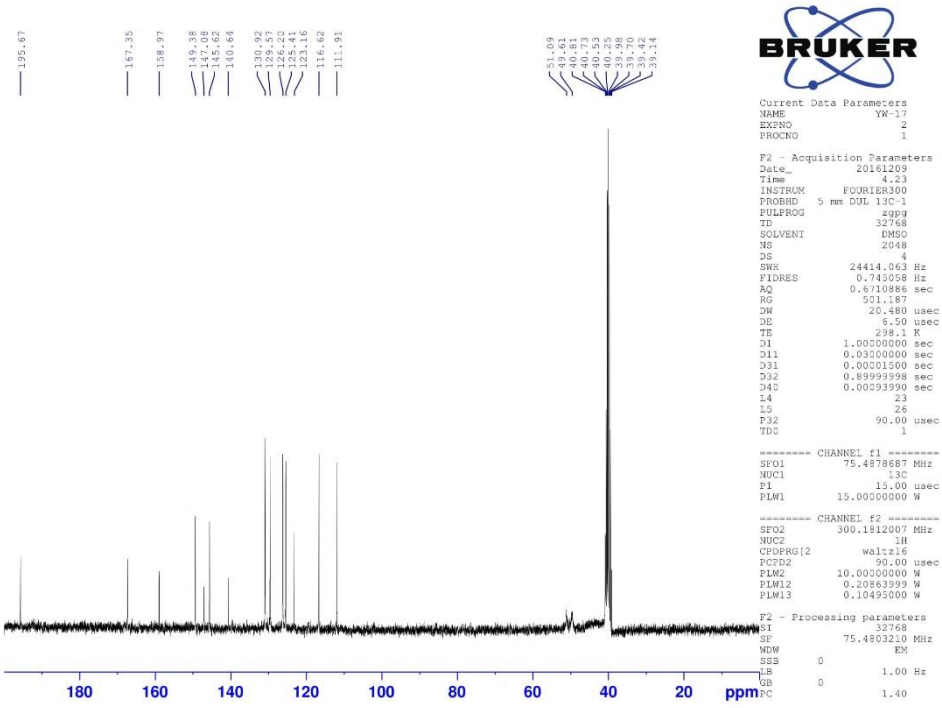

Figure 4.67. [13]C-NMR *Spectrum of Compound **4q***

Formula Predictor Report - YW-17_34.lcd

Page 1 of 1

Data File: C:\LabSolutions\Data\Analiz\GTuran\YW-17_34.lcd

Elmt	Val.	Min	Max	Elmt	Val.	Min	Max	Elmt	Val.	Min	Max	Elmt	Val.	Min	Max	Use Adduct
H	1	7	25	O	2	1	7	Cl	1	0	1	I	3	0	0	H
C	4	17	30	F	1	0	1	Br	1	0	0					
N	3	4	7	S	2	2	3	Ru	2	0	0					

Error Margin (ppm): 10
HC Ratio: unlimited
Max Isotopes: 3
MSn Iso RI (%): 10.00

DBE Range: 14.0 - 19.0
Apply N Rule: yes
Isotope RI (%): 1.00
MSn Logic Mode: AND

Electron Ions: both
Use MSn Info: no
Isotope Res: 10000
Max Results: 500

Event#: 1 MS(E+) Ret. Time : 4.080 -> 4.307 Scan# : 613 -> 647

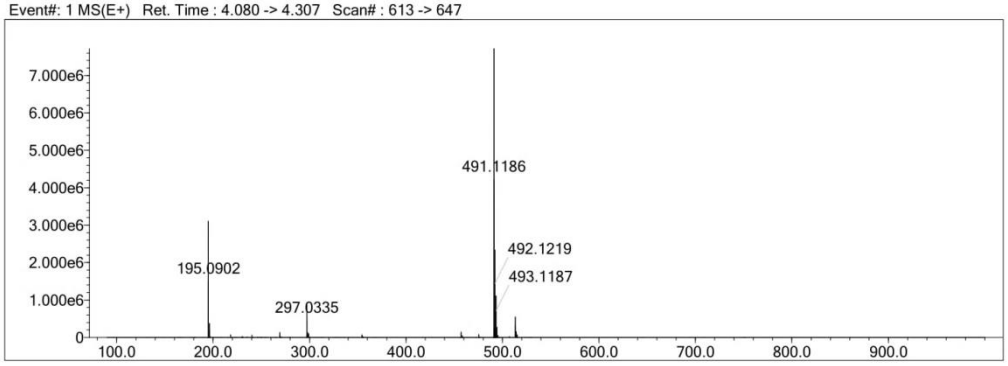

Measured region for 491.1186 m/z

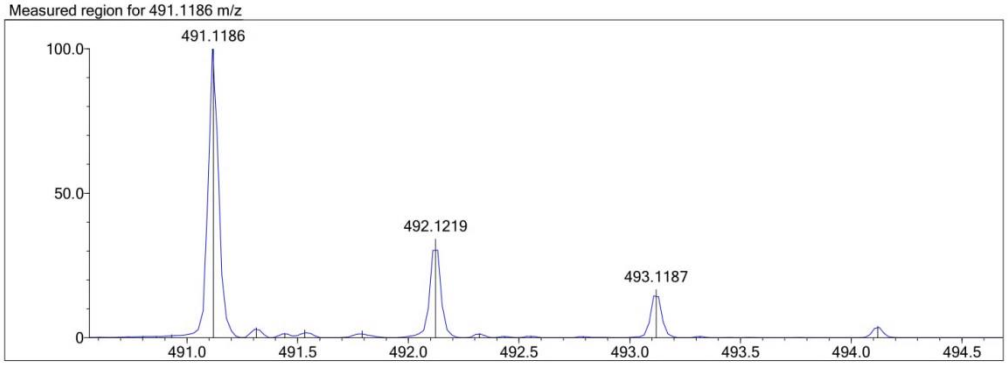

C25 H22 N4 O3 S2 [M+H]+ : Predicted region for 491.1206 m/z

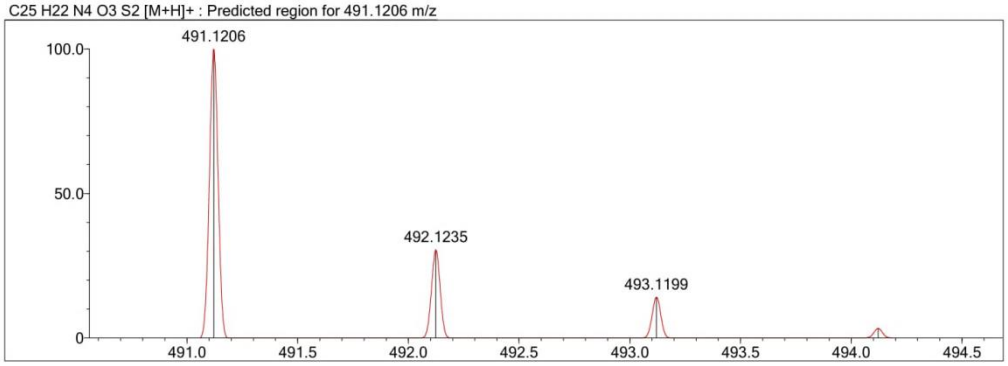

Rank	Score	Formula (M)	Ion	Meas. m/z	Pred. m/z	Df. (mDa)	Df. (ppm)	Iso	DBE
1	78.64	C25 H22 N4 O3 S2	[M+H]+	491.1186	491.1206	-2.0	-4.07	85.18	17.0

Figure 4.68. *Mass Specturum of Compound* ***4q***

2-(9-Acridinylamino)-2-oxoethyl morpholine-4-carbodithioate (4r)

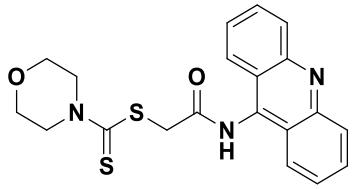

Yield: 89.2%, **M.p.**: 237.8 °C.

FTIR (ATR, cm^{-1}): 3232 (amide N-H), 2864-2949 (aliphatic C-H), 1653 (amide C=O), 1417-1423 (C=N and C=C), 1273 (C=S), 1001(C-O-C of morpholine), 864-758 (out of plane C-H bending).

^{1}H-NMR (300 MHz, DMSO-*d*$_6$; δ, ppm): 3.71-3.72 (4H, d, *J* =4.29 Hz, morpholine $C_{3,5}$-H), 4.01 and 4.25 (4H, two bs, morpholine $C_{2,6}$-H), 4.65 (2H, s, CO$\underline{CH_2}$), 7.58-7.63 (2H, t, *J* =7.54 Hz, Ar-H), 7.82 -7.87 (2H, t, *J*=7.57 Hz, Ar-H), 8.15-8.18 (2H, d, *J*=8.73 Hz, Ar-H), 8.26-8.29 (2H, d, *J*=8.63 Hz, Ar-H), 11.06 (1H, s, -NH-).

^{13}C-NMR (75 MHz, DMSO-*d*$_6$; δ, ppm): 50.87 (CH_2), 51.78 (CH_2), 66.08 (CH_2), 123.16 (C), 125.33 (CH), 126.23 (CH), 129.60 (CH), 130.93 (CH), 140.56 (C), 149.39 (C-9 in 9-aminoacridine), 167.35 (C=O), 195.70 (C=S).

HRMS (m/z): $[M+H]^+$ calcd for $C_{20}H_{19}N_3O_2S_2$: 398.0991. ; found 398.0977.

DOPNALAB

	Item	Value
	Acquired Date&Time	29.12.2016 15:19:06
	Acquired by	System Administrator
	Filename	C:\Users\dopnalab\Desktop\derya\wiam\yw-181.ispd
	Spectrum name	yw-181
	Sample name	YW-18
	Sample ID	
	Option	
	Comment	
	No. of Scans	10
	Resolution	4 [cm-1]
	Apodization	Happ-Genzel

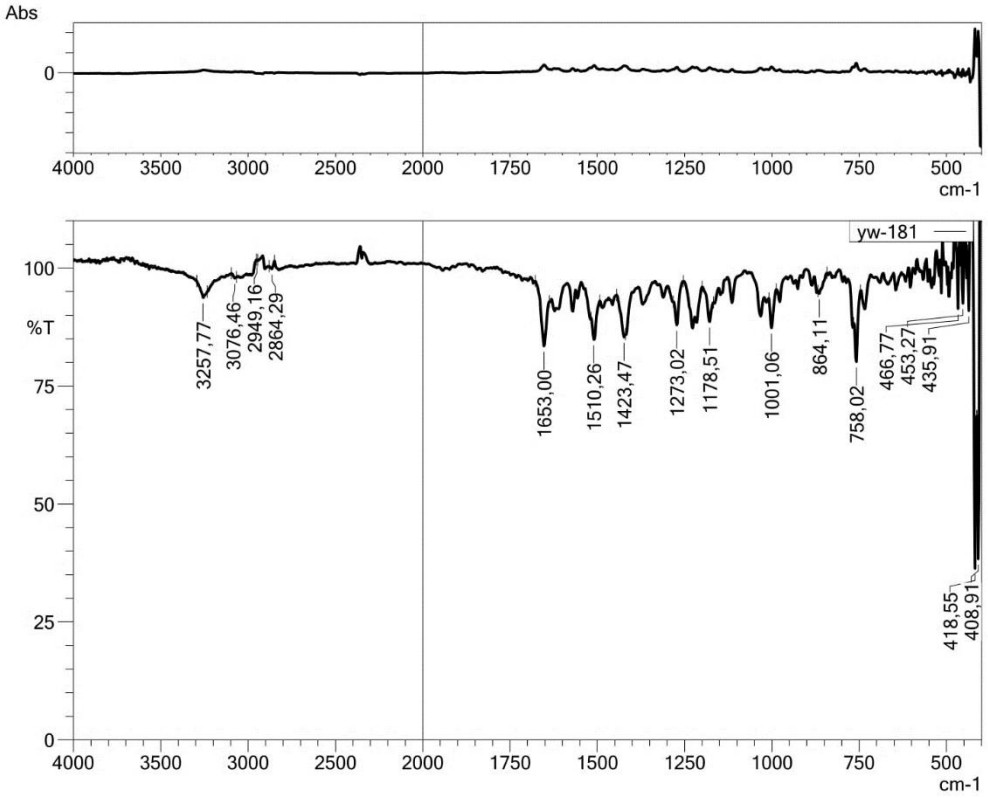

Figure 4.69. *IR Specturum of Compound* ***4r***

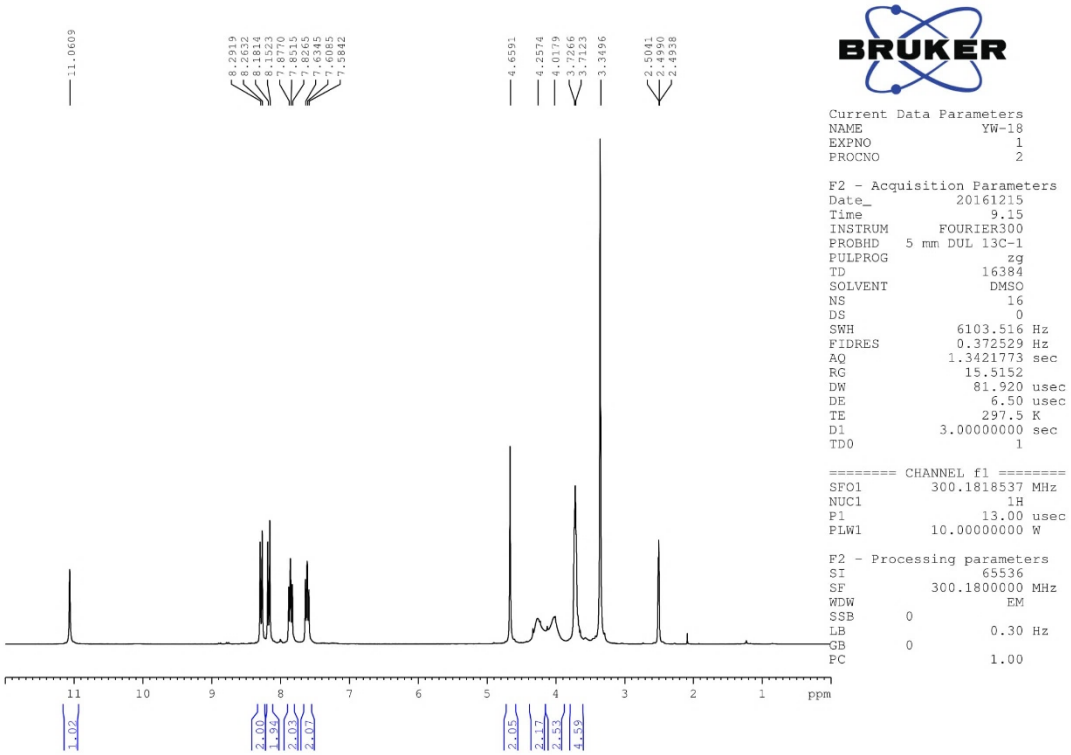

Figure 4.70. *The [1]H-NMR Specturum of Compound **4r***

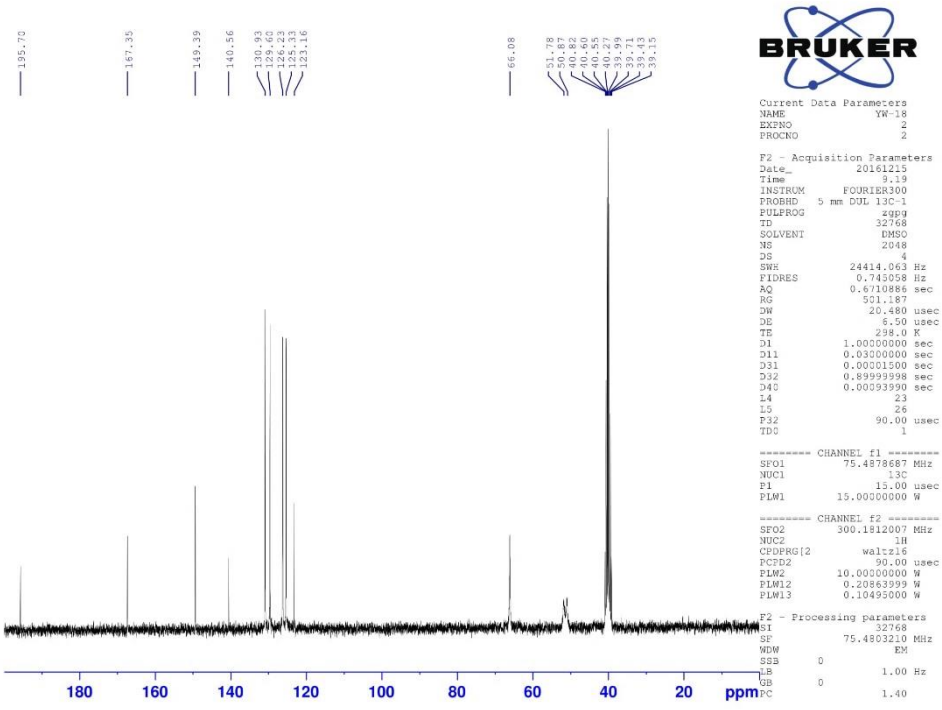

Figure 4.71. *The [13]C-NMR Specturum of Compound **4r***

Formula Predictor Report - YW-18_35.lcd

Page 1 of 1

Data File: C:\LabSolutions\Data\Analiz\GTuran\YW-18_35.lcd

Elmt	Val.	Min	Max	Elmt	Val.	Min	Max	Elmt	Val.	Min	Max	Elmt	Val.	Min	Max	Use Adduct
H	1	7	25	O	2	1	7	Cl	1	0	0	I	3	0	0	H
C	4	17	30	F	1	0	0	Br	1	0	0					
N	3	3	7	S	2	2	3	Ru	2	0	0					

Error Margin (ppm): 10
HC Ratio: unlimited
Max Isotopes: 3
MSn Iso RI (%): 10.00

DBE Range: 10.0 - 20.0
Apply N Rule: yes
Isotope RI (%): 1.00
MSn Logic Mode: AND

Electron Ions: both
Use MSn Info: no
Isotope Res: 10000
Max Results: 500

Event#: 1 MS(E+) Ret. Time : 3.693 -> 3.933 Scan# : 555 -> 591

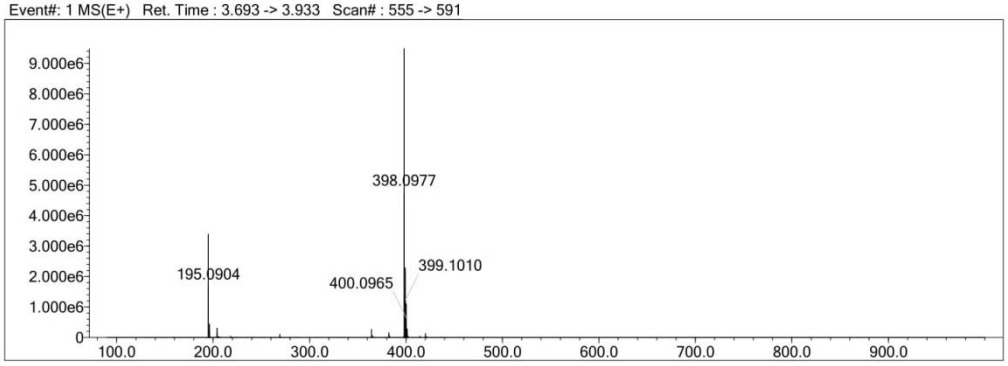

Measured region for 398.0977 m/z

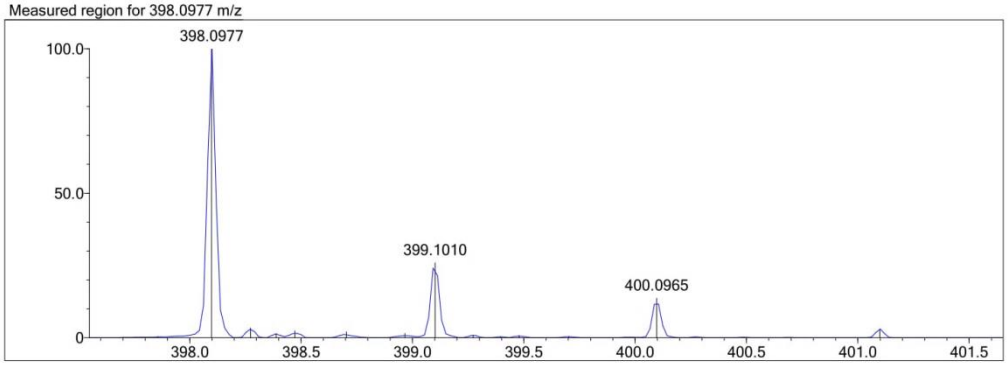

C20 H19 N3 O2 S2 [M+H]+ : Predicted region for 398.0991 m/z

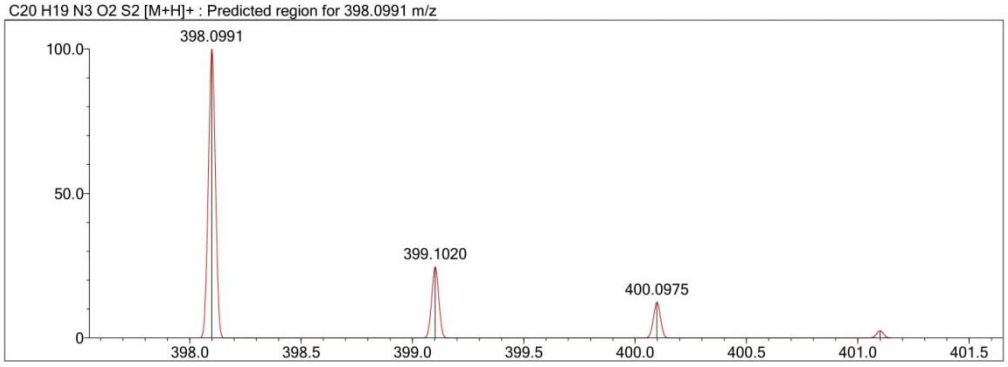

Rank	Score	Formula (M)	Ion	Meas. m/z	Pred. m/z	Df. (mDa)	Df. (ppm)	Iso	DBE
1	93.70	C20 H19 N3 O2 S2	[M+H]+	398.0977	398.0991	-1.4	-3.52	100.00	13.0

Figure 4.72. *Mass Specturum of Compound* ***4r***

2-(9-Acridinylamino)-2-oxoethyl piperidine-1-carbodithioate (4s)

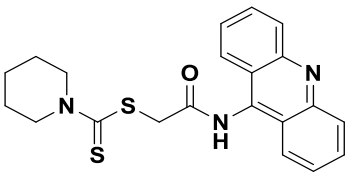

Yield: 84.4%, **M.p.**: 265.4 °C.

FTIR (ATR, cm^{-1}): 3255 (amide N-H), 2904-2983 (aliphatic C-H), 1653 (amide C=O), 1417 (C=N and C=C), 1217 (C=S), 1001(C-N of piperidine), 758 (out of plane C-H bending).

^{1}H-NMR (300 MHz, DMSO-*d*$_6$; δ, ppm): 1.64 (6H, s, piperidine – CH_2), 3.96 and 4.25 (4H, two s , piperidine $\underline{CH_2}$-N-$\underline{CH_2}$), 4.62 (2H, s, CO$\underline{CH_2}$), 7.57-7.61 (2H, t, *J*=6.55 Hz, Ar-H), 7.82 -7.86 (2H, t, *J*=6.85 Hz, Ar-H), 8.14-8.16 (2H, d, *J*=8.34 Hz, Ar-H), 8.26-8.29 (2H, d, *J*=8.46 Hz, Ar-H), 11.14 (1H, s, -NH-).

^{13}C-NMR (75 MHz, DMSO-*d*$_6$; δ, ppm): 23.94 (CH_2), 26.00 (CH_2), 51.67 (CH_2), 53.10 (CH_2), 123.16 (C), 125.42 (CH), 126.16 (CH), 129.56 (CH), 130.91(CH), 140.68 (C), 149.38 (C-9 in 9-aminoacridine), 167.54 (C=O), 193.73 (C=S).

HRMS (m/z): $[M+H]^+$ calcd for $C_{21}H_{21}N_3OS_2$: 396.1199. ; found 396.1184.

DOPNALAB

	Item	Value
	Acquired Date&Time	29.12.2016 15:21:47
	Acquired by	System Administrator
	Filename	C:\Users\dopnalab\Desktop\derya\wiam\yw-191.ispd
	Spectrum name	yw-191
	Sample name	YW-19
	Sample ID	
	Option	
	Comment	
	No. of Scans	10
	Resolution	4 [cm-1]
	Apodization	Happ-Genzel

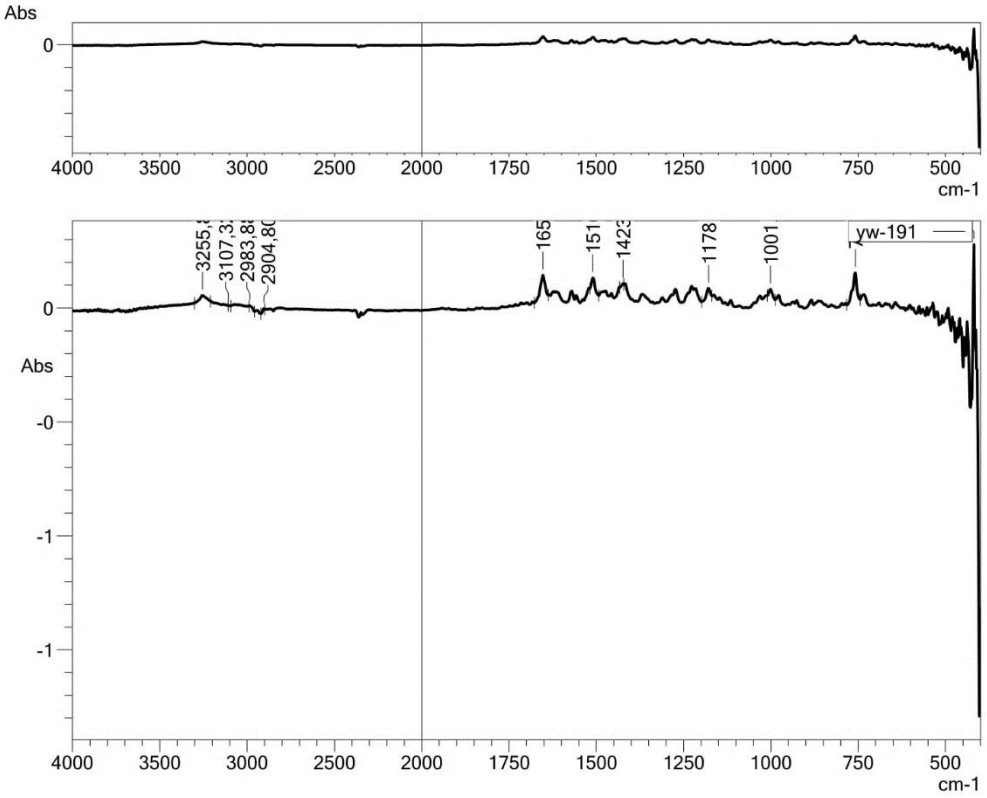

Figure 4.73. *IR Specturum of Compound **4s***

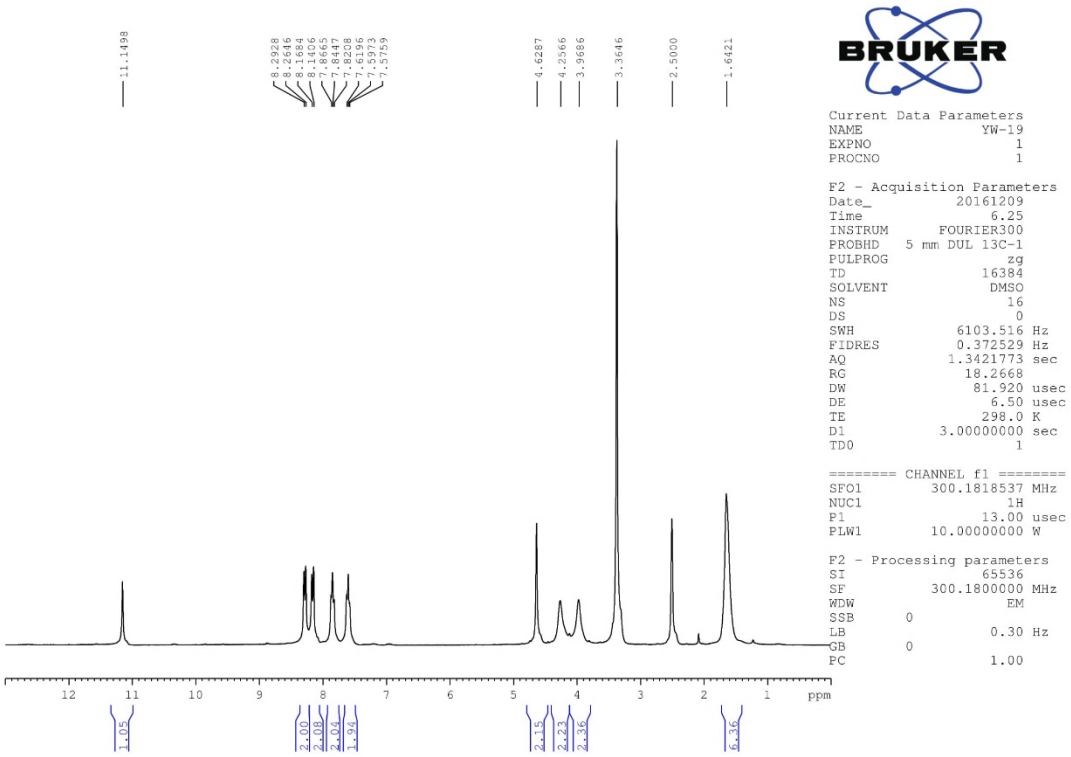

Figure 4.74. *The [1]H-NMR Specturum of Compound **4s***

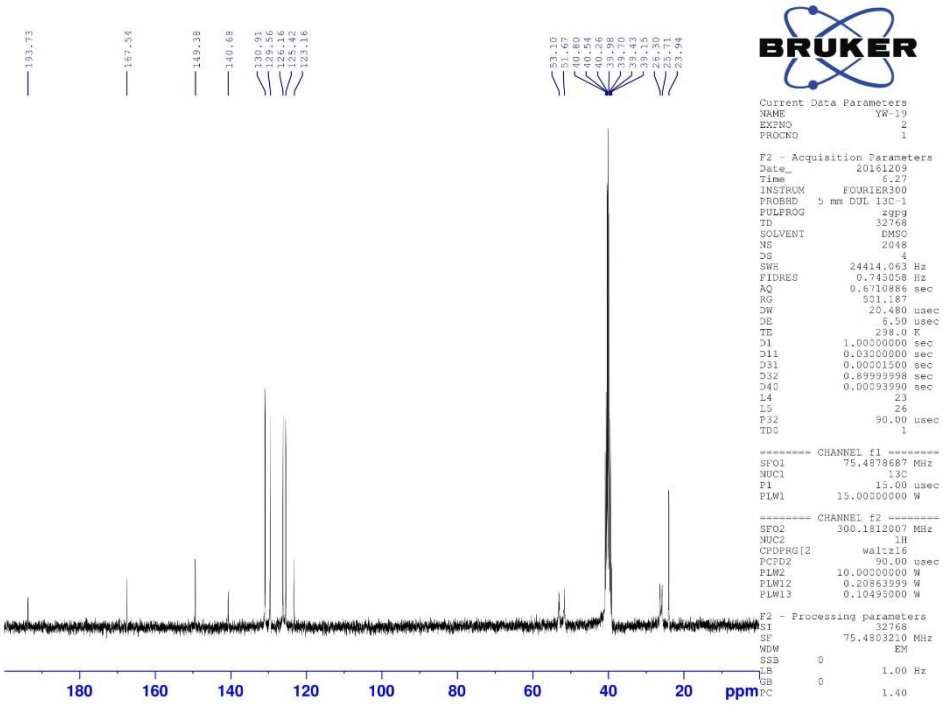

Figure 4.75. *The [13]C-NMR Specturum of Compound **4s***

Formula Predictor Report - YW-19_36.lcd

Page 1 of 1

Data File: C:\LabSolutions\Data\Analiz\GTuran\YW-19_36.lcd

Elmt	Val.	Min	Max	Elmt	Val.	Min	Max	Elmt	Val.	Min	Max	Elmt	Val.	Min	Max	Use Adduct
H	1	7	25	O	2	1	7	Cl	1	0	0	I	3	0	0	H
C	4	17	30	F	1	0	0	Br	1	0	0					
N	3	3	7	S	2	2	3	Ru	2	0	0					

Error Margin (ppm): 10
HC Ratio: unlimited
Max Isotopes: 3
MSn Iso RI (%): 10.00

DBE Range: 10.0 - 20.0
Apply N Rule: yes
Isotope RI (%): 1.00
MSn Logic Mode: AND

Electron Ions: both
Use MSn Info: no
Isotope Res: 10000
Max Results: 500

Event#: 1 MS(E+) Ret. Time : 4.653 -> 4.853 Scan# : 699 -> 729

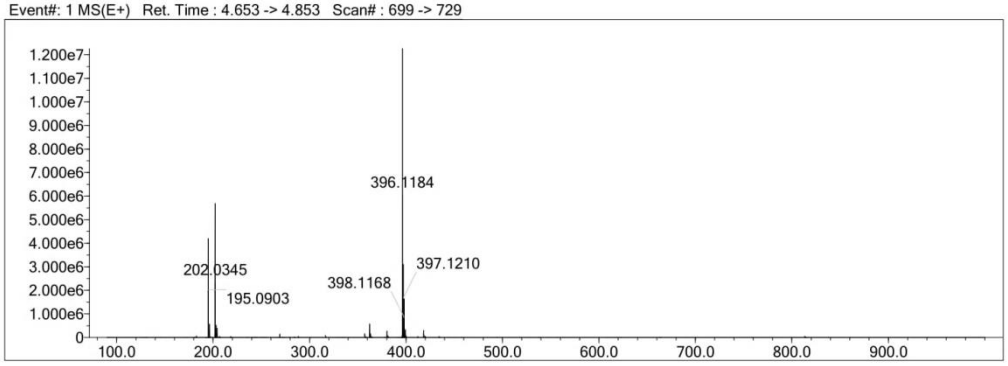

Measured region for 396.1184 m/z

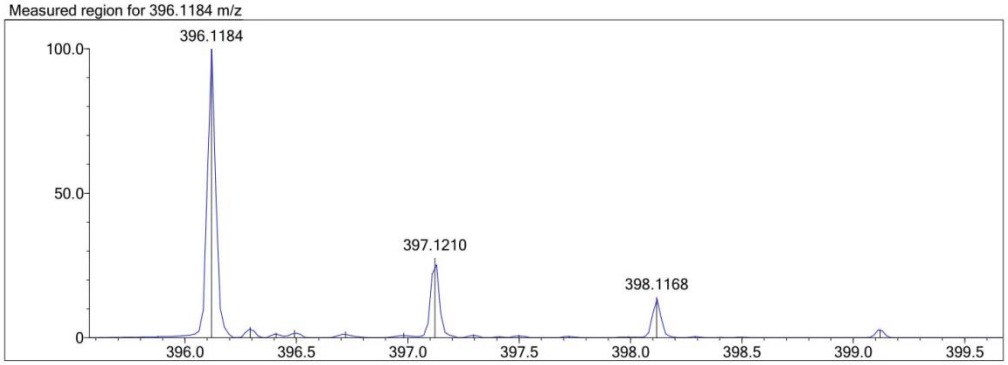

C21 H21 N3 O S2 [M+H]+ : Predicted region for 396.1199 m/z

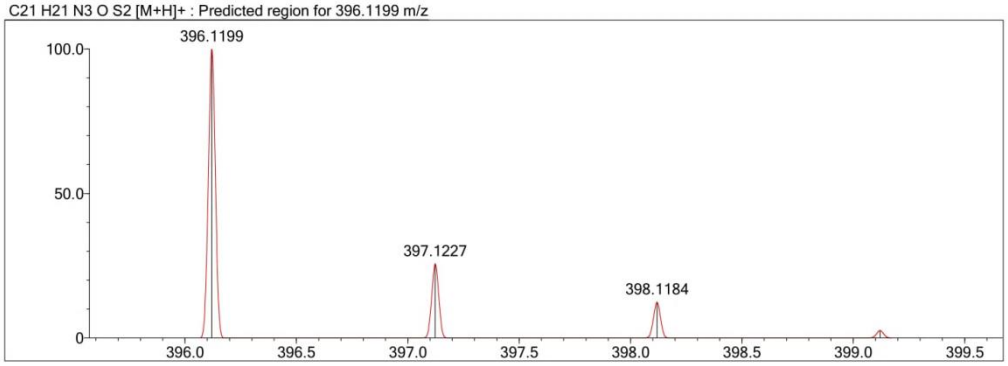

Rank	Score	Formula (M)	Ion	Meas. m/z	Pred. m/z	Df. (mDa)	Df. (ppm)	Iso	DBE
1	93.03	C21 H21 N3 O S2	[M+H]+	396.1184	396.1199	-1.5	-3.79	100.00	13.0

Figure 4.76. *Mass Specturum of Compound* ***4s***

2-(9-Acridinylamino)-2-oxoethyl 2-methylpiperidine-1-carbodithioate (4t)

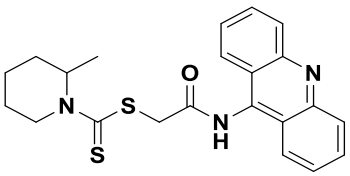

Yield: 93.3%, **M.p.**: 265.4 °C.

FTIR (ATR, cm^{-1}): 3255 (amide N-H), 2924 (aliphatic C-H), 1653 (amide C=O), 1417-1463 (C=N and C=C), 1215-1263 (C=S), 1001(C-N of piperidine), 758 (out of plane C-H bending).

^{1}H-NMR (300 MHz, DMSO-*d*$_6$; δ, ppm): 1.19-1.25 (9H, m, piperidine – CH_2, -CH_3), 4.26-4.30 (3H, m, piperidine - CH_2-, - CH-), 4.61 (2H, s, CO$\underline{CH_2}$), 7.60 (2H, t, *J*=7.50 Hz, Ar-H), 7.85 (2H, t, *J*=7.50 Hz, Ar-H), 8.16 (2H, d, *J*=8.64 Hz, Ar-H), 8.28 (2H, d, *J*=8.67 Hz, Ar-H), 10.94 (1H, s, -NH-).

^{13}C-NMR (75 MHz, DMSO-*d*$_6$; δ, ppm): 18.48 (CH_3), 18.67 (CH_2), 25.66 (CH_2), 26.19 (CH_2), 52.20 (CH_2), 54.56 (CH), 123.16 (C), 125.35 (CH), 126.17 (CH), 129.59 (CH), 130.91 (CH),140.26 (C), 149.38 (C-9 in 9-aminoacridine), 167.58 (C=O), 194.33 (C=S).

HRMS (m/z): $[M+H]^+$ calcd for $C_{22}H_{23}N_3OS_2$: 410.1355 ; found 410.1338.

DOPNALAB

	Item	Value
	Acquired Date&Time	29.12.2016 15:24:37
	Acquired by	System Administrator
	Filename	C:\Users\dopnalab\Desktop\derya\wiam\yw-201.ispd
	Spectrum name	yw-201
	Sample name	YW-20
	Sample ID	
	Option	
	Comment	
	No. of Scans	10
	Resolution	4 [cm-1]
	Apodization	Happ-Genzel

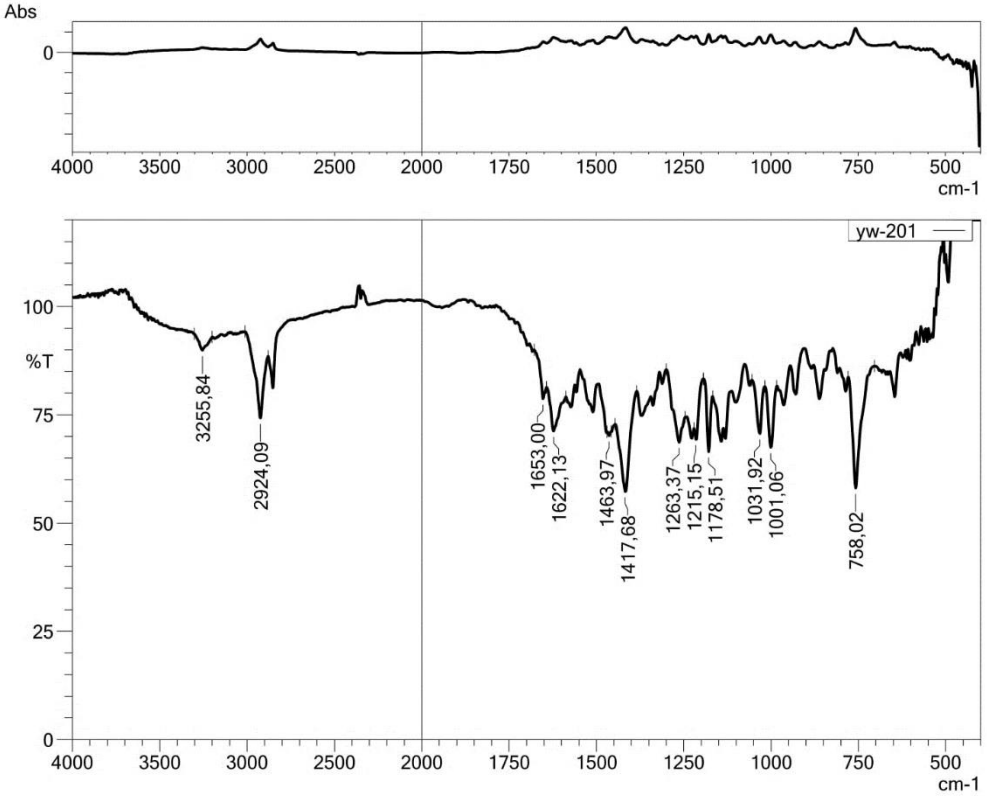

Figure 4.77. *IR Specturum of Compound* ***4t***

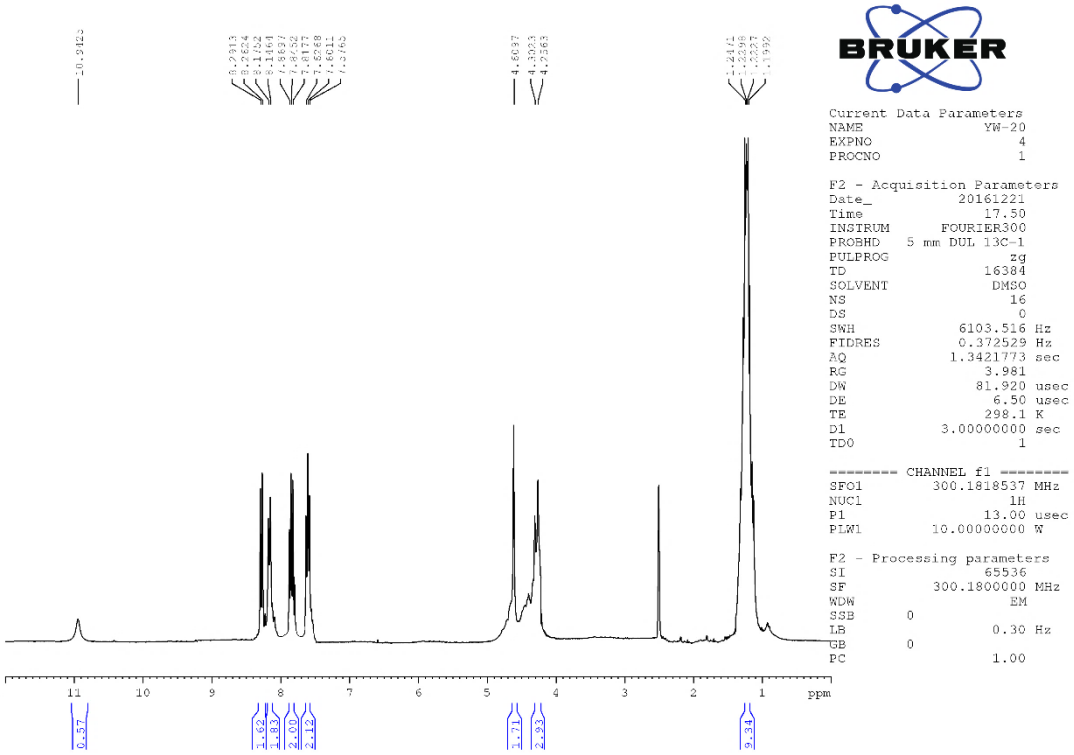

Figure 4.78. *The [1]HNMR Specturum of Compound* ***4t***

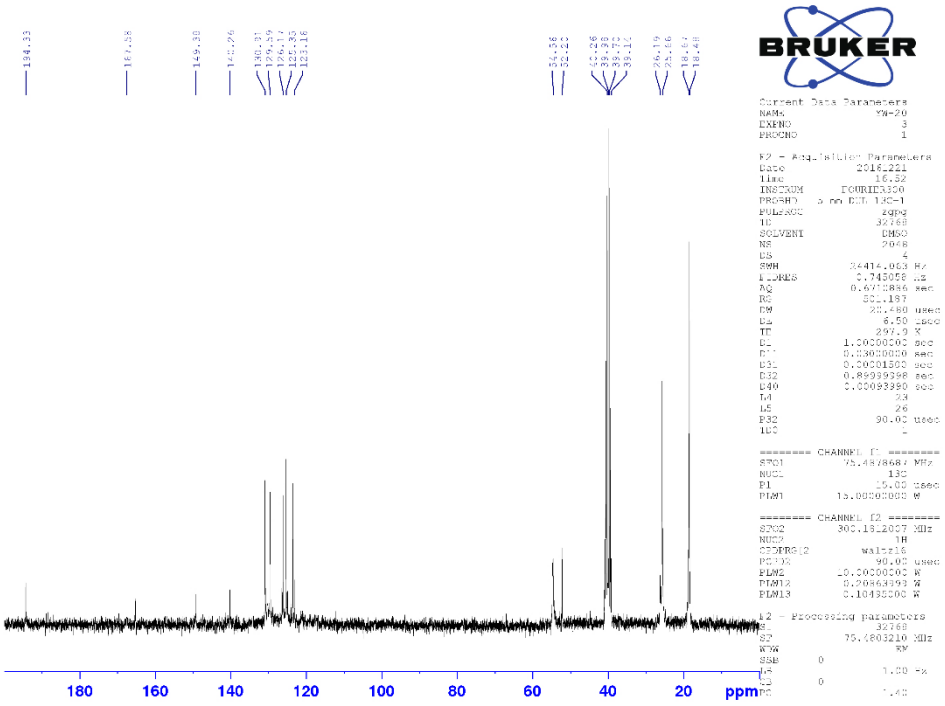

Figure 4.79. *The [13]CNMR Specturum of Compound* ***4t***

Formula Predictor Report - YW-20_10.lcd

Page 1 of 1

Data File: C:\LabSolutions\Data\Analiz\GTuran\YW-20_10.lcd

Elmt	Val.	Min	Max	Elmt	Val.	Min	Max	Elmt	Val.	Min	Max	Elmt	Val.	Min	Max	Use Adduct
H	1	23	40	O	2	0	15	Cl	1	0	0	I	3	0	0	H
C	4	22	30	F	1	0	0	Br	1	0	0					
N	3	0	3	S	2	0	2	Ru	2	0	0					

Error Margin (ppm): 5
HC Ratio: unlimited
Max Isotopes: 3
MSn Iso RI (%): 10.00

DBE Range: 0.0 - 30.0
Apply N Rule: yes
Isotope RI (%): 1.00
MSn Logic Mode: AND

Electron Ions: both
Use MSn Info: no
Isotope Res: 10000
Max Results: 500

Event#: 1 MS(E+) Ret. Time : 5.147 -> 5.253 - 6.480 -> 7.429 Scan# : 773 -> 789 - 973 -> 1115

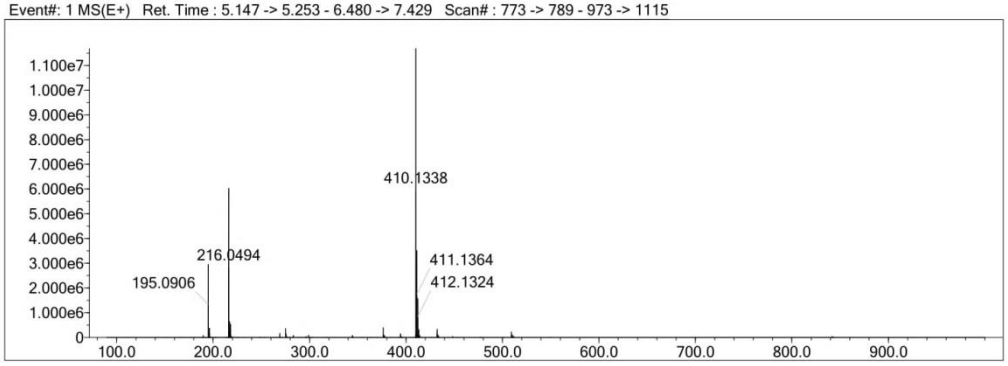

Measured region for 410.1338 m/z

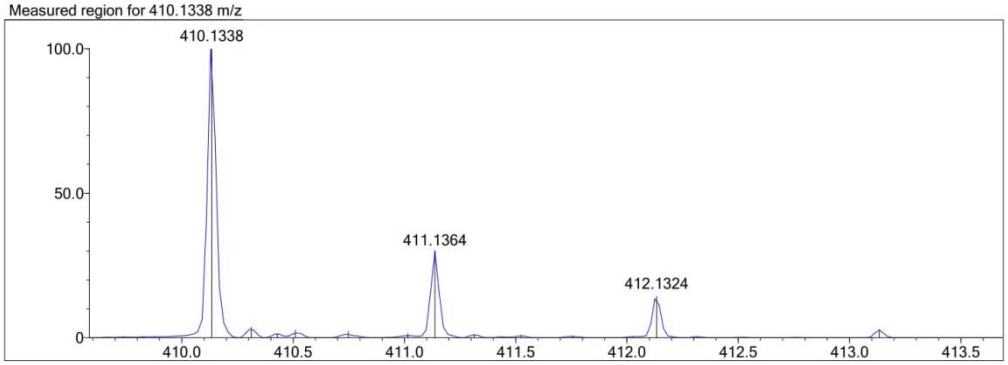

C22 H23 N3 O S2 [M+H]+ : Predicted region for 410.1355 m/z

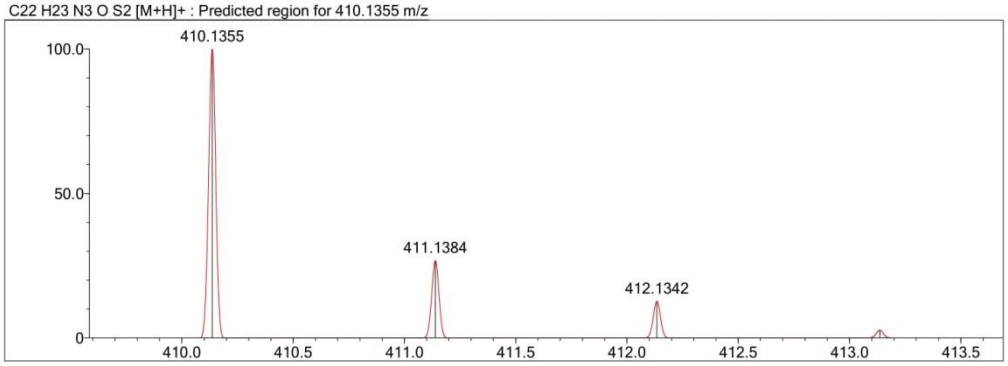

Rank	Score	Formula (M)	Ion	Meas. m/z	Pred. m/z	Df. (mDa)	Df. (ppm)	Iso	DBE
1	74.28	C22 H23 N3 O S2	[M+H]+	410.1338	410.1355	-1.7	-4.14	80.61	13.0

Figure 4.80. *Mass Specturum of Compound* ***4t***

2-(9-Acridinylamino)-2-oxoethyl 4-benzylpiperidine-1-carbodithioate (4u)

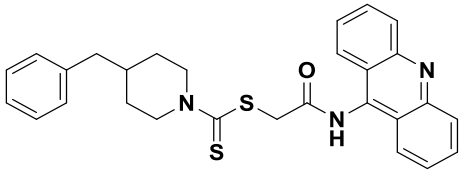

Yield: 90.7%, **M.p.**: 265.4 °C.

FTIR (ATR, cm^{-1}): 3261 (amide N-H), 2852-2922 (aliphatic C-H), 1653 (amide C=O), 1452-1570 (C=N and C=C), 1261 (C=S), 1016 (C-N of piperidine), 758 (out of plane C-H bending).

^{1}H-NMR (300 MHz, DMSO-*d*$_6$; δ, ppm): 1.22-1.26 (5H, m, piperidine – CH_2, -CH), 3.04-3.08 (2H, m, piperidine - CH_2-), 3.20-3.25 (2H, m, piperidine - CH_2-), 3.97 (2H, s, C_6H_5-$\underline{CH_2}$-), 4.61 (2H, s, CO$\underline{CH_2}$), 7.58 (2H, t, *J*=7.60 Hz, Ar-H), 7.67 (2H, t, *J*=7.50 Hz, Ar-H), 7.77-7.86 (5H, m, Benzyl –CH), 8.15 (2H, d, *J*=8.70 Hz, Ar-H), 8.28 (2H, d, *J*=8.67 Hz, Ar-H).

^{13}C-NMR (75 MHz, DMSO-*d*$_6$; δ, ppm): 37.12 (CH), 42.04 (CH_2), 48.74 (CH_2), 50.63 (CH_2), 54.56 (CH_2), 122.44 (C), 125.50 (CH), 125.97 (CH), 126.38 (CH), 128.68 (CH), 129.47 (CH), 130.34 (CH), 130.91 (CH), 132.15 (CH), 140.33 (C), 149.23 (C-9 in 9-aminoacridine), 167.61 (C=O), 193.93 (C=S).

HRMS (m/z): $[M+H]^+$ calcd for $C_{28}H_{27}N_3OS_2$: 486.1668 ; found 486.1654.

DOPNALAB

	Item	Value
	Acquired Date&Time	29.12.2016 15:27:26
	Acquired by	System Administrator
	Filename	C:\Users\dopnalab\Desktop\derya\wiam\yw-211.ispd
	Spectrum name	yw-211
	Sample name	YW-21
	Sample ID	
	Option	
	Comment	
	No. of Scans	10
	Resolution	4 [cm-1]
	Apodization	Happ-Genzel

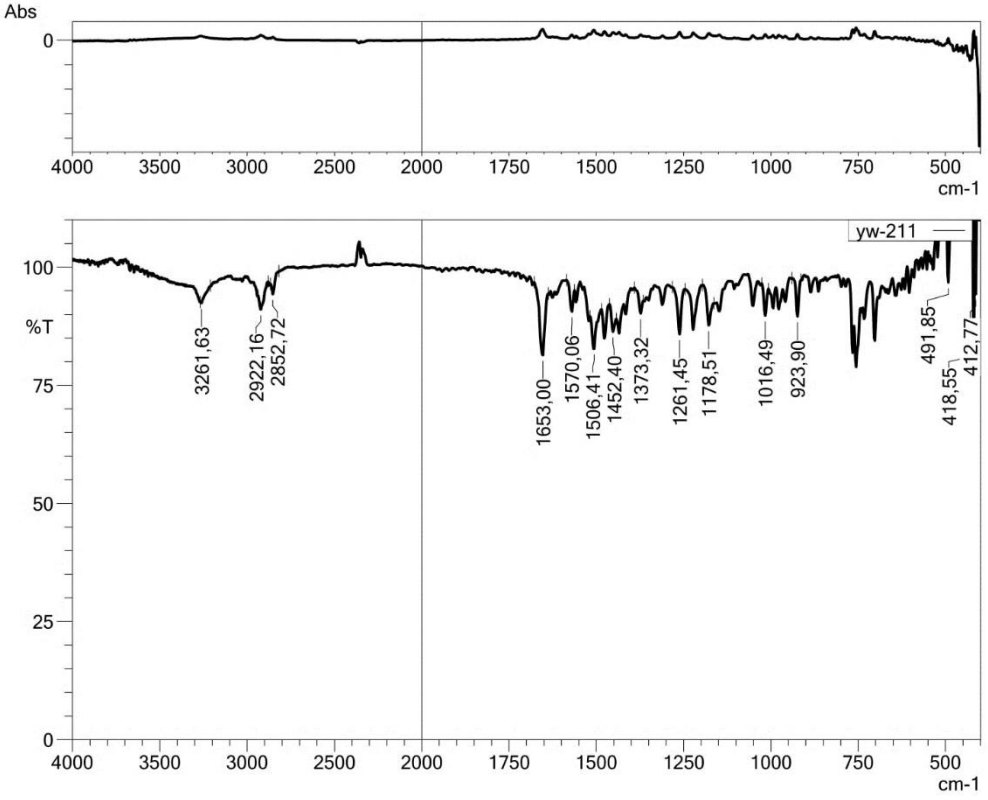

Figure 4.81. *IR Specturum of Compound* ***4u***

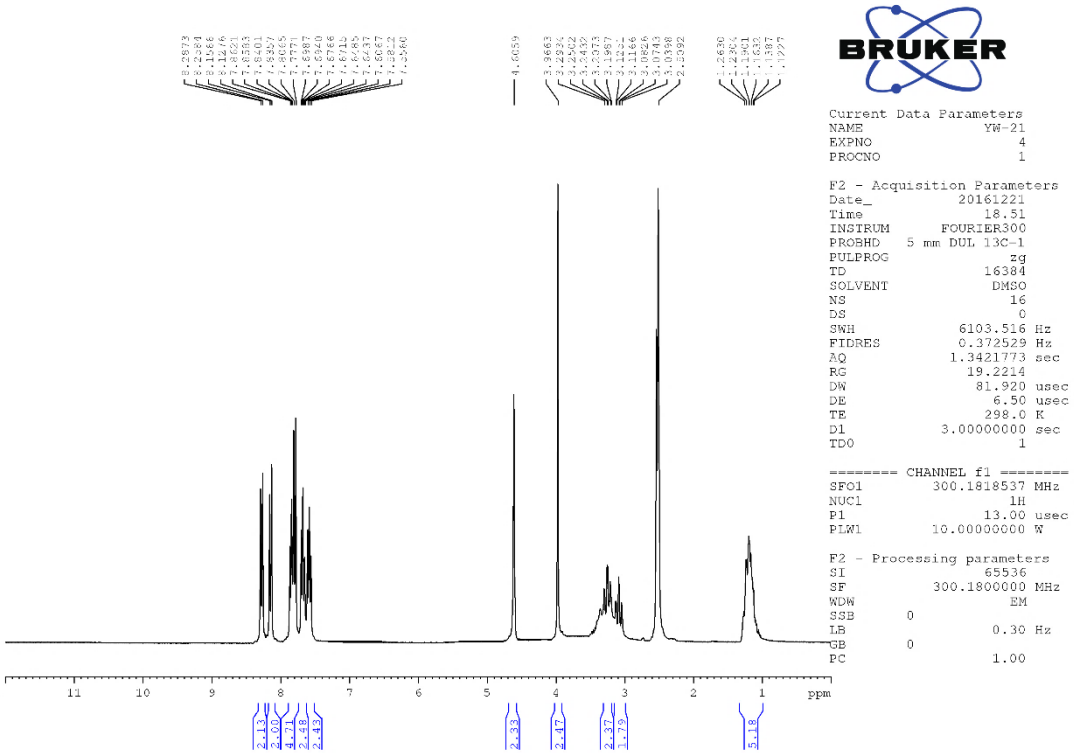

Figure 4.82. *The [1]HNMR Specturum of Compound* ***4u***

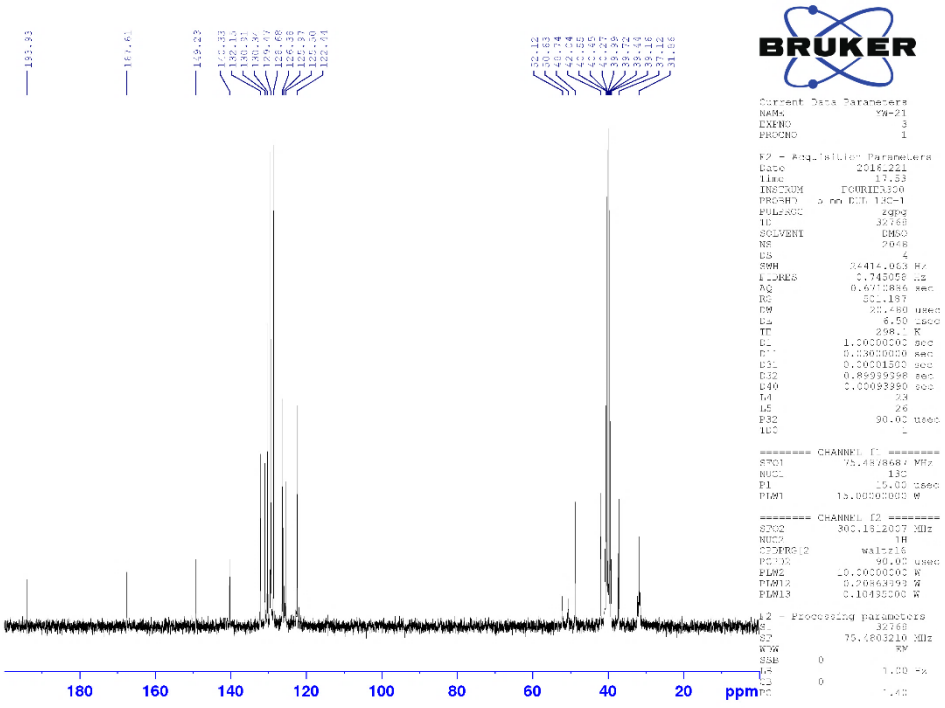

Figure 4.83. *The [13]CNMR Specturum of Compound* ***4u***

Formula Predictor Report - YW-21_38.lcd

Page 1 of 1

Data File: C:\LabSolutions\Data\Analiz\GTuran\YW-21_38.lcd

Elmt	Val.	Min	Max	Elmt	Val.	Min	Max	Elmt	Val.	Min	Max	Elmt	Val.	Min	Max	Use Adduct
H	1	7	30	O	2	1	7	Cl	1	0	0	I	3	0	0	H
C	4	17	30	F	1	0	0	Br	1	0	0					
N	3	3	7	S	2	2	3	Ru	2	0	0					

Error Margin (ppm): 10
HC Ratio: unlimited
Max Isotopes: 3
MSn Iso RI (%): 10.00

DBE Range: 14.0 - 20.0
Apply N Rule: yes
Isotope RI (%): 1.00
MSn Logic Mode: AND

Electron Ions: both
Use MSn Info: no
Isotope Res: 10000
Max Results: 500

Event#: 1 MS(E+) Ret. Time : 6.067 -> 6.333 Scan# : 911 -> 951

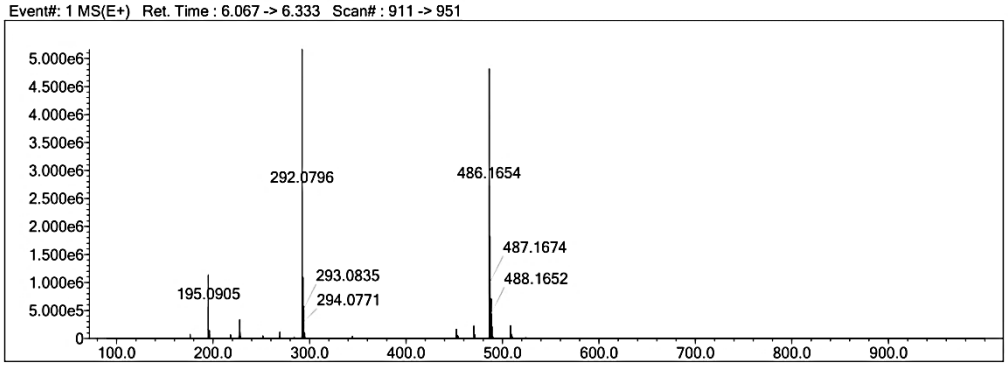

Measured region for 486.1654 m/z

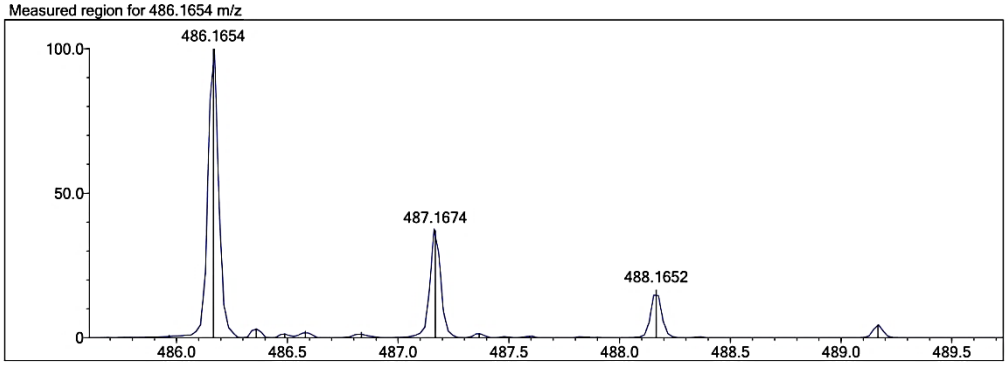

C28 H27 N3 O S2 [M+H]+ : Predicted region for 486.1668 m/z

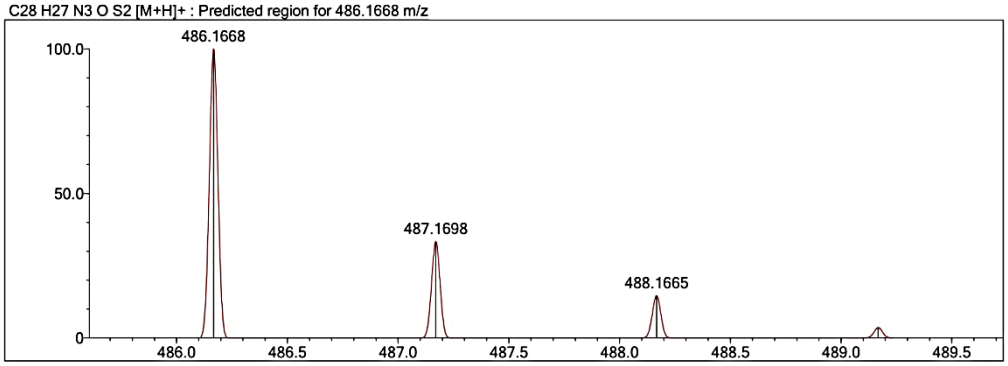

Rank	Score	Formula (M)	Ion	Meas. m/z	Pred. m/z	Df. (mDa)	Df. (ppm)	Iso	DBE
1	95.30	C28 H27 N3 O S2	[M+H]+	486.1654	486.1668	-1.4	-2.88	100.00	17.0

Figure 4.84. *Mass Specturum of Compound* ***4u***

4.2. Chemistry

The synthesis of 2-(9-acridinylamino)-2-oxoethyl piperazinyl/piperidinyl/morpholinylcarbodithioate derivatives **(4a-4u)** was accomplished as indicated by (**Scheme 3.1**). The starting compounds sodium *N*-substituted piperazine dithiocarbamates **(1)** were prepared in accordance with literatures method **Figure 4.85** shows the proposed reaction mechanism suggested for *N*-substituted piperazine dithiocarbamates.

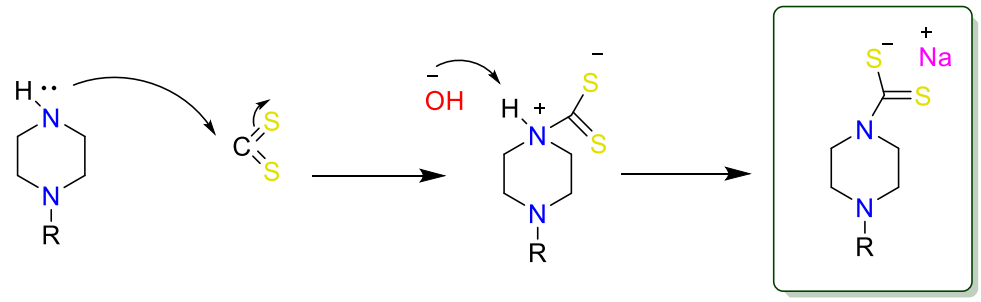

Figure 4.85. *The Proposed Reaction Mechanism Suggested for Sodium N-Substituted Piperazine Dithiocarbamates*

In the second step, 9-Aminoacridine was acetylated with chloroacetyl chloride to give *N*-(9-acridinyl)-2-chloroacetamide derivatives (**2**) (Wang et al., 2005, p.4667-4678). (**Figure 4.86**) shows the acetylation reaction mechanism suggested for the same derivatives.

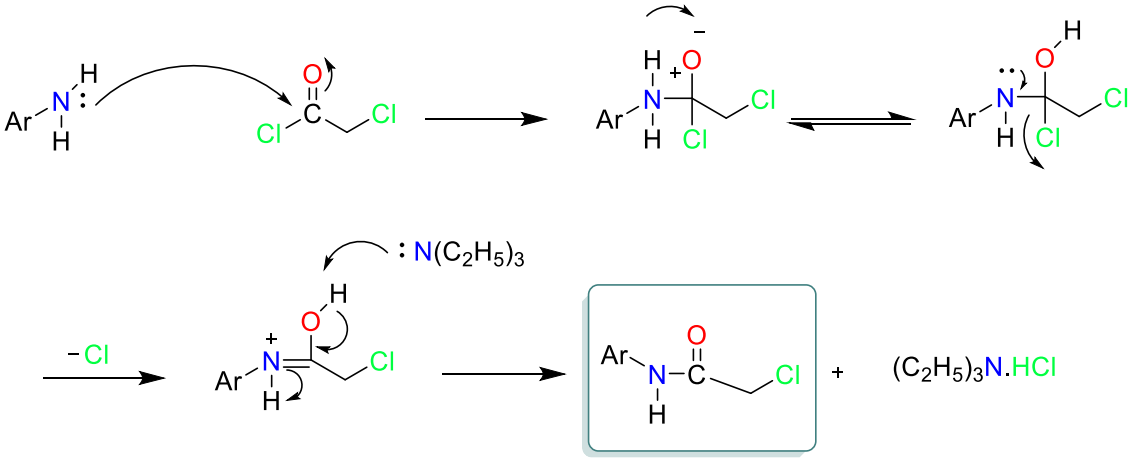

Figure 4.86. *The Proposed Reaction Mechanism Suggested for 9-Aminoacridine Acetylation*

The newly synthesized derivatives (**4a-4u**), were obtained by taking the advantage of three-steps protocol based on the treatment of *N*-(9-acridinyl)-2-chloroacetamide derivatives (**2**) with appropriate sodium *N*-substituted piperazine/piperidine/morpholine dithiocarbamates (**1**). The yields of the final synthesized compounds differed in the interim of 81.0-97.0 %. The structures of all synthesized compounds were elucidated by IR spectroscopy, mass spectrometry and ^{1}H-NMR and ^{13}C-NMR spectrometry. All new molecules indicated logical analytical and spectroscopic information in great concurrence with their structures, and after that they submitted to biological evaluation tests.

For instance, IR analysis of the compounds (**4a-4u**) showed characteristic absorption band at 3223-3352 cm^{-1} because of amide (N-H) group. The formation of amide was further affirmed by ^{1}H-NMR spectra which displayed downfield appearance of a singlet at 10.94-11.22 ppm. Since the protons that are involved in hydrogen bonding (like -OH and -NH) can come anywhere in the proton NMR spectrum. Sometimes they may also be absent. This because they are susceptible to many factors such as solvation, acidity, concentration and temperature, it can often be difficult to seen (Silverstein and Webster, 1998, p.166-167), because of this we not observed the amide proton and OH proton in compounds **4u** and **4e**, respectively. Bands due to C=O was seen at 1651-1676 cm^{-1}. Likewise, stretching bands due to thiocarbonyl (C=S) was seen at 1209-1284 cm^{-1}. The other Stretching bands in the IR spectra belonging to aromatic and aliphatic regions were observed in the assessed regions. Thus, aromatic C-H out-of-plane deformation modes due to monocyclic and polycyclic rings (acridine) noted easily and was appeared at 705-999 cm^{-1} and was in accordance with the literature values (Wang and Griffiths, 1995, p.229-236). There are some regular groups which exist in all synthesized final compounds, they might be viewed as verifications of the presence of (thiocarbamoylthio)acetamide residue of the objective compounds. In the ^{1}H-NMR spectra, the signal because of $COCH_2$ methylene protons, display in all compounds and appeared 4.60-4.68 ppm, as singlets. Aliphatic protons of piperazine, piperidine and morpholine were seen at 2.41-4.45, 1.19-4.30 and 3.71- 4.25 ppm, respectively. All other aromatic protons owing to phenyl ring and alkyl protons owing to methyl, methoxy substituents of the ring were determined at expected ranges. Additionally, the protons of dimethyl amino groups were seen at 2.08-2.18 ppm in accordance to the literature data (Zengin, 2014, p.1094-1101). The placement of 9-aminoacridine peaks is as the following: The C_1-H and C_4-H appeared as doublets situated at 6.81 and 8.14 ppm; the

C_2-H and C_3-H appeared as triplets situated at 6.67 and 7.87 ppm, respectively. In all compounds, the 9-aminoacridine the C_1-H/C_8-H and C_4-H/C_5-H signals appear at higher chemical shifts than those derived from C_2-H/C_7-H and C_3-H/C_6-H. This effect is likely due to the off-shielding influence of neighboring O atoms of the NHCO portion and the endocyclic N atom respectively (Krzyminski et al., 2011, p.401-409).

The nonappearance of -NH_2 signs is demonstrate that the acetylation was happening progressively. In addition, the protons of -CH_2 and -NH on the acetamide group peaked in the range of 4.60-4.68 ppm and 10.94-11.22 ppm, respectively, in line with the literature data (Modh et al., 2013, p.793-804). In the ^{13}C-NMR spectra, the major shifts might be attributed to the amide carbonyl peaks which observed at 167.33-167.61 ppm area while S-CH_2 and C=S peaks appeared as singlets at 42.97-52.20 and 193.73-195.70 ppm, respectively which confirmed the proposed dithiocarbamic acid ester structure (Turan-Zitouni et al., 2013, p.509–514). The proton-decoupled ^{13}C spectra for compounds containing both fluorine and protons can be quite complicated and difficult to interpret. This is because of the powerful and long-range fluorine-carbon couplings (Schilling, 1982, p.30-49). In the compound, **4n** the CF_3 splitting observed in the following manners as expected: the first C-F_3 coupling appeared as a quartet at δ 125.00 with a large J-coupling which corresponds to the carbon bonded to F_3 (q, *J*=214.9 Hz, CF_3). The rest of the C-F couplings were seen at δ 125.60 (q, *J*=3.6 Hz, trifluoromethylphenyl $C_{3,3'}$) and 129.96 (q, *J*=39.8 Hz, trifluoromethylphenyl C_4). In the compound **4p** where we have 4-fluorophenylpiperazine we can identify four doublets at 115.90 (d, *J*=21.8 Hz, fluorophenyl $C_{3,3'}$), 117.90 (d, *J*=7.5 Hz, fluorophenyl $C_{2,2'}$), 147.42 (d, *J*=2.3 Hz, fluorophenyl C_1) and 156.78 (d, *J*=234.8 Hz, fluorophenyl C_4) in accordance to the data generated through literature (Levent et al., 2016, p.510-519).

4.3. Inhibition Potency of the Compounds

For clear understanding to the inhibitory potency of the newly synthesized compounds along with acquiring effective knowledge about SAR, and because our in-depth analysis showed that the incorporation of a 9-aminoacridine moiety to our designed compounds contributes weakly to the AChE inhibition activity but, strongly increase the inhibition activity toward BChE (**Table 4.1, 4.2 and 4.3**). This section is divided into three main parts because the inhibitory activity against BChE of the synthesized compounds was sensitive to a substituent and the type of heterocyclic ring present in the structures.

4.3.1. Part 1. Substituted piperazine series (4a-4q)

This class of derivatives **(4a-4q)** offered a wide range of anti-ChE activity (expressed as the concentration required to inhibit 50% of this activity (IC_{50}) ranging from 0.015 to 2.038 µM (BChE) (Figure 4.87) and only 45.945µM for (AChE). Compounds (**4a**, **4b**, **4e**, **4i**, **4m**, **4n** and **4o**) possessing piperazine with (dimethylamino-ethyl), (dimethylamino-propyl), 2-hydroxyethyl, 4-chlorophenyl, 4-benzhydryl, 4-(trifluoromethyl)benzyl and 4-methylbenzyl respectively, shows more potent BChE inhibitory activity than other derivatives in the series. Furthermore, compounds (4a, 4b, 4e, 4m, and 4o) exhibited better BChE inhibition (IC_{50}; 0.092-1.420 µM) in compare with the positive control, donepezil, by 18.3-1.2-fold.

From the 7 active derivatives featuring this series compound **4n** exhibited intermediate inhibitory activity against AChE (IC_{50}; 45.945 µM) and superior BChE inhibition activity (IC_{50} value of 0.015 µM and selectivity index to BChE of 3.063) which was 112.2-fold more than that of donepezil (IC_{50};1.683 µM). Consequently, it has been chosen for the kinetic studies.

Along these lines, the accompanying SAR perceptions can be drawn from the inhibition potency data in this series: (**i**): Structurally, a substitution of a trifluoromethyl group at the 4^{th} position of the piperazine ring is responsible for this change in potency, in addition, it was reported that the carbonyl of the acetamido group ($COCH_2$) was essential for activity and it already presented in this compound and in all our synthesized compounds (Sugimoto et al., 2000, p.303-317). Furthermore, a benzyl ring which found in the donepezil, a benzylpiperidine derivative may play a significant role in determining the inhibitory activity for **4n** compound since in vitro tests showed that substitution of the benzyl ring specifically by a fluorine atom enhances activity (Omran et al., 2005, p. 1222-1245) and this is exactly which is present in the compound **4n** which exhibited the strongest inhibition against BChE in this series. Finally, we may attribute the strong activity of this compound to the increase in lipophilicity. In general, to add halogen substituents will increase the lipophilicity of your molecules: the element becomes bigger, is more polarized and the London dispersion forces are increased accordingly (http-16). As these forces are quite important for lipophilic substances to interact with other molecules such as enzymes and this will support the theory that polar groups are not suitable to target BChE. (**ii**): The piperazine ring with bulky moieties had a good anti-BChE activity (**4m**, IC_{50} 0.092 µM). This result improved the finding of some reported

researches about the ability of BChE to bind with more bigger substituents ideally, since its structure composed of more open core (Krátký et al., 2016, p.191) (**iii**): If we are talking about the other active derivatives in this series we cannot ignore the effects of side chain in 4th position of piperazine ring since a short side chain does not permit the terminal amino to achieve the choline restricting site, while an exorbitantly long side chain expands the adaptability and disturbance of the total molecular structure, which was more likely to cause the side chain to not deeply reach the enzyme active part, along these lines influencing the combination of the compounds and enzymes (Li et al., 2016, p.1-11). So, if the end groups are the same which is the dimethylamino the lenghth of the chain is critical. The terminal amino must be linked with the parent piperazine ring by 2-3 carbon **(n: 2, 3)** this will positively be affected the inhibitory activity against BChE as in the case of compounds **4a** and **4b** (IC_{50}; 0.226 and 0.264 µM) (de Paula et al., 2009, p.3754–3759). (**iv**): On the contrary, the presence of the OH group instead of dimethylamino in the end of the chain produce active compound against BChE but with less IC_{50} value as in the compound **4e** (IC_{50};1.420 µM). The explanation behind this decline can be clarified by a negative inductive effect of the oxygen, which brings down the electron density of the amine nitrogen, finally leading to a decrease of its H-bonding ability (Sonmez et al., 2017, p. 285–297). So, according to the results of the present study, it indicated that not only the replacement of aminoalkylgroups but also the linker length between amino-alkyl side chain and piperazine ring were important for anti- BChE activity. (**v**): Methyl substituent in the para position of the benzyl piperazine led to compounds **4o** which exhibited selective BChE inhibition activity with IC_{50} value of 1.071µM. Consequently, 4-methyl along with benzyl piperazine derivatives exhibited improvements to the anti-BChE profiles. (**vi**): Interestingly, compound **2i** showed the weakest inhibitory activity in comparing with other active compounds (IC_{50} 2.038µM). Therefore, the Cl substitutions on phenyl ring have a notable influence on BChE inhibition activity, be that as it may, in second place in terms of BChE inhibition. (**vii**): When compared the above observation of the active to the inactive derivatives in this series we can noted that the presence of any group directly bind to the 4th position in piperidine ring did not significantly affect ChE inhibition activity (**4c and 4g**). Due to a double bond contributes weakly to the ChE inhibition activity (Kuca, Jun, and Musilek, 2006, p. 269-277) for this reason compound **4q** was inactive. Unsubstituted and substituted-phenylpiperazine derivatives (**4d, 4f, 4h and 4p**) exhibited a complete loss of

ChE inhibition activity, thus the presence of nitro, methoxy and fluoro substituents are produce no improvements to the anti-BChE activity, except for compound **2i**. Pyrimidine, cyclohexyl and unsubstituted benzyl piperazine moieties **(4j, 4l and 4k)** didn't generate anti-BChE activity at all.

4.3.2. Part 2. Morpholine (4r)

The replacement of piperazine with a morpholine bioisoster as in the case of compound **4r** negatively affects the activity against both AChE and BChE enzymes. The reason for this decrease can be clarified again as explained before by a negative inductive impact of the oxygen, on the morpholine moiety which brings down the electron density of the amine nitrogen leading to a decrease of its H-bonding capability. In addition, it may be due to decrease in hydrophobicity which associates to the theory that polar groups are not reasonable to target BChE (Mohamed et al., 2011, p. 2269-2281).

4.3.3. Part 3. Piperidine and substituted piperidine series (4s-4u)

Regardedless to the Donepezil, which is a benzylpiperidine derivative the bioisosterical replacement of piperazine with piperidine generally lead to selective BChE inhibition (**4t**, with IC_{50} value of 1.515 μM), except for **4s** and **4u** whose inhibitory activity against both AChE and BChE completely lost.

Accordingly, the anti- BChE was sensitive to a substituent at the 2-position of the piperidine ring (**4t**) which was almost 1.2-fold more than that of Donepezil while piperidine ring itself (**4s**) and benzyl- piperidine (**4u)** showed no effect on both ChEs enzymes. For a better understanding, the anti-BChE activity data related to the structure for all three-substituted series (**4a-4u**) is graphically summarized in Figure 4.88.

Based on the BChE enzyme structure which mentioned before in introduction section, BChE contains smaller residues which permit bulkier substrates to enter into the active site (Nicolet et al., 2003, p.41141-41147) and because of our most active derivatives are big molecules especially the lead compound **4n** is considered a bulky molecule, in addition the presence of three flour atoms in its structure, this may explain in part why these derivatives have more tendency to inhibit BChE. Furthermore, since there are some studies suggested that BChE is associated with and may play a role in AD plaque disposition as has been stated before (Guillozet et al., 1997, p.909-918), in like manner the active derivatives because of their anti-BChE activity, may also be able indirectly to affect the subpopulation of beta amyloid plaques.

Table 4.1. *Inhibitory Activity (%) of the Compounds **4a-4u** Against AChE and BChE*

	AchE Inhibition(%) ±SD		BChE Inhibition(%) ±SD	
Compound	**10^{-3} M**	**10^{-4} M**	**10^{-3} M**	**10^{-4} M**
4a	60.13 ±1.54	17.03 ±0.48	99.13 ±3.21	91.13 ±2.94
4b	79.95 ±1.78	32.41 ±1.01	98.16 ±3.11	82.50* ±2.07
4c	50.73 ±2.21	5.11 ±0.09	45.18 ±0.94	22.70 ±0.70
4d	55.62 ±1.14	31.64 ±0.45	77.75 ±1.79	40.19 ±0.49
4e	48.67 ±1.51	7.09 ±0.64	97.00 ±3.16	95.98* ±2.88
4f	77.65 ±2.42	4.70 ±0.27	77.60 ±1.60	12.80 ±0.87
4g	26.90 ±0.83	10.44 ±0.66	78.11 ±2.24	33.65 ±0.89
4h	30.87 ±1.01	15.23 ±0.69	84.02 ±2.35	12.64 ±0.46
4i	86.41 ±2.91	35.91 ±1.57	99.37 ±3.41	69.51* ±1.16
4j	69.08 ±1.67	2.88 ±0.18	92.87 ±2.84	27.86 ±1.07
4k	58.74 ±1.69	8.62 ±0.22	74.62 ±2.75	25.14 ±1.42
4l	56.11 ±2.46	3.90 ±0.09	84.88 ±3.34	45.88 ±1.62
4m	71.23 ±2.15	25.43 ±1.21	99.65 ±3.86	98.96* ±3.47
4n	80.99 ±2.65	63.21* ±1.76	99.49 ±2.97	99.03* ±3.26
4o	94.97 ±3.61	25.30 ±1.01	98.64 ±3.86	74.83* ±2.17
4p	98.66 ±2.98	48.40 ±1.18	93.27 ±3.07	48.65 ±1.14
4q	68.60 ±1.57	16.35 ±0.39	92.00 ±3.44	39.90 ±1.36
4r	68.20 ±1.69	37.33 ±1.03	91.26 ±3.42	45.30 ±1.88
4s	44.51 ±0.96	32.17 ±1.23	86.72 ±3.07	38.40 ±0.74
4t	81.22 ±2.77	15.94 ±0.42	96.06 ±3.61	55.00* ±1.74
4u	69.30 ±1.28	25.88 ±0.74	32.20 ±0.59	29.50 ±0.48
Donepezil	99.48 ±3.29	98.56 ±2.87	82.24 ±2.91	71.65 ±2.16
Tacrine	99.16 ± 2.49	97.29 ± 3.24	99.27± 2.86	98.61 ± 3.71

Table 4.2. *Inhibitory Activity (%) of the Active Compounds Against BChE*
**Compounds Were Selected for Second Step*

Compounds	BChE Inhibition (%) ±SD					BChE IC_{50} (µM)±SD
	10^{-5} M	10^{-6} M	10^{-7} M	10^{-8} M	10^{-9} M	
4a	84.80 ±2.76	52.10 ±1.04	39.90 ±0.81	28.24 ±0.54	19.69 ±0.99	0.226 ±0.008
4b	70.30 ±1.80	46.10 ±0.74	41.80 ±0.81	33.04 ±0.78	26.35 ±0.77	0.264 ±0.015
4e	57.53 ±1.89	29.52 ±1.07	24.26 ±0.54	18.89 ±0.84	10.77 ±0.58	1.420 ±0.080
4i	44.32 ±0.79	38.72 ±0.82	33.65 ±0.45	26.52 ±0.80	25.73 ±0.70	2.038 ±0.068
4m	90.78 ±3.92	80.30 ±2.56	40.34 ±0.61	30.24 ±0.70	18.98 ±0.20	0.092 ±0.001
4n	92.51 ±2.86	81.28 ±1.25	49.33 ±0.58	43.73 ±1.11	39.25 ±0.22	0.015 ±0.001
4o	46.33 ±0.91	42.99 ±0.97	35.48 ±0.67	25.36 ±0.49	16.54 ±0.56	1.071 ±0.051
4t	49.04 ±0.68	41.33 ±0.41	35.75 ±0.53	30.66 ±0.59	28.50 ±0.66	1.515 ±0.077
Donepezil	59.24 ±1.54	54.27 ±1.16	38.14 ±0.89	15.29 ±0.61	9.23 ±0.08	1.683 ±0.214
Tacrine	94.27 ±3.19	91.68 ±2.82	84.27 ±2.12	46.27 ±1.09	22.49 ±0.70	0.0068 ±0.0011

Table 4.3. *Inhibitory Activity (%) of the **4n** Compound Against AChE*

	AChE Inhibition (%) ±SD					IC_{50} (µM))±SD
	10^{-5} M	10^{-6} M	10^{-7} M	10^{-8} M	10^{-9} M	
4n	22.41 ±0.80	14.56 ±0.76	11.31 ±0.61	8.43 ±0.38	6.91 ±0.27	45.945 ±1.581
Donepezil	95.30 ± 1.64	92.15 ± 1.88	81.36 ± 1.41	41.78 ± 0.84	25.62 ± 0.58	0.0077 ±0.0008
Tacrine	95.95 ±2.16	75.05 ±2.21	36.64 ±1.94	20.40 ±0.67	17.05 ±0.44	0.147 ±0.004

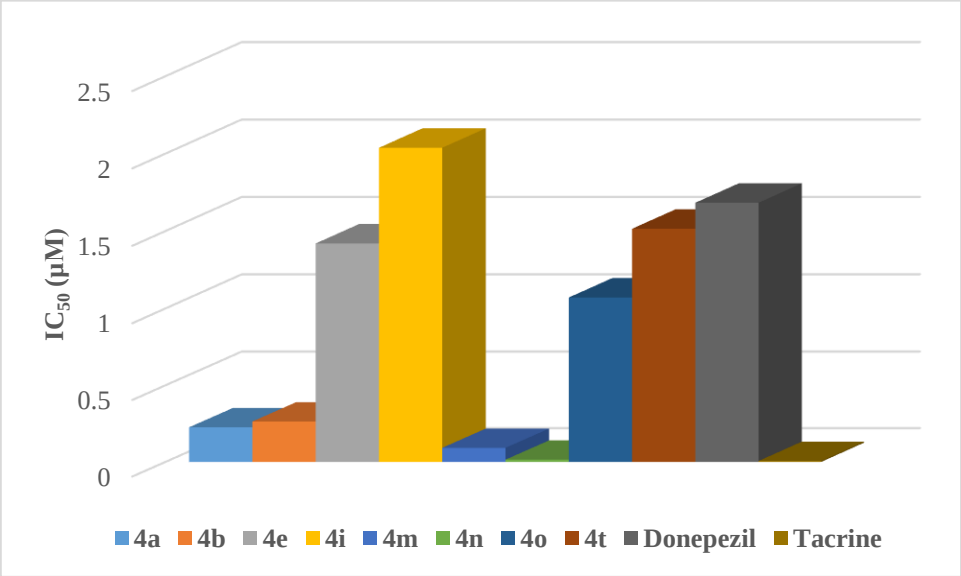

Figure 4.87. *BChE Inhibition Activity, Represented by IC_{50} of Active Derivatives and Standard Drugs*

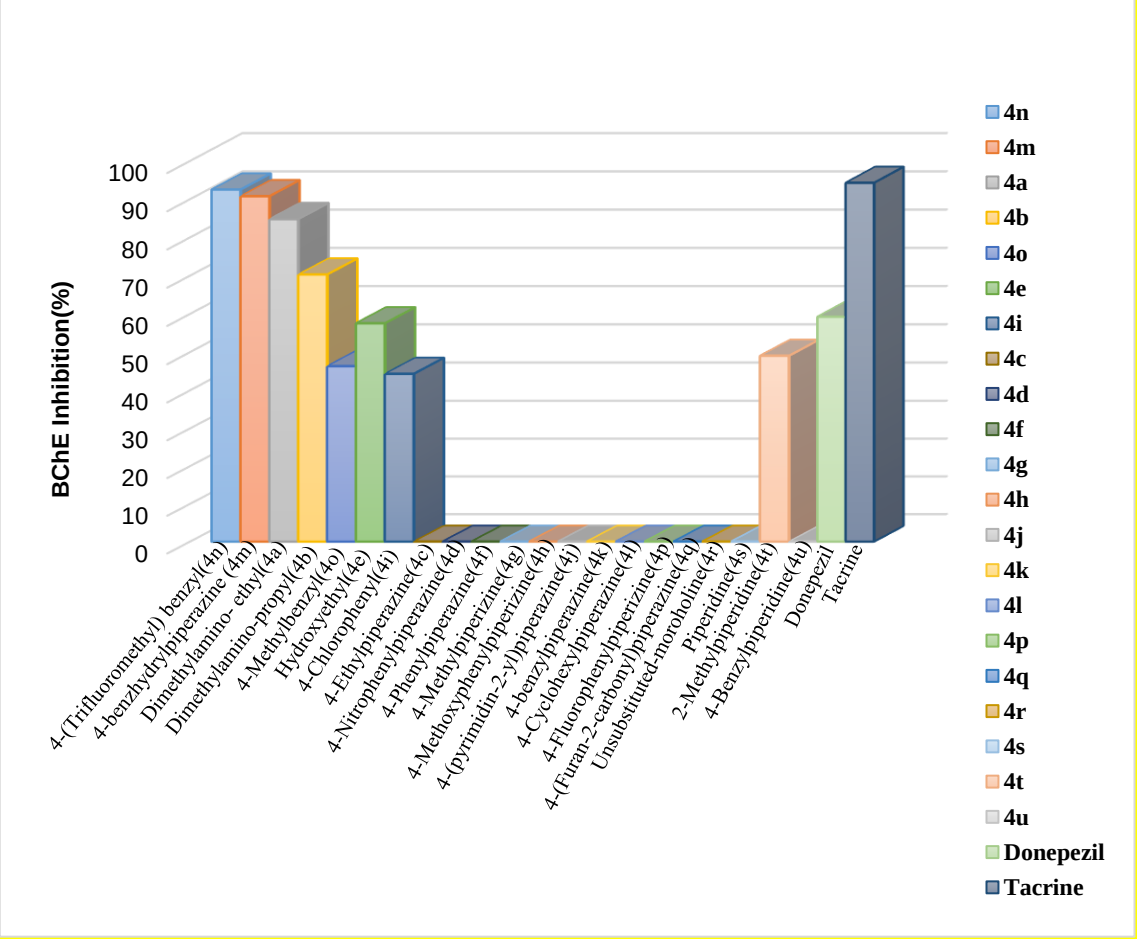

Figure 4.88. *Anti-BChE Activity Data for All Three-Substituted Series (4a-4u)*
**Data was Taken Against 10^{-5}(µM) From Synthesized Compounds and Standards Drugs*

4.4. Kinetics Characterization of BChE Inhibition

Understanding how to recognize the types of inhibitors is vital, but much of the drug discovery process focuses instead upon deciding whether one inhibitor is more viable than another. This determination requires evaluation of an inhibitor's power. The two most basic values for evaluating an inhibitor's effect are IC_{50} and Ki (Lucier, McDaniel and Matthews,1971, p.520-530).

To recognize the type of inhibition exerted by the analogs on BChE, the Michaelis-Menten equation is an equation of a hyperbolic curve which has been used a lot for this purpose. But, since it is difficult to determine the characteristic points of the hyperbolic curve, it is necessary to translate another equation whose graph is linear to facilitate experimentally examining the Vmax and Km of an enzyme. By reversing the Michaelis-Menten equation and dividing it by its multipliers. The conversion of the Michaelis-Menten equation to an equilibrium and to graphing Vmax and Km values can be found. Drawn this graph by this way is known as the Lineweaver-Burk Curve (Schneider, 1984, p. 646-653). We select compound **4n**, which shows the best activity, to study the inhibition kinetics of BChE. After the absorbance values and substrate concentrations obtained as a result of the tests a Lineweaver-Burk graph was drawn. 1 / S on the x-axis in graphics (1 / substrate concentrations), 1 / V representing (1 / velocity of the reaction) on the y axis Values. There are two different points in the graphs showing the presence and absence of the inhibitor. In addition, we noticed that every single straight line in Figure 4.89 was intersected in the second quadrant of the coordinate axis, which characterizes a typical mixed inhibition. In addition, graphical examination of the corresponding Lineweaver–Burk plot showed both increased slopes (decreased Vmax) and intercepts (higher Km) at higher inhibitor concentration (Table 4.3.). This pattern indicated a mixed-type inhibition, as well. Since the inhibition constant Ki can be determined using the secondary plots. As long as the Ki calculation is an effective tool for measuring the affinity of an enzyme for its substrate and it is easily determined by using the secondary plots of the Lineweaver-Burk equation. The graphical investigations of a secondary plot for calculation of steady-state inhibition constant (Ki) for the lead compound **4n** (Ki = 0.0259μM) is presented in (Figures 4.90). A small Ki means that the inhibitor is bound firmly, and the amount of active enzyme present will be small so the inhibitory effect will be strong and as a result we may consider this value a good sign

since it is not so far from that of tacrine (reported Ki = 0.012 μM against ^{HS}BChE) (Ahmed et al.,2006, p.165-171) for future research into that compound.

When the small-molecule ligand was bound with the BChE active center (CAS), the type of inhibition of the enzyme was classified as competitive inhibition; by contrast, when the small-molecule ligand was acted on the PAS, the enzymatic inhibition was classified as non-competitive inhibition. When the active molecule ligand acted on both CAS and PAS, the enzymatic inhibition was designated as mixed inhibition (Wang et al., 2010, p. 1415-1423). Nonetheless, various studies suggested the lack of a PAS at BChE gorge entry many other studies clarify its association with neurotoxic aggregates in the brain via an undetermined mechanism (Greig et al., 2005, p.17213-17218; Darvesh, Hopkins and Geula, 2003, p. 131-138). In this manner, we estimated that the compound **4n** interacted with the two BChE functional sites CAS and PAS (Li et al., 2016, p.1-11); consequently, the **4n** showed a strong inhibitory effect and predictable with our outline design strategy. This conclusion was verified by subsequent molecular docking procedure.

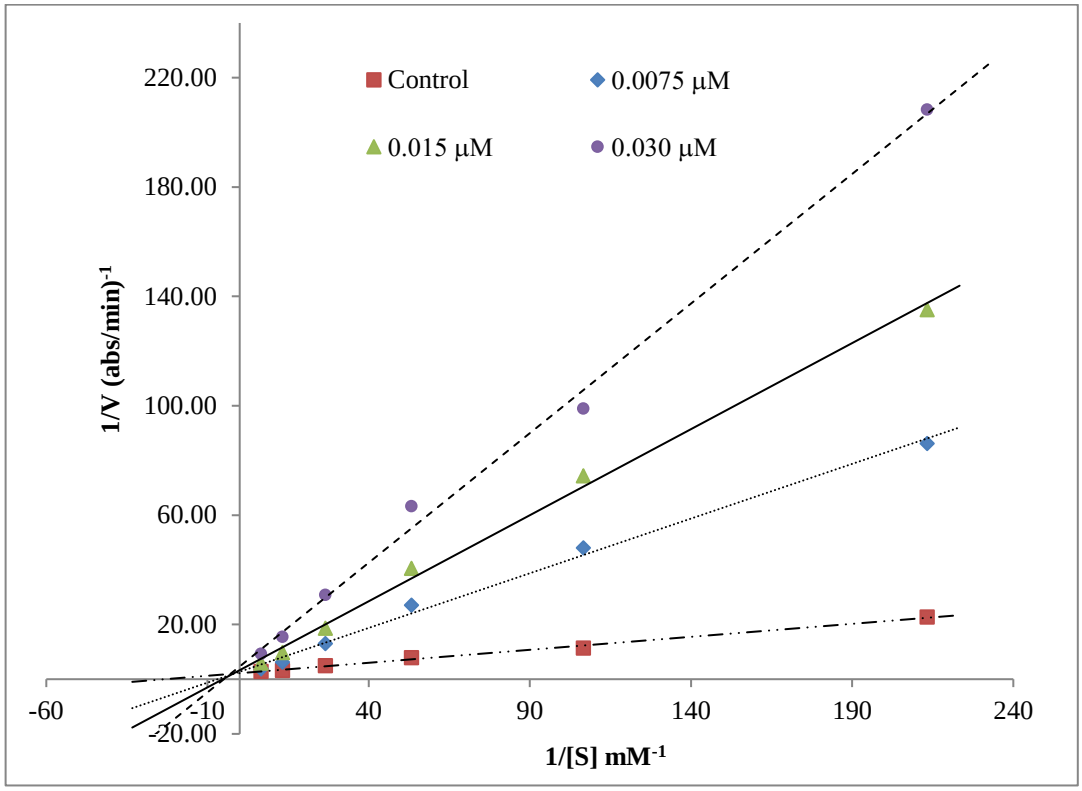

Figure 4.89. *Lineweaver–Burk Plot for the Inhibition of BChE by Compound **4n** at Different Concentrations of Substrate (ATC)*

Table 4.4. *To Prove a Mixed-Type Inhibition*

Concentration	Vmax	Km
0.030	0.21	0.20
0.015	0.30	0.19
0.0075	0.37	0.15
0	0.45	0.04

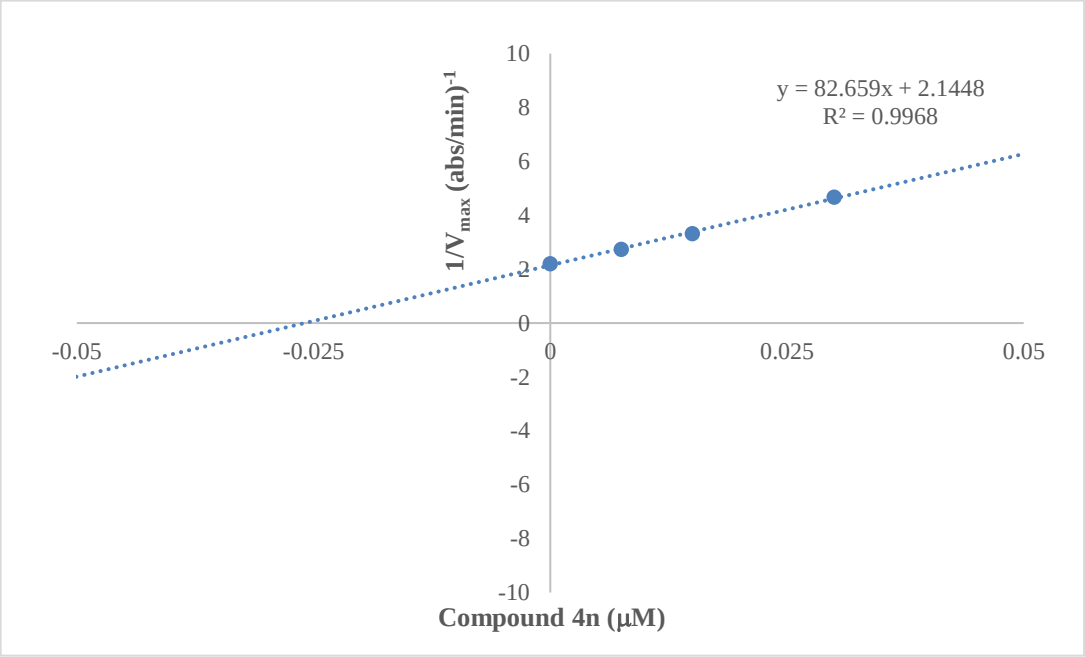

Figure 4.90. *Secondary Plot for Calculation of Steady-State Inhibition Constant (Ki =0.0259 µM against BChE) of Compound* ***4n***

4.5. Molecular Docking

Computational chemistry assumes an imperative part in understanding a derivative's biological profile and supporting the acquired SAR. Therefore, to explore a possible interacting mode of the lead compound **4n** and to evaluate the effects of structural modifications on BChE enzyme activity molecular docking was performed and carried out by using the X-ray crystal structure of hBChE in complex with tacrine (PDB ID: 4BDS) (Nachon et al., p. 393-399,2013) obtained from Protein Data Bank server (http-17). First, tacrine was docked to enzyme active site to validate the docking procedure. The same interactions in the literature about tacrine were gained (Nachon et al., p. 393-399, 2013). Thus, the procedure has proven validity. When two-dimensional poses are examined, two amino acids are noted for their interactions (Figure 4.91). The aromatic ring of tacrine establishes π-π interaction with the indole of Trp82. Furthermore, there is a hydrogen bond between the 9-amino group of tacrine and the carbonyl of Hid438. The three-dimensional interactions of tacrine with BChE (Figure 4.92) clarify this binding mode, along with some studies which clarify that the inhibitory activity against BChE occurs by π-π stacking interaction with the Trp82 residue (Li et al., 2016, p.1-11) and this will support our finding, as well.

The docking poses of compound **4n**, showing two and three-dimensional interactions, are presented in Figure 4.93 and 4.94. According to the poses, there were three main patterns of interaction. One of them was almost identical to the arrangement of tacrine which was a binding to the Hid438 in the catalytic triad of BChE enzyme, but by a π- π interaction between the phenyl ring of the lead structure and the imidazole-Hid438 of the enzyme, cocaine which is rapidly hydrolyzed by BChE binds with the same amino acid (Xie et al., 1999, p.83; Stewart et al., 1977, p.1557-1564). The second pattern is the hydrogen bond which established between the carbonyl group of a compound **4n** and amino group of Thr120 and finally, there is another hydrogen bond between one fluoro atom of the three fluoro methyl group which already present in **4n** and amino group of Gly115. These results demonstrate that the three-main pattern of interaction of a lead **4n** make a significant contribution for improving the effective binding with BChE and may in part clarify that why the compound **4n** is more active than the other derivatives in the series. Based on these outcomes and because of the common capacity and nature of BChE active site is unclear; we trust in that our picked-up data after this docking study may profit the future review for the catalysis mechanism of BChE with various recently synthesized medications.

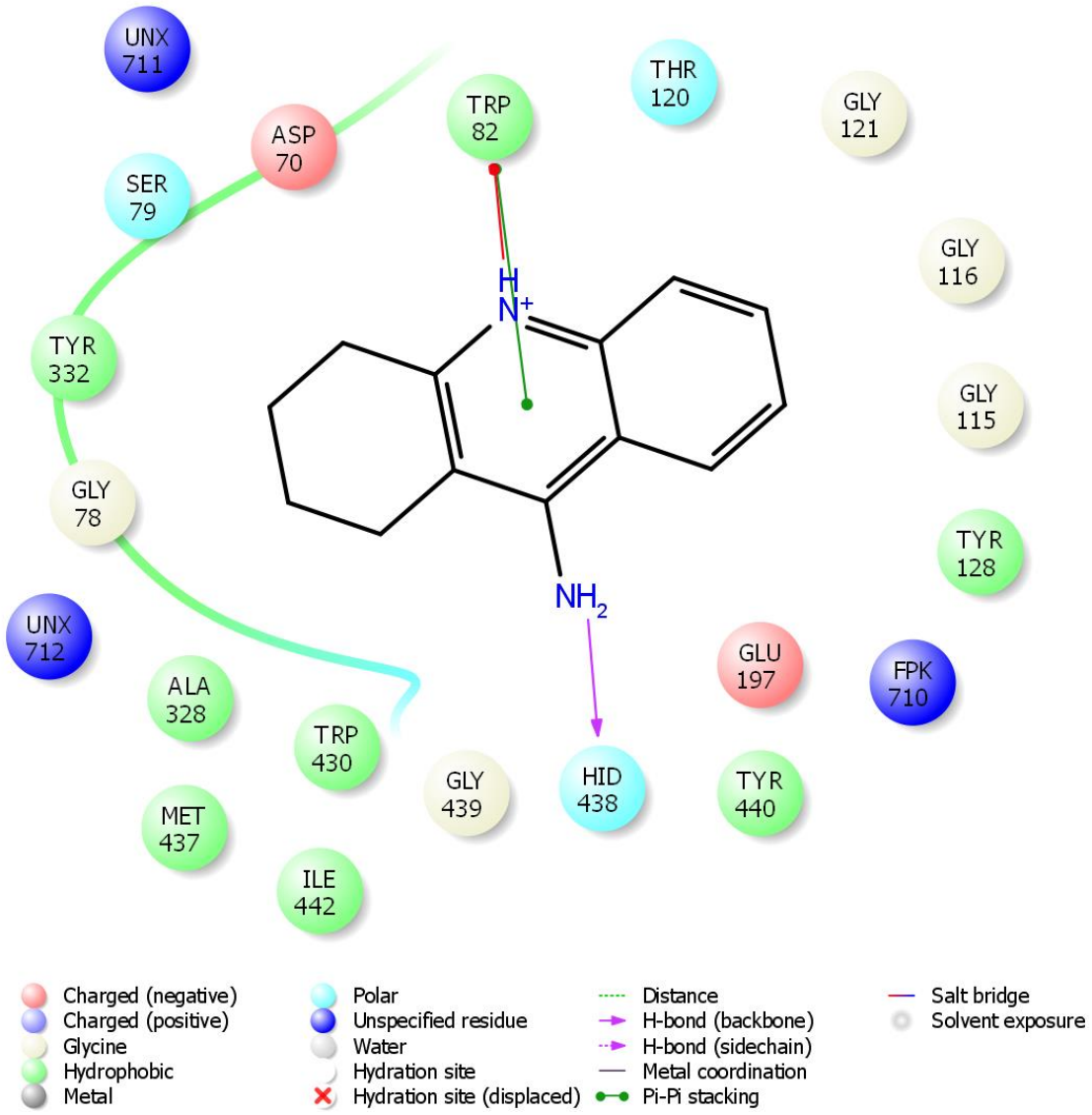

Figure 4.91. *Two-Dimensional Interaction of Tacrine with BChE.*

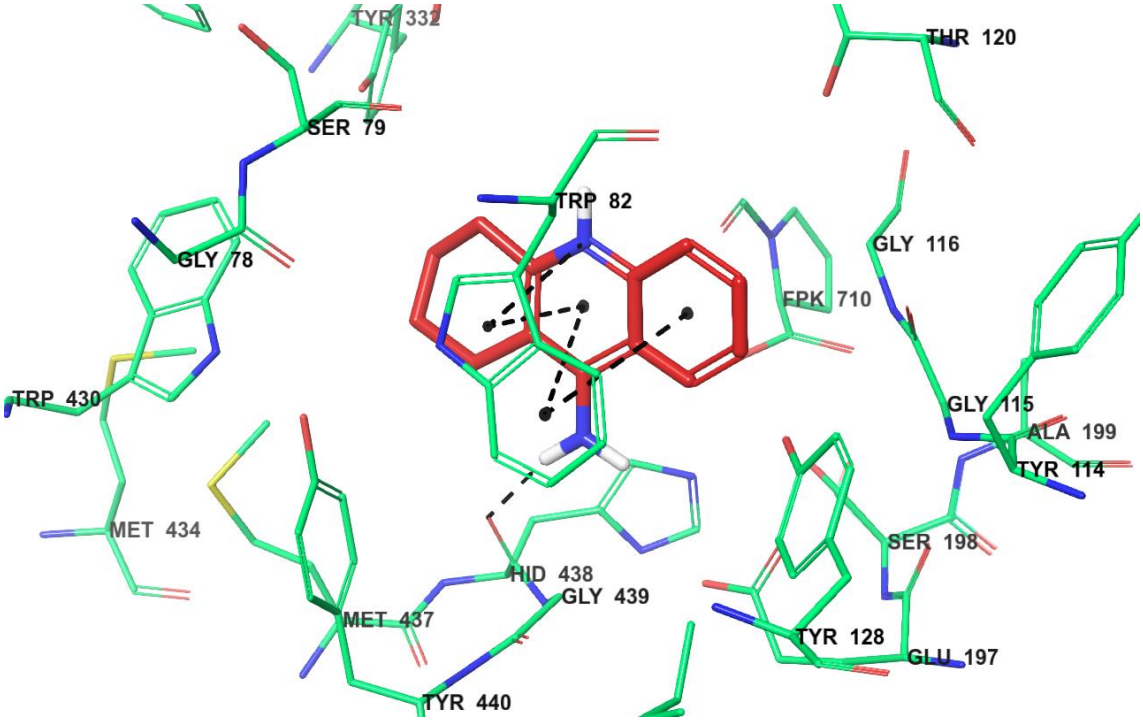

Figure 4.92. *Three-Dimensional Interaction of Tacrine with BChE*

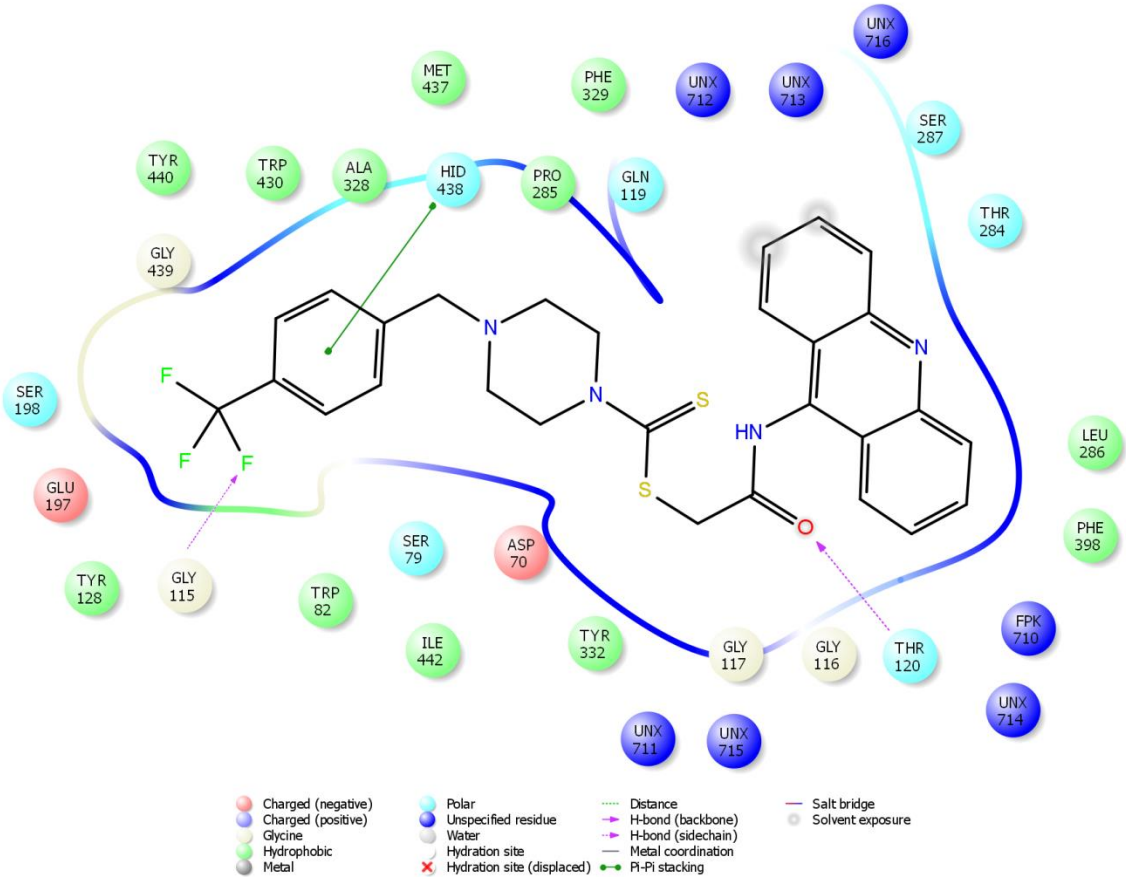

Figure 4.93. *Two-Dimensional Interaction of Compound **4n** with BChE*

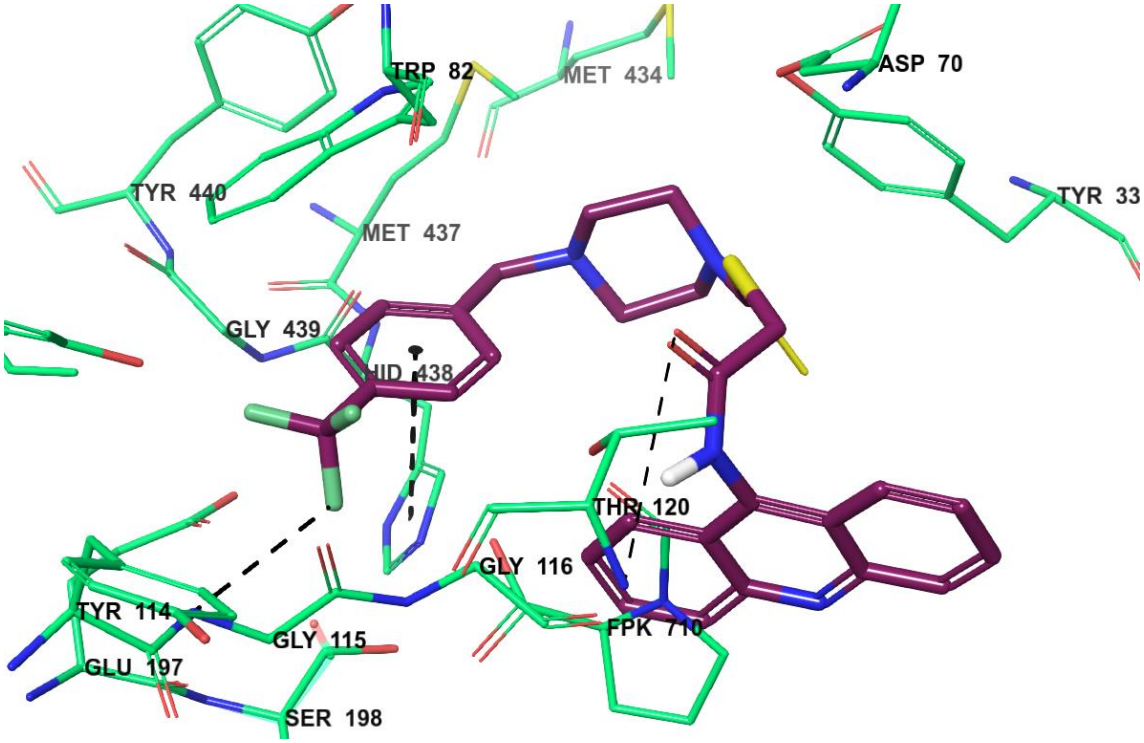

Figure 4.94. *Three-Dimensional Interaction of Compound **4n** with BChE*

4.6. 3D Structure of the Active Compounds

The 3D structure of the active compounds (**4a, 4b, 4e, 4i, 4m, 4n, 4o and 4t**) was visualized by using the Molinspiration Galaxy 3D Structure Generator. The 3D molecular structures help us to interactively examine the compounds from various display modes, including visualization of various surface properties, such as molecular lipophilicity potential (MLP) which encoded by violet- blue colors and polar surface area (PSA) which encoded by yellow and red colors.

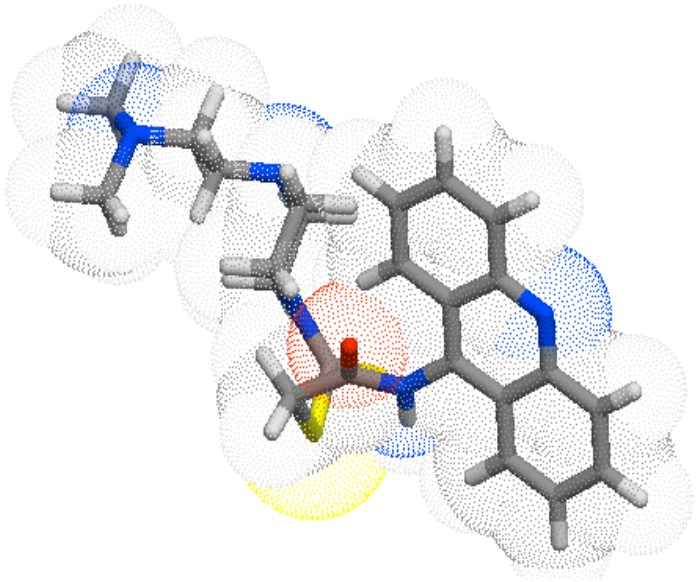

Figure 4.95. *3D Structure of the Compound 4a*

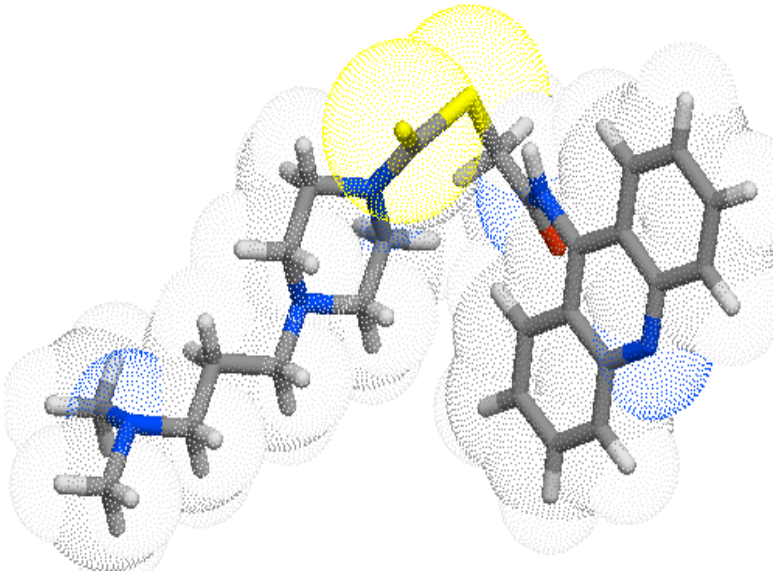

Figure 4.96. *3D Structure of the Compound 4b*

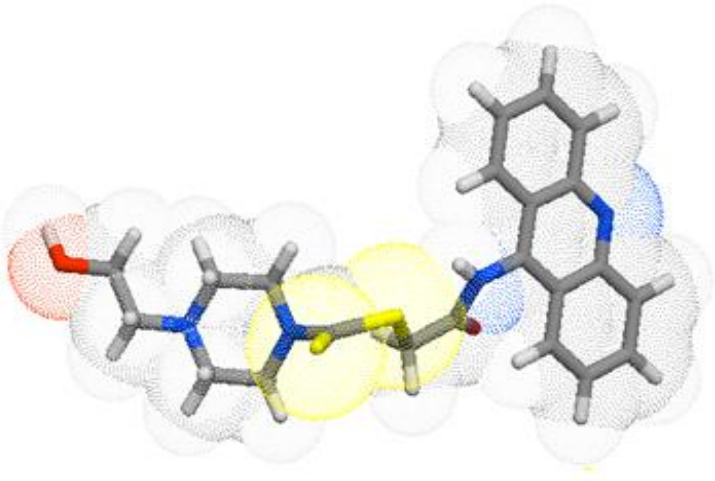

Figure 4.97. *3D Structure of the Compound 4e*

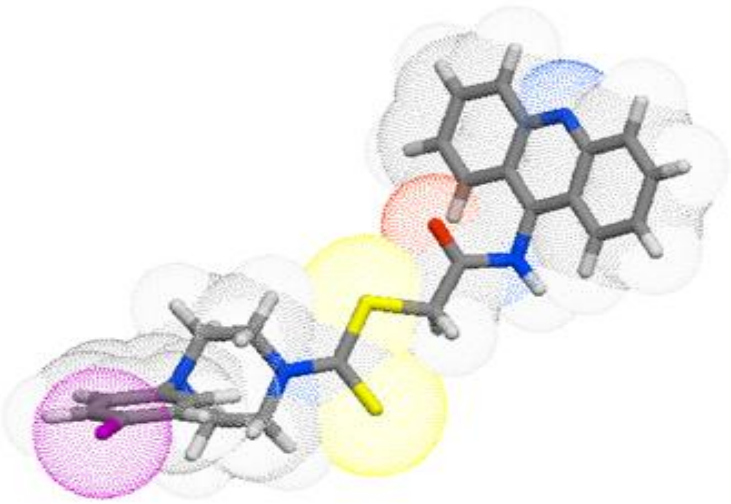

Figure 4.98. *3D Structure of the Compound 4i*

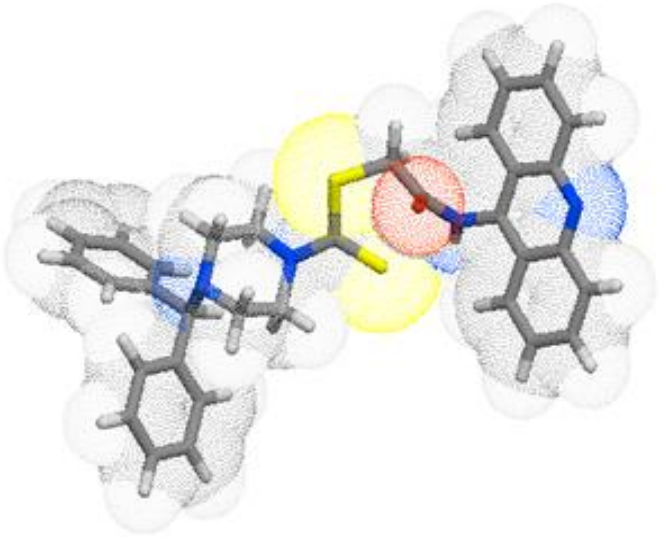

Figure 4.99. *3D Structure of the Compound 4m*

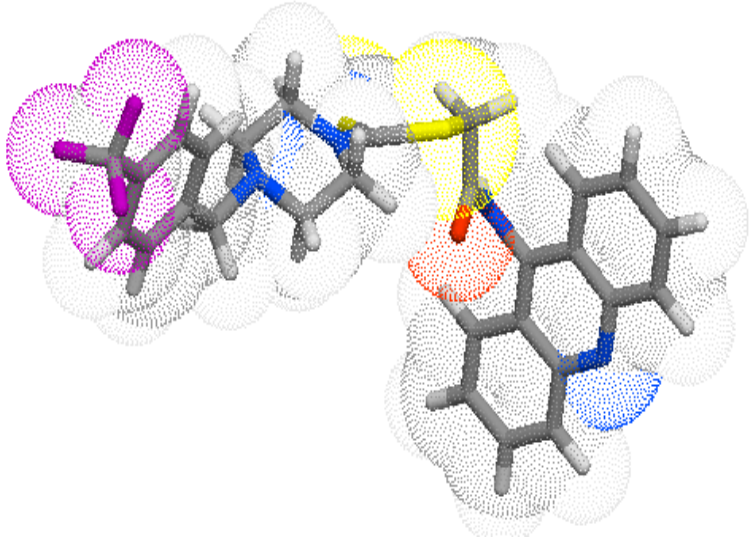

Figure 4.100. *3D Structure of The Compound* ***4n***

**We Can Visualize Easily the Lipophilic Part of Trifluoro-Methyl (Encoded by Violet Color) Which Responsible for Inhibition Activity. In Addition, the Orientation of Compound Is Somewhat Like What We Have Seen in Docking Procedure*

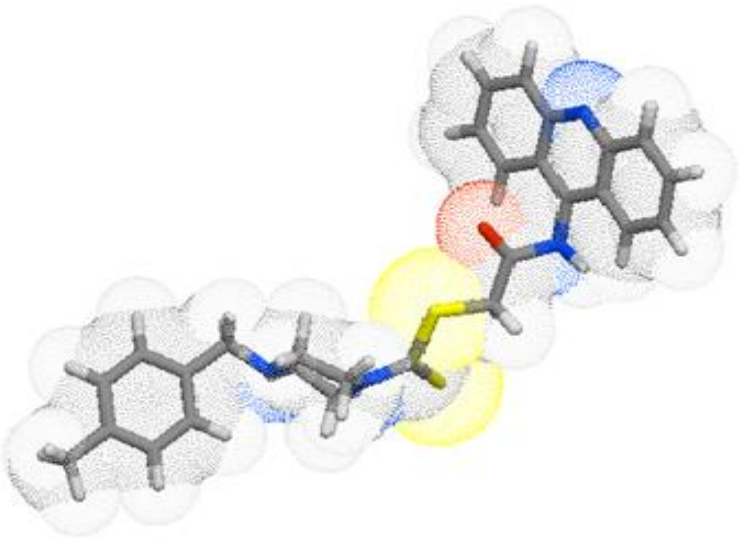

Figure 4.101. *3D Structure of the Compound 4o*

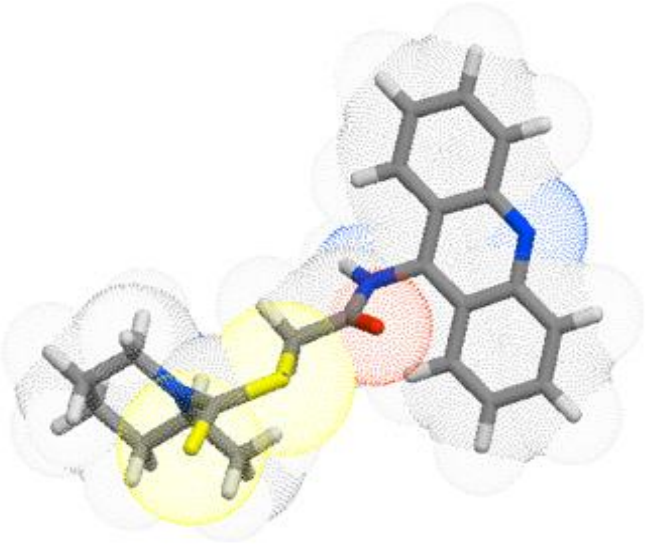

Figure 4.102. *3D Structure of the Compound 4t*

4.7. MTT Cell Viability Assay and Selectivity Indexes

The active compounds (**4a, 4b, 4e, 4i, 4m, 4n, 4o and 4t)** were chosen as the candidates to further study on the potential danger impact on the mouse fibroblast healthy cell line (NIH3T3). After incubating the cells to active compounds for 24 h, the cell feasibility was tried by the 3-(4,5-dimethylthiazol-2-yl)-2,5-diphenyltetrazolium (MTT) examines. As demonstrated all active compounds at 0.000316μM-1000 μM did not indicate noteworthy impact on cell viability. Furthermore, after each experiment the % inhibition values were calculated for each concentration of test substances. IC_{50} values of the substances were determined by non-linear regression analysis over the calculated % inhibition values and the cytotoxic properties of the substances were interpreted. As mentioned above, IC_{50} values of compounds (**4a, 4b, 4e, 4i, 4m, 4n, 4o and 4t**) were determined to be 0.226, 0.264, 1.420, 2.038, 0.092, 0.015, 1.071 and 1.515 μM respectively, according to BChE enzyme inhibitor activity. The IC_{50} values of these compounds on the NIH3T3 cell line were calculated to be 26.81, 25.64, 324.90, >1000, 214.18, >1000, >1000 and 154.20 μM, respectively (Table 4.5). The utilization of selectivity measurements in medication disclosure is an imperative parameter to evaluate the potential safety profile of the newly synthesized compounds. In addition, is preferable for a drug to have a high safety profile. Accordingly, the SI results of active derivatives has shown that compounds exhibit enzyme inhibition at a concentration 97.12 - to 66.66 $\times 10^3$ fold lower than the concentration at which they show cytotoxic activity against NIH3T3 cells (Figure 103). This proposed that our active derivatives were nontoxic to NIH3T3 cells and may be reasonable compounds to inhibit BChE.

Table 4.5. *Cytotoxicity and Selectivity Indexes for Active Derivatives*

Compound	IC_{50} (µM) against NIH3T3	IC_{50} (µM) for BChE	*SI for BChE
4a	26.81	0.226	118.62
4b	25.64	0.264	97.12
4e	324.90	1.420	228.80
4i	>1000	2.038	490.67
4m	214.18	0.092	2.328×10^3
4n	>1000	0.015	66.666×10^3
4o	>1000	1.071	933.70
4t	154.20	1.515	101.78

* The Ratio of IC_{50} Against NIH3T3 to IC_{50} for BChE.

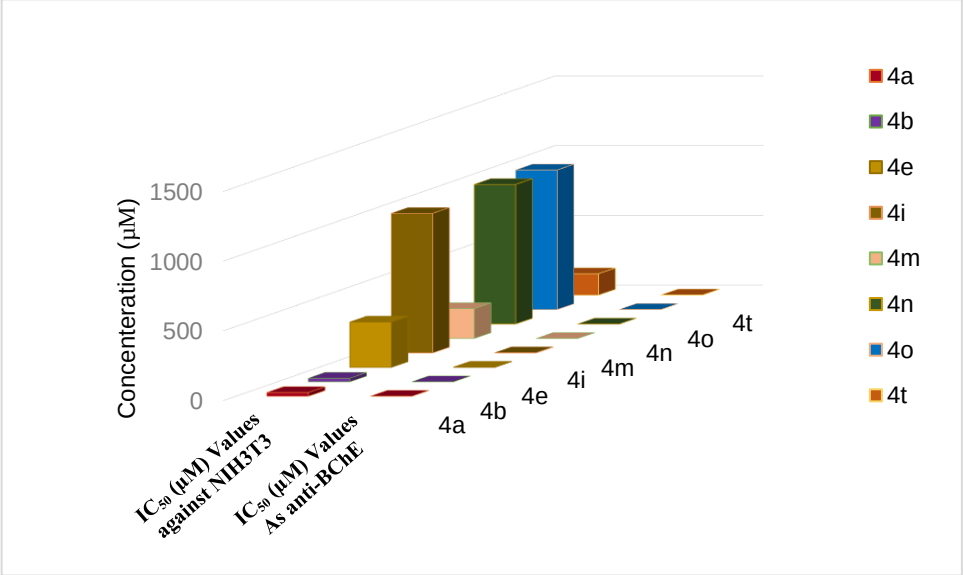

Figure 4.103. *Graphical Comparison of Concentrations*

4.8. BBB Permeability and Drug-Likeness Score (DLS)

BBB permeability is exceptionally basic for medications that particularly target and focus on the CNS. The failure of the medication particles to penetrate the BBB constitutes a major obstacle for CNS drug candidates and ought to be considered in new drugs discovery efforts. In this way, BBB permeability of the most active derivatives was

computed by a CBLigand-BBB forecast server. This predictor uses two different algorithms as AdaBoost and Support Vector Machine (SVM), combining with four different fingerprints, employed to predict if a compound can pass (+) or cannot pass (-) the BBB. As presented in Table 4.6, all calculations for selected compounds resulted as BBB (+), which is necessary for compounds plan to act as ChEs inhibitors (Goodwin et al., 2005, p.477-483).

Drug-likeness score (DLS) was additionally figured out for all active compounds on the Molsoft's chemical fingerprints mode consisting of 5K of marketed drugs from World Drug Index (positives) and 10K of carefully selected nondrug compounds (negatives) (http-17). According to this program, DLS score was observed to be near 1.26-2.21 this proposes may give hints about a decent pharmacokinetics profile for the active synthesized compounds, which facilitate and fortifies their therapeutic significance in the future study.

Table 4.6. *Drug-Likeness Score (DLS) and BBB Permeability of the Active Compounds*

Comp.	DLS	BBB Perm.
4a	2.21	+
4b	2.16	+
4e	1.73	+
4i	1.80	+
4m	1.88	+
4n	1.40	+
4o	1.54	+
4t	1.26	+
Tacrine	0.97	+
Donepezil	0.91	+

5. CONCLUDING REMARKS AND FUTURE RECOMMENDATIONS

Because of the complicated nature of AD, scientists are trying to discover one medication to cure this illness, in any event not until the ailment reason is better understood. Until that day, it is likely that a multitarget-treatments, symptomatic and disease adjusting, is the way which must be looking for. As a result, twenty one of 2-(9-acridinylamino)-2-oxoethyl-piperazinyl/piperidinyl/morpholinylcarbodithioate derivatives (**4a-4u**) were designed and synthesized through efficient synthetic procedure and screened for their inhibition power toward ChEs. Eight derivatives (**4a, 4b, 4e, 4i, 4m, 4n, 4o** and **4t**) demonstrated a specific and promising action against BChE, from which only one compound (**4n**) created generally inhibition for both enzymes with IC_{50} value of 0.015 µM and selectivity index to BChE of 3.063 which was 112.2-fold more than that of donepezil (IC_{50}1.683 µM) and only 45.945 µM for AChE. Molecular modeling and BChE analysis were conducted to investigate the docking of lead compound **4n** inside the target enzyme and to confirm their natural profile. Moreover, the result of cytotoxic activity against NIH3T3 cells indicated that the all active derivatives do not show any signs of cytotoxicity up to >1000 µM in the cell lines tested, suggesting a high level of safety when using these moieties. In like manner, BBB and DLS studies indicated the relative successfulness of the most active derivatives.

Nonetheless, there are still some important points to investigate inside this thesis and some of these points are illustrated below.

- Our advancement towards ChE inhibitors could be extended out with wide series of derivatives to figure out the structure-activity relationship and to enhance the inhibitory activities.
- *In-vivo* pharmacokinetic profile may have conducted in the future for active derivatives to assess their capability to develop into the therapeutic agents.
- Due to the multi-pathogenesis of AD, the classical approach regulating at one target might be deficient in this mind complicated disease. Subsequently, the multitarget approach in medication outline for the treatment of AD incorporates for example double inhibitors of ChE and monoamine oxidase must be done later.

REFERENCES

Abraham, A.J. (2003). Cannon, J.G (Ed.), Burger's medicinal chemistry and drug discovery. *Cholinergic* inside (p. 39-108). New Jersey.

Abu Mohsen, U. (2014). Synthesis and Biological Activity of Some Thiazole Derivatives with Dithiocarbamate side chain. *Int. J. Pharm. Sci. Rev. Res.*,29, 222-228.

Abu Mohsen, U. (2014). Studies on Benzimidazole Dithiocarbamate Derivatives as Acetycholinesterase Inhibitors. *World Journal of Pharmacy and Pharmaceutical Sciences*, 3,10-19.

Adler, M., Sweeney, R.E., Hamilton, T.A., Lockridge, O., Duysen, E.G., Purcell, A.L., and Deshpande, S.S. (2011). Role of acetylcholinesterase on the structure and function of cholinergic synapses: insights gained from studies on knockout mice. *Cellular and Molecular Neurobiology*, 31, 909-920.

Al-Ghorbani, M., Bushra Begum, A., Zabiulla Mamatha, S. V. and Ara Khanum. S. (2015). Piperazine and morpholine: Synthetic preview and pharmaceutical applications. *J. Chem. Pharm. Res.,* 7(5), 281-301.

Ali, M.A., Ismail, R., Choon, T.S., Kumar, R.S., Osman, H., Arumugam, N., Almansour, A.I., Elumalai, K., Singh, A. (2012). AChE inhibitor: A regio- and stereoselective 1,3-dipolar cycloaddition for the synthesis of novel substituted 5,6-dimethoxyspiro[5.3']-oxindolespiro-[6.3"]-2,3-dihydro-1H-inden-1"-one-7-(substituted aryl)-tetrahydro-1H-pyrrolo[1,2-c][1,3]thiazole. *Bioorg. Med. Chem. Lett.,* 22, 508-511.

Alonso, D., Dorronsoro, I., Rubio, L., Mun˜oz, P., Garcı´-Palomero, E., Del Monte, M., Bidon-Chanal, A., Orozco, M. Luque, F. J., Castro, A., Medinaa, M. and Martı´nez, A. (2005). Donepezil–tacrine hybrid related derivatives as new dual binding site inhibitors of AChE. *Bioorganic & Medicinal Chemistry,*13, 6588–6597.

Altıntop, M. D., Gurkan-Alp, A. S., Ozkay, Y., Kaplancıklı, Z. A. (2013). Synthesis and biological evaluation of a series of dithiocarbamates as new cholinesterase inhibitors. *Arch. Pharm.*, 2013, 346, 571.

Altıntop, M.D., Gurkan-Alp, A.S., Özkay, Y. and Kaplancıklı, Z.A. (2013). Synthesis and biological evaluation of a series of dithiocarbamates as new cholinesterase inhibitors. *Arch. Pharm. Chem. Life Sci.,* 346, 571–576.

Altıntop, M.D., Özdemir, A., Atlı, Ö., Cantürk, Z., Baysal, M. and Kaplancıklı, Z.A. (2016). Synthesis and evaluation of new thiazole derivatives as potential antimicrobial agents. *Letters in Drug Design & Discovery,* 13, 1-9.

Altıntop, M.D., Özdemir, A., Kaplancikli, Z.A., Turan-Zitouni, G., Temel, H.E. and Akalın-Çiftçi, G. (2013). Synthesis and biological evaluation of some pyrazoline derivatives bearing a dithiocarbamate moiety as new cholinesterase inhibitors, *Arch. Pharm. Chem. Life Sci.,* 346, 189-199.

Ames, B.N., Sims, P. and Grover, P. L. (1972). Epoxides of carcinogenic polycyclic hydrocarbons are frameshift mutagens. Science. 176, 47–49.

Anders, W. and Martin, P. (2010). The global economic impact of dementia. *Alzheimer's Disease International (ADI),* 1-56.

Andreani, A., Cavalli, A., Granaiola, M., Leoni, A., Locatelli, A., Morigi, R., Rambaldi, M., Recanatini, M., Roda, A. (2006). Synthesis and screening for anticholinesterase activity of (1-benzyl-4-oxopiperidin-3ylidine) methylindoles and pyrroles related to Donepezil. *J. Med. Chem.,* 44, 4011–4014.

Aytemir, M.D., Calis, U., Ozalp, M. (2004). Synthesis and evaluation of anticonvulsant and antimicrobial activities of 3-hydroxy-6-methyl-2-substituted -4H-pyran -4-one derivatives. *Arch. Pharm. Pharmaceutical Medicinal Chemistry*, 337, 81-288.

Ballard, C.G. (2002). Advances in the treatment of Alzheimer's disease: benefits of dual cholinesterase inhibition. *Eur. Neurol.,* 47, 64–70.

Barril, X., Orozco, M. and Luque, F.J. (2001). Towards improved acetylcholinesterase inhibitors: a structural and computational approach. *Mini Rev. Med. Chem*., 1(3), 255-266.

Berridge, M. V., Herst, P. M., Tan, A. S. (2005). Tetrazolium dyes as tools in cell biology: new insights into their cellular reduction. *Biotechnol. Annu. Rev.,* 11, 127-152.

Bolognesi, M.L., Andrisano, V., Bartolini, M., Cavalli, A., Minarini, A., Recanatini, M., Rosini, M., Tumiatti, V. and Melchiorre, C. (2005). Heterocyclic inhibitors of AChE acylation and peripheral sites. *Farmaco*.,60(6-7), 465-473.

Bourne, Y., Taylor, P., Radic, Z. and Marchot, P. (2003). Structural insights into ligand interactions at the acetylcholinesterase peripheral anionic site. *EMBO J.,* 22 (1), 1-12.

Brooks, G.T. (1989). Herausgeber: L.A. Damani (Ed.). Sulphur Containing Drugs and Related Organic Compounds: Chemistry, Biochemistry, and Toxicology. *Metabolism of Sulphur Functional Groups* inside (p.62). Chichester.

Cen, D., Brayton, D., Shah, B., Meyskens, F. L. and Farmer, P.J. (2004). Disulfiram facilitates intracellular Cu uptake and induces apoptosis in human melanoma cells. *J. Med. Chem.,* 47, 6914–6920.

Clark, C.M. and Karlawish. J.H. (2003). Alzheimer disease: current concepts and emerging diagnostic and therapeutic strategies. *Ann Intern Med*., 138, 400–10.

Cummings, J.L. (2004). Alzheimer's disease. *N Engl J Med.,* 351, 56–67.

Darvesh, S., Grantham, DL., and Hopkins, DA. (1998). Distribution of butyrylcholinesterase in the human amygdala and hippocampal formation. *The Journal of Comparative Neurology*, 393, 374-390.

Darvesh, S., Hopkins, D. A., Geula, C. 2003. Neurobiology of butyrylcholinesterase. *Nat. Rev. Neurosci.,* 4, 131-138.

David, W., Mukesh, A., Zhiqing, X., Goutam, K. (2015). Novel HDMX inhibitors and their use for cancer treatment, U.S. Patent, No: WO 2015153535.

De Paula, A.A.N., Martins, J.B.L., dos Santos, M.L., Nascente, L. de C., Romeiro, L.A.S., Areas, T.F.M.A., Vieira, K.S.T., Gambo, N.F., Castro, N.G., Gargano, R. New potential AChE inhibitor candidates. (2009). *European Journal of Medicinal Chemistry*, 44, 3754–3759.

Demir Özkay, Ü., Can, Ö. D., Sağlık, B. N., Acar Çevik, U., Levent, S., Özkay, Y., Ilgın, S., Atlı, Ö. (2016). Design, synthesis, and AChE inhibitory activity of new benzothiazole–piperazines. *Bioorg. Med. Chem. Lett.*, 26, 5387-5394.

Denny, W.A. (2002). Acridine derivatives as chemotherapeutic agents. *Curr. Med. Chem.* 9, 1655-65.

Dhanasekaran, S., Perumal, P., and Palayan, M. (2015). In-vitro Screening for acetylcholinesterase enzyme inhibition potential and antioxidant activity of extracts of Ipomoea aquatica Forsk: therapeutic lead for Alzheimer's disease. *Journal of Applied Pharmaceutical Science*, 5, 012-016.

Dhooghe, M. and De Kime, N. (2006). Synthetic approaches towards 2-iminothiazolidines: An overview. *Tetrahedron*, 2006, 62, 513–535.

Dimond, A.E., J. W. Heuberger, J.W. and Horsfall, J.G. (1943). A water-soluble protectant fungicide with tenacity. *Phytopathology*, 33, 1095–1097.

Dvir, H., Silman, I., Harel, M., Rosenberry, TL., and Sussman, JL. (2010). Acetylcholinesterase: From 3D structure to function. *Chemico-Biological Interactions*, 187, 10-22.

Eddleston, M., Buckley, N.A., Eyer, P., and Dawson, A.H. (2008). Management of acute organophosphorus pesticide poisoning. *The Lancet*, 371, 597-607.

Eicher, T. Hauptmann. S. (2003). T. Eicher, S. Hauptmann (Eds.). The Chemistry of Heterocycles. Structure, Reactions, Syntheses, and Applications. *The Structure of Heterocyclic Compounds* inside (p.1-5). Weinheim.

Elio, S., Schelterns, P., H Feldman, H. (2003). Treatment of Alzheimer's disease; current status and new perspectives. *The Lancet Neurology*, 2, 539–547.

Ellman, G.L., Courtney, K.D., Andres, V. and Feather-Stone, R.M. (1961). A new and rapid colorimetric determination of acetylcholinesterase activity. *Biochem. Pharmacol.*, 7, 88-95.

Frank, D. Popp. (1962). Polyphosphoric Acid in the Bernthsen Reaction. *Org. Chem.*, 27 (7), 2658–2659.

Galy, J. P., Morel, S., Boyer, G., J. and Elguero, J. (1996). Tetracyclic derivatives of acridine - heterofused acridines. *Journal of Heterocyclic Chem.*, 33, 1551-1560.

Garcia-Alloza, M., Gil-Bea, F.J., Diez-Ariza, M., Chen, CPLH., Francis, P.T., Lasheras, B., and Ramirez, M.J. (2005). Cholinergic–serotonergic imbalance contributes to cognitive and behavioral symptoms in Alzheimer's disease. *Neuropsychologia*, 43, 442-449.

Garcia-Fontan, S., Rodriguez-Seoane, P. (1993). Spectroscopic study of cadmium(II) complexes with heterocyclic dithiocarbamate ligands. *Inorganica Chimica Acta.*, 211, 211-215.

Gauthier, S. (2002). Advances in the pharmacotherapy of Alzheimer's disease. *Canadian Medical Association Journal*, 166, 616-623.

Glide, version 7.1, Schrödinger, LLC, New York, NY, (2016).

Gniazdowski, M., Szmigiero, L. (1995). Nitracrine and its congeners--an overview. *Gen.Pharmacol*., 26, 473-81.

Goodwin, J.T., Clark, D.E. (2005). In Silico Predictions of Blood-Brain Barrier Penetration: Considerations to "Keep in Mind". *Prespect. Pharmacol.***,** 315, 477-483.

Greig, N. H., Utsuki, T., Ingram, D. K., Wang, Y., Pepeu, G., Scali, C., Yu, Q., Mamczarz, J., Holloway, H. W., Giordano, T., Chen, D., Furukawa, K., Sambamurti, K., Brossi, A., Lahiri, D. K. (2005). Selective butyrylcholinesterase inhibition elevates brain acetylcholine, augments learning and lowers Alzheimer β-amyloid peptide in rodent. *Proc. Natl. Acad.*, 102, 17213-17218.

Greig, N.H, Lahiri, D. K, Sambamurti, K. (2002). Butyrylcholinesterase: an important new target in Alzheimer's disease therapy. *Int Psychogeriatr*.,14 ,1:77-91.

Guerra, M., Cartaud, A., Cartaud, J., and Legay, C. (2005). Acetylcholinesterase and molecular interactions at the neuromuscular junction. *Chemico-Biological Interactions,* 157, 57-61.

Guillozet, A.L., Smiley, J.F., Marsh, D.C et al. 1997. Butyrylcholinesterase in the life cycle of amyloid plaques. *Ann Neurol.,* 42, 909-918.

Gullino, M.L., Tinivella, F., Garibaldi, A., Kemmitt, G.M, Bacci, L. and Sheppard, B. (2010). Mancozeb: Past, Present, and Future. *Plant Disease*, 94,1076-1087.

Gundogdu-Karaburun, N. (2014). Synthesis and biological activity of thiazole dithiocarbamate derivatives. *Lett. Drug Des. Discov.,* 11 (6), 814-823.

Guo, J., Hurley, M. M., Wright, J. B. and Lushington, G. H. (2004). A docking score function for estimating ligand-protein interactions: application to acetylcholinesterase inhibition. *J. Med. Chem*., 47(22), 5492-5500.

Hamid, R., Rotshteyn, Y., Rabadi, L., Parikh, R. and Bullock, P. (2004). Comparison of alamar blue and MTT assays for high through-put screening. *Toxicol In Vitro,*18, 703-10.

Hamulakova, S., Janovec, L., Hrabinova, M., Spilovska, K., Korabecny, J., Kristian, P., Kuca, K and Imrich, J. (2014). Synthesis and Biological Evaluation of Novel Tacrine Derivatives andTacrine−Coumarin Hybrids as Cholinesterase Inhibitors. *American Chemical Society*, 57, 7073−7084.

Harel, M., Schalk, I., Ehret-Sabatier, L., Bouet, F., Goeldner, M., Hirth, C., Axelsen, PH, Silman, I., and Sussman, JL. (1993). Quaternary ligand binding to aromatic residues in the active-site gorge of acetylcholinesterase. *Proceedings of the National Academy of Sciences of the United States of America*, 90, 9031-9035.

Hayat, F., Rehman, Z. & Haleem Khan, M. (2017). Two new heteroleptic ruthenium(II) dithiocarbamates: synthesis, characterization, DFT calculation and DNA binding. *Journal of Coordination Chemistry,* 70, 279–295.

Hitchcock, S.A., Pennington, L.D. (2006). "Structure - Brain Exposure Relationships". *J Med. Chem.,* 49, 7559–7583.

Hoey, S. E., Williams, R. J., Perkinton, M. S.2009. Synaptic NMDA receptor activation stimulates α- secretase amyloid precursor protein processing and inhibits amyloid-β production. *J. Neurosci.,* 29, 4442-4460.

Johnson, G. and Moore, S.W. (2006). The peripheral anionic site of acetylcholinesterase: structure, functions and potential role in rational drug design. *Curr. Pharm. Des.*, 12(2), 217-225.

Johnson, G., and Moore, S.W. (2006). The peripheral anionic site of acetylcholinesterase: structure, functions and potential role in rational drug design. *Current Pharmaceutical Design*, 12, 217-225.

Jourdan, F. (1885). New syntheses of derivatives of hydroacridine and acridine. *Ber.*, 18, 1444-56.

Kálai, K., Altman, R., Maezawa, I., Balog, M., Morisseau, C., Petrlova, J., Hammock, B.D., Jin, L.W., Trudell, J.R., Voss, J.C., Hideg.K. (2014). Synthesis and functional survey of new Tacrine analogs modified with nitroxides or their precursors. *European Journal of Medicinal Chemistry*, 77, 343-350.

Kapanda Coco N., Masquelier, Julien Labar, Geoffray., Muccioli Giulio G., Poupaert, Jacques H., Lambert Didier, M. (2012). Synthesis and Pharmacological Evaluation of 2,4-Dinitroaryldithiocarbamate Derivatives as Novel Monoacylglycerol Lipase Inhibitors. *Journal of Medicinal Chemistry*, 55, 5774-5783.

Karaburun, A.c., Kaplancikli, Z.a., Gundogdu-Karaburun, N., Demirci, F. (2011). Synthesis, antibacterial and antifungal activities of some carbazole dithiocarbamate derivatives. *Letters in Drug Design & Discovery*, 8, 811-815.

Karali, N., Apak, I., Ozkirimli, S., Gursoy, A., Dogan, S.U., Eraslan, A. and Ozdemir, O. (1999). Synthesis and pharmacology of new dithiocarbamic acid esters derived from phenothiazine and diphenylamine. *Arch. Pharm Med Chem.*, 332, 422-426.

Kaufman, SE., Donnell, RW., Aiken, DC, and Magee, C. (2011). Prolonged Neuromuscular Paralysis Following Rapid-Sequence Intubation with Succinylcholine. *The Annals of Pharmacotherapy*, 45, 21.

Koellner, G., Steiner, T., Millard, C.B., Silman, I and Susssman, J. L. (2002). A neutral molecule in a cation-binding site: specific binding of a PEG-SH to acetylcholinesterase from Torpedo californica. *J. Mol. Biol*., 2002, 320(4), 721-725.

Korabecny, J., Musilek, K., Holas, O., Binder, J., Zemek, F., Marek, J., Pohanka, M., Opletalova, V., Dohnal, V., and Kuca, K. (2010). “Synthesis and in vitro evaluation of N-alkyl-7-methoxytacrine hydrochlorides as potential cholinesterase inhibitors in Alzheimer disease.” *Bioorganic and Medicinal Chemistry Letters*, 20, 6093–6095.

Krátký, M., Štěpánková, S., Vorčáková, K., Švarcová, M., and Vinšová, J. (2016). Novel cholinesterase inhibitors based on o-aromatic n,n-disubstituted carbamates andthiocarbamates. *Molecules*, 21, 191.

Kryger, G., Harel, M., Giles, K., Toker, L., Velan, B., Lazar, A., Kronman, C., Barak, D., Ariel, N., Shafferman, A., Silman, I., and Sussman, JL. (2000). Structures of recombinant native and E202Q mutant human acetylcholinesterase complexed with the snake-venom toxin fasciculin-II. *Acta Crystallographica Section D: Biological Crystallography*, 56, 1385-1394.

Kryger, G., Silman, I. and Sussman, J.L. (1998). Three-dimensional structure of a complex of E2020 with acetylcholinesterase from Torpedo californica. *J. Physiology*, 92(3-4), 191-194.

Krzyminski, K., Malecha, P., Zadykowicz, B., Wróblewska, A., Błazejowski J. (2011).^{1}H and ^{13}C-NMR spectra, structure and physicochemical features of phenyl acridine-9-carboxylates and 10-methyl-9-(phenoxycarbonyl)acridinium trifluoromethanesulphonates – alkyl substituted in the phenyl fragment. *Spectrochimica Acta Part A* ,78, 401–409.

Kuca, K., D. Jun, and Musilek, K. (2006). Structural requirements of acetylcholinesterase reactivators. *Mini-Reviews in Medicinal Chemistry*, 6, 269-277.

Kumar, J., Chawla, G., Akhtar, M., Sahu, K., Rathore, V., Sahu, S. (2013). Design, synthesis and pharmacological evaluation of some novel derivatives of 1-{[3-(furan-2-yl)-5-phenyl-4,5-dihydro-1,2-oxazol-4-yl]methyl}-4-methyl piperazine. *Arab. J. Chem.*, 10 (1), 141-149.

kumar, R., kaur, M., and kumarı, M. (2012). Acridıne: a versatile heterocyclic nucleus. *acta poloniae pharmaceutica - drug research*, 69, 3-9.

Kumar, P., Kumar,R., and Prasad, D.N. (2013). Synthesis and anticancer study of 9-aminoacridine derivatives. *Arabian Journal of chemistry*, 6 , 79-85.

Kuppukkannu, R., Corrado, R., Gurunathan-Senthilkumar, S. (2016). Mono and trivalent thallium-sulfur interactions and their influence on the formation of nano thallium sulphide: single crystal X-ray structural and spectral studies on thallium(I)/(III)-cyclohexylpiperazine dithiocarbamates. *New Journal of Chemistry*, 40, 2489-2500.

Lemke, T.L, Williams, D.A., Roche, V.F. and Zito, S.W. (2008). E. Kim Fifer (Eds.), Foye's Principles of Medicinal Chemistry. *Drugs affecting cholinergic transmission* inside (p.361-391). Philadelphia.

Leurs, R., Bakker, R. A., Timmerman, H., de Esch, I. 2005.The histamine H3 receptor: from gene cloning to H3 receptor drugs. *J. Nat. Rev. Drug Discov*., 4, 107-120.

Levent, S., Acar Çevik, U., Sağlık, BN., Özkay, Y., Devrim Can, Ö., Demir Özkay, Ü., & Uçucu, Ü. (2016). Anticholinesterase activity screening of some novel dithiocarbamate derivatives including piperidine and piperazine moieties. Phosphorus, *Sulfur, and Silicon and the Related Elements*, 191, 1-6

Levent, S., Gerstmeier, J., Olgaç, A., Nikels, F., Garscha, U., Carotti, A., Macchiarulo, A., Werz, O., Banoglu, E., Çalışkan.B. (2016). Synthesis and biological evaluation of C (5)-substituted derivatives of leukotriene biosynthesis inhibitor BRP-7. *European Journal of Medicinal Chemistry*, 122, 510-519.

Li, B., Stribley, J.A., Ticu, A et al.2000. Abundant tissue butyrylcholinesterase and its possible function in the acetylcholinesterase knockout mouse. *J Neurochem.*,75, 1320-1331.

Li, Z., Mu, C., Wang, B., and Jin, J. (2016). Graveoline analogs exhibiting selective acetylcholinesterase inhibitory activity as potential lead compounds for the treatment of alzheimer's disease. *Molecules*, 21, 1-11.

Lieske, C.N., Gepp, R.T., Clark, J.H., Meyer, H.J., Blumbergs, P. and Tseng, C.C. (1991). Anticholinesterase activity of potential therapeutic 5-(1,3, 3-trimethylindolinyl) carbamates. *Journal of Enzyme Inhibition*, 5, 215–223.

LigPrep, version 3.8, Schrödinger, LLC, New York, NY, (2016).

Lipinski, C.A., Lombardo, F., Dominy, B.W.and Feeney, P.J. (2012). Experimental and computational approaches to estimate solubility and permeability in drug discovery and development settings.Adv. *Drug Deliv. Rev*., 64, 4–17.

Liston, D., Nielsen, J., Villalobos, A., Chapin, D., Jones, S., Hubbard, S., Shalaby, I., Ramirez, A., Nason, D., and White, W. (2004). Pharmacology of selective acetylcholinesterase inhibitors: implications for use in Alzheimer's disease. *European Journal of Pharmacology*, 486, 9-17.

Lucier, G.W., McDaniel, O.S., Matthews, H.B., Microsomal rat liver UDP glucuronyltransferase. (1971). Effects of piperonyl butoxide and other factors on enzyme activity. *Archiv. Biochem. Biophysics*, 145, 520–530.

Madalageri, P. M. and Kotresh, O. (2012). Synthesis, DNA protection and antimicrobial activity of some novel chloromethyl benzimidazole derivatives bearing dithiocarbamates. *J. Chem. Pharm. Res.*, 4 (5), 2697–2703.

Madalageri, P.M. and Kotresh, O. (2012). Synthesis, DNA protection and antimicrobial activity of some novel chloromethyl benzimidazole derivatives bearing dithiocarbamates. *Journal of Chemical and Pharmaceutical Research*, 4, 2697–2703.

Maestro, version 10.6, Schrödinger, LLC, New York, NY, (2016).

Mafud-Ana, C., Gambardella-Maria-Teresa, P. (2011). Sodium piperidine-1-carbodithioate dihydrate. *Acta Crystallographica*, 67, 942.

Mandalapu, D., Kushwaha, B., Guptaa, S., Singhc, N., Shukla, Kumar, J., Tanpula, D.K., Sankhwar, S.N., Maikhuri, J.P., Siddiqi, M.I., Lald, J., Gupta, G., Sharma, V.L.(2016)2-Methyl-4/5-nitroimidazole derivatives potentiated against sexually transmitted Trichomonas: Design, synthesis, biology and 3D-QSAR study. *European Journal of Medicinal Chemistry*,124, 820–839.

Massoulie, J., Pezzementi, L., Bon, S., Krejci, E. and Vallette, F.M. (1993). Molecular and cellular biology of cholinesterases. *Prog. Neurobiol.*, 41, 31–91.

Mehta, M., Adem, A., and Sabbagh, M. (2012). New Acetylcholinesterase Inhibitors for Alzheimer’s Disease. *International Journal of Alzheimer’s Disease*, 2012,1-8.

Melnikova, I. (2007). Therapies for Alzheimer's disease. *Nat Rev Drug Discov.*, 6, 341-342.

Meng, F.C., Mao, F., Shan, W.J., Qin, F., Huang, L., Li, X.S. (2012). Design, synthesis, and evaluation of indanone derivatives as acetylcholinesterase inhibitors and metalchelating agents. *Bioorg. Med. Chem. Lett.*, 22, 4462-4466.

Meshnick, S. R. and Dobson, M. J. (2001). P. J. Rosenthal (Ed.), Antimalarial Chemotherapy: Mechanisms of Action, Resistance, and New Directions in Drug Discovery. *The History of Antimalarial Drugs* inside (p.15-25). Humana, Totowa.

Mesulam, M., Guillozet, A., Shaw, P., Levey, A., Duysen, E., and Lockridge, O. (2002). Acetylcholinesterase knockouts establish central cholinergic pathways and can use butyrylcholinesterase to hydrolyze acetylcholine. *Neuroscience*, 110, 627-639.

Mesulam, M.M., Geula, C. 1994. Butyrylcholinesterase reactivity differentiates the amyloid plaques of aging from those of dementia. *Ann Neurol.*, 36:722-727.

Miller, D. and Latimer, R. (1962). The Kinetics of the decomposition and synthesis

Modh, R., Kumar, S.P., Jasrai, Y.T., Chikhalia, K.H. (2013). Design, synthesis, biological evaluation, and molecular modeling of coumarin–piperazine derivatives as acetylcholinesterase inhibitors. *Arch. Pharm. Chem. Life Sci.*, 346, 793-804.

Mohamed, T., Zhao, X., Habib, LK., Yang, J., and Praveen Rao, PPN. (2011). Design, synthesis and structure-activity relationship (SAR) studies of 2,4-disubstituted pyrimidine derivatives: dual activity as cholinesterase and aβ-aggregation inhibitors. *Bioorg Med Chem.*, 19, 2269–2281.

Mohammadi-Khanaposhtani, M., Saeedi, M., Zafarghandi, NS., Mahdavi, M., Sabourian, R., Razkenari, E.K., Alinezhad, H., Khanavi, M., Foroumadi, A., Shafiee, A. and Akbarzadeh, T.(2015). Potent acetylcholinesterase inhibitors: design, synthesis, biological evaluation, and docking study of acridone linked to 1,2,3-triazole derivatives. *Eur J Med Chem.*,6, 799-806.

Mohsen ,U.A., Kaplancikli ,Z.A., Özkay,Y. and Yurttaş,L. **(**2015). Synthesis and Evaluation of Anti-Acetylcholinesterase Activity of Some Benzothiazole Based New Piperazine-dithiocarbamate Derivatives. *Drug Res.*, 65,176-183.

Monser, L.and Adhoum, N. (2002). Modifled activated carbon for the removal of copper, zinc, chromium and cyanide from wastewater. *Sep. Purif. Technol*., 26,137-146.

Morrin Acheson. R. (1973). N.R. Raulins.The Chemistry of Heterocyclic Compounds. *Acridines* inside (p. 28–29). Burlington.

Mumford, H., and Troyer, JK. (2011). Post-exposure therapy with recombinant human BChE following percutaneous VX challenge in guinea-pigs. *Toxicology Letters*, 206, 29-34.

Mushtaq Ahmed, Jo˜ao Batista T. Rocha, Ma´ısa Corrˆea, Cinthia M. Mazzanti, Rafael F. Zanin, Andr´e L.B. Morsch, Vera Maria Morsch, Maria R.C. Schetinger. (2006). Inhibition of two different cholinesterases by tacrine. *Chemico-Biological Interactions*, 162,165–171.

Nachon, F., Carletti, E., Ronco, C., Trovaslet, M., Nicolet, Y., Jean, L., Renard, PY. (2013). Crystal structures of human cholinesterases in complex with huprine W and tacrine: elements of specificity for anti-Alzheimer's drugs targeting acetyl- and butyryl-cholinesterase. *Biochem. J.*, 453, 393-399.

Nachon, F., Carletti, E., Ronco, C., Trovaslet, M., Nicolet, Y., Jean, L., Renard, PY. (2013). Crystal structures of human cholinesterases in complex with huprine W and tacrine: elements of specificity for anti-Alzheimer's drugs targeting acetyl- and butyryl-cholinesterase, *Biochem. J.* 453, 393-399.

Ngamelue, M., Homma, K., Lockridge, O., and Asojo, O. (2007). Crystallization and X-ray structure of full-length recombinant human butyrylcholinesterase. *Acta Crystallographica Section F: Structural Biology and Crystallization Communications* 63, 723-727.

Nicolet, Y., Lockridge, O., Masson, P., Fontecilla-Camps, J., and Nachon, F. (2003). Crystal structure of human butyrylcholinesterase and of its complexes with substrate and products. *Journal of Biological Chemistry*, 278, 41141-41147.

of some dithiocarbamates. *Can. J. Chem.*, 40, 246- 255.

Omran, Z., Cailly, T., Lescot, E., Oliveira Santos, J.S., Agondanou, J.H., Lisowski, V., Fabis, F., Godard, A.M., Stiebing, S., Flem, G.L et al. (2005). Synthesis and

biological evaluation as AChE inhibitors of new indanones and thiaindanones related to donepezil. *Eur. J. Med. Chem*., 40, 1222–1245.

Onder, N.I., Incesu, Z., Ozkay, Y. (2015). Synthesis and Evaluation of New Dithiocarbamic Acid 6,11-Dioxo-6,11-dihydro-1H-anthra[1,2-d]imidazol-2-yl Methyl Esters. *Archiv der Pharmazie*, 348, 508-517.

Özkay, Y., Yurttaş, L., Mohsen, U. A., Sever, B., Hussein, W., Öztürk, Ö., Sağlık, B. N., Acar, U., Erdoğan, Ö. N., Pekbağ, A., Kaplancıklı, Z. A. (2014). Study on thiazolyl-hydrazone derivatives as acetylcholinesterase inhibitors. *MUSBED*, 4, 39-42.

Pákáski, M., Kálmán, J. (2008). Interactions between amyloid and cholinergic mechanisms in Alzheimer's disease. *Neurochem. Int.*, 53, 103–111.

Parveena, N., Shaha, A., Zeb Khana, S., Ud-Din Khanc, S., Ali Ranac, U., Farkhondeh, F., Hassan Shaha, A., Naeem Ashiqd, M., Raufa, A., Qureshia, R., Zia-ur, R., and Kraatzb, H-B.(2015).Synthesis, Spectroscopic Characterization, pH Dependent Electrochemistry and Computational Studies of Piperazinic Compounds.*Journal of The Electrochemical Society*, 162,32-39.

Pelayo, C., Jordi, R.E., Diego, M.T., Albert, B., Josep, Eladi, B., Nuria Maria, V., Xavier; B., Modesto, O., Francisco Javier, L. (2000). New tacrine-huperzine A hybrids (huprines): highly potent tight-binding acetylcholinesterase inhibitors of interest for the treatment of Alzheimer's disease. *Journal of Medicinal Chemistry*, 43, 4657-4666.

Pliska, V., Testa, B., and Waterbeemd, H.V.D. (1996). H. van de Waterbeemd and R. Mannhold. Lipophilicity in Drug Action and Toxicology. *Lipophilicity descriptors for structure–property correlation studies: overview of experimental and theoretical methods and a benchmark of log P calculations* inside (p.401-415). New York.

Pohanka, M. (2011). Cholinesterases, a target of pharmacology and toxicology. *Biomed. Pap. Med. Fac. Univ. Palacky Olomouc Czech. Repub*., 155 (3), 219-229.

Rakonczay, Z. (2003). Potencies and selectivities of inhibitors of acetylcholinesterase and its molecular forms in normal and Alzheimer's disease brain. *Acta Biol. Hung.,* 54(2),183-189.

Rakonczay, Z. and Brimijoin, S. (1988). Monoclonal antibodies to human brain acetylcholinesterase: properties and applications. Cell. Mol. *Neurobiol.,* 8 (1), 85-93.

Reisberg, B., Kenowsky, S., Franssen, E., Souren, L.E.M., Shulman, E., Steinberg, G., Aronstein, Z. and Auer, S. (1996). Slowing the progression of Alzheimer Disease: Towards a Science of Alzheimer Disease care. *Caring*, 2(2), 2-4.

Ripoll, D.R., Faerman, C.H, Axelsen, P.H., Silman, I. and Sussman, J. L. (1993). An electrostatic mechanism for substrate guidance down the aromatic gorge of acetylcholinesterase. *Proc.Natl. Acad. Sci. USA.* 90(11), 5128-5132.

Sağlık, BN., Özkay, Y., DemirÖzkay, Ü., and Gençer, HK. (2014). Synthesis and Biological Evaluation of Some Novel Dithiocarbamate Derivatives. *Journal of Chemistry,* 2014,1-9.

Samadi, A., Marco-Contelles, J., Soriano, E., Alvarez-Pérez, M., Chioua, M., Romero, A., González-Lafuente, L., Gandía, L., Roda, J.M., López, M.G., Villarroya, M., García, A.G. and Ríos Cde, L. (2010). "Multipotent drugs with cholinergic and neuroprotective properties for the treatment of Alzheimer and neuronal vascular diseases.I. Synthesis, biological assessment, and molecular modeling of simple and readily available 2-aminopyridine-, and 2-chloropyridine-3,5-dicarbonitriles". *Bioorganic and Medicinal Chemistry,*18, 5861–5872.

Scarpini, E., Scheltens, P. and Feldman, H. (2003). Treatment of Alzheimer's disease: current status and new perspectives. *Lancet Neurol.*, 2, 539–47.

Schneider, R.W. (1984). Effects of nonpathogenic strains of fusarium oxysporum on celery root infection by F. oxysporum f. sp. apii and a novel use of the Limeweaver-Burk double reciprocal plot tecnique. *Eco. Epidem.,* 74, 646-653.

Schrödinger, LLC, New York, NY, (2016).

Sclan, S., Saillon, A., Franssen, E., Hugonot-Diener, L., Saillon, A. and Reisberg, B. (1996). The Behavioral Pathology in Alzheimer's disease Rating Scales (BEHAVE-AD): Reliability and Analysis of symptom category scores. *International journal of Geriatric Psychiatry,* 11, 819-830.

Selkoe, D. J. 2002. Alzheimer's disease is a synaptic failure. *Science*, 298, 789-791.

Shen, Y., Sheng, R., Zhang, J., He, Q., Yang, B., Hua, Y. (2008). 2-Phenoxy-indan-1-one derivatives as acetylcholinesterase inhibitors. A study on the importance of modifications at the side chain on the activity. *Bioorg. Med. Chem.*, 16, 7646–7653.

Shen, Z.X. (2004). Future perspectives of AD research and clinical practice. *Med, Hypotheses*, 63, 298–307.

Shih-Hsien Wang and R. Griffiths. (1995). Resolution enhancement of diffuse reflectance i.r. spectra of coals by Fourier self-deconvolution: C-H stretching and bending modes. The Science and Technology of Fuel and Energy. 64,229-236.

Silverman, R.B. (2004). R.B. Silverman.The Organic Chemistry of Drug Design and Drug Action. *Lead Discovery and Lead Modification* inside (p. 11–12). Burlington.

Silverstein, R.M., Webster, F.X. (1998). R.M Silverstein, F.X. Webster (Eds.). Spectrometric identification of organic compounds. Proton magnetic resonance spectrometry inside (p.166-167). NewYork.

Sonmez, F., Kurt, B.Z., Gazioglu, I., Basile, L., Dag, A., Cappello, V., Ginex, T., Kucukislamoglu, M., & Guccione.S. (2017). Design, synthesis and docking study of novel coumarin ligands as potential selective acetylcholinesterase inhibitors. *Journal of enzyme inhibition and medicinal chemistry,* 32, 285–297.

Stewart, DJ., Inaba, T., Tang, BK. and Kalow, W. (1977). Hydrolysis of cocaine in human plasma by cholinesterase. *Life Sci.*, 20, 1557–1564.

Sugimoto, H., Yamanishi, Y., Limura, Y., Kawakami, Y. (2000). Donepezil hydrochloride (E 2020) and other acetylcholinesterase inhibitors. *Curr. Med. Chem.,*7, 303–317.

Sussman, J.L., Harel, M., Frolow, F., Oefner, C., Goldman, A., Toker, L. and Silman, I. (1991). Atomic structure of acetylcholinesterase from Torpedo californica: a prototypic acetylcholine-binding protein. *Science,* 253(5022), 872-879.

Szolar, O. H. J. (2007). Environmental and pharmaceutical analysis of dithiocarbamates. *Analytica Chimica Acta.,* 582, 191–200.

Takemura, Y., Ju-ichi. M., Ito, C., Furukawa, H. and Tokuda H. (1995). Studies on the inhibitory effects of some acridone alkaloids on Epstein-Barr virus activation. *Planta Med*., 61, 366-8.

Tayeb, H.O., Yang, H.D., Price, B.H. and Tarazi, F.I. (2012). Pharmacotherapies for Alzheimer's disease: beyond cholinesterase inhibitors. *Pharmacol. Ther.*, 34(1), 8-25.

Tisdale, W.H and Williams, I. (1934). Disinfectant, U.S. Patent, No: 1,972,961.

Turan-Zitouni, G., Özdemir, A. and Güven, K. (2005). Synthesis of some 1-[(N,Ndisubstituted thiocarbamoylthio)acetyl]3-(2-thienyl)-5-aryl-2-pyrazoline derivatives and investigation of their antibacterial and antifungal activities. *Arch. Pharm. Chem.Life,* 338, 96–104.

Turan-Zitouni, G., Ozdemir, A., Kaplancikli, Z.A., Altintop, M.D., Temel, H.E., Akalın Çiftçi, G. (2013). Synthesis and biological evaluation of some thiazole derivatives as new cholinesterase inhibitor. *J. Enzyme Inhib. Med.Chem.,* 28 (3), 509–514.

Turan-Zitouni, G., Ozkay, Y., Ozdemir, A., Kaplancikli, Z.A., Altintop, MD. (2011). Synthesis of some benzothiazole based piperazine-dithiocarbamate derivatives and evaluation of their anticancer activities. *Letters in Drug Design & Discovery.*, 8, 830-837.

Vernino, S., Sandroni, P., Singer, W., and Low, PA. (2008). Invited Article: Autonomic ganglia: Target and novel therapeutic tool. *Neurology*,70, 1926-1932.

Viktor, E. and Jiri, N. (1906). Local anesthetics derived from acylaminoacridine. *Chemicke Listy pro Vedu a Prumysl*, 51, 1906-8.

Wales, P.C. and Helliker, P.E. (2002). Evaluation of Methyl Isothiocyanate as a Toxic Air Contaminant. *California Environmental Protection Agency*, 1-3.

Wang, B., Mai, Y.C., Li, Y., Hou, J.Q., Huang, S.L., Ou, T.M., Tan, J.H., An, L.K., Li, D., Gu, L. Q et al. (2010). Synthesis and evaluation of novel rutaecarpine derivatives and related alkaloids derivatives as selective acetylcholinesterase inhibitors. *Eur. J. Med. Chem.*, 45, 1415–1423.

Wang, X., Bhatia, P.A., Daanen, J.F., Latsaw, S.P., Rohde, J., Kolasa, T., Hakeem, A.A., Matulenko, M.A., Nakane, M., Uchic, M.E., Miller, L.N., Chang, R., Moreland, R.B., Brioni, J.D. and Stewart, A.O. (2005). Synthesis and evaluation of 3-aryl piperidine analogs as potent and efficacious dopamine D4 receptor agonists. *Bioorg. Med. Chem.*, 13(15), 4667-4678.

Waugh, J.S. (1982). Theory of broadband spin decoupling. *J. Magn. Reson.*, 50,30–49.

Weiner, M. F and Gray, K. F. (1994). Balancing Psychosocial and Psychopharmacologic measures in Alzheimer Disease. *The American Journal of Alzheimer's Care and Related Disorders and Research*, 9(4), 6-12.

Weinreb, O., Amit, T., Bar-Am, O. and Youdim, M. B. H. (2011). "A novel anti-Alzheimer's disease drug, ladostigil. neuroprotective, multimodal brain-selective monoamine oxidase and cholinesterase inhibitor." *International Review of Neurobiology*,100, 191–215.

Westrop, G. D., Georg, I. and Coombs, G. H. (2009). The Mercaptopyruvate Sulfurtransferase of Trichomonas vaginalis Links Cysteine Catabolism to the production of Thioredoxin Persulfide *J. Biol. Chem.*, 284, 33485-33494.

Wynne, J. H., Jensen, S. D. and Snow, A. W. (2003). Facile One-Pot Synthesis of S-Alkyl Thiocarbamates. *J. Org. Chem.*, 68, 3733–3735.

Xie, W., Altamirano, CV., Bartels, C.F, Speirs, RJ., Cashman, JR., Lockridge, O. (1999). An improved cocaine hydrolase: the A328Y mutant of human butyrylcholinesterase is 4-fold more efficient. *Mol Pharmacol.*,55, 83.

Xue, L., Ko, M-C., Tong, M., Yang, W., Hou, S., Fang, L., Liu, J., Zheng, F., Woods, JH., Tai, H-H., and Zhan, C-G. (2011). Design, preparation, and characterization of

high-activity mutants of human butyrylcholinesterase specific for detoxification of cocaine. *Molecular Pharmacology* ,79, 290-297.

Yin, H. D., Xue, S. C., Wang, C. H. (2006). Synthesis, characterization of di-t-butyltin piperazine carbodithioato complexes $tBu_2Sn(Cl)S2CN(CH_2CH_2)_2NR$ and crystal structures of $tBu_2Sn(Cl)S_2CN(CH_2CH_2)_2NEt$ and $tBu_2Sn(Cl)S_2CN(CH_2CH_2)_2NBz$. Polish Journal of Chemistry, 80, 873-880.

Yurttaş, L., Kaplancıklı, Z.A., Özkay, Y. (2013). Design, synthesis and evaluation of new thiazole-piperazines as acetylcholinesterase inhibitors. *J. Enz. Inh. Med. Chem.*, 28, 1040–1047.

Yurttas, L., Ozkay, Y., Demirci, F., Goger, G., Ulusoylar Y., Safak; Abu Mohsen, U., Ozturk, O., Kaplancikli, Z.A. (2014). Synthesis, anticandidal activity and cytotoxicity of some thiazole derivatives with dithiocarbamate side chains. *Turkish Journal of Chemistry*, 38, 815-824.

Zahradni, R. and Zuman, P. (1958). Carbaminate, Monothiocarbaminate und Dithiocarbaminate. VIII. Polarographische Studie der Kinetik und des Mechanismus des Zerfalls von Dithiocarbaminosauren in saurem Milieu. *Chem. listy* 52, 231.

Zeisel, J. and Raia, P. (2000). Non-pharmacological Treatment for Alzheimer Disease: A mindbrain approach. *American Journal of Alzheimer Disease and Other Dementias*, 15(6), 331-340.

Zengin, H., Yenilmez, H.Y., Burat, A.K., Bayir, Z.A. (2014). Synthesis and characterization of novel 2-{[2-(dimethylamino)ethyl](methyl)amino} ethoxy-substituted metallophthalocyanines. *Turk J Chem.*, 38, 1094-1101.

Zeynep Soyer, Z., Uysal, S., Parlar, S., Ayse Hande Tarikogullari Dogan, A.H. T & Alptuzun, V. (2016). Synthesis and molecular docking studies of some 4-phthalimidobenzenesulfonamide derivatives as acetylcholinesterase and butyrylcholinesterase inhibitors. *Journal of Enzyme Inhibition and Medicinal Chemistry*,13-19, 2016.

Zhiyong, Y., Fei., W., Vesna., M., Xiaofeng, L., Qiuzhi Cindy, C., Yan, Z.B., Dou, B., Ping, Q. (2007). Evaluation of copper-dependent proteasome-inhibitory and apoptosis-inducing activities of novel pyrrolidine dithiocarbamate analogues. *International Journal of Molecular Medicine,* 20, 919-925.

Zhou, J., Hu, X., Zhang, H., Qian, H., Huang, W., Qi, F., Zhang, Y. (2009). Synthesis and Biological Evaluation of 5,6-Dihydro-benzo[c] acridin-7-ol Derivatives as Anti-Alzheimer's Disease Drugs.*Letters in Drug Design & Discovery*, 6, 623-628.

Zuman, P. and Zahradnik, R. (1957). Kinetik und Mechanismus der Zersetzung der Dithiocarbaminsauren in saurer Lbsung. Polarographische Studie *Z. physik. Chem.*, 208, 135.

[1]http://www.who.int/mental_health/publications/dementia_report_2012/en/(Cited:

26.01.2017).

[2]https://en.dailypakistan.com.pk/lifestyle/happy-birthday-alois-alzheimer-its-been-110-years-since-dementia-was-discovered/(Cited:11.01.2017).

[3]https://www.nia.nih.gov/alzheimers/topics/alzheimers-basics(Cited:19.01.2017).

[4](http://neuropathology-web.org/chapter9/chapter9bAD.html)(Cited:30.01.2017).

[5]http://www.pbs.org/wnet/brain/episode5/alzheimers/ (Cited:31.01.2017).

[6]https://www.researchgate.net/figure/41412544_fig7_Fig-7-Schematic-view-of-the-active-site-gorge-of-Tc-AChE-The-bottom-of-the-gorge-is (Cited: 01.02.2017).

[7]https://www.wessexscene.co.uk/science/2015/05/14/pint-of-science-time-flies-a-brain-perspective/(Cited: 02.02.2017).

[8]https://en.wikipedia.org/wiki/Acridine (Cited:03.02.2017).

[9]http://chempedia.info/page/24009611820515310100316924213407617409511805104 6/ (Cited:23.02.2017).

[10]http://en.wikipediaorg/wiki/Acriflavine (Cited: 02.02.2017).

[11]http://www.inchem.org/documents/ehc/ehc/ehc78(Cited:04.02.2017).

[12]http://www.who.int/ipcs/publications/pesticides_hazard/en/(Cited:04.02.2017).

[13]http://www.molinspiration.com/cgi-bin/galaxy?smiles=CN(C)CCN4CCN(C(%3DS)SCC(%3DO)Nc2c1ccccc1nc3ccccc23)CC4(Cited:24.02.2017)

[14]http://www.cbligand.org/BBB/index.php(Cited:27.02.2017)

[15]http://molsoft.com/about.htm(Cited:02.03.2017)

[16]https://www.researchgate.net/post/Why_do_halogen_substituents_make_molecules_more_lipophilic(Cited:04.03.2017)

[17](www.pdb.org).